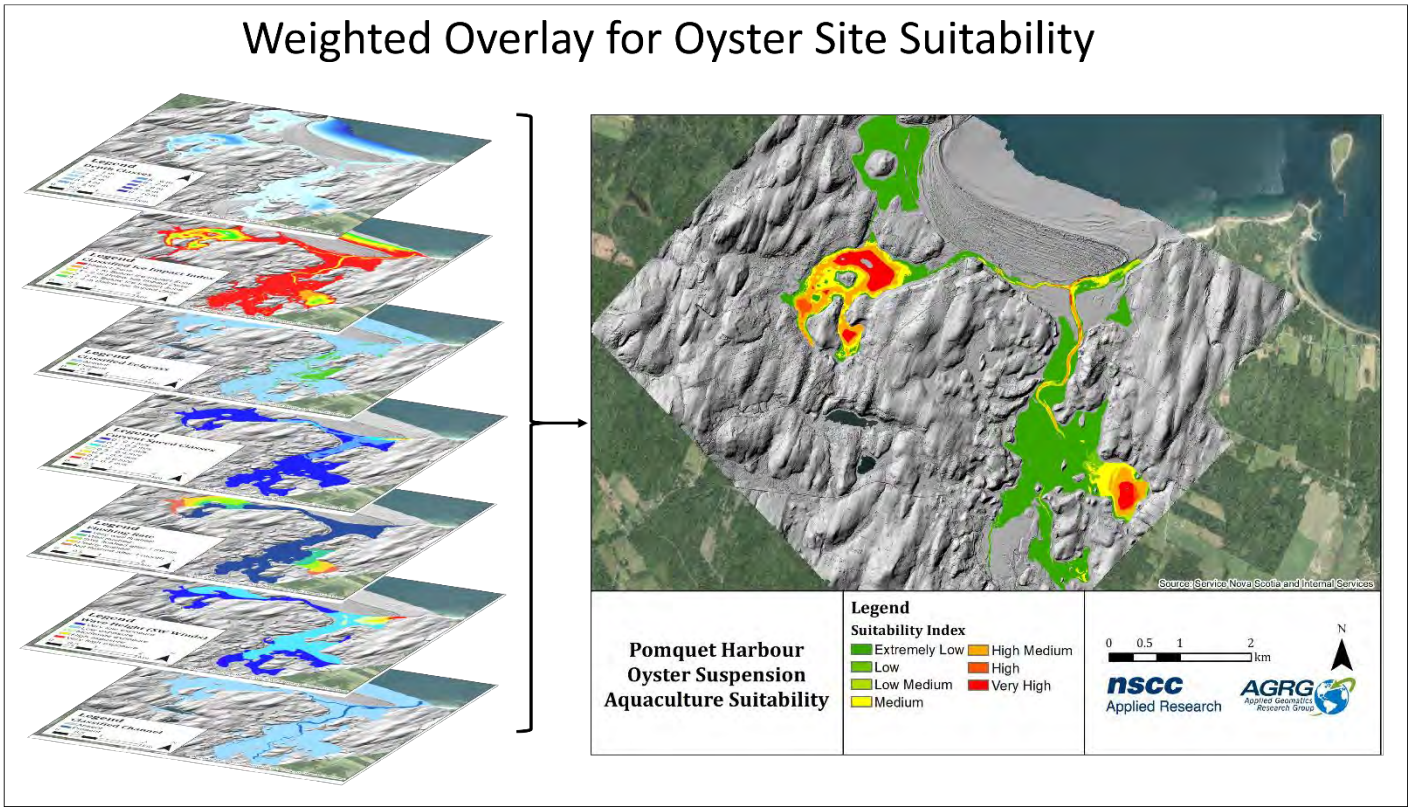

DEVELOPMENT OF A BAY MANAGEMENT TOOL TO SUPPORT SUSTAINABLE AQUACULTURE FOR PAQTNKEK MI'KMAW NATION using Bathymetric Lidar, Hydrodynamic Modelling, and GIS

Prepared by

Tim Webster, PhD, Nathan Crowell,
Dedipya Kodavati, Jesse Siegel,
Emma Laskey
Applied Geomatics Research Group
NSCC, Middleton
Tel. (902)825 5475
email: tim.webster@nscc.ca

Submitted to

Paqtnkek Mi'kmaw Nation

How to cite this work and report:

Webster, T., Crowell, N., Kodavati, D., Siegel, J., and Laskey, E. 2021. Development of a Bay Management Tool to Support Sustainable Aquaculture for Paqtnkek Mi'kmaw Nation using Bathymetric Lidar, Hydrodynamic Modelling, and GIS. Technical report, Applied Geomatics Research Group, NSCC Middleton, NS.

Copyright and Acknowledgement

The Applied Geomatics Research Group of the Nova Scotia Community College maintains full ownership of all data collected by equipment owned by NSCC and agrees to provide the end user who commissions the data collection a license to use the data for the purpose they were collected for upon written consent by AGRG-NSCC. The end user may make unlimited copies of the data for internal use; derive products from the data, release graphics and hardcopy with the copyright acknowledgement of **"Data acquired and processed by the Applied Geomatics Research Group, NSCC"**. Data acquired using this technology and the intellectual property (IP) associated with processing these data are owned by AGRG/NSCC and data will not be shared without permission of AGRG/NSCC.

Executive Summary

The Applied Geomatics Research Group of NSCC supplied data for Pomquet Harbour based on their aircraft-mounted topo-bathymetric lidar sensor and camera to collect land and sea elevation data and high-resolution air photos. Topo-bathymetric lidar is a relatively new remote sensing technology that uses lasers to acquire accurate measurements of the topography of the land and the bathymetry of the seabed. Bathymetric lidar depth penetration is limited by water clarity and therefore the survey must be completed under optimal conditions to maximize data quality. NSCC supplied data from an Acoustic Doppler Current Profiler (ADCP) deployed for one month in Pomquet Harbour. Supplemental bathymetry data were collected using a multibeam echo sounder for an area where the lidar sensor did not penetrate to the seabed. Maps were generated from the lidar data including a Digital Elevation Model (DEM) of the land and seabed, an intensity map that provides data on the seabed cover, and a high resolution (50 cm) multispectral aerial photo ortho-mosaic. A Mike-21 hydrodynamic model was developed to simulate current speeds and direction within the harbour under normal tidal conditions and in the case of a 1.5 m storm surge. The model was used to characterize harbour circulation, calculate flushing rates, and track the fate of particles that represent oyster spat. The layers for a GIS suitability map of potential oyster aquaculture sites include the development of a bottom classification map derived from the lidar and photo products, showing substrate cover, modelled currents, flushing time, water depth and depth below the ice impact zone among other GIS layers. The GIS suitability layers were classified and ranked in preparation for the GIS overlay to show optimal locations for aquaculture sites. The suitability maps were influenced by advice from DFO, NSFA, and CMAR. A web-based GIS mapping system was developed to display the GIS layers (model output, lidar-derived layers, etc.) and suitability maps. Suitability maps can be customized using the web-tools by assigning weights and scores to each GIS layer to determine suitability. See the User Guide to understand how the GIS layer selection and how the weighting-scoring of map classes function to construct suitability maps.

Table of Contents

Executive Summary ii

Table of Contents iii

Table of Figures vi

List of Tables xi

1 Introduction 12

1.1 Project Description 12

1.2 Background and Study Area 12

2 Methods 13

2.1 Lidar Sensor Specifications and Installation 13

2.2 Lidar Survey Details 15

2.3 Lidar Data Processing 16

2.4 Multibeam Survey 16

2.4.1 Data Collection 16

2.4.2 Data Processing 19

2.5 Ground Truthing 19

2.5.1 GPS points 19

2.5.2 Video Ray 20

2.5.3 Acoustic Doppler Current Profiler (ADCP) 24

2.6 GIS Datasets 32

2.6.1 Traditional Ecological Knowledge (TEK) 32

2.6.2 Oyster Stock Survey Data 35

2.6.3 Temperature and Salinity 38

2.6.4 Supporting Data 40

2.6.5 Land Use 41

2.6.6 Intertidal Zone 43

2.6.7 Channel Map....44
2.6.8 Ice Impact Zone....45
2.6.9 Depth Map....46
2.7 Eelgrass....48
2.8 Hydrodynamic Modelling....49
2.8.1 Mesh Generation....49
2.8.2 Boundary Conditions....51
2.8.3 Hydrodynamic Simulation....52
2.8.4 Transport Module Simulation (Flushing time)....53
2.8.5 Spectral Waves Module Simulation....53
2.8.6 Particle Tracking....53
3 Results....54
3.1 Digital Elevation Model (DEM)....54
3.2 Digital Surface Model (DSM)....55
3.3 Intensity....56
3.4 Orthophoto....59
3.5 Eelgrass....61
3.6 Acoustic Doppler Current Profiler (ADCP)....62
3.7 Hydrodynamic Model Products....66
3.7.1 Mean and Maximum Currents....66
3.7.2 Significant Wave Height (Hs)....69
3.7.3 Flushing Rate....71
3.7.4 Storm Surge....73
3.7.5 Particle Tracking....76
4 Validation....80
4.1 Lidar Validation....80

4.1.1 Topographic Validation 80
4.1.2 Bathymetric Validation 80
4.2 Hydrodynamic Model Validation 81
5 Aquaculture Suitability Index 87
5.1 GIS Data Layers 87
5.2 Weighted Overlay Suitability Model 89
5.3 Suitability Model Parameter Weighting 89
6 Web Visualization 92
6.1 Aquaculture Suitability Modeller 93
7 Conclusion 97
8 Acknowledgements 99
9 References 99
10 Appendix 1: Number of Oysters per Length 100
11 Appendix 2: Hillshade Models 108
12 Appendix 3: Pomquet AFF Aquaculture Suitability Modeller User Guide 110
Getting Started 111
12.1 GIS Data Layers 113
12.1.1 Traditional Ecological Knowledge (TEK): Molluscs 114
12.1.2 Channel Location 115
12.1.3 Classified Depth from Low Tide 116
12.1.4 Classified Dominant Wave Height 117
12.1.5 Classified Flushing Rate 118
12.1.6 Classified Mean and Maximum Monthly Current Speed 119
12.1.7 Classified Eelgrass 121
12.1.8 Ice Impact-Free 122
12.1.9 NS Marine Aquaculture Leases 123

12.2 Suitability Modeller Tool 124

Table of Figures

Figure 1: Pomquet Harbour, NS, the study area used for the Bay Management Tool project. 13
Figure 2: Principals of topo-bathymetric lidar. The system utilizes two lasers, a near-infrared and a green laser to surface the land and marine topography. Inset of green laser waveform. 14
Figure 3: (A): Aircraft used for lidar survey; (B): display seen by lidar operator in-flight; (C): main body of sensor (left) and laser pointing through a hole cut in the bottom of the plane (right); (D): large red circles are the lasers; the RCD30 lens (right) and low-resolution camera (left). 14
Figure 4: Flight lines for 2018 lidar surveys in Pomquet and Afton River, NS. 15
Figure 5: AGRG Boston Whaler with deployed multibeam system on an arm that rotates to submerge the echo sounder. 17
Figure 6: Pomquet lidar seamless Digital Surface Model with 2020 multibeam survey trajectory (dark points), and SVP drop location. 18
Figure 7: Sound Velocity Profile taken in Pomquet Harbour on October 23rd, 2020. 18
Figure 8: Global Positioning System (GPS) points for validating the topo-bathymetric lidar overlaid on a Colour Shaded Relief (CSR) lidar Digital Surface Model (DSM). 20
Figure 9: (A) The left side of the figure shows a Video Ray ROV; (B) The right side shows a Video Ray control unit. 21
Figure 10: Video ray track obtained from the GPS units Garmin (autonomous >5 m accuracy) and Leica GS 14 (RTK corrections < 0.05 m accuracy) overlaid on a CSR. 22
Figure 11: The right side of the figure shows screen shots from video taken using a Video Ray ROV, with the location of the video shown marked on the orthophoto to the left. The video frames were matched using time stamps from the video correlated with time stamps from the Leica GNSS log. The site at location (A) shows the bottom type as focus. The dark patch at location (B) is Sand (60)/Moss (30)/Fucus (10) along with oyster shells. Location (C) shows the presence of rock and eelgrass. Location (D) shows moss and algae in deeper water farther from shore than the previous three locations. 24
Figure 12: (A) ADCP deployment location in Pomquet Harbour; (B) Sentinel V20 on a frame being deployed from Boston Whaler. 25
Figure 13: Sample "Basic" post-processing setting window. 26
Figure 14: Parameters set up in the processing tab of WavesMon. 28
Figure 15: Water binned current speed (m/s). X-axis represents time and consists of approximately 30 days. 29
Figure 16: Wind speed at nearby Tracadie weather station. 29

Figure 17: Binned Water Velocity, Northern Component. 29
Figure 18: Binned Water Velocity, Eastern Component. 29
Figure 19: Binned Water Velocity, 'Up' Component. 30
Figure 20: Binned Water Direction, corrected for true north. The repeating pattern represents the daily tidal cycles. 30
Figure 21: A plot showing the Hs (top graph), Tp (middle graph) and WL (bottom graph) during the ADCP deployment time frame. 30
Figure 22: Wind data from the Tracadie station (top graph) plotted with the ADCP Significant Wave Height (Hs) (bottom graph) in metres. 31
Figure 23: Wave Height Spectra and Directional Spectrum on June 26th, 2018 at 13:00. Top graph shows the significant wave height (Hs). Bottom graph is a rose diagram showing where the direction the waves are coming from and their period. 32
Figure 24: Migratory fish presence identified from Traditional Ecological Knowledge. 33
Figure 25: Mollusc presence identified from Traditional Ecological Knowledge. 34
Figure 26: Invasive species presence as reported by the Department of Fisheries and Oceans (DFO). 35
Figure 27: Location of oyster stock surveys conducted by Robin Stuart on behalf of Paqtnkek First Nation. 36
Figure 28: Location of oyster survey stations with significant oyster habitat as identified by Robin Stuart on behalf of Paqtnkek First Nation. 37
Figure 29: Number of Oysters Times Average Size (mm) was determined by multiplying the total number of recorded oysters by the mean size at each station during oyster stock surveys conducted by Robin Stuart on Paqtnkek First Nation's behalf. 38
Figure 30: Temperature data collected at each station during oyster stock surveys conducted by Robin Stuart on Paqtnkek First Nation's behalf 39
Figure 31: Salinity data collected at each station during oyster stock surveys conducted by Robin Stuart on Paqtnkek First Nation's behalf. 40
Figure 32: Aquaculture leases in Pomquet Harbour as of November 2020. Most recent information is available at http://novascotia.ca/fish/aquaculture/site-mapping-tool/ 41
Figure 33: The Nova Scotia Department of Lands and Forestry Forest Resource Inventory land use classification, with simplified categories. 43
Figure 34: The intertidal zone, defined as the region on the elevation model between 0.45 m (HHWLT) and -1.01 m (LLWLT). 44
Figure 35: Classified channel obtained from the depth layer. 45

Figure 36: The Ice Impact Zone is defined as the level of HHWLT to 1 metre below LLWLT, with the ice impact-free zone divided into 1-metre increments below the impact zone. 46
Figure 37: Continuous depth model, with depth relative to LLWLT. 47
Figure 38: Classified depth model, with 1 m depths relative to Lower Low Water Large Tide. 48
Figure 39: Mesh generated using Mike Mesh Generator tool showing fine resolution in channel and small branches of the harbour. 50
Figure 40: Mesh file showing bathymetry plotted using Mike plot Composer. 51
Figure 41: Predicted Tide obtained from http://tbone.biol.sc.edu/tide/ at Antigonish harbour plotted using Mike Plot Composer. 52
Figure 42: Wind data from Tracadie ECCC station. 52
Figure 43: Number of particles released per hour from the station in the simulation. 54
Figure 44: Colour shaded relief model generated from the digital elevation model. 55
Figure 45: Colour shaded relief model generated from the digital surface model. 56
Figure 46: Intensity map of the lidar return data that incorporates all green laser returns above and below the water line (HHWLT). 57
Figure 47: Normalized intensity map of the lidar return data that incorporates lidar returns below the water line (HHWLT). 58
Figure 48: Colour shaded relief intensity model generated from the digital elevation model and lidar intensity data. 59
Figure 49: True colour image (50 cm), generated from the RCD30 orthophoto mosaic. 60
Figure 50: False colour NIR image (50 cm), generated from the RCD30 orthophoto mosaic with band combinations near infrared, green, and blue. 61
Figure 51: Classified eelgrass presence in Pomquet Harbour. 62
Figure 52: Frames from the ADCP animation. Upper left graph shows the wind direction and speed from the Tracadie weather station. The bottom left graph shows the water level above the sensor. The right graph shows the 30 cm bins of current velocity (magnitude and direction) as well the depth averaged current (green line and circle). (A) Currents during low tide with strong southerly winds. (B) Currents during high tide with moderate southerly winds. 63
Figure 53: Frame from the ADCP animation for June 26th storm surge. Upper left graph shows the wind direction and speed from the Tracadie weather station. The bottom left graph shows the water level above the sensor. The right graph shows the 30 cm bins of current velocity (magnitude and direction) as well the depth averaged current (green line and circle). 64

Figure 54: Wind from Tracadie weather station (top) and average current velocity from the ADCP (bottom) for the June-July 2018. 65
Figure 55: Wind from Tracadie weather station (top) and water height above the ADCP (bottom) for the June-July 2018. 65
Figure 56: Mean of current magnitudes (m/s) during a 33-day simulation of the hydrodynamic model displayed as a continuous raster. 66
Figure 57: Mean of current magnitudes (m/s) during a 33-day simulation of the hydrodynamic model classified into seven speed categories. 67
Figure 58: Maximum value of current magnitudes (m/s) during a 33-day simulation of the hydrodynamic model displayed as a continuous raster. 68
Figure 59: Maximum value of current magnitudes (m/s) during a 33-day simulation of the hydrodynamic model classified into thirteen speed categories. 69
Figure 60: The continuous dominant wave height layer was generated by applying strong south-southwest winds to the model. 70
Figure 61: The classified dominant wave height layer was generated from modelled exposure to a south-southwest wind. 71
Figure 62: The continuous flush layer was generated from the minimum concentration left in the harbour after a 33-day simulation of the hydrodynamic model. The blue indicates faster flushing rates than the red areas. 72
Figure 63: The minimum concentration left in the harbour after the hydrodynamic model simulation was classified into five flushing classes. 73
Figure 64: Maximum water level during storm surge, modelled in Mike 21 and a contour at high tide. Inset shows the water level in Church Cove. 74
Figure 65: Mean Current magnitudes during a storm event modelled in Mike 21 Flex Mesh. 75
Figure 66: Maximum current magnitudes during a storm event modelled in Mike 21 Flex Mesh. 76
Figure 67: Simulated oyster spat concentrations during the initial model timesteps. 77
Figure 68: Modelled spat distribution during an outgoing tide scenario. Highest concentrations were observed in the northwestern bay which exhibited minimal tidal distribution. 78
Figure 69: Modelled spat distribution during an incoming tide scenario. Highest concentrations were observed in the southeastern bay where onshore forcing concentrated particles on the north shore. 79
Figure 70: Validation statistics for topographic points. 80
Figure 71: Validation statistics for bathymetric points. 81

Figure 72: Simulated water levels from the Mike FM hydrodynamic model (blue dash) show good agreement with ADCP observations (blue line) over the validation period in contrast to tidal predictions (orange line). 82
Figure 73: Residual water level (+ observation above simulation, - observation below simulation; green line) plotted against wind velocity components as Wind U (+ East, - West; grey dash) and Wind V (+ North, - South; grey line) showing inverse relation between residual water level and V component velocity. 83
Figure 74: Simulated and observed current velocities presented as Velocity U (+ East, - West; top) and Velocity V (+ North, - South; bottom) showing a dominant V component in both the simulated and observed currents with a high degree of variation between the modelled and observed values. 84
Figure 75: Comparison of incoming spring and neap tidal currents which were found to produce complex and variable eddy patterns over the ADCP validation point (red). 85
Figure 76: Simulated current magnitudes and directions modelled during the peak flow of an incoming tide. 86
Figure 77: The Pomquet Aquaculture Suitability Index includes seven classified raster layers: depth from low tide, ice impact-free depth, eelgrass presence, average monthly current speed, flushing rate, dominant wave height, and the channel location. 91
Figure 78: Pomquet Harbour Oyster Suspension Aquaculture Suitability map. 92
Figure 79: Pomquet AFF suitability web application, https://agrgims.cogs.nscc.ca/PomquetAFF/ 93
Figure 80: Location of suitability modeller tool on the Pomquet AFF web application. 94
Figure 81: Partial list of layers available to conduct suitability analysis. 94
Figure 82: Relative importance assigned to each layer in the suitability analysis, as determined by the user. 95
Figure 83: The suitability model will appear in the list of layers when the analysis is complete. 96
Figure 84: Output of suitability model. The visualization of the model will change as the user selects different layers and assigns different values of relative importance. Scores go from least suitable (1) to most suitable (9). 96
Figure 85: Chart of the suitability model generated by drawing a polygon around the area of interest. 97
Figure 86: Count values of the 0 – 20 mm oyster shell size class collected at each station during oyster stock surveys conducted by Robin Stuart on Paqtnkek First Nation's behalf. 100
Figure 87: Count values of the 20 – 30 mm oyster shell size class collected at each station during oyster stock surveys conducted by Robin Stuart on Paqtnkek First Nation's behalf. 101
Figure 88: Count values of the 30 – 40 mm oyster shell size class collected at each station during oyster stock surveys conducted by Robin Stuart on Paqtnkek First Nation's behalf. 102
Figure 89: Count values of the 40 – 50 mm oyster shell size class collected at each station during oyster stock surveys conducted by Robin Stuart on Paqtnkek First Nation's behalf. 103

Figure 90: Count values of the 50 – 60 mm oyster shell size class collected at each station during oyster stock surveys conducted by Robin Stuart on Paqtnkek First Nation's behalf. 104
Figure 91: Count values of the 60 – 80 mm oyster shell size class collected at each station during oyster stock surveys conducted by Robin Stuart on Paqtnkek First Nation's behalf. 105
Figure 92: Count values of the 80 – 100 mm oyster shell size class collected at each station during oyster stock surveys conducted by Robin Stuart on Paqtnkek First Nation's behalf. 106
Figure 93: Count values of the >100 mm oyster shell size class collected at each station during oyster stock surveys conducted by Robin Stuart on Paqtnkek First Nation's behalf. 107
Figure 94: Hillshade generated from the digital elevation model. 108
Figure 95: Hillshade generated from the digital surface model. 109

List of Tables

Table 1: Summary of lidar surveys, 2018. 15
Table 2: Lidar point classification values and descriptions. 16
Table 3: Wave and Currents Setup for the Sentinel V20 for the Pomquet deployment. 26
Table 4: NS Department of Lands and Forestry Land Use layer definitions. 42
Table 5: Tidal range values obtained from Canadian Hydrographic Services (CHS) relative to CGVD2013. 43
Table 6: Data layers utilized by the Web Application and its components. 88
Table 7: Data layers used to inform the Aquaculture Suitability Map. 90

1 Introduction

1.1 Project Description

Paqtnkek Mi'kmaw Nation (PMN) is a First Nations community near Antigonish, NS. The name Paqtnkek, meaning "by the bay", is a distinction emphasizing the importance of the local bay and its resources to the Mi'kmaw people. For this science partnership project, PMN collaborated with the Nova Scotia Community College's (NSCC) Applied Geomatics Research Group (AGRG) to carry out research on sustainable aquaculture development in Pomquet Harbour, NS. The AGRG has been conducting remote sensing research, mapping, and analysis since 2000 and specialize in coastal zone applications. Part of the motivation of this project was the result of a previous project conducted by AGRG for Monique Niles, DFO Science, Gulf Region where an aquaculture suitability map was developed for Little Harbour as well as an interactive website (AGRG, 2018) "Aquaculture Decision Support Tool Demonstration Project. Technical report". A proposal was submitted to the Atlantic Fisheries Fund which is funded by Department of Fisheries and Oceans (DFO) and the Nova Scotia Fisheries and Aquaculture (NSFA) by PMN to build the appropriate layers for a web-based suitability and mapping tool for Pomquet Harbour.

1.2 Background and Study Area

Studies show that there is an abundance of natural shellfish seed (oyster, bay scallops) in the Pomquet Harbour, suggesting that the harbour is an ideal shellfish larvae nursery beyond the current experimental lease. Paqtnkek Mi'kmaw Nation, with the assistance from Ulnooweg Development Group, wishes to apply to NS Fisheries and Aquaculture for oyster aquaculture leases, but requires quantitative information on the biophysical conditions of the harbour to suggest optimal lease locations. PMN began a commercial oyster spat collection business in Pomquet Harbour in 2016, with varying degrees of success. Quantitative biophysical information is required to improve the success of the oyster spat collection industry so that it can be developed into a commercially viable operation with the potential to improve access to seed for the whole province. The biophysical information provided by AGRG will help in site selection and farm management for full oyster production.

Pomquet Harbour is a small, shallow, estuary near Antigonish, NS, connected to the eastern Northumberland Strait by a narrow channel inlet (Figure 1). Monks Head Harbour is located north of the Pomquet Harbour and is connected by a narrow channel. Church Cove and areas around Île à Magotte island are deeper than rest of the harbour.

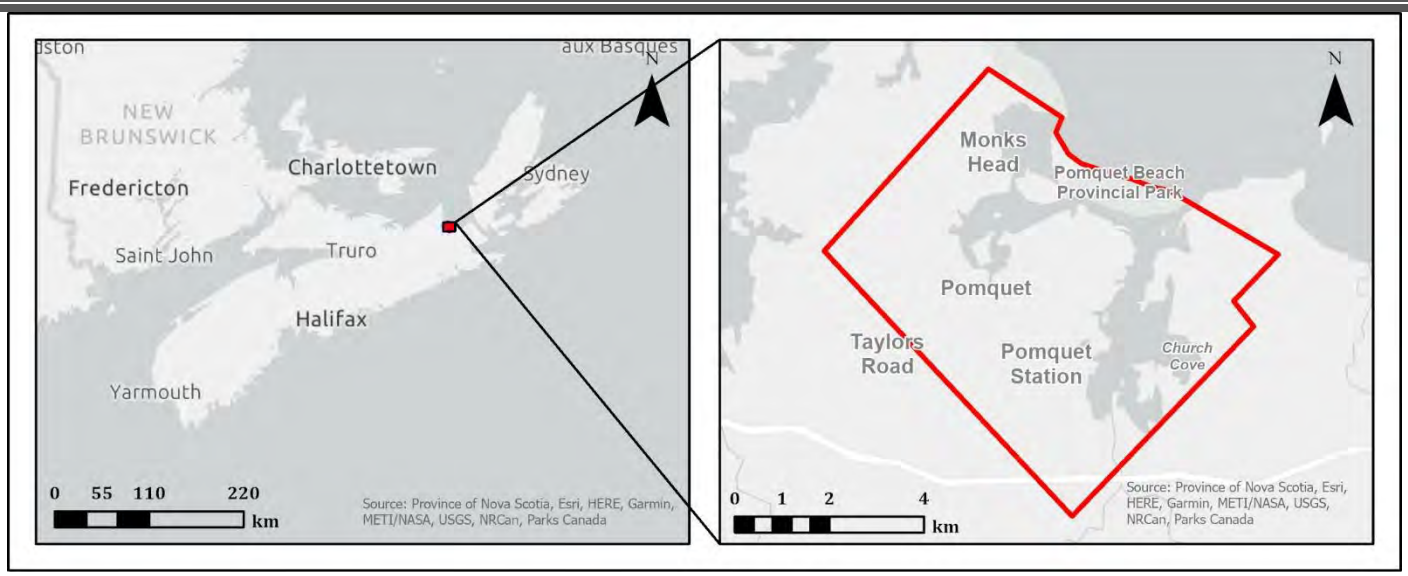

Figure 1: Pomquet Harbour, NS, the study area used for the Bay Management Tool project.

2 Methods

2.1 Lidar Sensor Specifications and Installation

The lidar sensor used in this study was a Chiroptera 4X integrated topo-bathymetric lidar sensor equipped with a 60-megapixel multispectral camera. The system incorporated a 1064 nm near-infrared laser for ground and sea surface returns and a green 515 nm laser for bathymetric returns (Figure 2). The lasers scanned in an elliptical pattern which enabled coverage from many different angles on vertical faces and resulted in fewer shadow effects in the data including those caused by wave interaction. The bathymetric laser was limited by water clarity and has a depth penetration rating of 1.5 x the Secchi depth (a measure of turbidity or water clarity using a black and white disk). The Leica RCD30 camera collected co-aligned RGB+NIR motion-compensated images which could be mosaicked into a single image in post-processing or analyzed frame by frame for maximum information extraction.

AGRG-NSCC does not own an aircraft, only the sensor. AGRG partnered with Leading Edge Geomatics to contract a twin-engine aircraft that was certified to carry the Chiroptera II sensor suite and had a hole suitable to house the sensor head. The lidar sensor was installed in the aircraft in Fredericton, NB. The laser systems and camera were calibrated and aligned with the navigation system which consisted of a survey-grade GPS mounted on the roof of the aircraft and an inertial measurement unit (IMU) mounted above the laser system (Figure 3a).

The system also included a 5-megapixel quality assurance camera that the lidar operator could view during the flight, along with the waveform of the returning green laser pulse and the flight plan (Figure 3b). The aircraft had a hole cut in the bottom for the laser to face the ground and installation involved fitting the sensor head into the hole (Figure 3c). Figure 3d shows the downward-facing portion of the sensor head, including the red (topographic) and green (bathymetric)

lasers, which shoot and return through the large red circles. The lenses on the left and right were the low and high-resolution cameras, respectively.

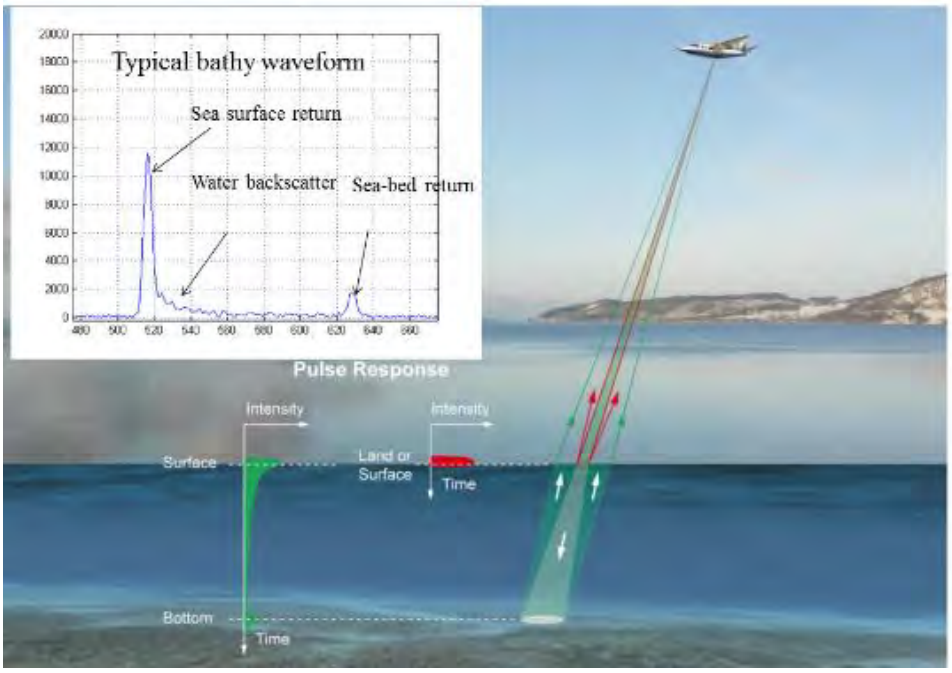

Figure 2: Principals of topo-bathymetric lidar. The system utilizes two lasers, a near-infrared and a green laser to surface the land and marine topography. Inset of green laser waveform.

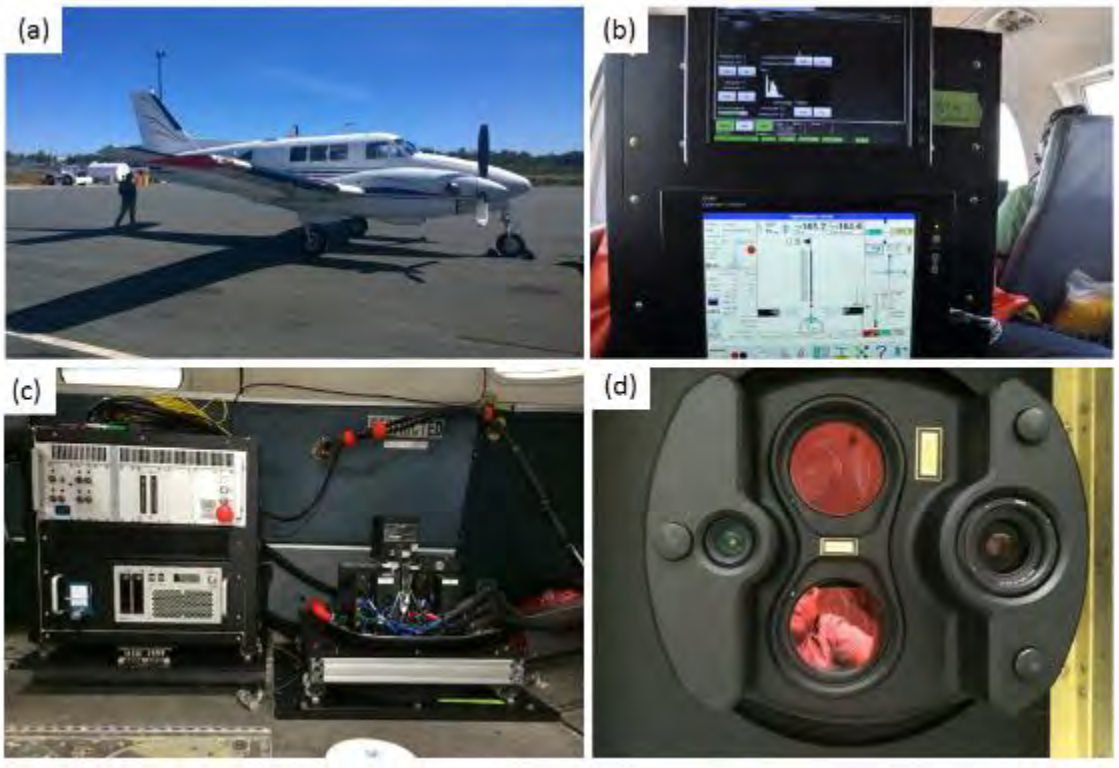

Figure 3: (a): Aircraft used for lidar survey; (b): display seen by lidar operator in-flight; (c): main body of sensor (left) and laser pointing through a hole cut in the bottom of the plane (right); (d): large red circles are the lasers; the RCD30 lens (right) and low-resolution camera (left).

2.2 Lidar Survey Details

The lidar survey was conducted on August 6th, 2018 (Table 1). The surveys were planned using Mission Pro software. The 54 flight lines are shown in Figure 4. The aircraft required ground-based high precision GPS data to be collected during the lidar survey to provide accurate positional data for the aircraft trajectory. The Nova Scotia Active Control Stations (NSACS) network was used to provide geodetic control from the Antigonish station which was used to process the trajectory of the aircraft. The NSACS network was also used to establish base station coordinates for real-time kinematic collection of ground truth data within the study area.

Survey	Lidar System	Survey Date	Survey Time (UTC)	Survey Duration	Number of Flight Lines	Flight Altitude (m)
Afton River and Pomquet Bay Part 1	Topo-Bathymetric	Aug 6	13:15	3 hours 20 mins	32	400
Afton River and Pomquet Bay Part 2	Topo-Bathymetric	Aug 6	17:15	2 hours 40 mins	22	400

Table 1: Summary of lidar surveys, 2018.

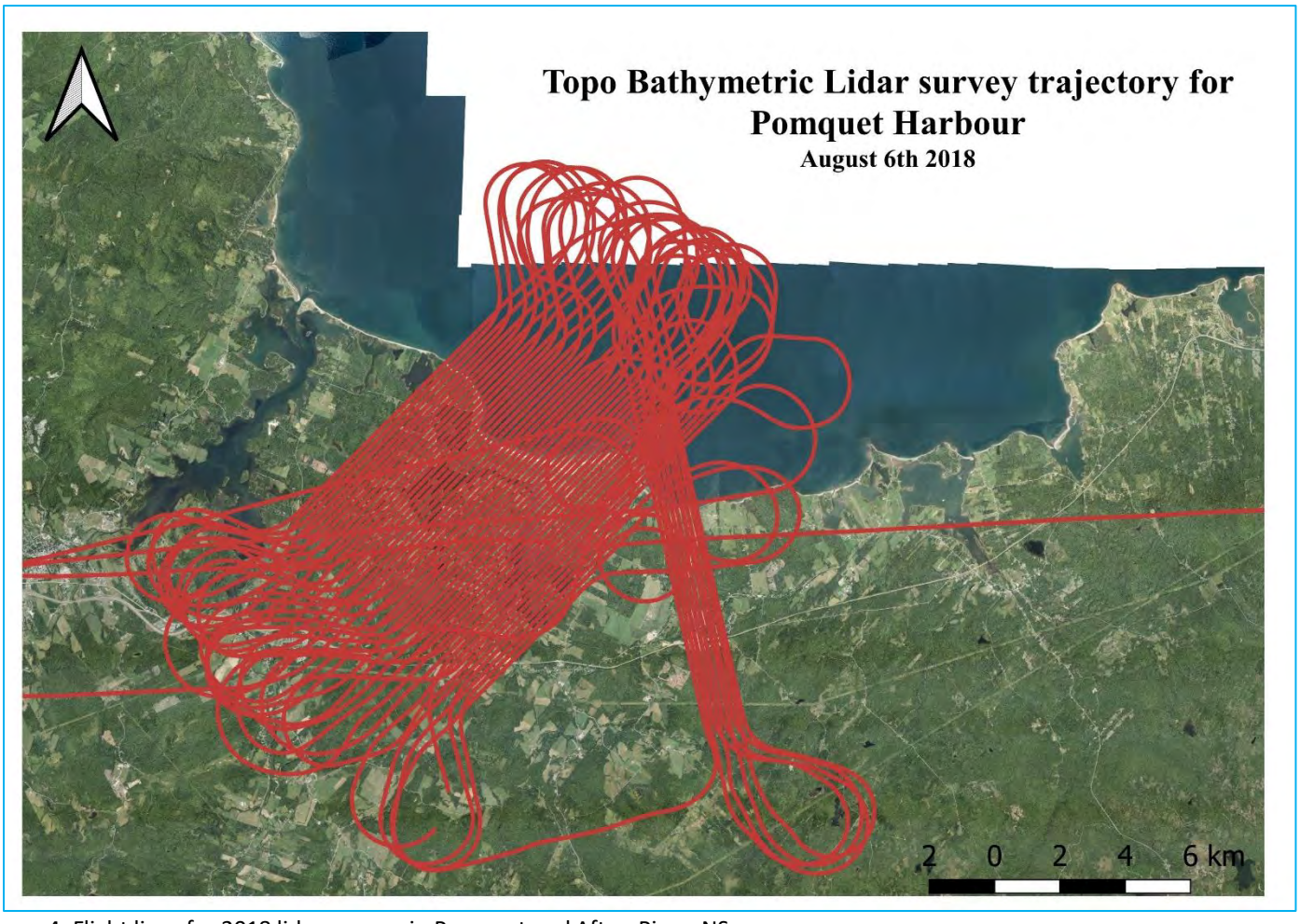

Figure 4: Flight lines for 2018 lidar surveys in Pomquet and Afton River, NS.

2.3 Lidar Data Processing

Aircraft GPS data were differentially corrected using base station observations, and the aircraft trajectory was calculated by linking the corrected GPS data with the aircraft attitude measured by an inertial measurement unit (IMU). Lidar Survey Studio (LSS) was used to process Chiroptera II waveforms, which were georeferenced into discrete points by linking laser returns to the processed aircraft trajectory to produce georeferenced point clouds in the LAS format. The data were inspected to ensure there was sufficient overlap (30%) and the AOI was fully covered by lidar returns.

The LAS files were read into TerraScan™ with the laser returns grouped by laser type so they could be easily separated, analyzed, and further refined. Points were classified into discrete classes based on their physical characteristics including relative geometry and reflective properties (Table 2).

Classification Value	Meaning
1	Unclassified
2	Ground
4	Medium vegetation
7	Low point (noise)
9	Topographic water surface
18	High noise
40	Bathymetric point
41	Bathymetric water surface
42	Derived water surface
80	Bathymetric vegetation

Table 2: Lidar point classification values and descriptions.

The original elevation of the lidar products were referenced to the same datum as the GPS unit they were collected with. This model is a theoretical Earth surface known as the ellipsoid, and elevations referenced to this surface are in ellipsoidal height (GRS80). The elevations were converted to orthometric heights relative to the Canadian Geodetic Vertical Datum of 2013 (CGVD2013).

The classification was further refined in ArcMap 10.8.3 and gridded at 1 m to produce a bare-earth, Digital Elevation Model (DEM), Digital Surface Model (DSM) and an Intensity model.

2.4 Multibeam Survey

2.4.1 Data Collection

A multibeam survey was conducted on Oct 23rd, 2020 in Church Cove where the ADCP (Acoustic Doppler Current Profiler) was deployed in 2018. The main intention for this survey was to fill in the area where the lidar did not penetrate due to the water quality on depth constraints. An R2sonic 2026 multibeam with an integrated Applanix Wavemaster Navigation unit was mounted on the 17' Boston Whaler along with two Global Positioning System (GPS) units to aid the position and heading of the vessel which was used to collect data for 14 survey lines (Figure 5).

Figure 5: AGRG Boston Whaler with deployed multibeam system on an arm that rotates to submerge the echo sounder.

The Whaler was launched from the marina at Bayfield, NS. Real-Time Kinematic (RTK) corrections were not applied during the survey. A single Sound Velocity Profile (SVP) was performed during the survey as the duration of the survey was only an hour. Data from the SVP was applied to the sonar pings in post-processing. The location of the SVP drop along with the multibeam survey lines is shown in Figure 6. The SVP exhibited a prominent thermocline (or halocline) at 1.5 – 2 m depth from the surface (Figure 7).

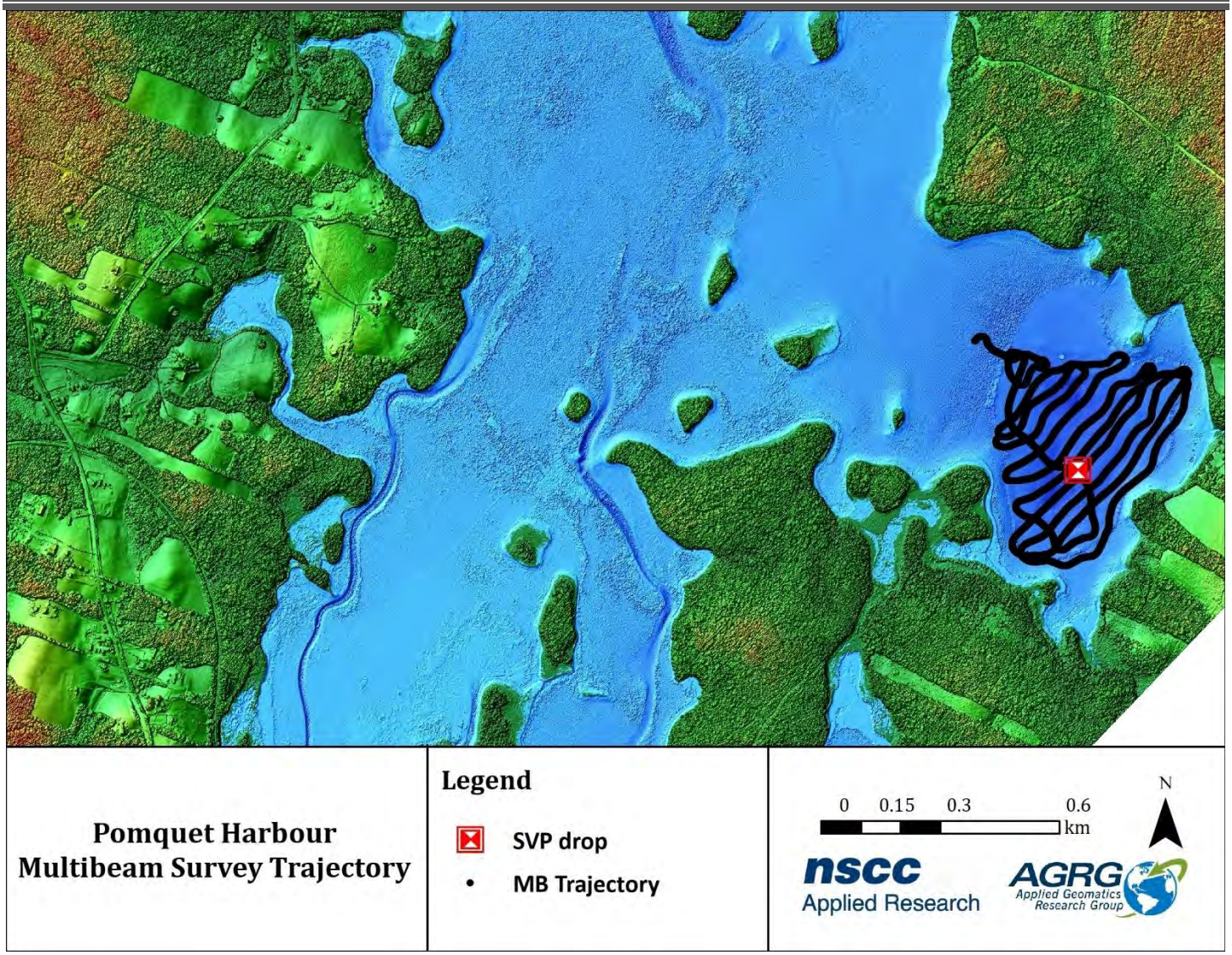

Figure 6: Pomquet lidar seamless Digital Surface Model with 2020 multibeam survey trajectory (dark points), and SVP drop location.

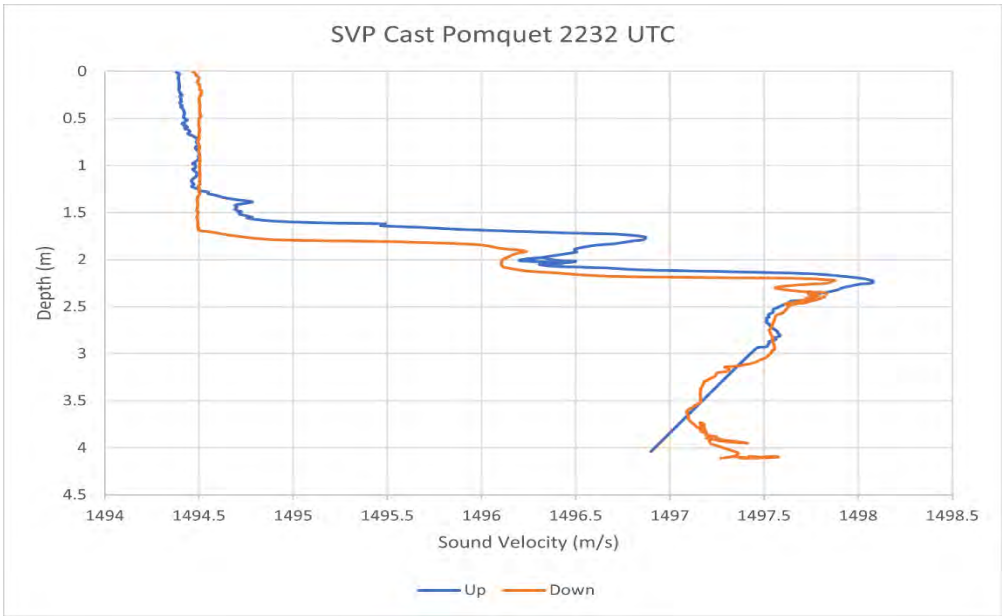

Figure 7: Sound Velocity Profile taken in Pomquet Harbour on October 23rd, 2020.

2.4.2 Data Processing

Multibeam data were processed using Qimera 2.1.1 software. Raw sonar files were cleaned using various filters for noise removal. Trajectory from the GPS and motion unit was post-processed in POSPac *MMS* with the active control station in Antigonish as the base station, resulting in a Smoothed Best Estimate of Trajectory (SBET) file that was applied to the sonar points. The post-processed sonar points were exported as LAS files. These files were gridded in ArcMap using the LAS dataset tools to obtain a raster. This raster was merged with the lidar data to obtain a continuous and complete raster.

2.5 Ground Truthing

2.5.1 GPS points

A total of 1,410 GPS points were collected on July 27th, 2018 to validate the lidar data, as shown in Figure 8. Out of these, 1,399 points were collected on hard surfaces using a Leica GS14 GPS receiver unit obtaining Real-Time Kinematic (RTK) corrections through SmartNet, which was mounted on a truck collecting data every second. 11 points were collected in the harbour using the GPS receiver threaded on a painter's pole. Other areas in the Harbour where the lidar did not penetrate to the seabed were supplemented with point soundings of nautical charts. These points were post-processed in Leica Geo Office with Antigonish as the base station to provide centimetre level precision.

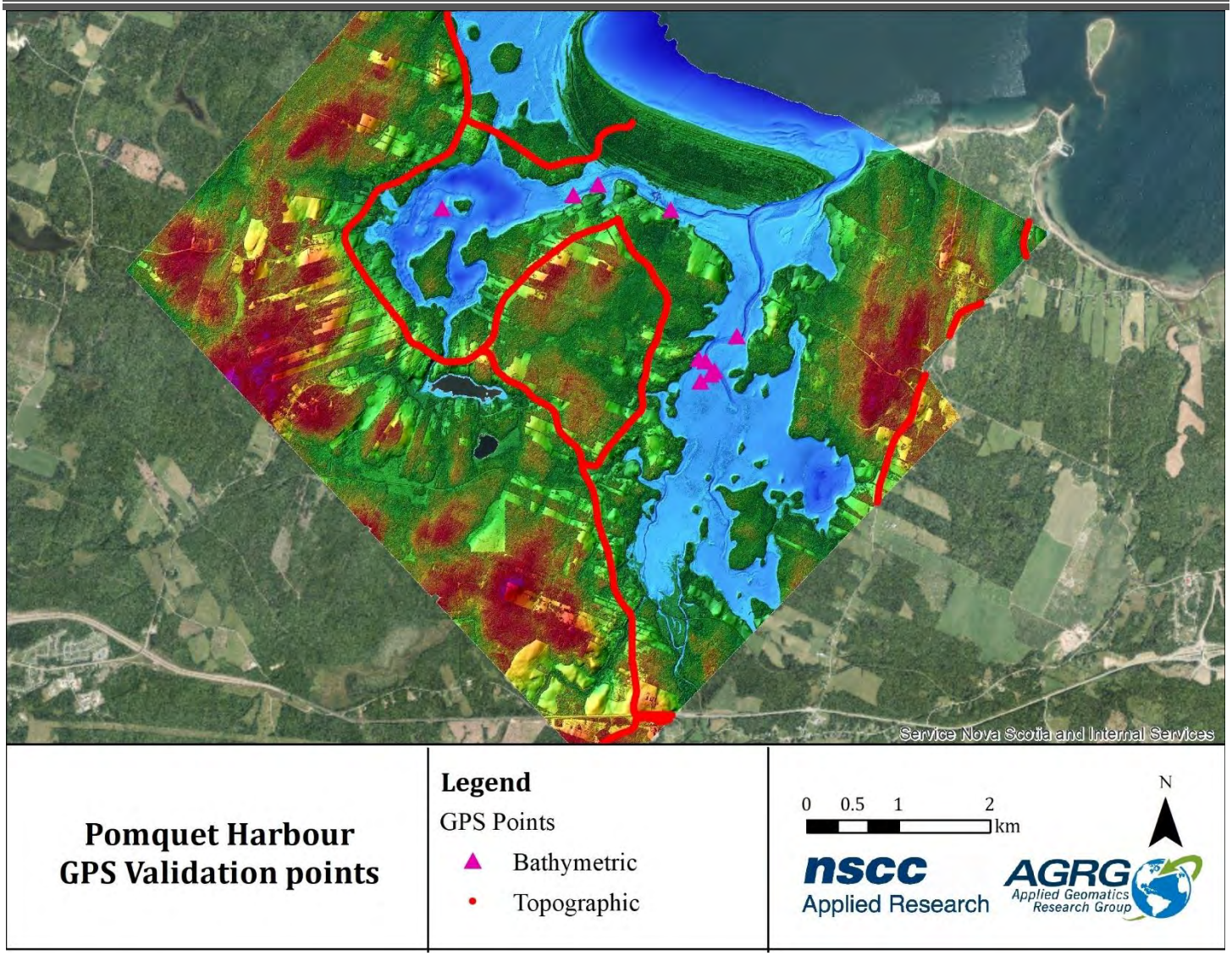

Figure 8: Global Positioning System (GPS) points for validating the topo-bathymetric lidar overlaid on a Colour Shaded Relief (CSR) lidar Digital Surface Model (DSM).

2.5.2 Video Ray

Underwater videos were collected on July 27th, 2018 using Video Ray Class I Remotely Operated Vehicle (ROV). The system consisted of the ROV, plus a control tether and reel, and was controlled by a deck box which included a laptop with preloaded control software and a joystick (Figure 9). The Video Ray was borrowed from NSCC's Oceans Technology program at the Ivany Campus, while the control unit was originally from Defence Research and Development Canada Atlantic, both of which are in Dartmouth, NS.

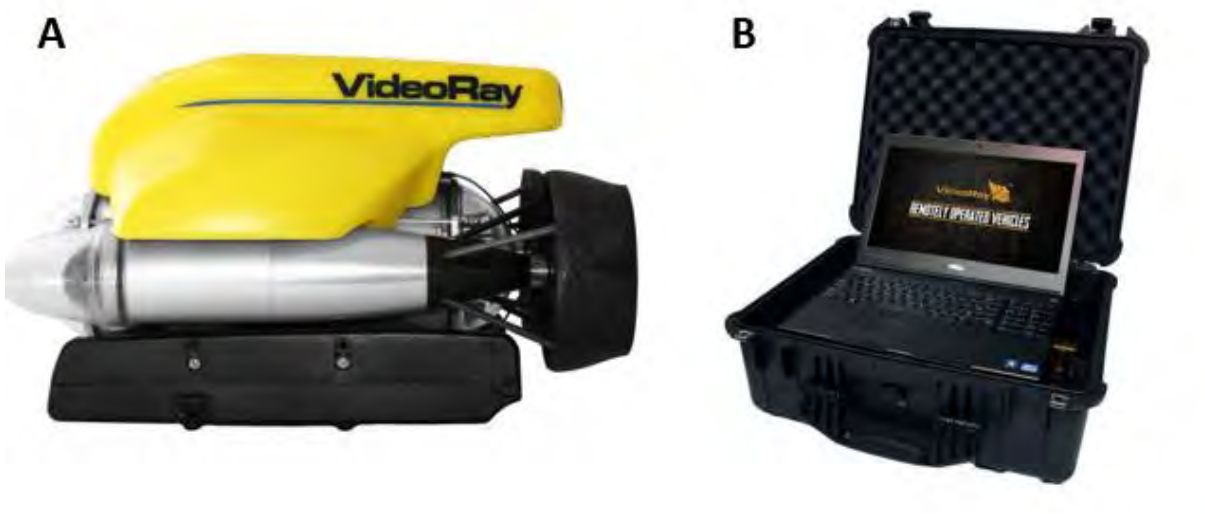

Figure 9: (A) The left side of the figure shows a Video Ray ROV; (B) The right side shows a Video Ray control unit.

The Video Ray had an integrated camera in the forward plexiglass bubble with pan and tilt capability. The piloting screen in the control unit displayed the camera view with heading, depth, and water temperature information overlaid on the video feed from the ROV. The control unit was used to take video using the Video Ray's camera.

The video ray was towed alongside AGRG's Boston Whaler with a 10 m tether which communicated the data to the control unit. A GPS receiver was mounted on the vessel to collect positions. The track from the GPS unit along with the Garmin (Boat GPS) is shown in Figure 10.

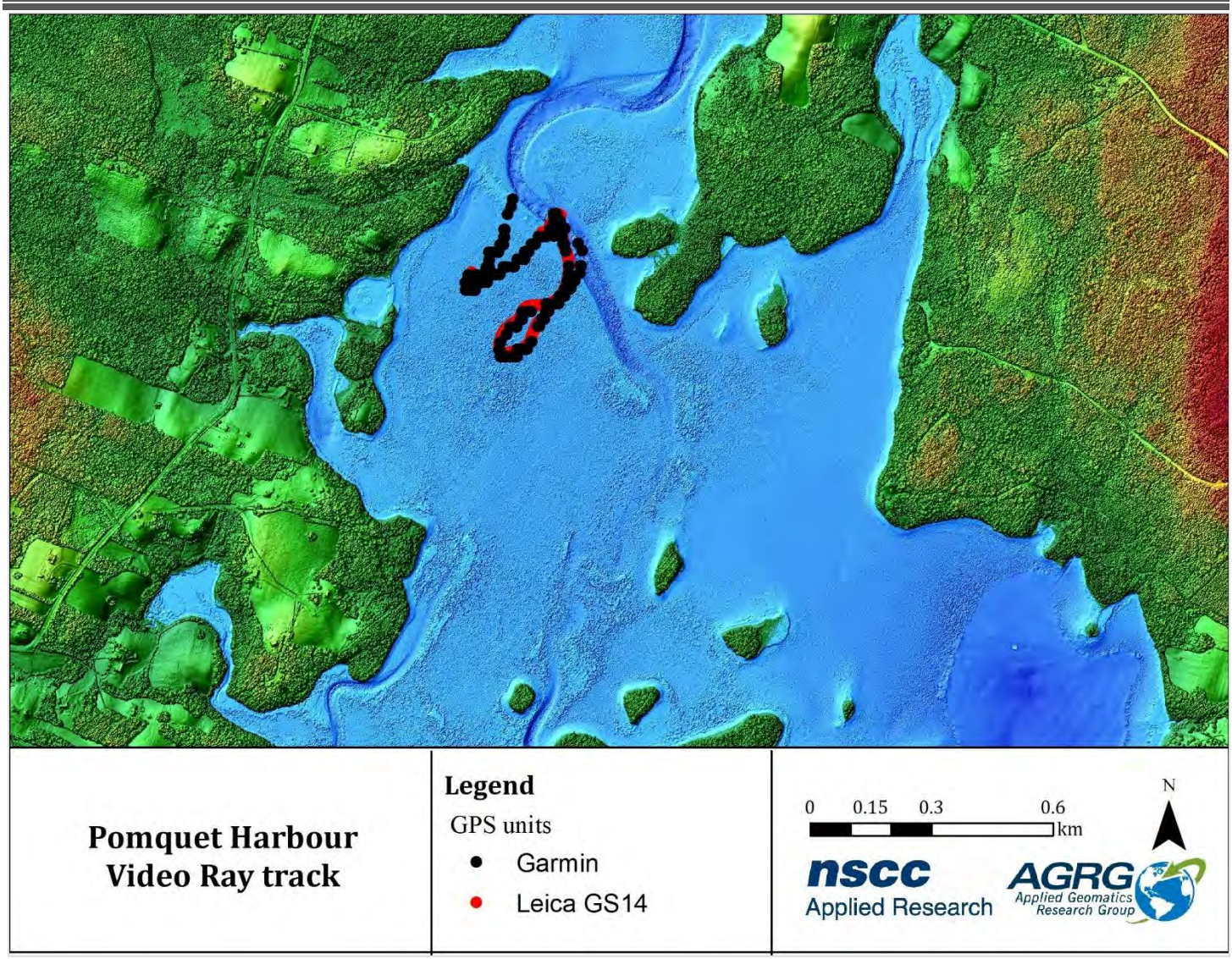

Figure 10: Video ray track obtained from the GPS units Garmin (autonomous >5 m accuracy) and Leica GS 14 (RTK corrections < 0.05 m accuracy) overlaid on a CSR.

The video obtained from the system showed that one area was dominated by moss and algae, while the other contained areas of fucus interspersed with bare rocky patches. The rocky areas (and probably the areas of subaquatic vegetation as well) were strewn with oyster shells, presumably the leftovers from harvesting operations. The various types of bottom coverage in the video ray survey site by matching the timestamp with the GPS points (Figure 11).

A

7/27/2018 11:47:01 AM
H: 214.8 °
D: 0.71 m
Temp: 23.0 °C

B

7/27/2018 11:48:14 AM
H: 299.2 °
D: 0.21 m
Temp: 23.1 °C

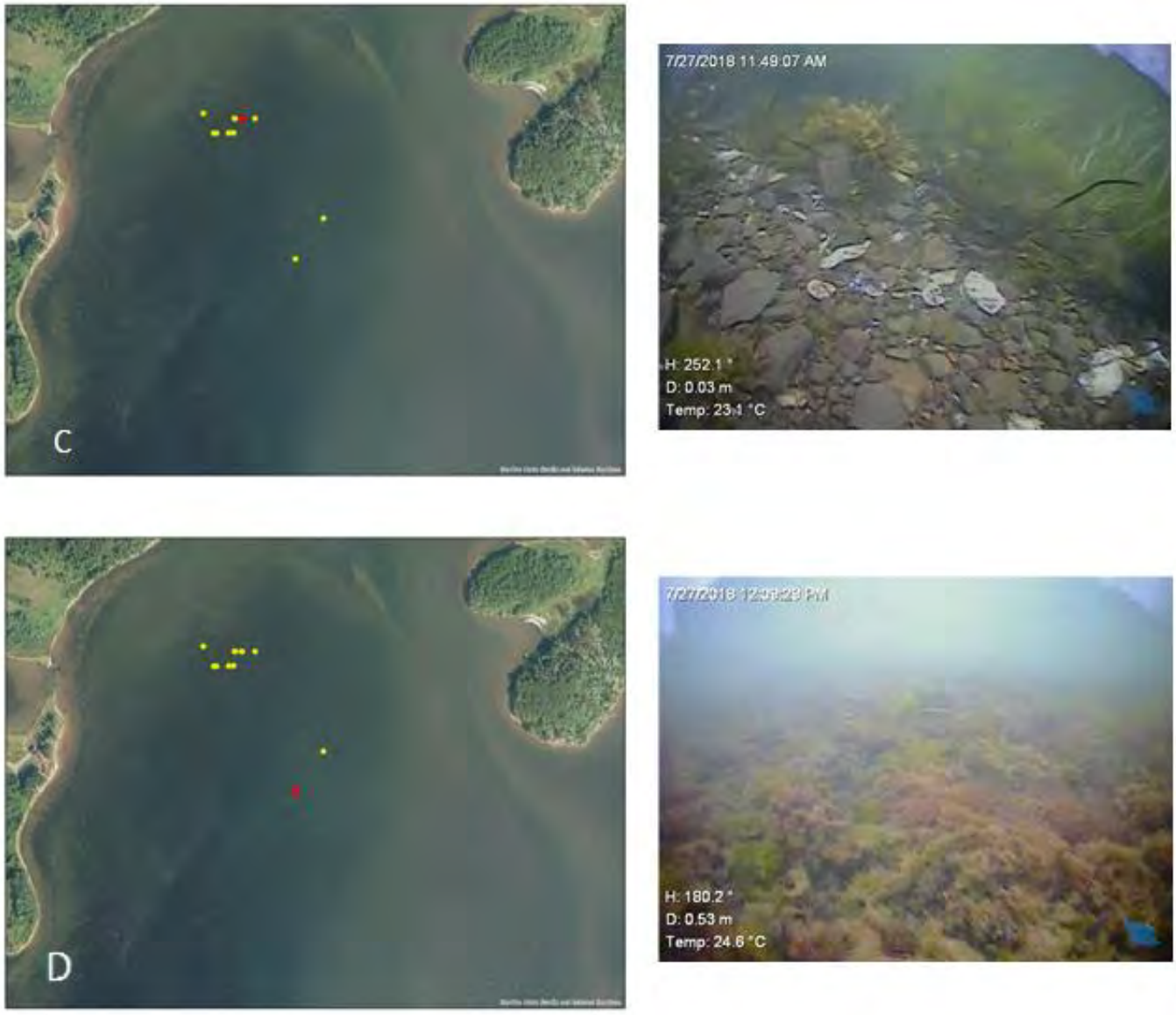

Figure 11: The right side of the figure shows screen shots from video taken using a Video Ray ROV, with the location of the video shown marked on the orthophoto to the left. The video frames were matched using time stamps from the video correlated with time stamps from the Leica GNSS log. The site at location (a) shows the bottom type as focus. The dark patch at location (b) is Sand(60)/Moss (30)/Fucus(10) along with oyster shells. Location (c) shows the presence of rock and eelgrass. Location (d) shows moss and algae in deeper water farther from shore than the previous three locations.

2.5.3 Acoustic Doppler Current Profiler (ADCP)

An ADCP measures water current velocities within the water column and waves. This is achieved through the Doppler effect of sound waves passing through a medium. The ADCP deployed in Church Cove was a Teledyne Sentinel V20 which had 5 transducers, a pressure and temperature sensors. Velocity was calibrated prior to deployment.

2.5.3.1 Deployment

The Sentinel V20 was deployed in Church Cove in Pomquet Harbour on June 7th, 2018 and recovered on the July 10th, 2018. The unit sat on the bottom of the harbour in the same location at an average depth of ~4.7 metres, recording data over

the course of 29 days, from 1800 UTC on the day it was deployed until 1900 UTC on the 4th of July 2018. The geographic location of the deployment site can be seen in Figure 12a.

The ADCP was mounted on a metal frame as shown in Figure 12b. Additional weights were added to the frame, and a 70-pound (lb) pyramid anchor was attached to the frame using a line sized to deployment depth (in this case ~ 5 m). A marker buoy was attached to the pyramid anchor to assist in recovering the instrument at the end of its deployment. Two zinc anodes were also attached to the frame to reduce galvanic corrosion.

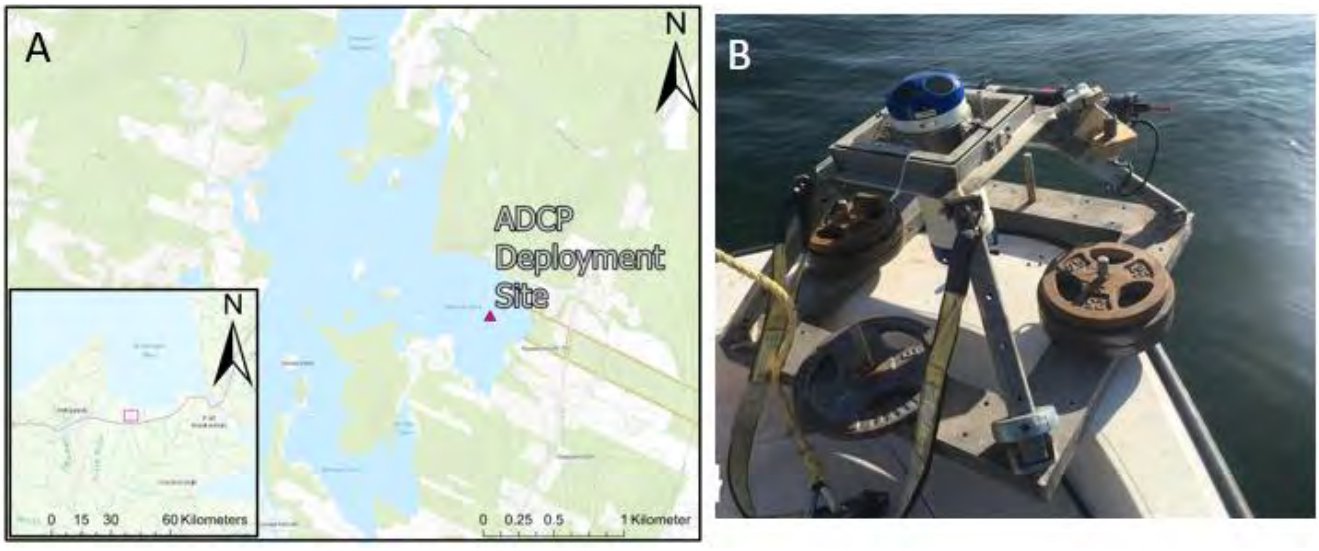

Figure 12: (a) ADCP deployment location in Pomquet Harbour; (b) Sentinel V20 on a frame being deployed from Boston Whaler.

2.5.3.2 Data Collection

The system was setup to collect tidal current data in 3 bursts of 3 minutes each in every hour on the clock, with 15 minutes between the start of each burst, and the first burst of each ensemble taking place 20 minutes past the hour as shown in Table 3. The waves profile collected one burst for 17.7 minutes on the hour every hour.

Waves Setup (Profile 1)	
Ensemble interval	3600 s
Ping interval	0.5 s
Number of pings	2100
Number of bursts	1
Sampling interval (ping interval x number of pings)/60 s	17.5 minutes
Cell size	0.3 m
Currents Setup (Profile 2)	
Ensemble interval	3600 s (1 hour)
Ping interval	1 s
Number of pings	180
Sampling interval (ping interval x number of pings)/60 s	3
Cell size	0.3
Depth of deployment	7.8 m (range)
Sequential offset	1200 s (20 mins)
Burst interval	900 s (15 mins)
Burst count	3

Table 3: Wave and Currents Setup for the Sentinel V20 for the Pomquet deployment.

The resultant data represents waves every hour and currents three times an hour at the 15-, 30- and 45-minute mark. Data were retrieved at the end of the deployment time to be processed in Velocity, developed by Teledyne, the manufacturers of the Sentinel V series of ADCP.

2.5.3.3 Data Processing

Currents

Processing for currents was done in Teledyne's Velocity software. The most basic processing settings that need to be taken into consideration before conducting any kind of analysis are displayed in Figure 13.

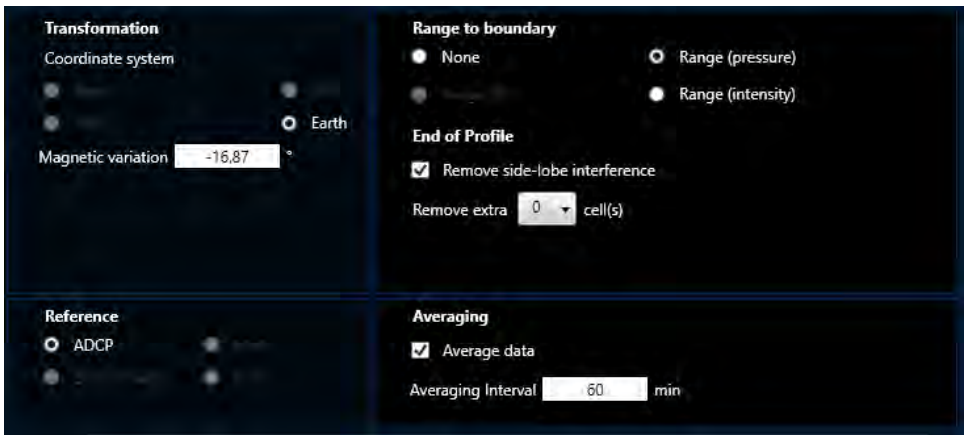

Figure 13: Sample "Basic" post-processing setting window.

Much of post-processing involved cleaning up the data, reducing interference, and ensuring that the information extracted was as accurate as possible. An averaging interval of 1 hour for the currents data was used as it best filled out the data without losing too much detail to be useful. The next step of currents processing was to remove *side lobe interference*, which removed the interference caused by currents near the measurement cells. *Range to boundary* typically remains set

to *Range (pressure)*, meaning the pressure transducer on the unit was used to determine the range to the water column boundary. Next, the *magnetic variation offset was supplied*. This step was necessary to correct the data to get the most correct representations of the vector components of the measured currents. As most compasses do, the one on board the Sentinel V20 detects its orientation by finding *magnetic north*. True north and magnetic north vary by latitude, longitude, and over time. Using the *Magnetic declination calculator* web tool found on *Natural Resources Canada*'s website, we determined this offset to input into Velocity.

Waves

Data were processed using Velocity 1.7.22 WavesMon 4.05 (a package within the Velocity software). A profile averaging an interval of 15 minutes was set to match the average current profile. As the ADCP sat in a frame above the seabed, the measurement in metres from the bottom to the sensor (60 cm) was added in the initial stages of the processing. The measurement was useful for applying the correct gain in the lower bins. In the more advanced options, a magnetic variation of -16.87 degrees was applied to calculate the direction information with respect to true north as shown in Figure 14. As the waves data were set up to be collected every hour for 17.5 minutes on the hour, the samples/bursts processed along with the frequency were adjusted to process all the data. Only the top three cells, which were 0.9 m from the water surface, were considered for height of the wave and direction spectrum.

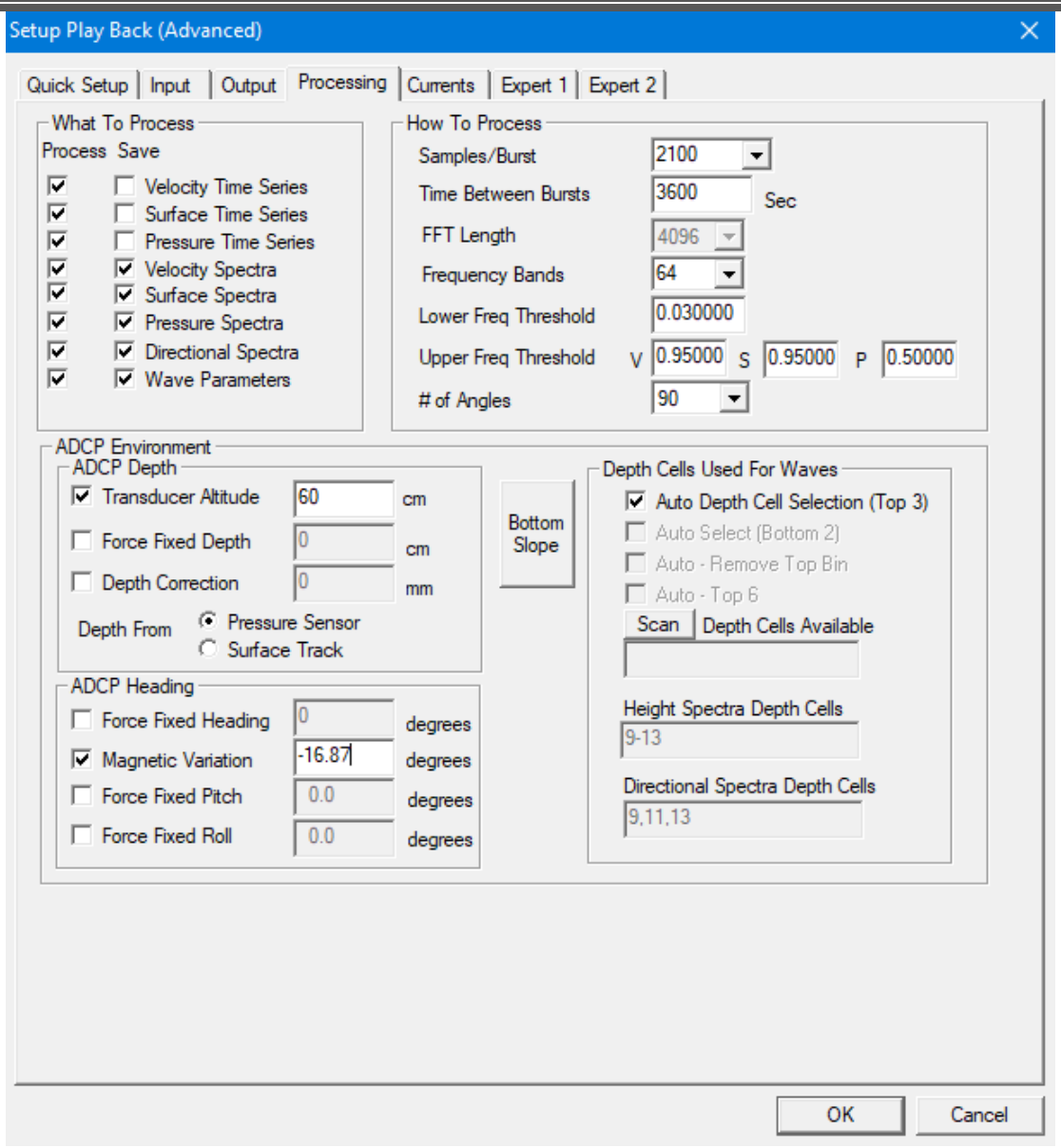

Figure 14: Parameters set up in the processing tab of WavesMon.

In the more advanced settings for the WavesMon package, expert 1 and 2 tabs were set such that data was processed with a sample rate at 2 Hz between ensembles. It was also set up so that all the time series for the duration was processed and flagged for bad data that exceeded four times the standard deviation. Only bursts with good data more than a threshold of 90% were processed, along with auto bias removal, and the negative values in the spectra were set up to be clipped.

2.5.3.4 Data Overview

Currents

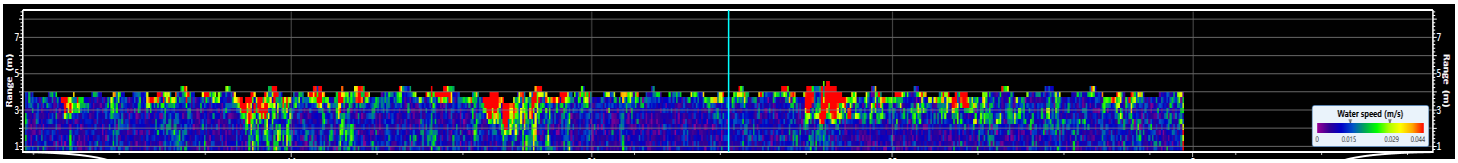

Figure 15: Water binned current speed (m/s). X-axis represents time and consists of approximately 30 days.

Within the protection of the sheltered Church Cove in Pomquet Harbour, the waters were typically calm and lacking dramatic changes in speed. Most of the water moved at 0.015 m/s or lower most days, as Figure 15 illustrates. We can also see that days with noticeable increase of water speed near the water's surface coincide with increases in wind speed in the hours prior (Figure 16). This increased water speed near the surface brings water up from the bottom of the water column. This can be seen especially on June 12th, June 18th, and June 25th. Red indicated the increase in water velocity/speed, and roughly one day later a dramatic spike in upward component of the currents can be seen in Figure 17, Figure 18 and Figure 19. An increase at the surface of the water also trickled down to the bins beneath it, over a period of hours, slowing as it reached the bottom. Figure 20 shows the effect of the tidal cycle on water flow in the harbour. The water current direction changed through the water column in a predictable way, with exception of the outliers previously mentioned. The current flow in a particular direction rose through the column over a period of roughly 6 hours, which is the amount of time it takes to go from a high tide to a low tide and vice versa.

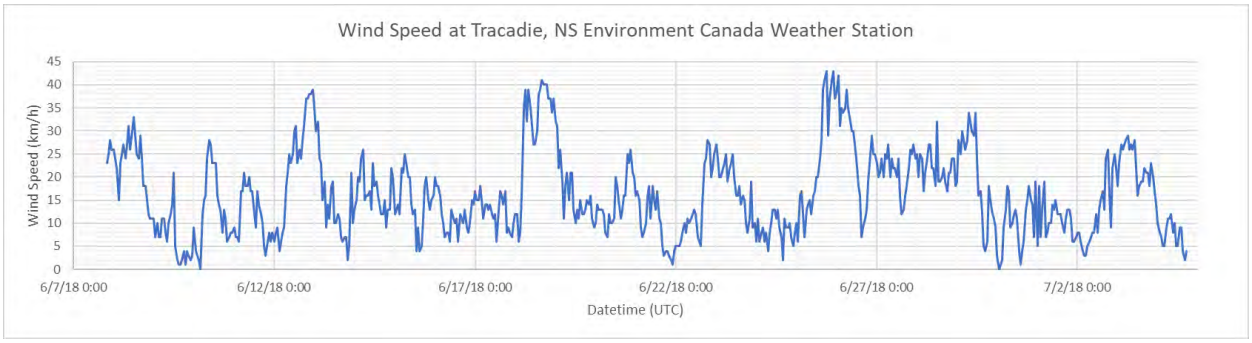

Figure 16: Wind speed at nearby Tracadie weather station.

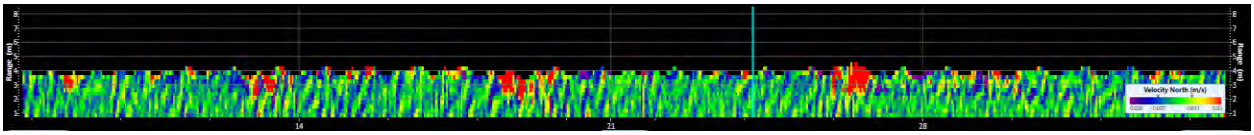

Figure 17: Binned Water Velocity, Northern Component.

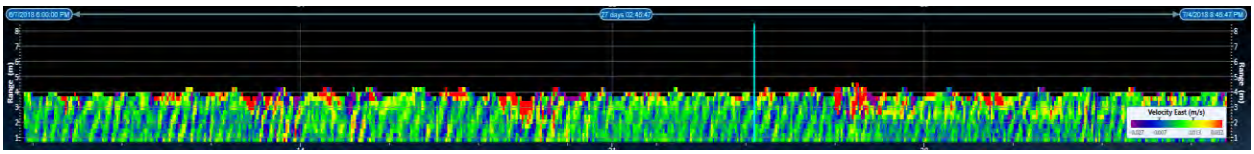

Figure 18: Binned Water Velocity, Eastern Component.

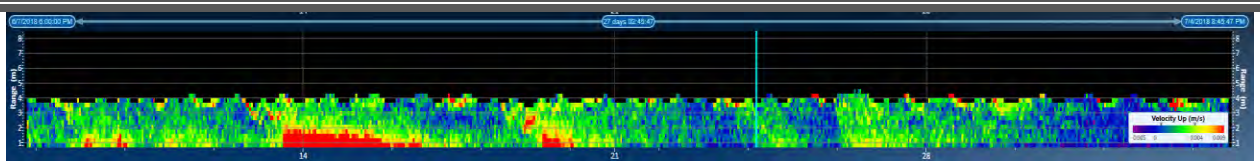

Figure 19: Binned Water Velocity, 'Up' Component.

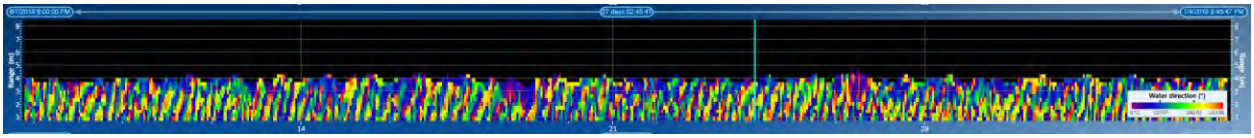

Figure 20: Binned Water Direction, corrected for true north. The repeating pattern represents the daily tidal cycles.

Waves

Data from WavesMon was exported in two formats: A Waves Log file containing the summary of the wave parameters, and a Waves record file to visualize the data in WaveView. A time series plot with Significant Wave height (Hs), Peak Period (Tp) along with the Water Level (WL) is shown in Figure 21.

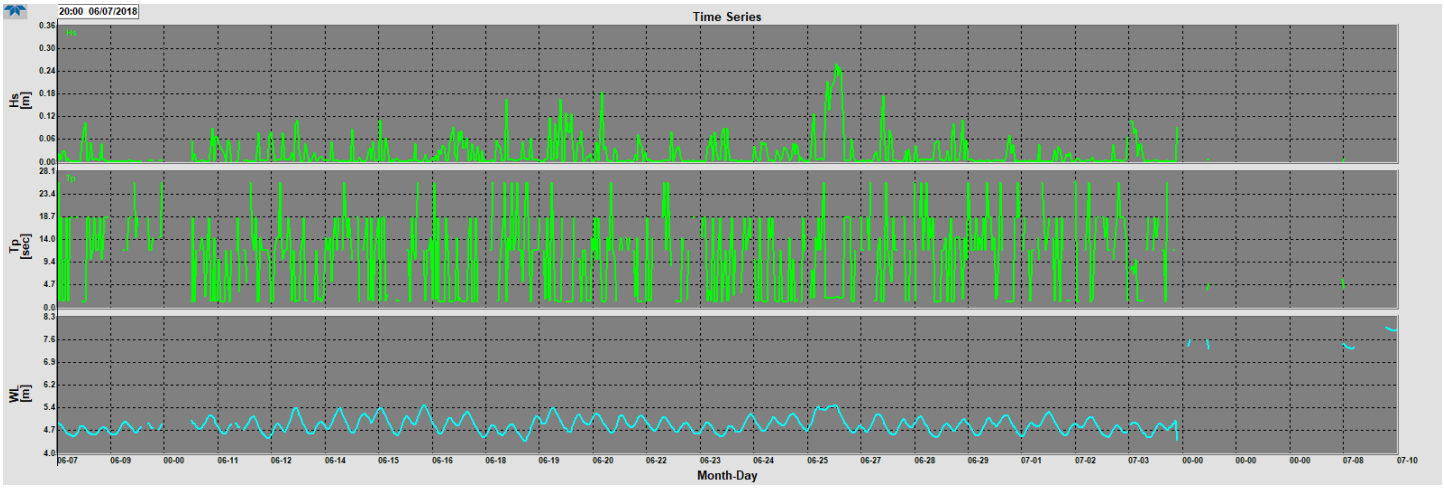

Figure 21: A plot showing the Hs (top graph), Tp (middle graph) and WL (bottom graph) during the ADCP deployment time frame.

Hs in the harbour was close to 10 cm with an average peak period of 1 second. An exception to this was during the major wind event that happened on June 26th, 2018, when it was 26 cm with the peak period of 1.86 seconds. The plot of wind data from Tracadie station and wave height shows that strong winds blowing in the south direction resulted in an increase in Hs on the 26th of June, 2018 (Figure 22).

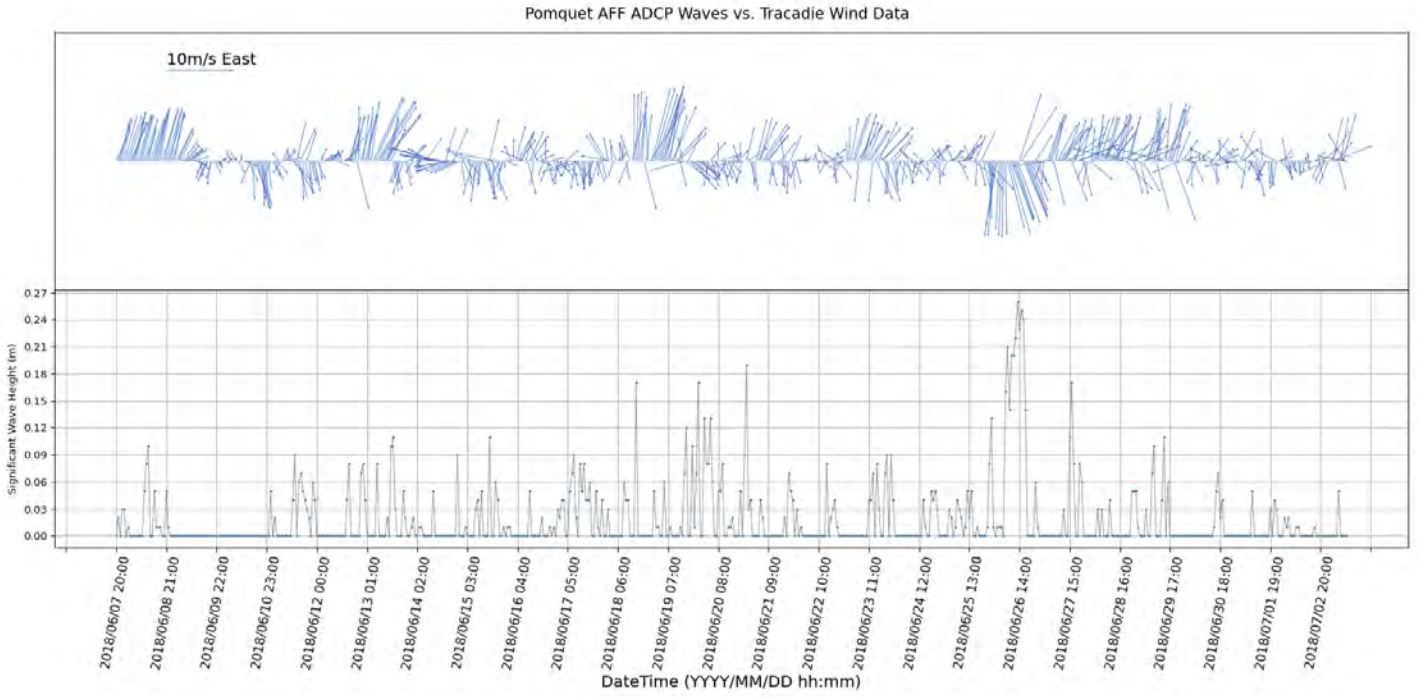

Figure 22: Wind data from the Tracadie station (top graph) plotted with the ADCP Significant Wave Height (Hs) (bottom graph) in metres.

The direction reported for wind and waves indicate where the wind was blowing from. For example, waves travelling to the west, as shown in Figure 23. The wave height spectra and directional spectrum plots exhibit the wave frequency and direction during the June 26th, 2018 event (Figure 23).

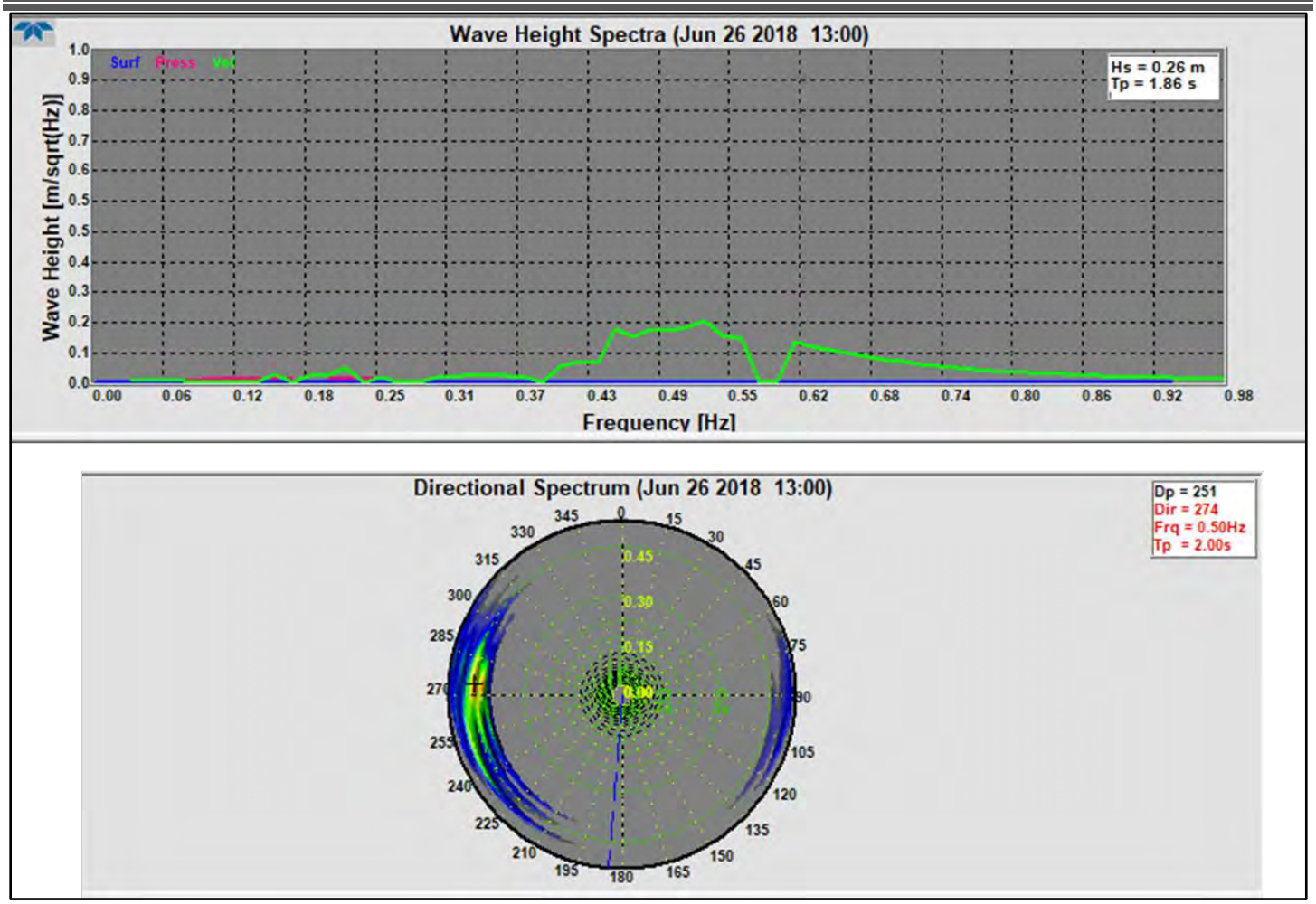

Figure 23: Wave Height Spectra and Directional Spectrum on June 26th, 2018 at 13:00. Top graph shows the significant wave height (Hs). Bottom graph is a rose diagram showing where the direction the waves are coming from and their period.

During the event on June 26th, there were high frequency waves. The dotted blue line is the average direction during the deployment period. Peak Direction (Dp) during the event was 251 degrees (waves are from the west travelling to the east).

2.6 GIS Datasets

2.6.1 Traditional Ecological Knowledge (TEK)

The Department of Fisheries and Oceans provided Traditional Ecological Knowledge (TEK) polygon data representing the habitat of several migratory fish species (alewife, American Eel, American smelt, Atlantic salmon, sea trout), molluscs (American oyster, blue mussel, quahog, razor clam, softshell clam) and invasive species (green crab). These layers were clipped to the Pomquet Harbour study area (Figure 24; Figure 25; Figure 26). The mollusc data layers were converted from polygons to binary presence/absence rasters for use in the web application's Suitability Modeller widget.

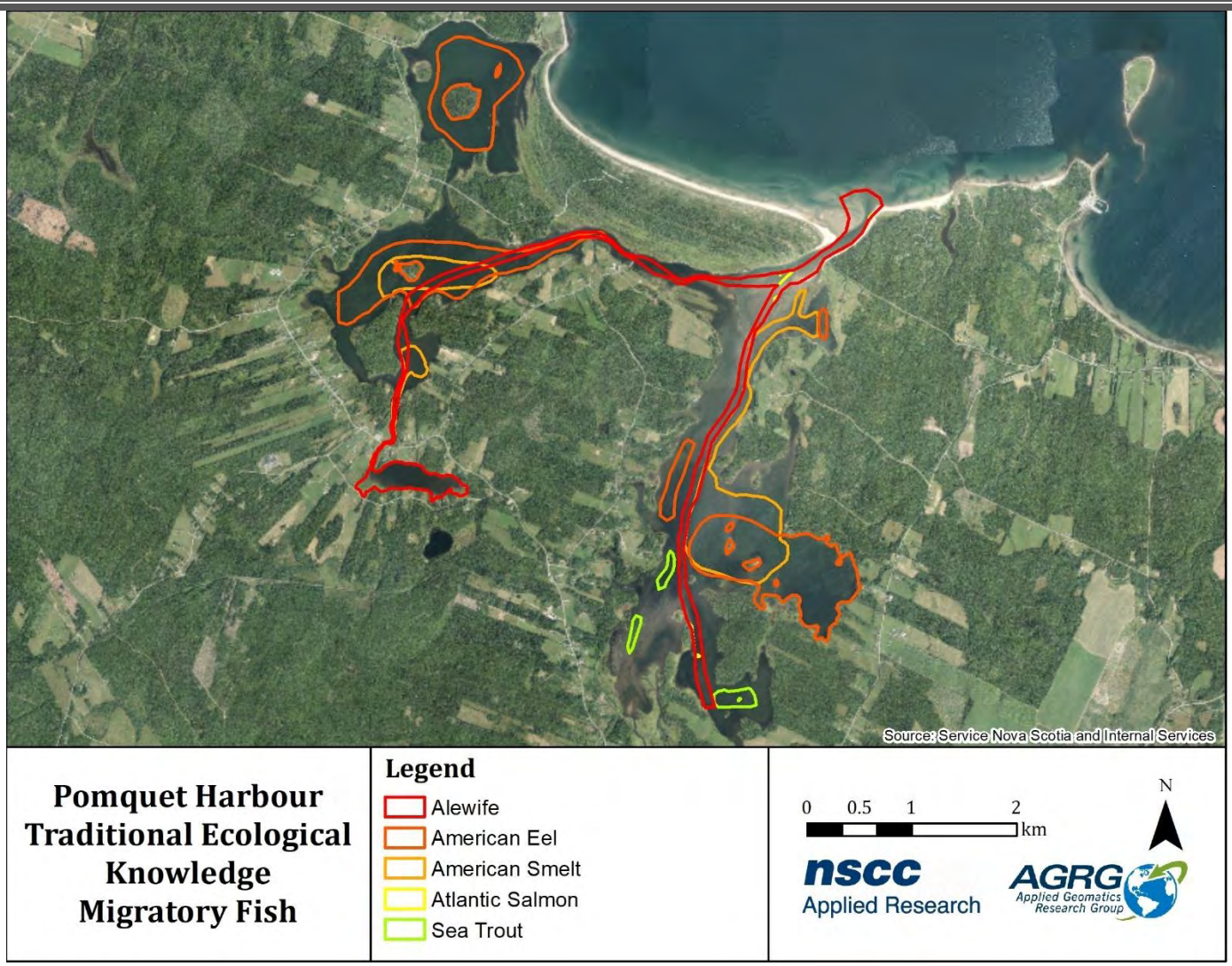

Figure 24: Migratory fish presence identified from Traditional Ecological Knowledge.

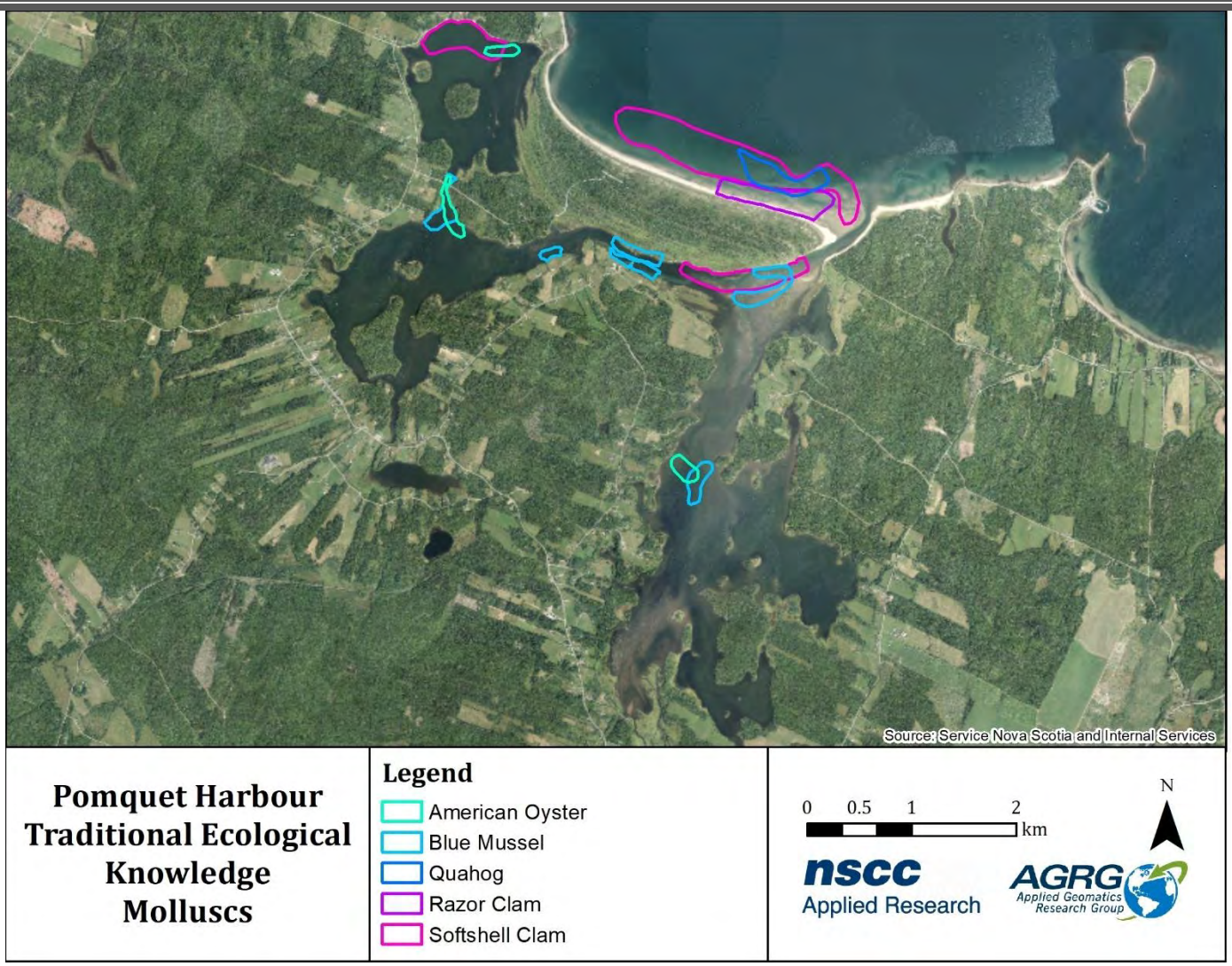

Figure 25: Mollusc presence identified from Traditional Ecological Knowledge.

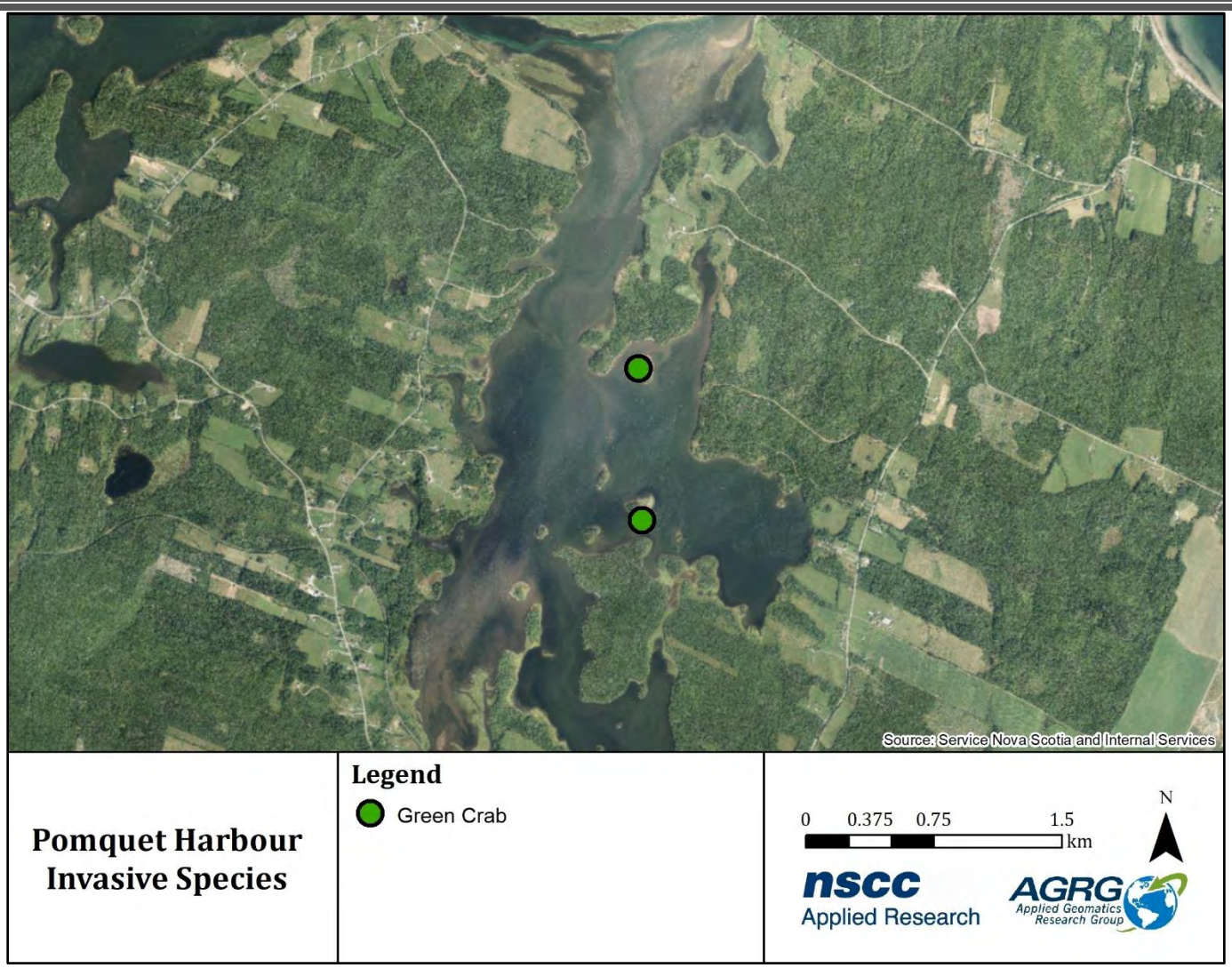

Figure 26: Invasive species presence as reported by the Department of Fisheries and Oceans (DFO).

American eels had the largest habitat extent of the migratory fish species present in Pomquet Harbour, with an area of 2.40 km^2. American smelt and alewife also had significant habitat extents, with areas of 1.42 km^2 and 0.98 km^2, respectively. The mollusc species with the largest habitat extent in Pomquet Harbour was the softshell clam (1.09 km^2). Green crabs were identified in two locations in Pomquet Harbour. Both observations were made in 2001 and were in the eastern bay.

2.6.2 Oyster Stock Survey Data

Secondary data for oyster stock surveys conducted at Pomquet Harbour in 2014 were obtained from Robin Stuart on behalf of Paqtnkek First Nation and in agreement with DFO (Stuart, 2014). The location of each of the 29 oyster surveys was used to generate the Wild Oyster Location layer (Figure 27). The Wild Oyster Spat Producer layer was extracted from the nine oyster survey sites identified as having a good oyster habitat (Figure 28).

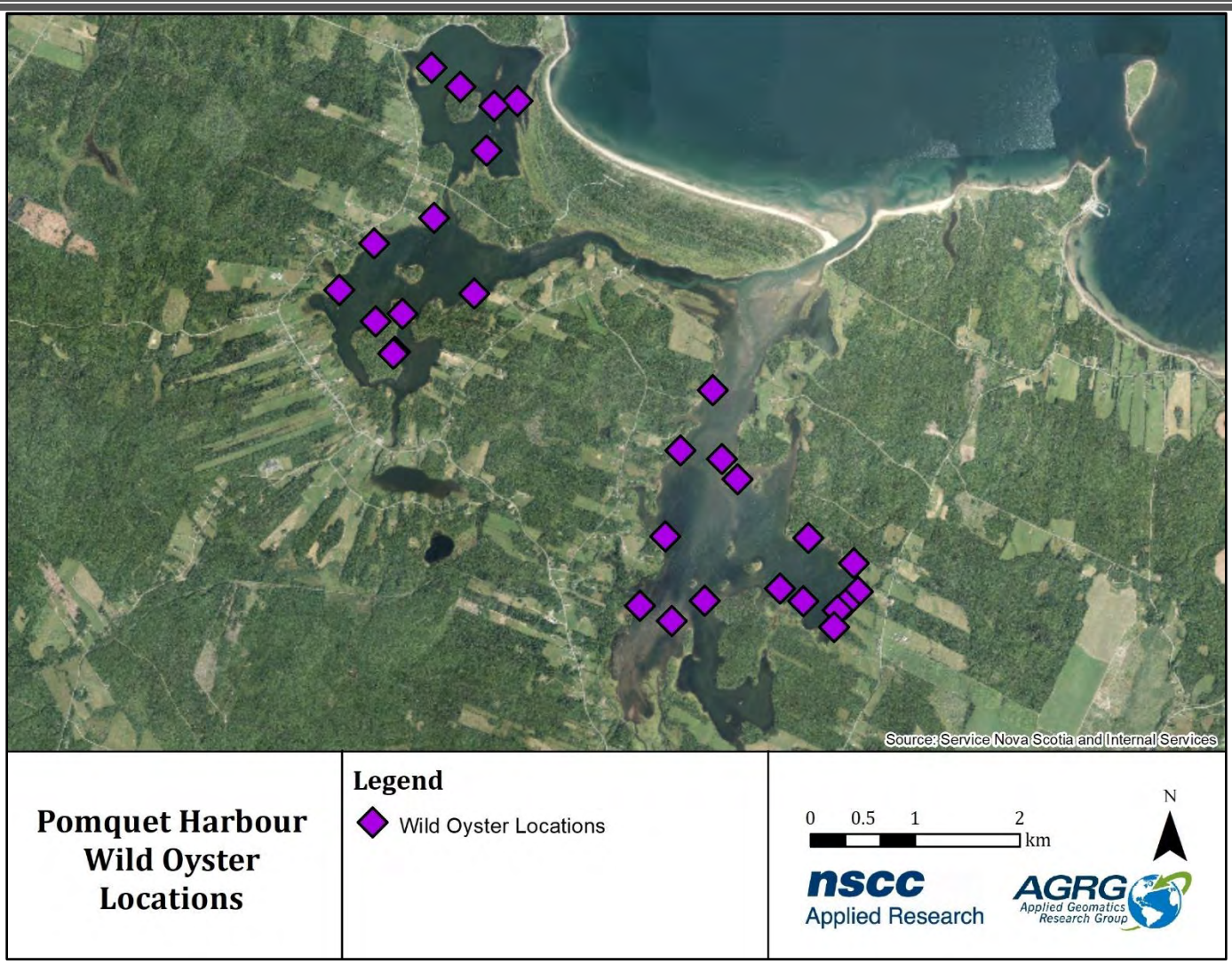

Figure 27: Location of oyster stock surveys conducted by Robin Stuart on behalf of Paqtnkek First Nation.

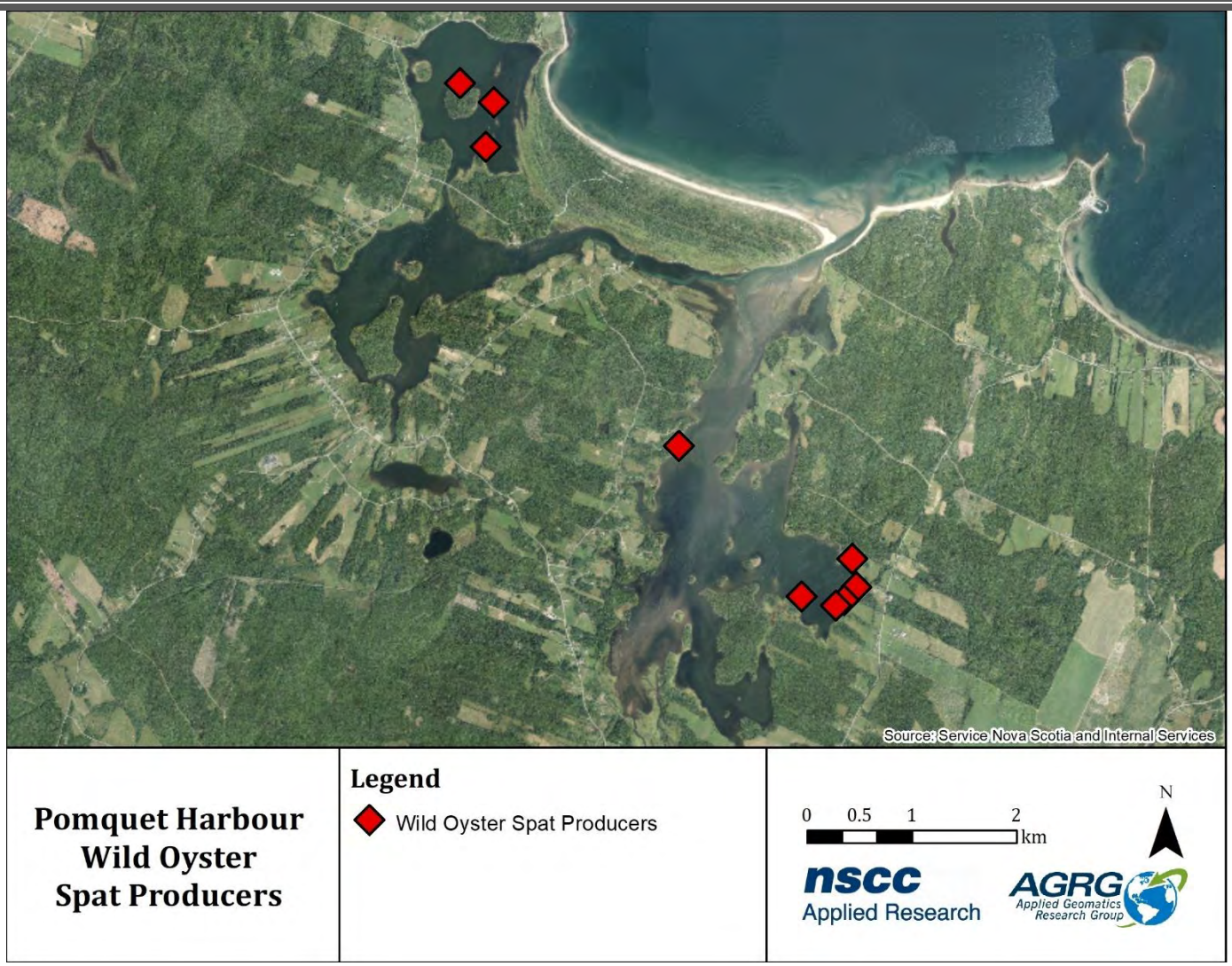

Figure 28: Location of oyster survey stations with significant oyster habitat as identified by Robin Stuart on behalf of Paqtnkek First Nation.

The Number of Oysters Times Average Size layer was generated by multiplying the total number of reported oysters by the mean size at each oyster sampling station (Figure 29). The oyster survey stations with the highest Number of Oysters Times Average Size (mm) were station 13 and station 21, with 27,696 mm and 17,399 mm, respectively. Station 13 was located near the western bay, and station 21 was in Monks Head Harbour.

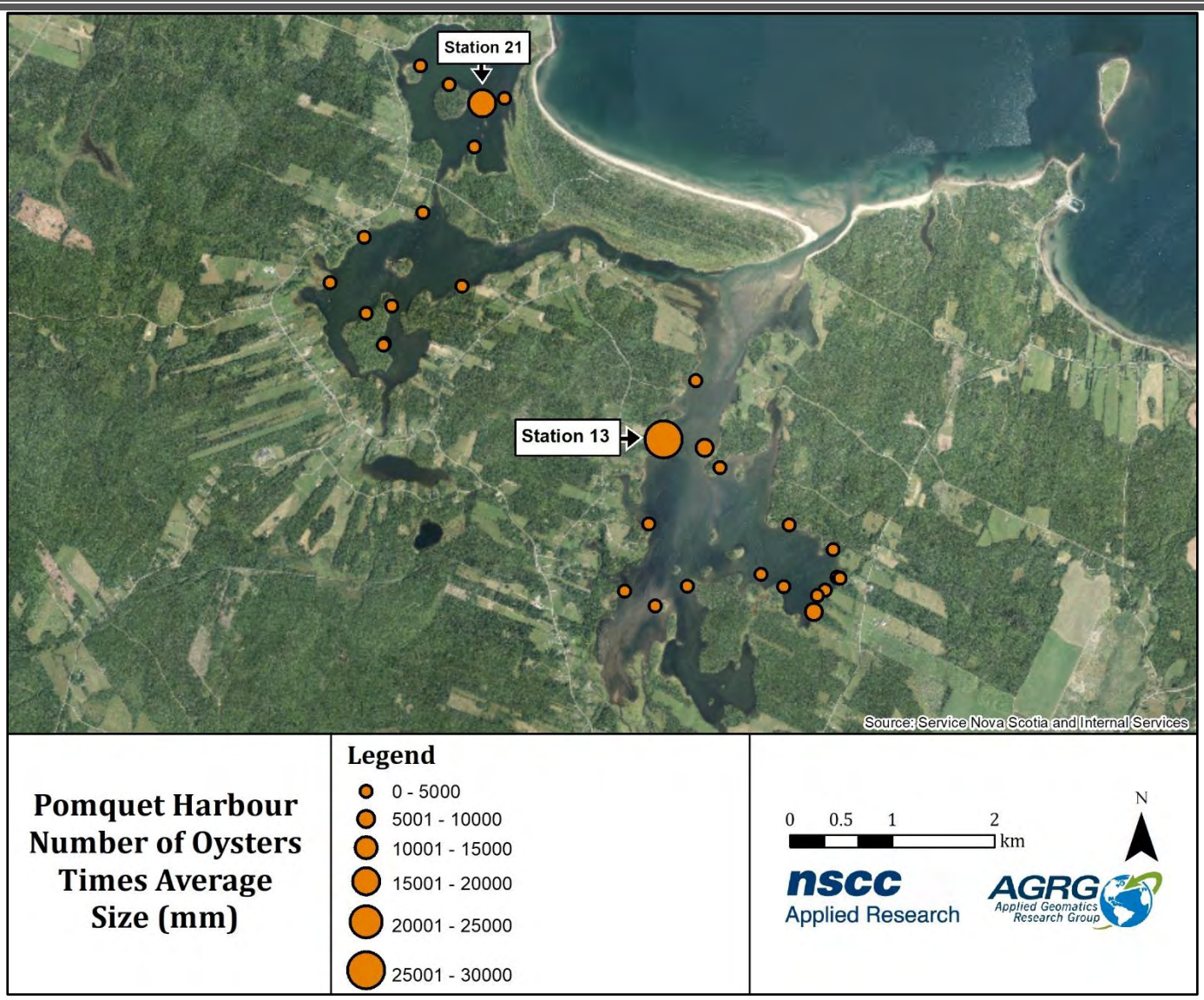

Figure 29: Number of Oysters Times Average Size (mm) was determined by multiplying the total number of recorded oysters by the mean size at each station during oyster stock surveys conducted by Robin Stuart on Paqtnkek First Nation's behalf.

Maps that show the count values of each oyster shell size class (e.g., 0 – 20 mm, 20 – 30 mm, 30 – 40 mm, 40 – 50 mm, 50 – 60 mm, 60 – 80 mm, 80 – 100 mm, and > 100 mm) at each sampling station have been included in Appendix 1: Number of Oysters per Length.

2.6.3 Temperature and Salinity

Temperature and salinity layers were extracted from data collected with a YSI salinity/temperature meter for each of the oyster stock survey locations (Figure 30; Figure 31). The temperature recorded during each survey ranged from 13.0°C to 16.8°C and had a mean value of 15.3°C. Salinity varied from 26 ppt and 28.7 ppt and had a mean value of 27.8 ppt.

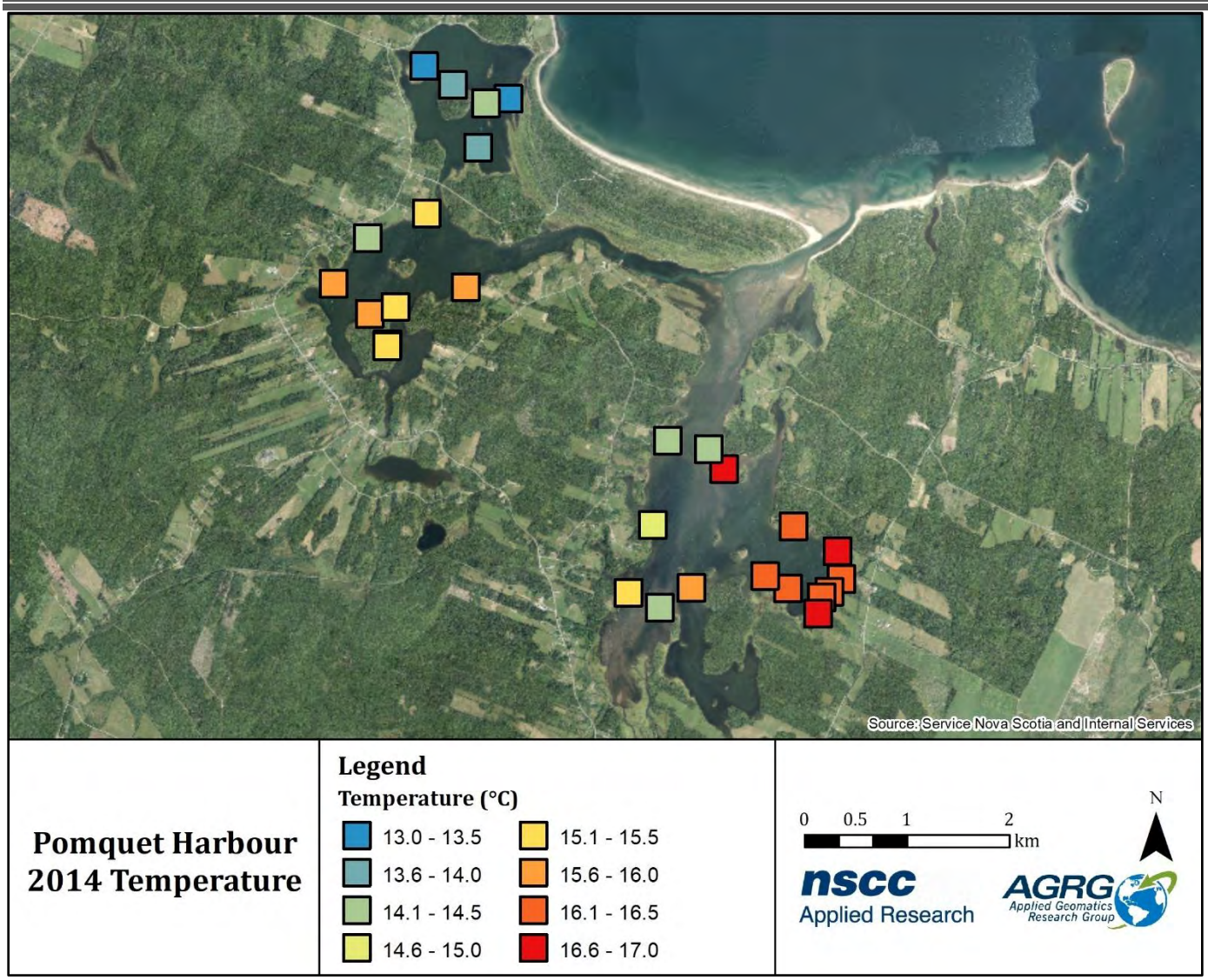

Figure 30: Temperature data collected at each station during oyster stock surveys conducted by Robin Stuart on Paqtnkek First Nation's behalf

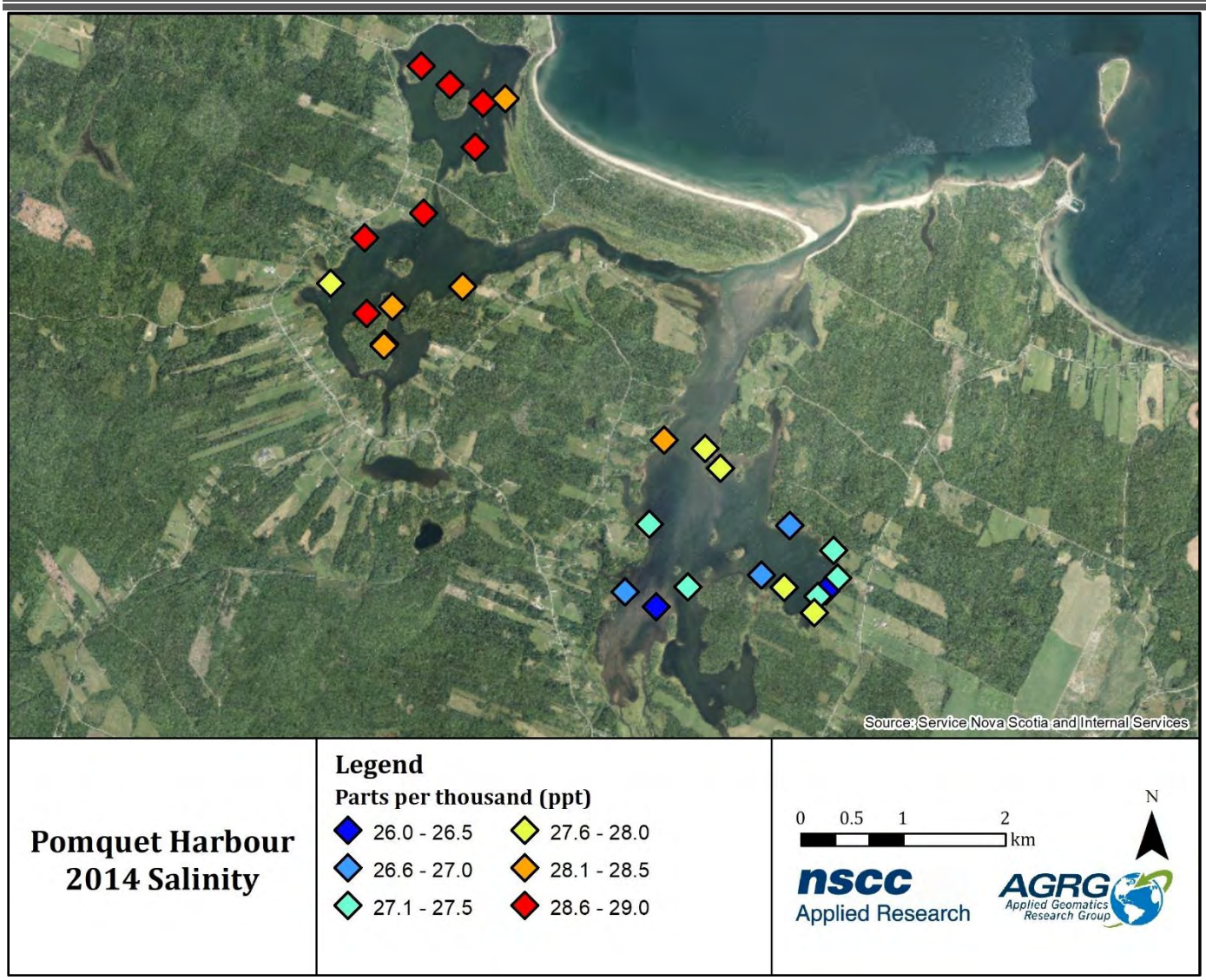

Figure 31: Salinity data collected at each station during oyster stock surveys conducted by Robin Stuart on Paqtnkek First Nation's behalf.

2.6.4 Supporting Data

Issued marine aquaculture leases along the Nova Scotian coast were obtained from the Nova Scotia Fisheries and Aquaculture (NSFA) website and clipped to the Pomquet Harbour study area (Figure 32). For use in the web application's Suitability Modeller widget, the aquaculture lease layer was converted from a polygon to a binary presence/absence raster.

Figure 32: Aquaculture leases in Pomquet Harbour as of November 2020. Most recent information is available at http://novascotia.ca/fish/aquaculture/site-mapping-tool/

As expected, the only license in Pomquet Harbour is an experimental license for American Oyster owned by Paqtnkek Mi'kmaw Nation. More information on Nova Scotia aquaculture leases is available through the NS Fisheries and Aquaculture web services.

2.6.5 Land Use

The Nova Scotia Department of Lands and Forestry provides a data layer called the Forest Resource Inventory which is used to describe the land use for all of Nova Scotia. The layer is derived from air photos and uses codes to define how land is being used (e.g., agriculture, forest, infrastructure). The Forest Resource Inventory layer for Antigonish County was updated in 2007. Several non-forested land codes (FORNON) were merged to reduce the number of classes. The final classes are represented in Table 4.

Merged Class	FORNON Code(s)
Agriculture	86, 91
Barren	84, 85
Beach	94
Cliffs, Dunes, Coastal Rocks	76
Forest	0, 1, 3, 5, 6, 7, 8, 9, 12, 20, 33, 38, 39
Forest Harvest (Clear Cuts)	60, 61
Infrastructure	92, 95, 96, 97, 98, 99
Lakes	77
Urban	87
Wetland	70, 71, 72, 73, 74, 75

Table 4: NS Department of Lands and Forestry Land Use layer definitions.

The land in the Pomquet study area was 61% forested (28.5 km^2), 19% agricultural (8.7 km^2), and has wetlands that cover approximately 7% (3.1 km^2) of the region (Figure 33). Clear-cuts, and cliffs/dunes/coastal rocks made up 4% (2.0 km^2) and 3% (1.5 km^2) of overall land use, respectively.

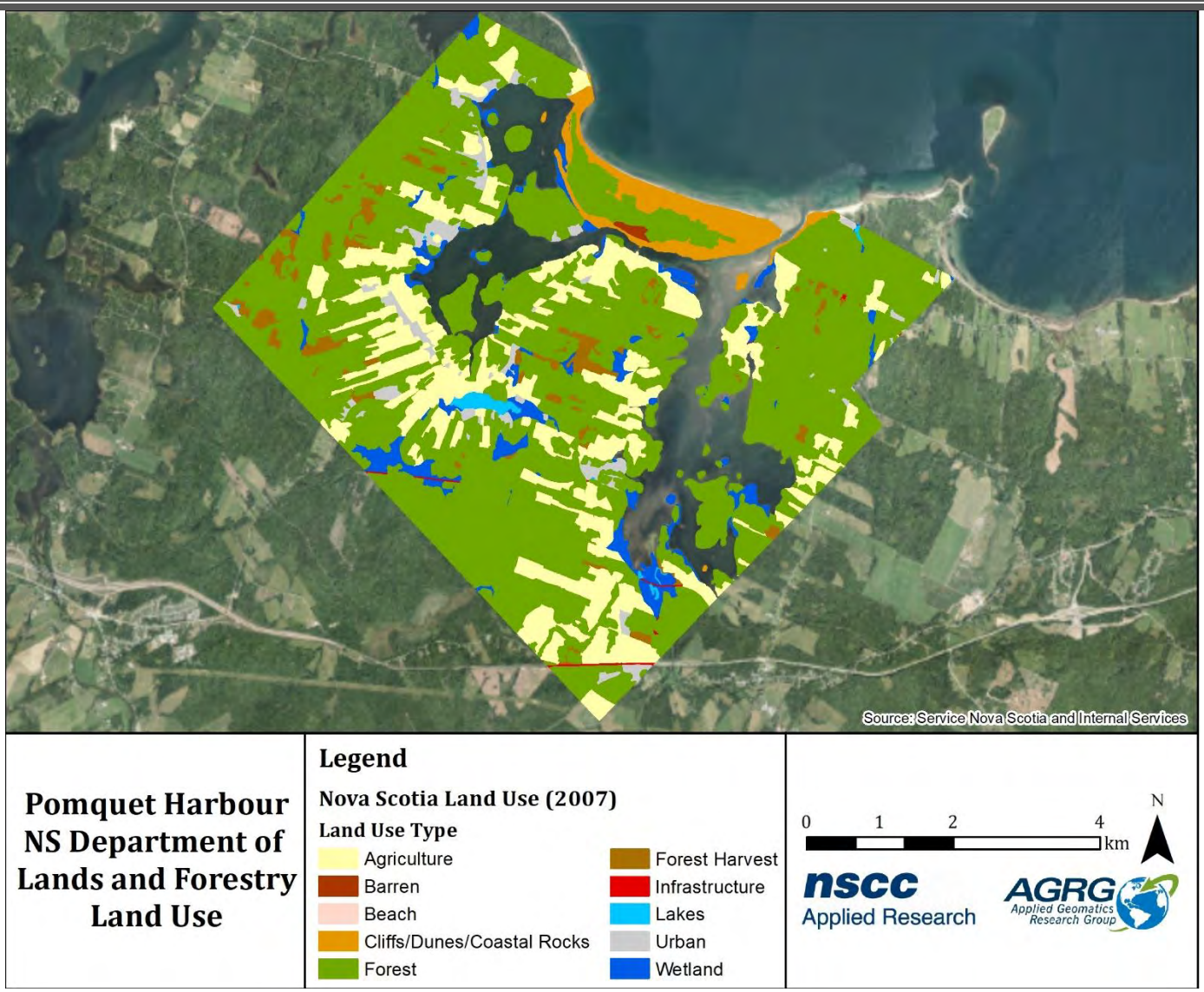

Figure 33: The Nova Scotia Department of Lands and Forestry Forest Resource Inventory land use classification, with simplified categories.

2.6.6 Intertidal Zone

The elevations between Lower Low Water Large Tide (LLWLT) and Higher High Water Large Tide (HHWLT) defined the intertidal zone. In Pomquet Harbour, LLWLT is -1.01 m, Mean Sea Level (MSL) is -0.20m and HHWLT is 0.45 m relative to CGVD2013. These values were provided by the Canadian Hydrographic Service (CHS) (Table 5). The values in between LLWLT and HHWLT were extracted from the Digital Elevation Model using Raster Calculator, and the resulting raster was cleaned using Majority Filter (Figure 34).

	CGVD2013
HHWLT	0.45 m
MSL	-0.20 m
LLWLT	-1.01 m

Table 5: Tidal range values obtained from Canadian Hydrographic Services (CHS) relative to CGVD2013.

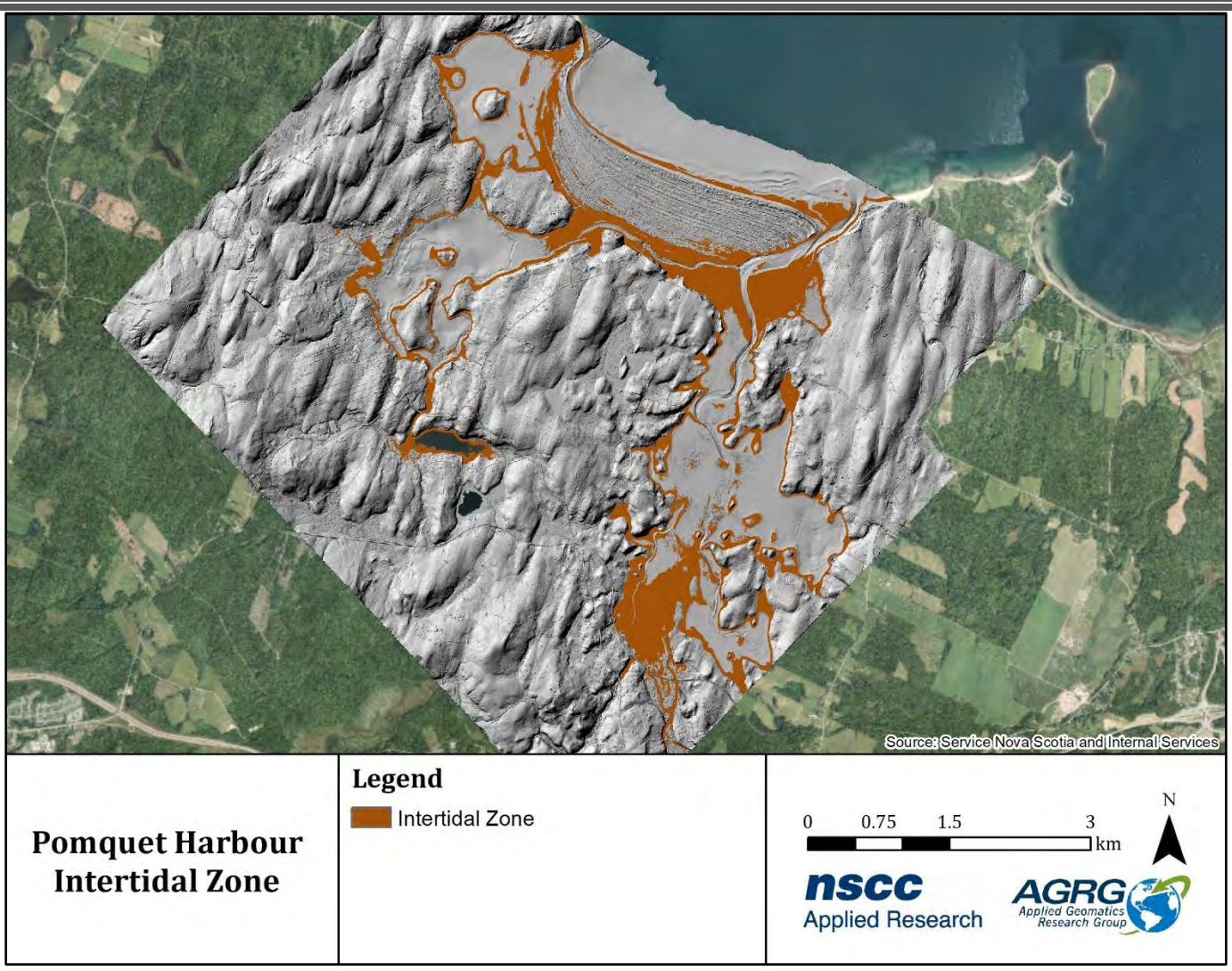

Figure 34: The intertidal zone, defined as the region on the elevation model between 0.45 m (HHWLT) and -1.01 m (LLWLT).

2.6.7 Channel Map

The channel location layer was derived from the continuous depth layer. Values above 2.2 m were selected from the depth layer and were reclassified. The reclassified raster was converted to polygons to remove speckle and deep areas. A few areas of the channel were digitized from the orthophoto and DEM. The final polygon layer was smoothed and converted to a raster to obtain the channel layer (Figure 35). The channel layer was converted to a presence/absence raster for use in ArcMap's Weighted Overlay tool and the web application's Suitability Modeller widget.

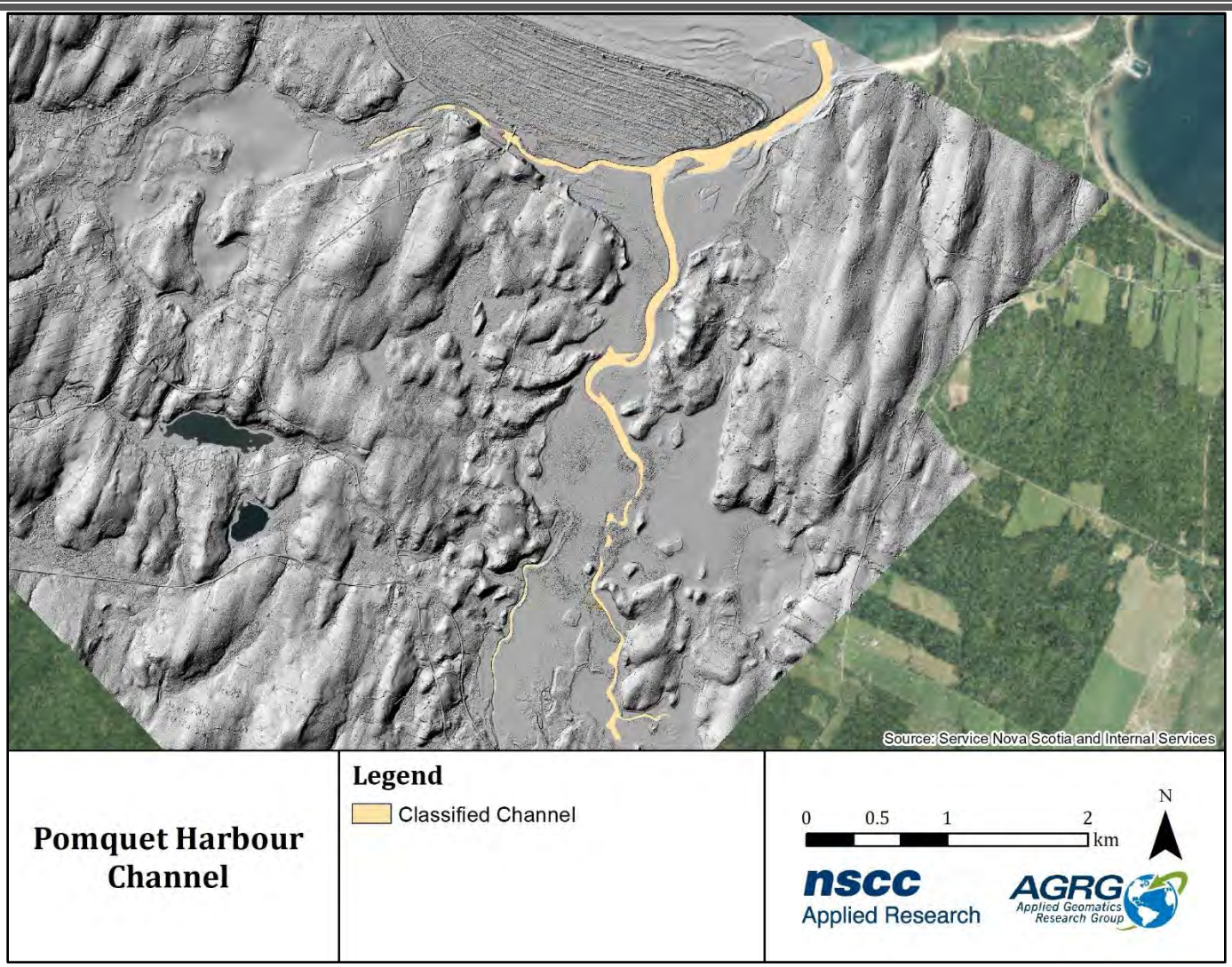

Figure 35: Classified channel obtained from the depth layer.

2.6.8 Ice Impact Zone

An Ice Impact Zone layer was derived from the seamless Digital Elevation Model (Figure 36). The ice impact zone was defined as the elevations between Higher High Water Large Tide (HHWLT) and 1 m below LLWLT. To generate this layer, the DEM was nullified in areas greater than HHWLT, and the ice impact zone was classified as the area between 0.45 m (HHWLT) and -2.01 m (LLWLT - 1 m). The ice-free zone was defined as values deeper than -2.01 m, classified into 1 m bins (e.g., -2.01 m, -3.01 m, -4.01 m, and -5.01 m). Small NoData holes were filled using the Elevation Void Fill function.

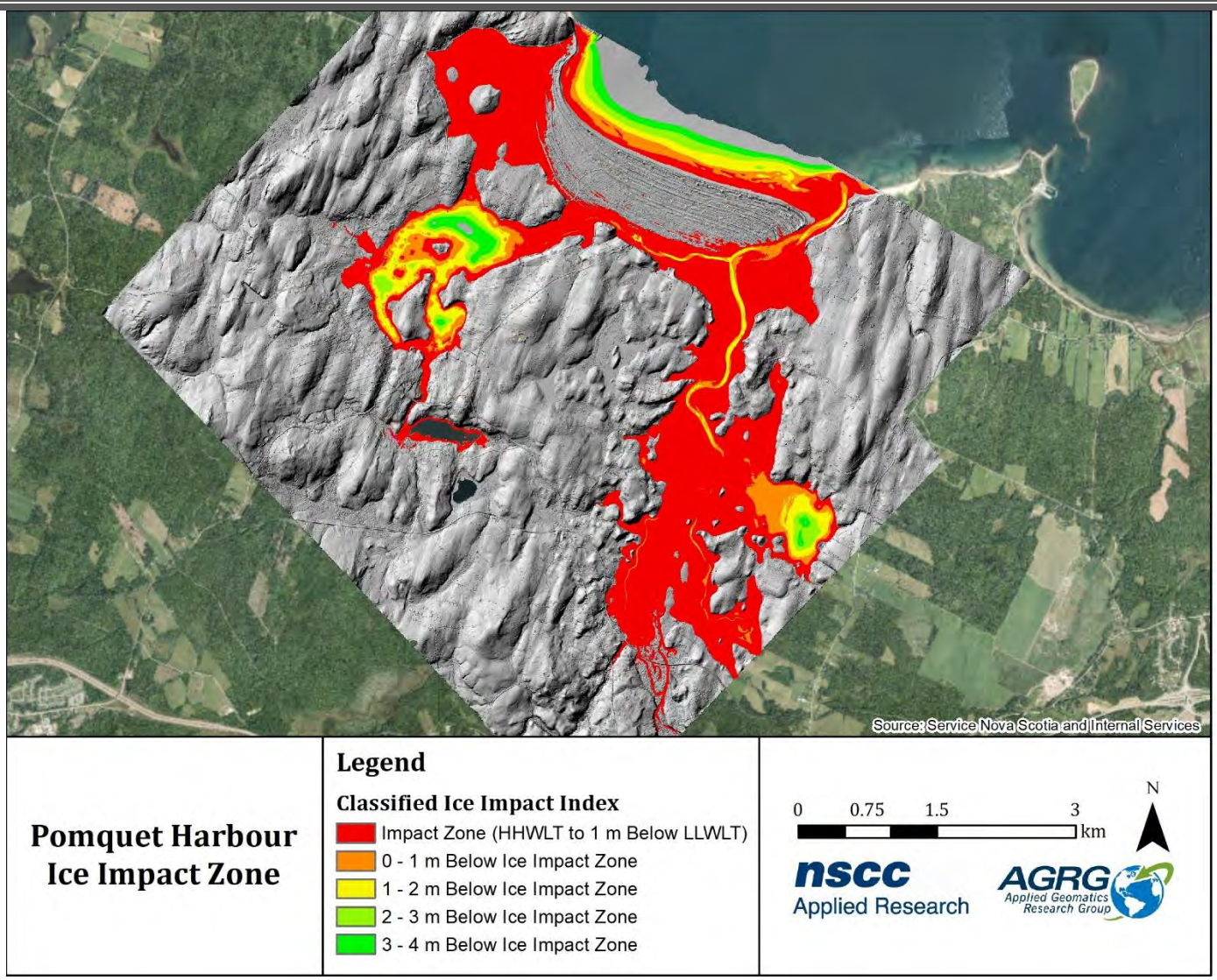

Figure 36: The Ice Impact Zone is defined as the level of HHWLT to 1 metre below LLWLT, with the ice impact-free zone divided into 1-metre increments below the impact zone.

Ice-impact zones were present over the majority of Pomquet Harbour. Ice-impact free zones were identified in the channel, the western bay, and a small portion of Church Cove (Figure 36).

2.6.9 Depth Map

Depth relative to Lower Low Water Large Tide (LLWLT) was generated by using the Raster Calculator tool in ArcMap to subtract the DEM from the LLWLT value (-1.01 m) and to nullify any value of the resulting raster greater than 0 m. This is shown as a Continuous Depth map in Figure 37. The Reclassify tool was then used to bin the Continuous Depth layer into 1 m bins to generate a Classified Depth layer (Figure 38). Small NoData holes were filled by applying the Elevation Void Fill Function in ArcMap's Image Analyst. The Majority Filter and Boundary Clean tools were also used on the Classified Depth layer to decrease speckle. One-metre contours relative to LLWLT were derived from the Classified Depth layer (Figure 38).

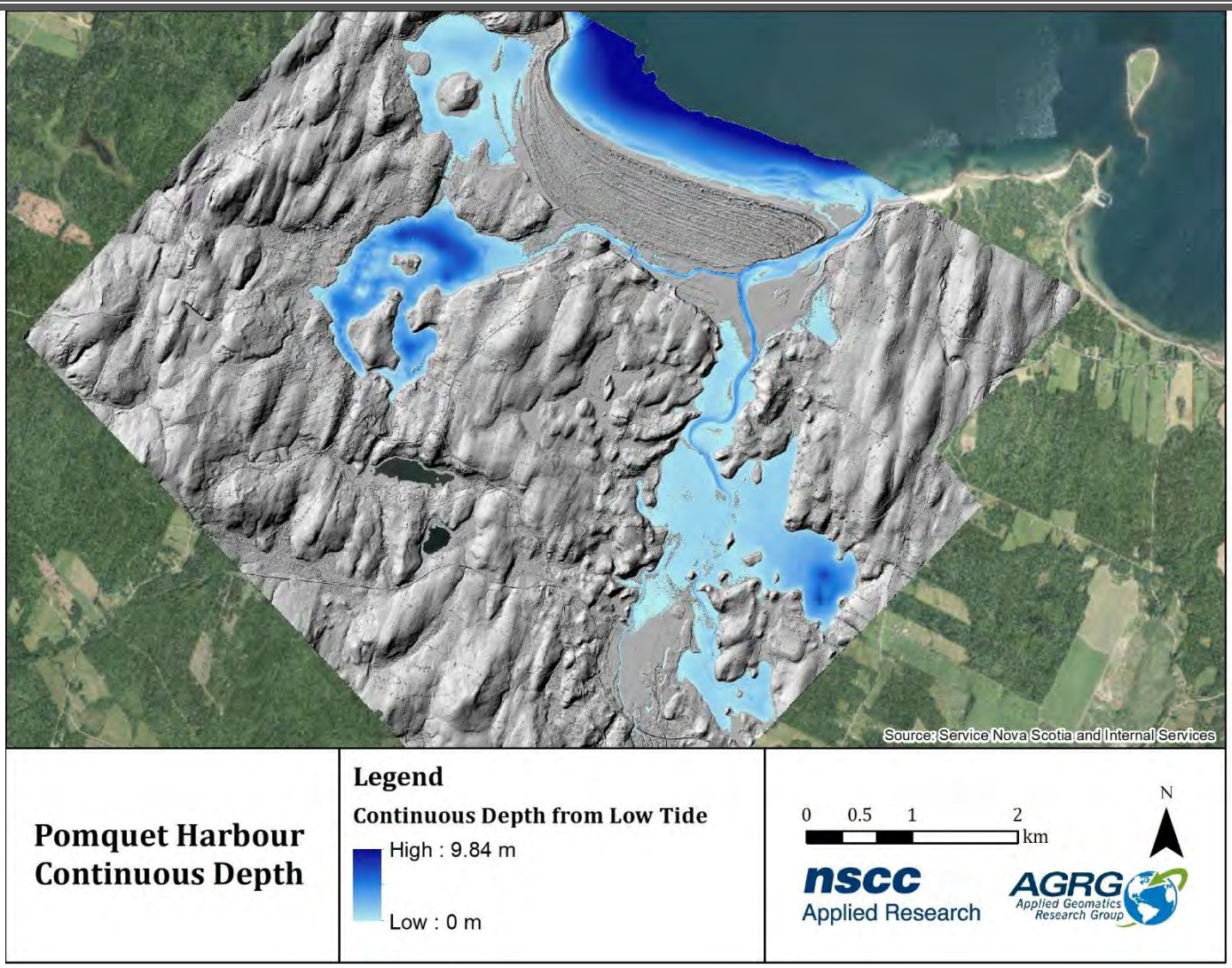

Figure 37: Continuous depth model, with depth relative to LLWLT.

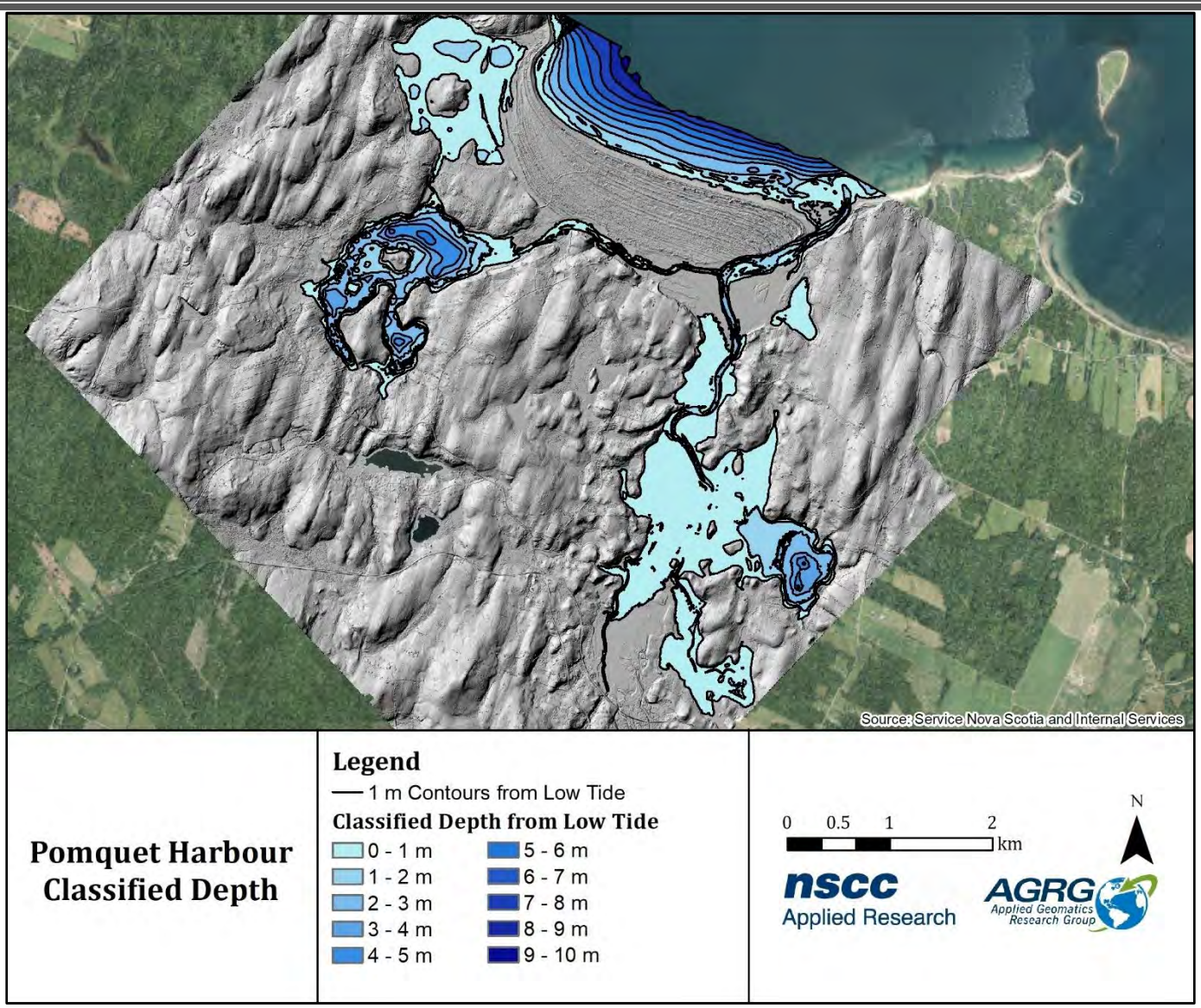

Figure 38: Classified depth model, with 1 m depths relative to Lower Low Water Large Tide.

The maximum depth in Pomquet Harbour was approximately 10 m below LLWLT with the deepest areas located seaward, near the mouth of the harbour, and in small portions of Church Cove and the western bay.

2.7 Eelgrass

The orthophoto imagery was combined with the lidar green laser intensity and the lidar seabed roughness and used in a Fuzzy K-Means unsupervised classification for cover material below the higher high-water line. The results of the classification tended to group features at too coarse of a level. The method was revised to include the use of band ratios from the orthophoto RGB bands. The band ratios help with variable light conditions between photo frame exposures and sun glint from the water surface. The band ratios were calculated using the following method: (B1 - B2)/(B1 + B2), which resulted in an image ranging from -1 to +1. These images were then scaled to a range of 0-255 and used for the Fuzzy K-Means unsupervised classification with an output of 16 classes. Some classes were aggregated to produce a final eelgrass presence and absence map since this was the only class that represented an ecosystem health indicator and steps should

be taken to avoid damaging eelgrass beds. There was minimal ground truth information available of the distribution of eelgrass and other benthic cover material (with the exception of the Video Ray transects which shows SAV). We reached out to various stakeholders and eelgrass experts for data and received some generalized areas from Sarah Silver Slayter, a student of Dr. David Garbary from the Biology department at St. FX University. We used these areas for a qualitative assessment and interpretation of the imagery and results.

2.8 Hydrodynamic Modelling

A hydrodynamic model (HD) was developed for the Pomquet Harbor using DHI Mike 21 Flow model Flex mesh application. A variety of modules within the Flex mesh were used to obtain the project outputs.

The model was used to produce four layers: flushing time, mean and maximum monthly currents, and significant wave height from the dominant wind direction and speed. Flushing time was determined using the transport module of Flex Mesh. Mean and maximum monthly current magnitudes were calculated directly using Mike 21 from the hydrodynamic model. The significant wave height was derived by applying strongest south winds to the Spectral Waves Module.

2.8.1 Mesh Generation

The hydrodynamic model was driven by two major inputs: a surface generated from bathymetric and land elevation points, and boundary conditions. As the Flex Mesh module works with meshes instead of a grid, a mesh was developed using the Mesh Generator tool in Mike Zero. Raw data for generating the mesh was land boundary (3 m contour) and bathymetry (resolution of 3 m) in XYZ format. Bathymetry was obtained from lidar, multibeam surveys and CHS chart data (converted to CGVD2013) where the lidar did not penetrate the deeper water. A mesh was generated with larger mesh resolution in the deep water and fine mesh resolution in the harbour and channel as shown in Figure 39. The mesh was interpolated using the linear interpolation method. The output mesh file contained geographical position information along with water depth at each node point.

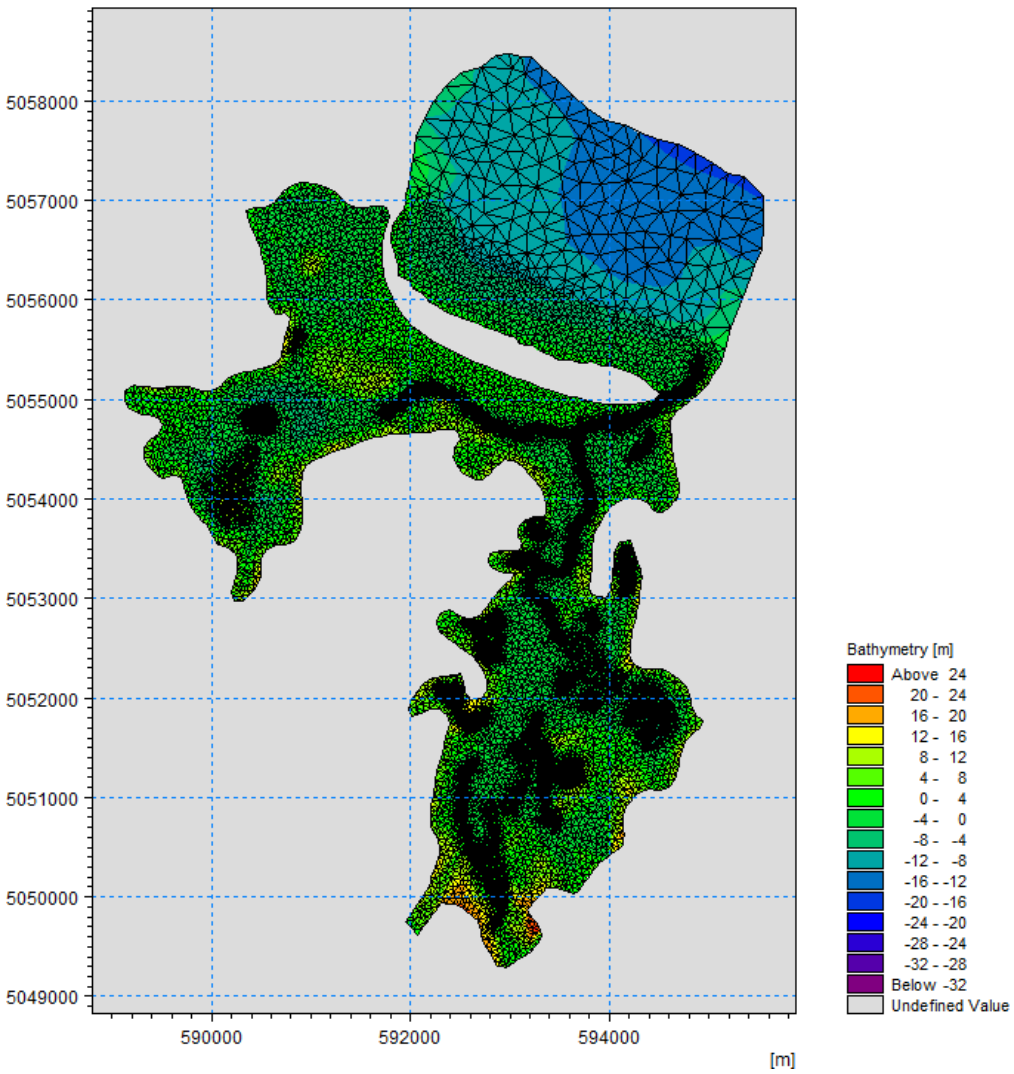

Figure 39: Mesh generated using Mike Mesh Generator tool showing fine resolution in channel and small branches of the harbour.

The mesh file showing the bathymetry with contours plotted using Plot Composer, a tool in Mike Zero, is as shown in Figure 40.

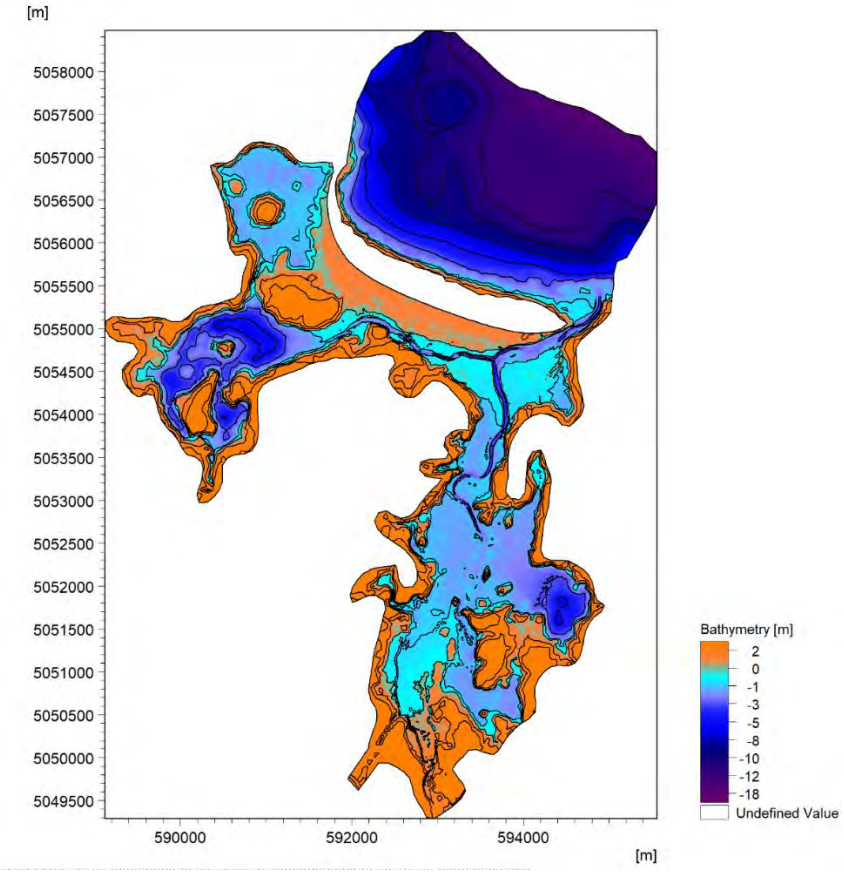

Figure 40: Mesh file showing bathymetry plotted using Mike plot Composer.

2.8.2 Boundary Conditions

The other major inputs for the models were the boundary conditions. Predicted tide generated by the XTide program, which was written by David Flater from Biological Sciences department, University of South Carolina, was extracted at the Antigonish Harbour station from Tbone tide website (Pentcheff). The tide file in chart datum (LLWLT) was converted to CGVD2013 and used to drive the model (Figure 41).

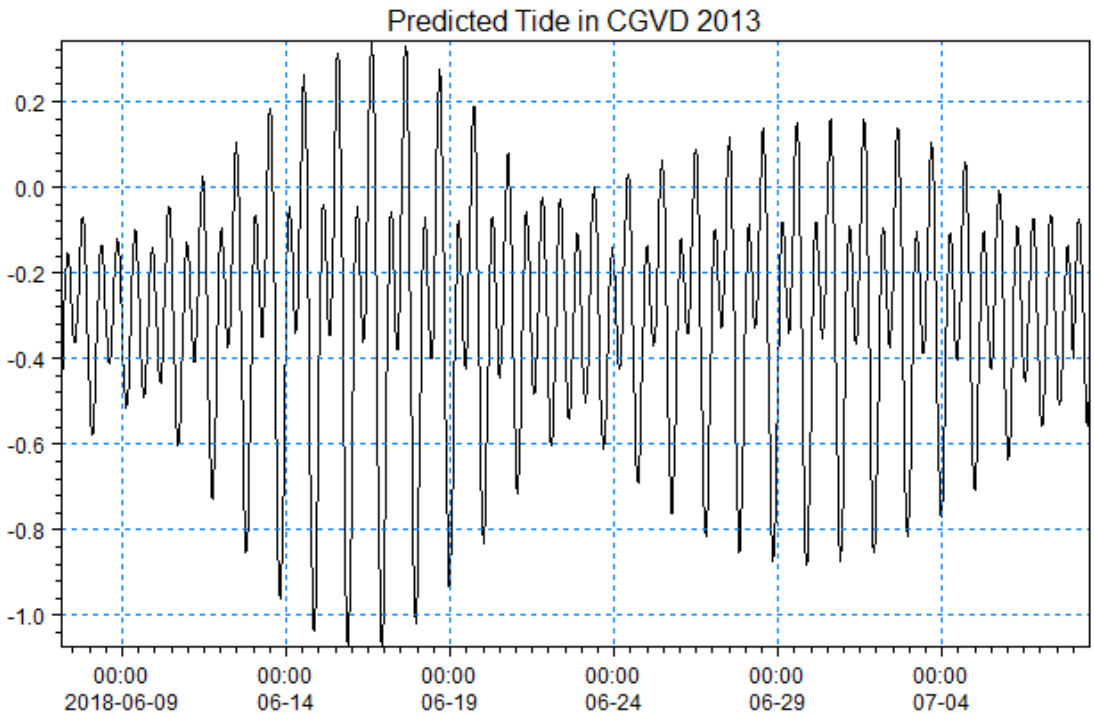

Figure 41: Predicted Tide obtained from http://tbone.biol.sc.edu/tide/ at Antigonish harbour plotted using Mike Plot Composer.

2.8.3 Hydrodynamic Simulation

The Hydrodynamic Model ran from the 5th of June to July 8th, 2018, a span of 33 days covering the one-month timeframe when the ADCP was deployed. Real time wind data obtained from the nearby Environment and Climate Change Canada station (ECCC) - Tracadie was also included in the model (Figure 42).

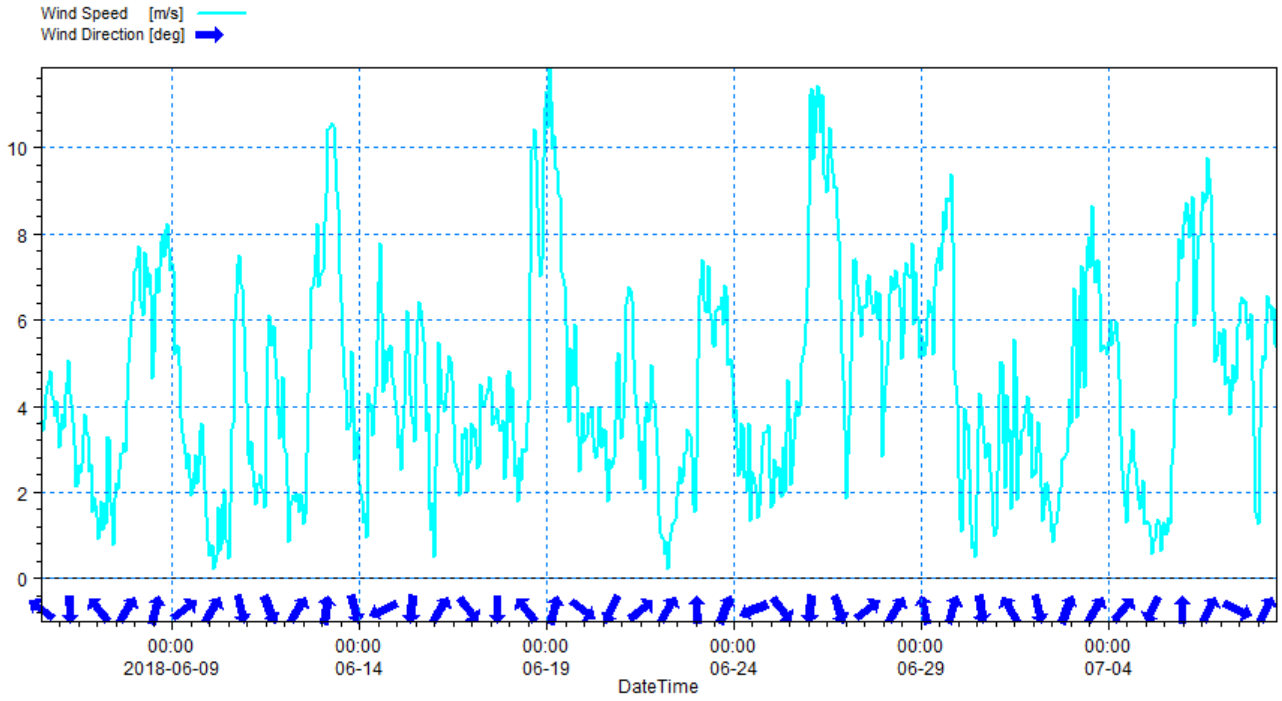

Figure 42: Wind data from Tracadie ECCC station.

For the hydrodynamic model, a temperature of 10 °C and salinity of 32 Practical Salinity Unit (PSU) were added to the model along with wind and bed resistance of 38 m^ (1/0)/s. Fresh water input was also included in the model to represent the streams draining into the harbour.

A storm surge value of 1.5 m was applied on the high tide to identify potential areas of flooding and changes in current speed. The value of 1.5 for a storm surge was typical for the type of storms that occur in the Maritimes. The hydrodynamic simulation ran for four tidal cycles to obtain water levels and currents.

2.8.4 Transport Module Simulation (Flushing time)

The Transport module in the Flex Mesh was used to calculate the minimum concentration that remained in the harbour based on the flow conditions. A concentration of one was added to the harbour on the first day and the model ran for a period of 33 days. Fresh water sources at four locations were also included with no concentration coming into the harbour. No decay factor was added. The results showed the time it took for the concentration to go to zero, thus replaced by fresh water while other areas still showed a concentration of 50%. The results were interpreted for flushing time estimates.

2.8.5 Spectral Waves Module Simulation

The Spectral wind wave model, which simulates growth and decay of wind generated waves and swell in coastal areas, was used to derive significant wave height (Hs) in the harbour. This simulation ran for four tidal cycles with south winds applied. Metrological data of Tracadie from 2003 to 2020 was summarized to obtain the significant winds in the region. When 15 m/s winds were applied, Hs in the harbour near the ADCP changed from 1 μm to 1 mm. Wave boundary conditions obtained from the ADCP waves data was used to drive the model.

2.8.6 Particle Tracking

The particle tracking module in the Flex Mesh of MIKE 21 was used to determine the fate of the suspended substance released from the best oyster sites in the harbour. The prime state for a female oyster to begin spawning is when they reach a size of 40 mm. Spawning is also dependent on environmental cues, where oysters prefer to spawn at water temperatures between 20°C to 30°C (68°F to 86°F) and at salinity levels above 10 ppt, which the harbour exhibits (Section 2.6.3 Temperature and Salinity) (Doiron, 2008). The fertilized eggs take about two weeks in the water column to reach the pediveliger stage (larva with a foot), which is when they begin to concentrate at the bottom of the river seabed system to search for a hard substrate. For this reason, the model ran for a period of one month with higher settling rate after the first two weeks.

As the female oyster releases a high number of eggs, only a fraction of them were considered by scaling the model's values to limit the simulation time. This number was obtained by summing the count of oysters in the size range of 30 mm to 100 mm and then assuming half of that number would be females. The resultant number was multiplied by 50 million, as each female oyster can produce that many eggs, and then divided by one million to facilitate the processing. These particles

were released per hour over a tidal cycle in the model at the best oyster locations (Figure 43). A horizontal dispersion constant of 0.002 m^2/s was also used along with water levels and bed resistance from the validated hydrodynamic model.

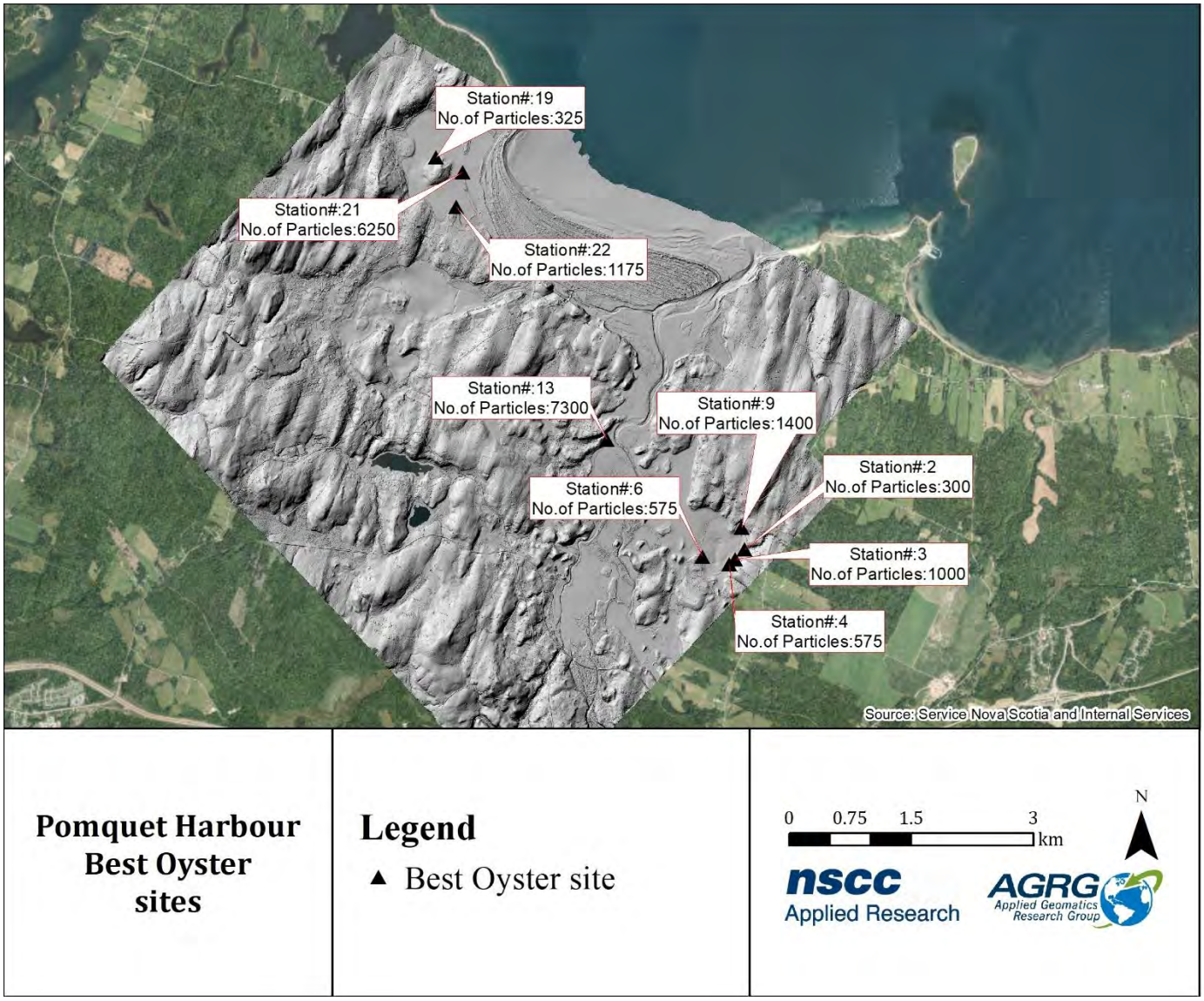

Figure 43: Number of particles released per hour from the station in the simulation.

3 Results

3.1 Digital Elevation Model (DEM)

The bathymetry obtained from the lidar, multibeam survey and CHS data, along with the topographic data from the Chiroptera topo-bathymetric lidar, is shown as a colour shaded relief (CSR) model in Figure 44. A hillshade model of the DEM is included in Appendix 2: Hillshade Models.

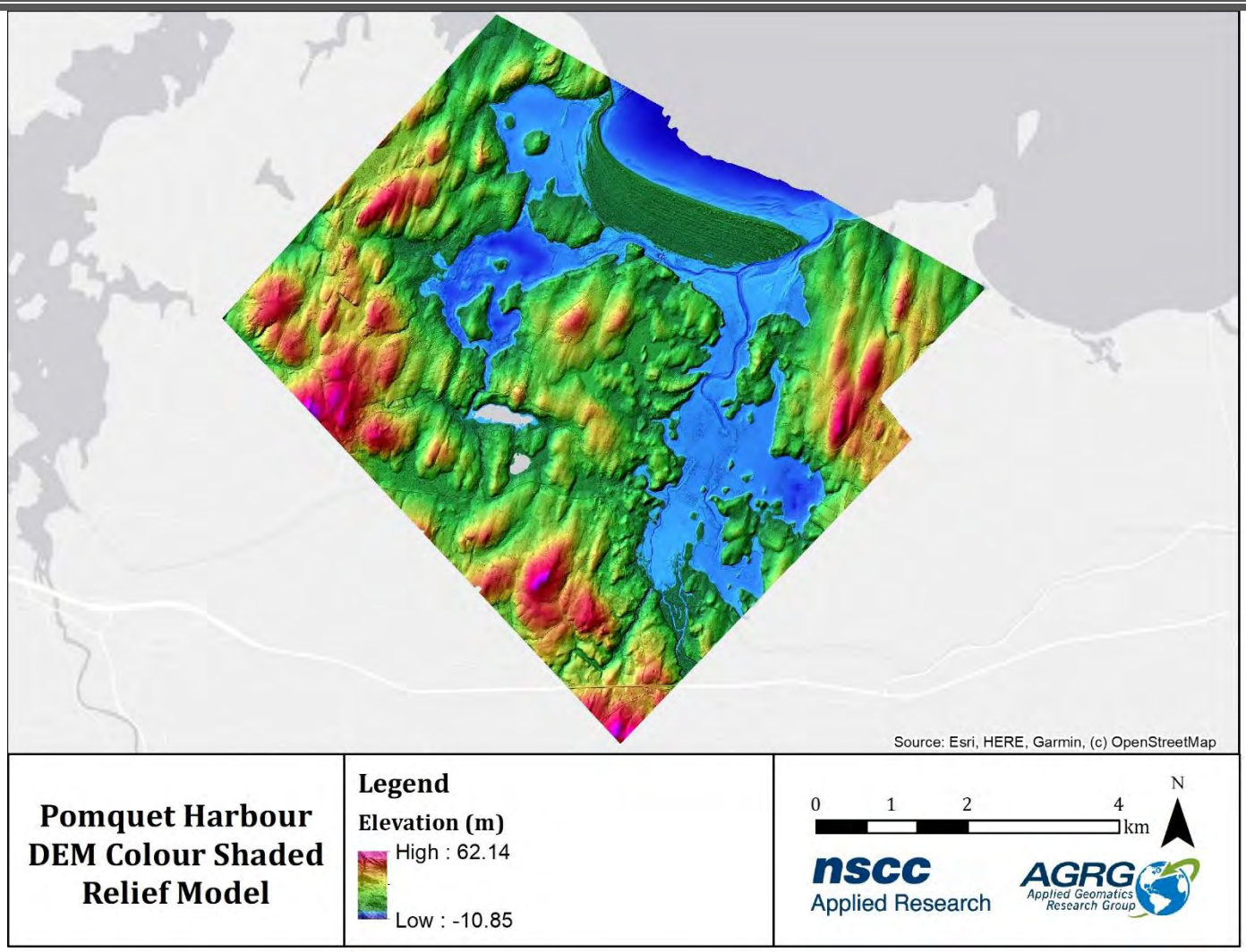

Figure 44: Colour shaded relief model generated from the digital elevation model.

3.2 Digital Surface Model (DSM)

The topo-bathymetric lidar survey, along with the multibeam data and CHS soundings, was processed into a digital surface model of the Pomquet study region. A DSM captured both the natural and built/artificial features of the environment whereas the DEM represented bare earth surface. This is presented as a colour shaded relief model in Figure 45. A hillshade model of the DSM is included in Appendix 2: Hillshade Models.

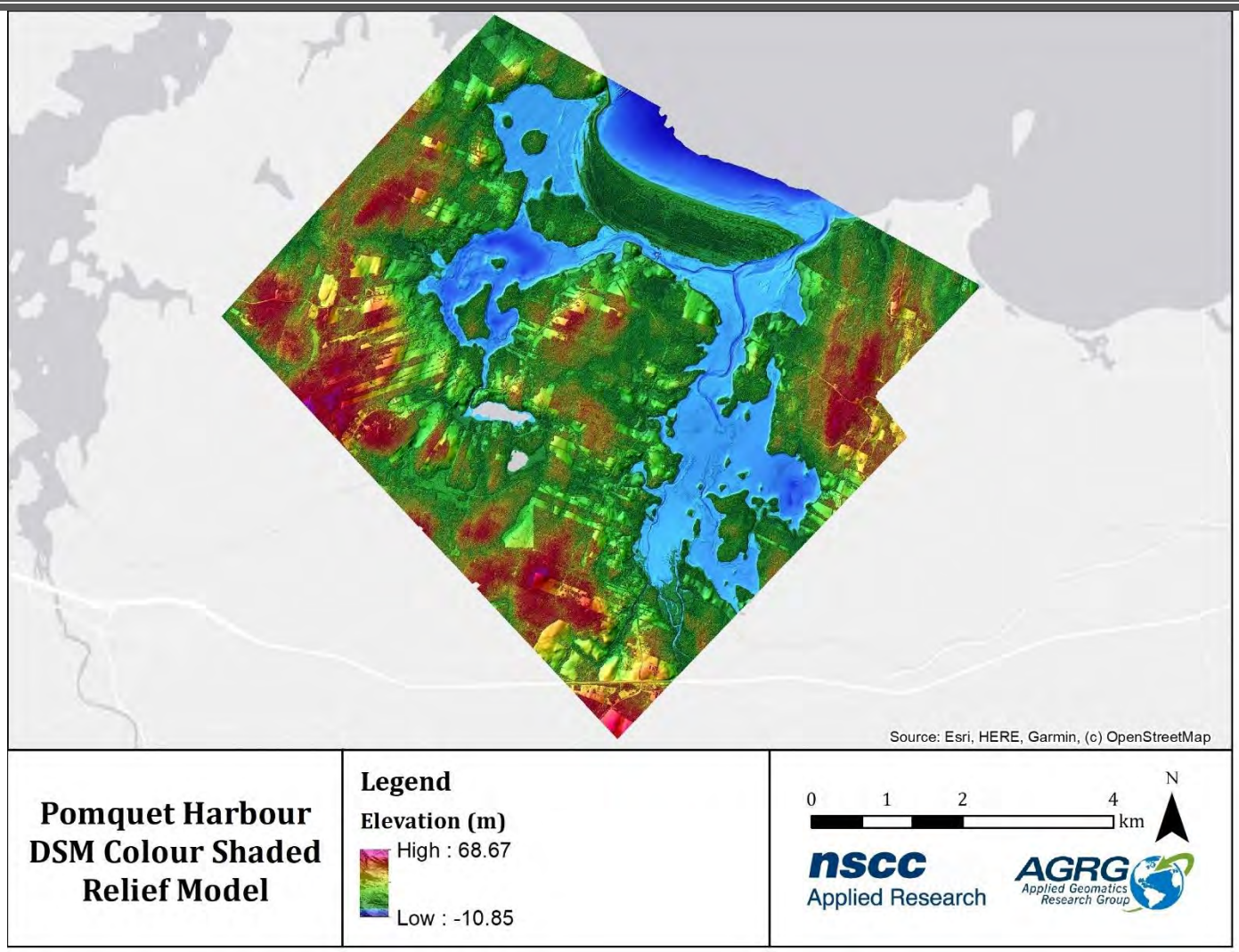

Figure 45: Colour shaded relief model generated from the digital surface model.

3.3 Intensity

The intensity model provided information on how much light was reflected by the ground and cover material surfaces that the green laser reflected off (Figure 46). Bright areas in the intensity model indicated that the laser reflected strongly off the land (e.g., sand), while dark areas indicated a weaker reflection of the laser (e.g., dark seaweed). The normalized bathymetric model compensated for the variation in depth in Pomquet Harbour and the impact on the amplitude of the reflected green laser pulses (Figure 47). A colour shaded relief of the intensity model is shown in Figure 48.

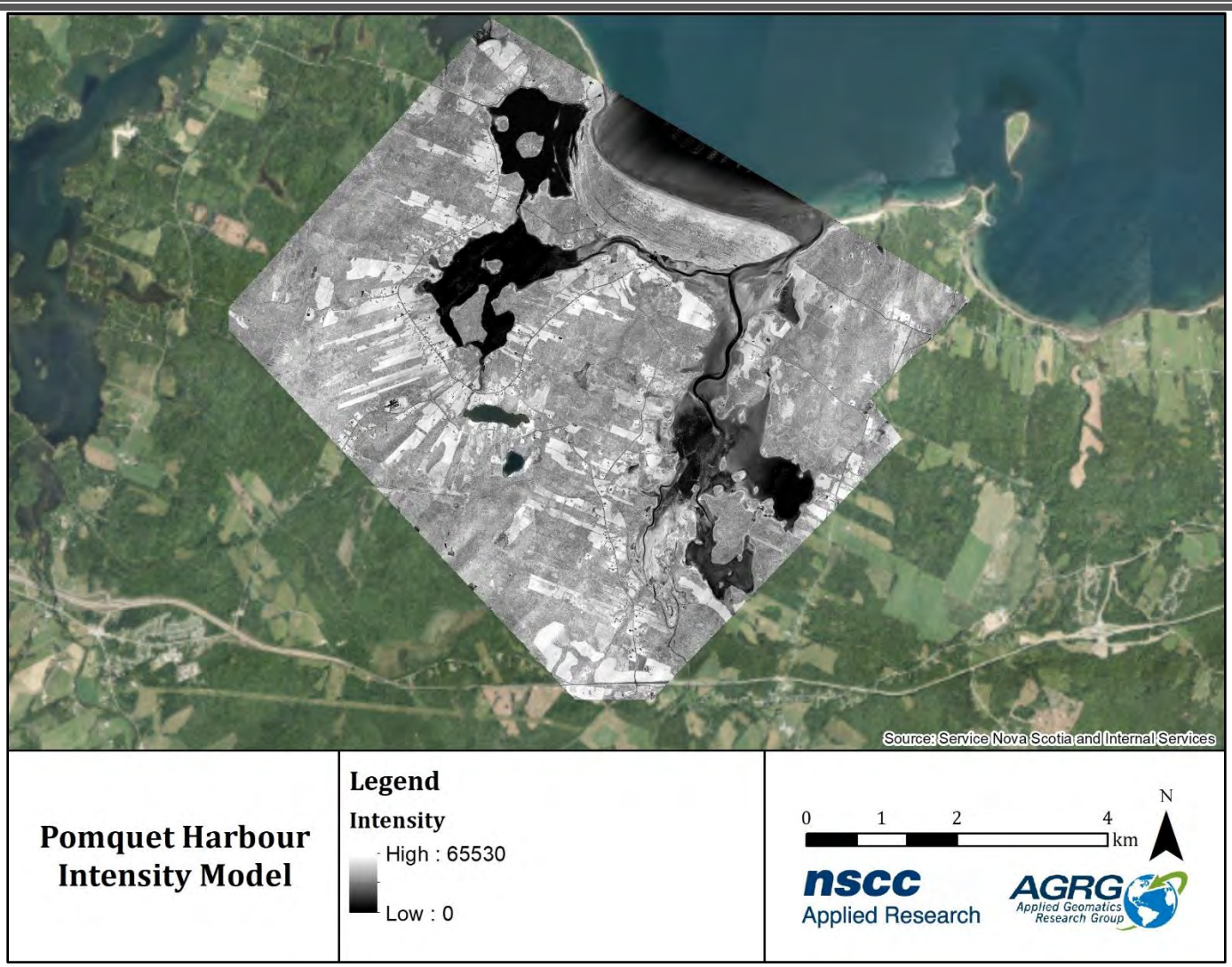

Figure 46: Intensity map of the lidar return data that incorporates all green laser returns above and below the water line (HHWLT).

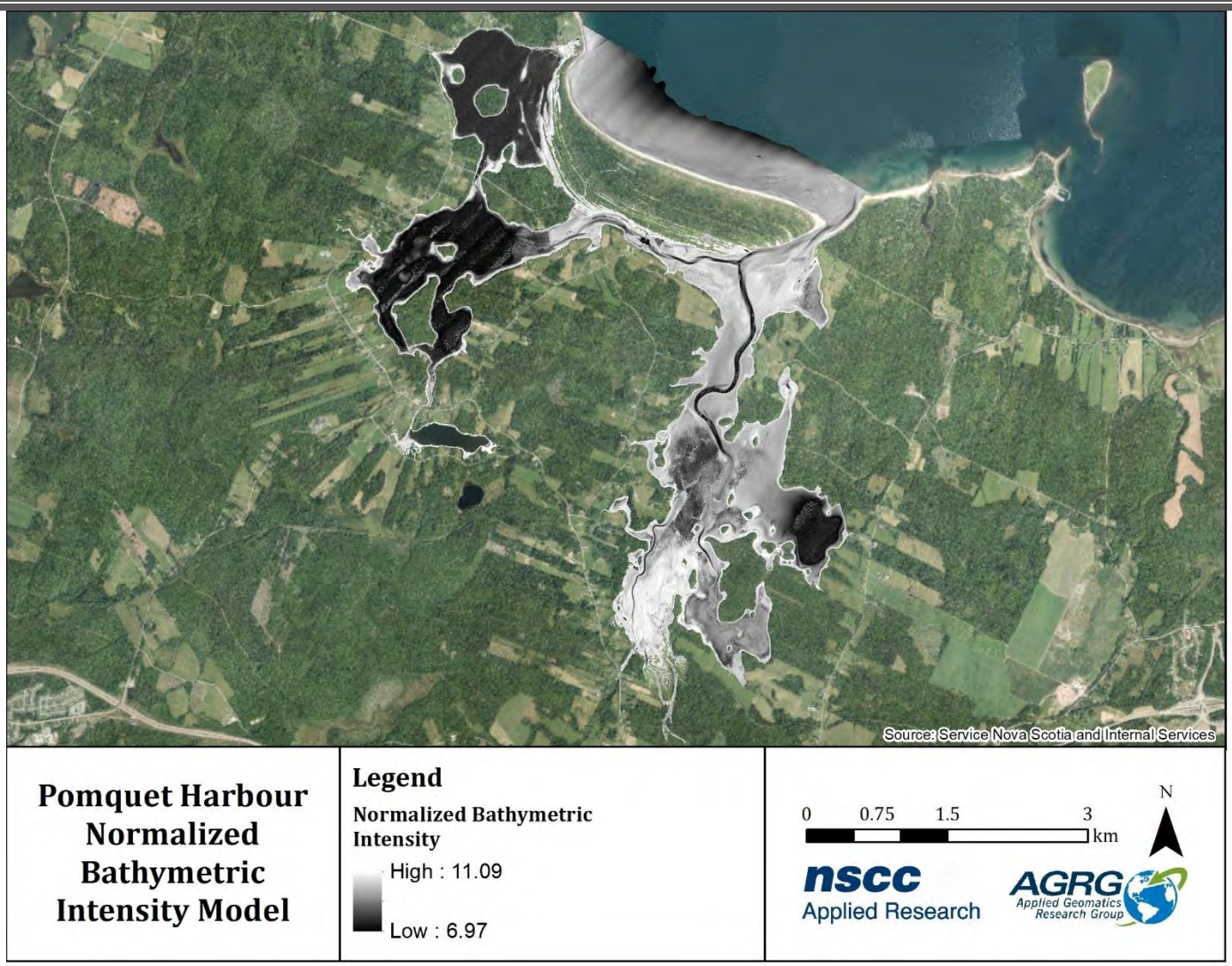

Figure 47: Normalized intensity map of the lidar return data that incorporates lidar returns below the water line (HHWLT).

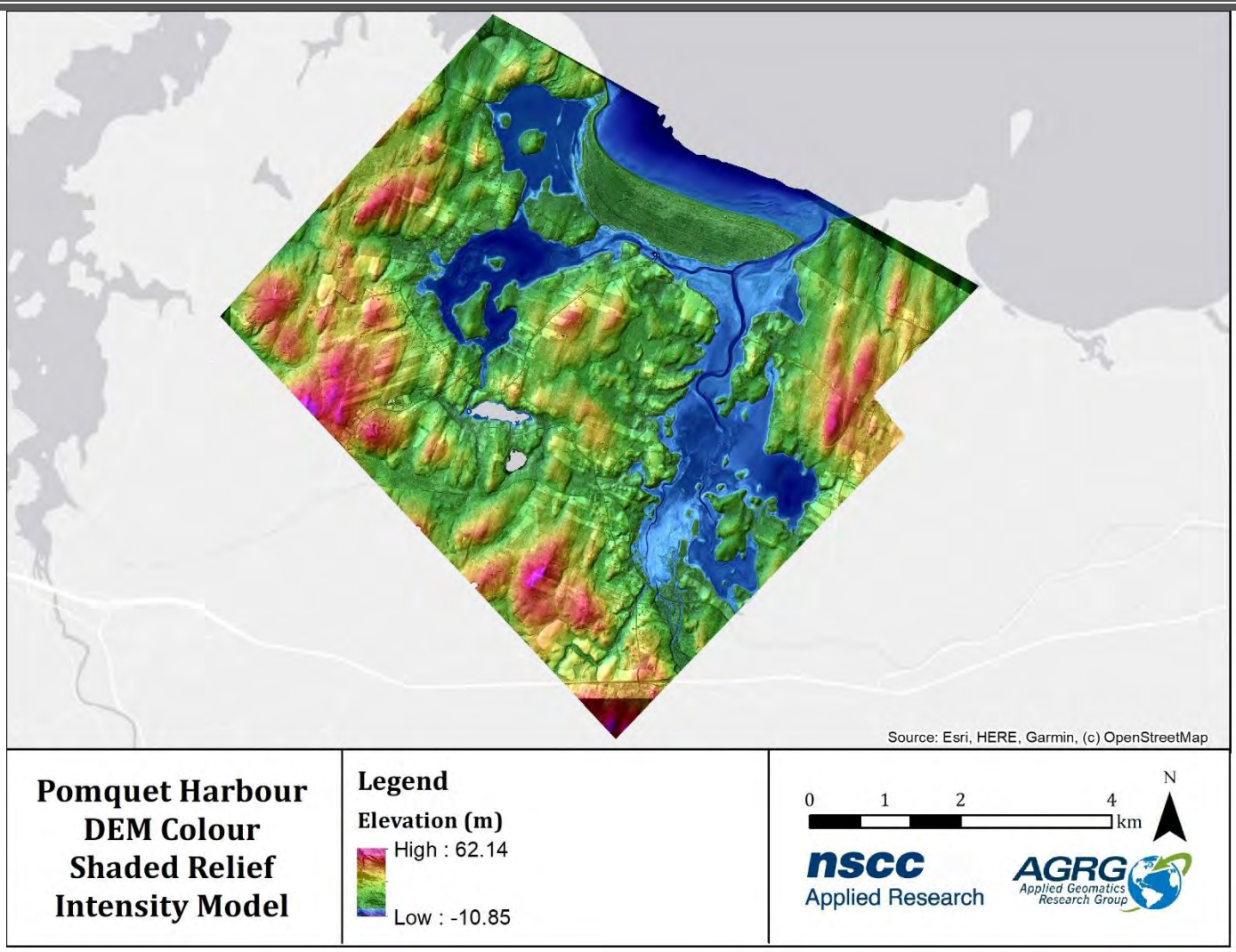

Figure 48: Colour shaded relief intensity model generated from the digital elevation model and lidar intensity data.

3.4 Orthophoto

The orthophoto layers were invaluable for assisting with the interpretation of the DEM, validating land use, and for use in the generation of lidar derived products, such as eelgrass. The orthophoto true colour mosaic (50 cm) showed areas of sand, vegetation, and identified the channel; the NIR orthophoto mosaic in shades of red was helpful in distinguishing between sand or pavement and vegetation on land (Figure 49; Figure 50).

The RCD30 imagery was processed using Agisoft Photoscan Professional. Captured imagery was georeferenced using an aerial triangulation model. Where photo positions were unable to be resolved, imagery was directly georeferenced using the known camera position and orientation. Photo orientations were calculated by linking the exterior orientation (EO) extracted from the aircraft trajectory GPS position (X, Y, Z) and the IMU attitude (omega, phi, kappa) at shutter events to the engineered internal orientation (IO) of the RCD30 (CCD dimensions, focal length, lens curvature). These orthophotos were displayed in the web application as a NIR image and an RGB image.

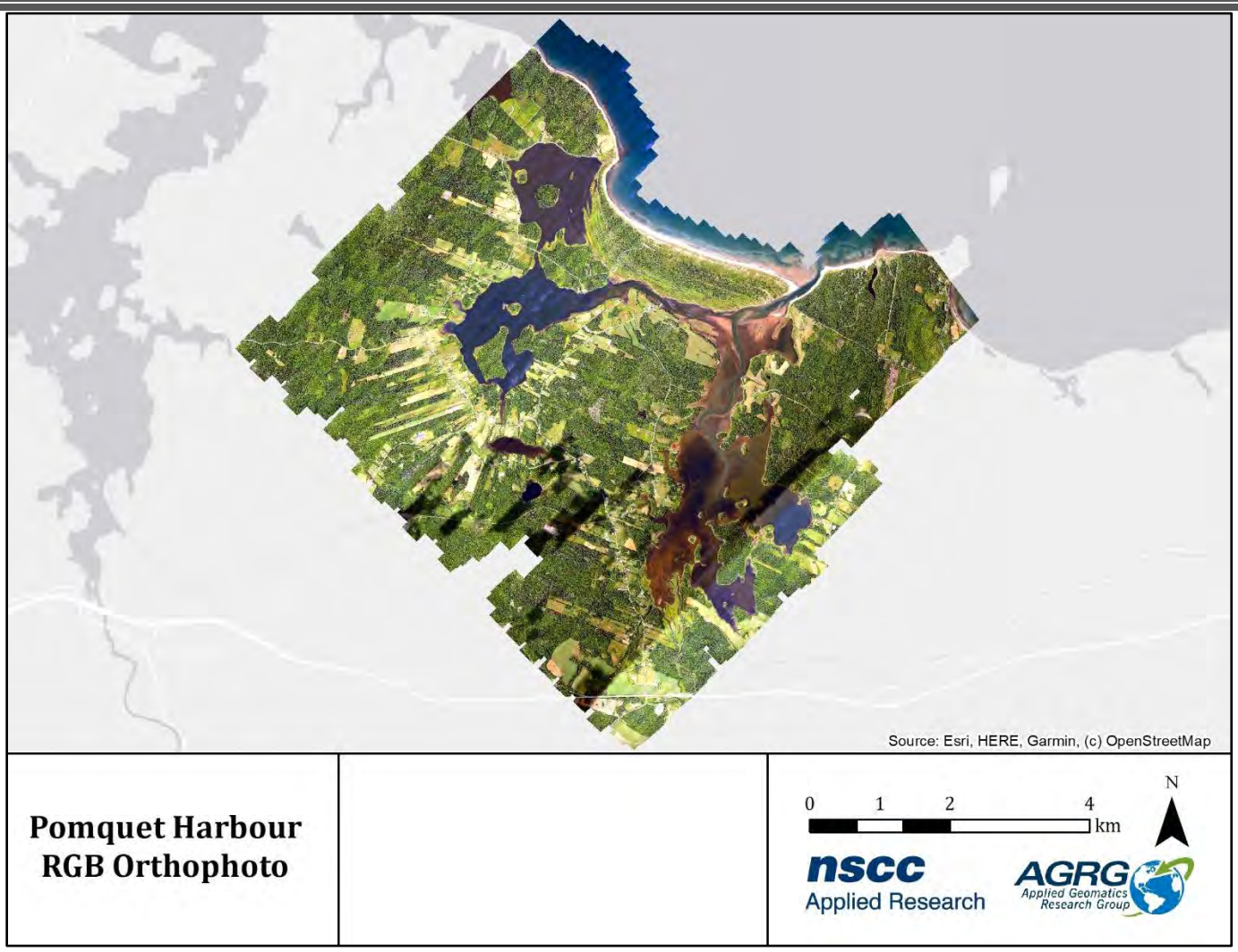

Figure 49: True colour image (50 cm), generated from the RCD30 orthophoto mosaic.

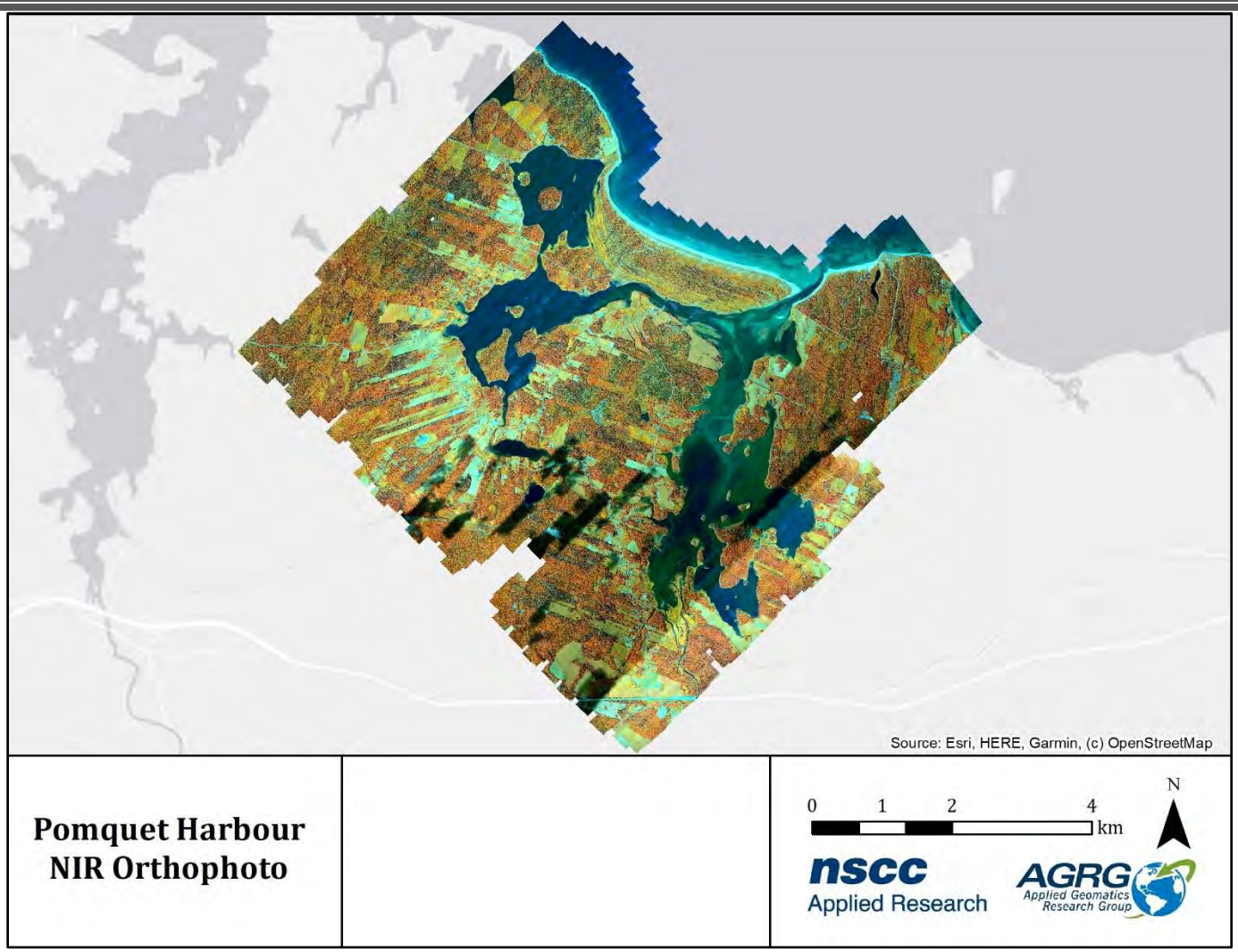

Figure 50: False colour NIR image (50 cm), generated from the RCD30 orthophoto mosaic with band combinations near infrared, green, and blue.

3.5 Eelgrass

The variation of the lighting condition across the survey area and the presence of cloud shadows affected the resultant classification, even after the use of band ratios. The results were validated qualitatively against interpreting the RGB orthophoto imagery. The map represented the healthiest eelgrass, although it may have underestimated the full extent of eelgrass presence as it did not pick up the outer boundary of some of the clumps (Figure 51).

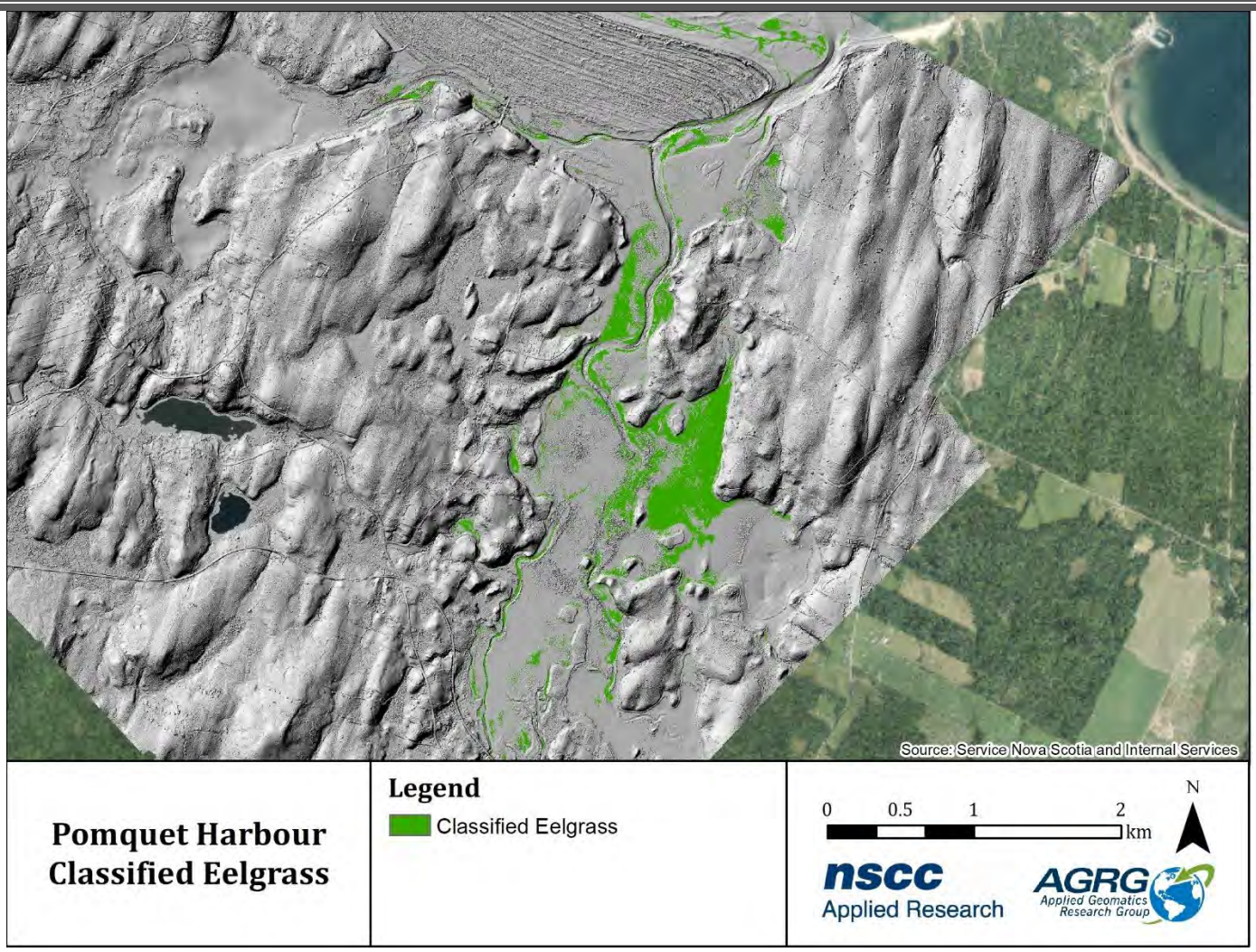

Figure 51: Classified eelgrass presence in Pomquet Harbour.

3.6 Acoustic Doppler Current Profiler (ADCP)

The ADCP measured waves on the hour and currents every 30 cm from the sensor to the sea surface every 15 minutes. In addition to measuring the current speed and direction for these vertical bins (30 cm increments), the ADCP also measured water level from a pressure sensor. The data were integrated into an animation to aid in visualizing the ADCP current and water level results in relation to wind speed and direction. Frames from the animation showed the water level and current speeds during normal tidal events with variable wind conditions (Figure 52). The current speed was denoted by the x and y-axis in m/s, and the direction by the four cardinal points (N, E, S, W red lines and text) and the water level above the sensor was denoted on the z-axis (m).

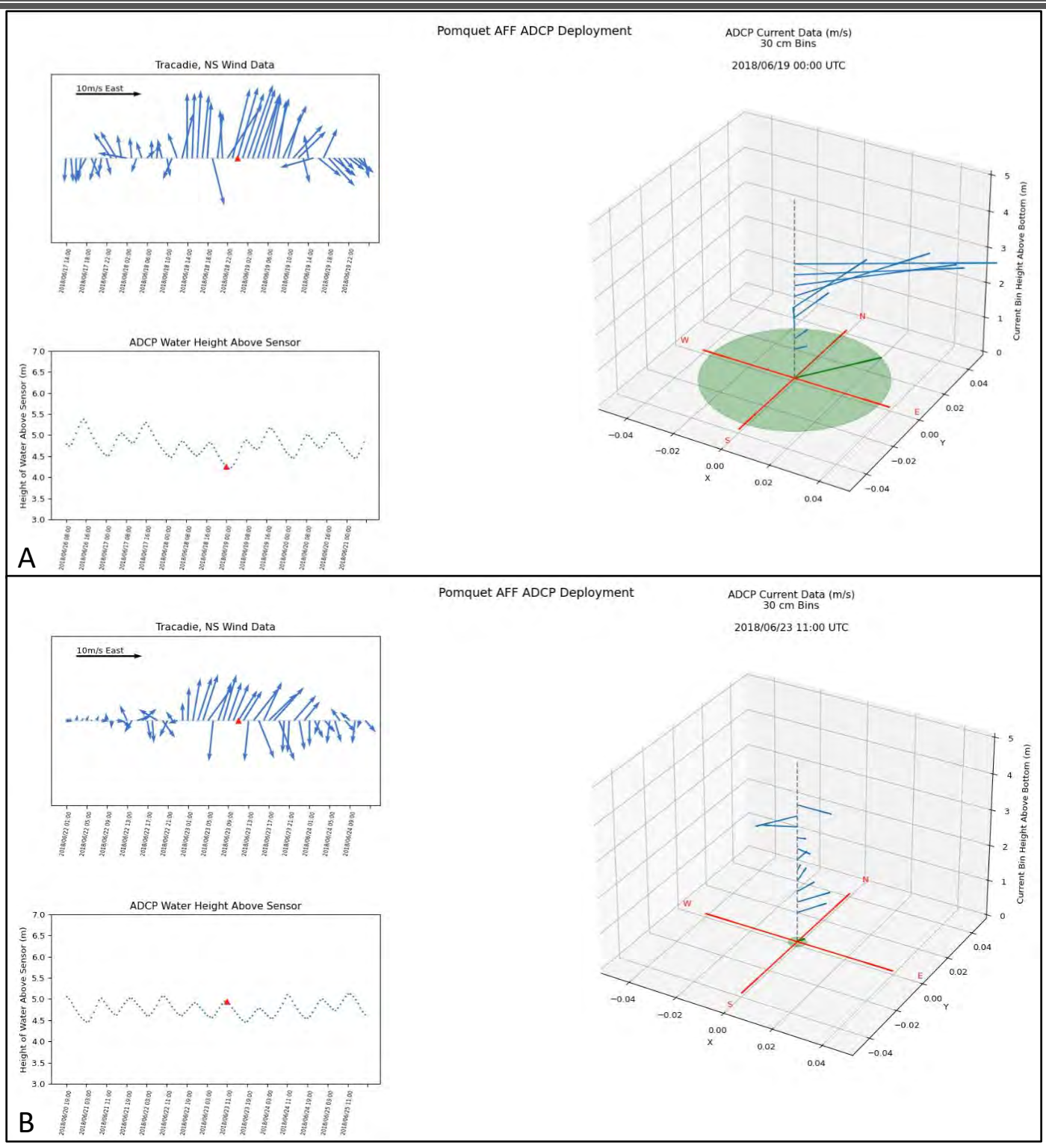

Figure 52: Frames from the ADCP animation. Upper left graph shows the wind direction and speed from the Tracadie weather station. The bottom left graph shows the water level above the sensor. The right graph shows the 30 cm bins of current velocity (magnitude and direction) as well the depth averaged current (green line and circle). (A) Currents during low tide with strong southerly winds. (B) Currents during high tide with moderate southerly winds.

The ADCP also captured two anomalous events on June 18-19 and a storm surge event on June 26th. Although the winds on June 26th were from the north-northeast, the currents increased dramatically to the northeast, and the water level increased by 20 cm (Figure 53).

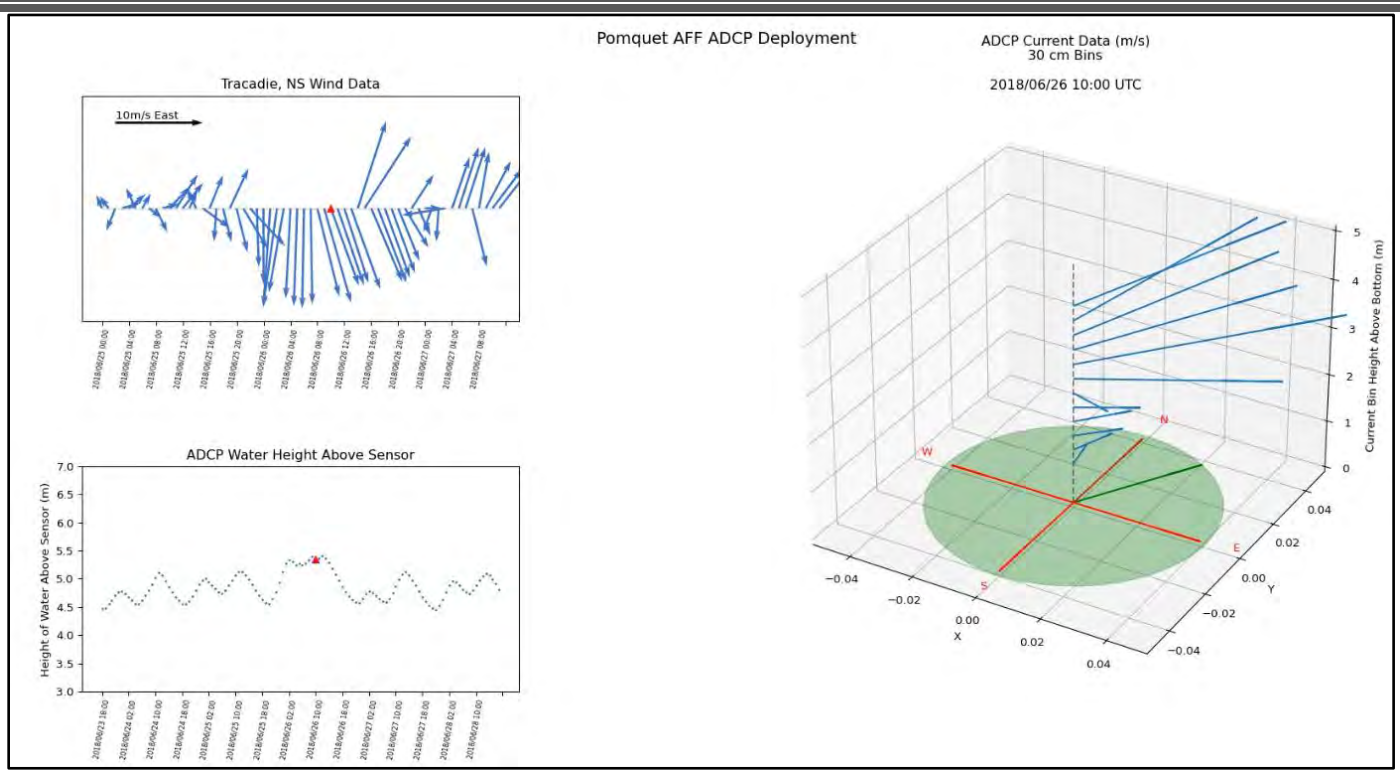

Figure 53: Frame from the ADCP animation for June 26th storm surge. Upper left graph shows the wind direction and speed from the Tracadie weather station. The bottom left graph shows the water level above the sensor. The right graph shows the 30 cm bins of current velocity (magnitude and direction) as well the depth averaged current (green line and circle).

The current speed and direction are strongly influenced by wind events even though Church Cove, where the ADCP was deployed, is quite sheltered (Figure 54). Although the currents increased during these events, it did not appear that the waves significantly increased, apart from June 26th, when waves reached magnitudes of 20-30 cm (Figure 22). The lack of significant waves was probably a result of the lack of fetch for the wind to generate large waves. The strong winds also affected the water level, for example, the strong southerly winds on June 19th produced a lower than usual water level and the strong northerly winds on June 26th produced higher than normal water levels (Figure 55).

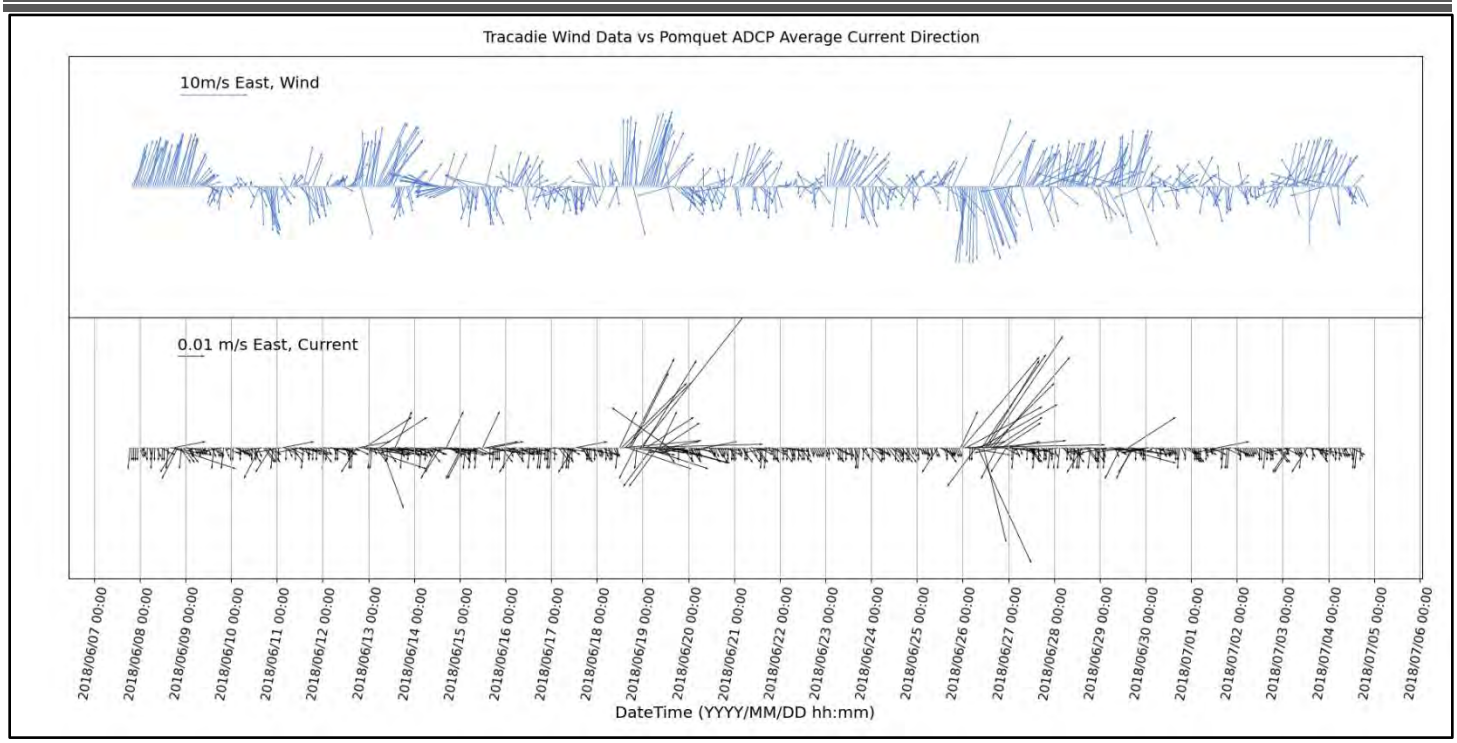

Figure 54: Wind from Tracadie weather station (top) and average current velocity from the ADCP (bottom) for the June-July 2018.

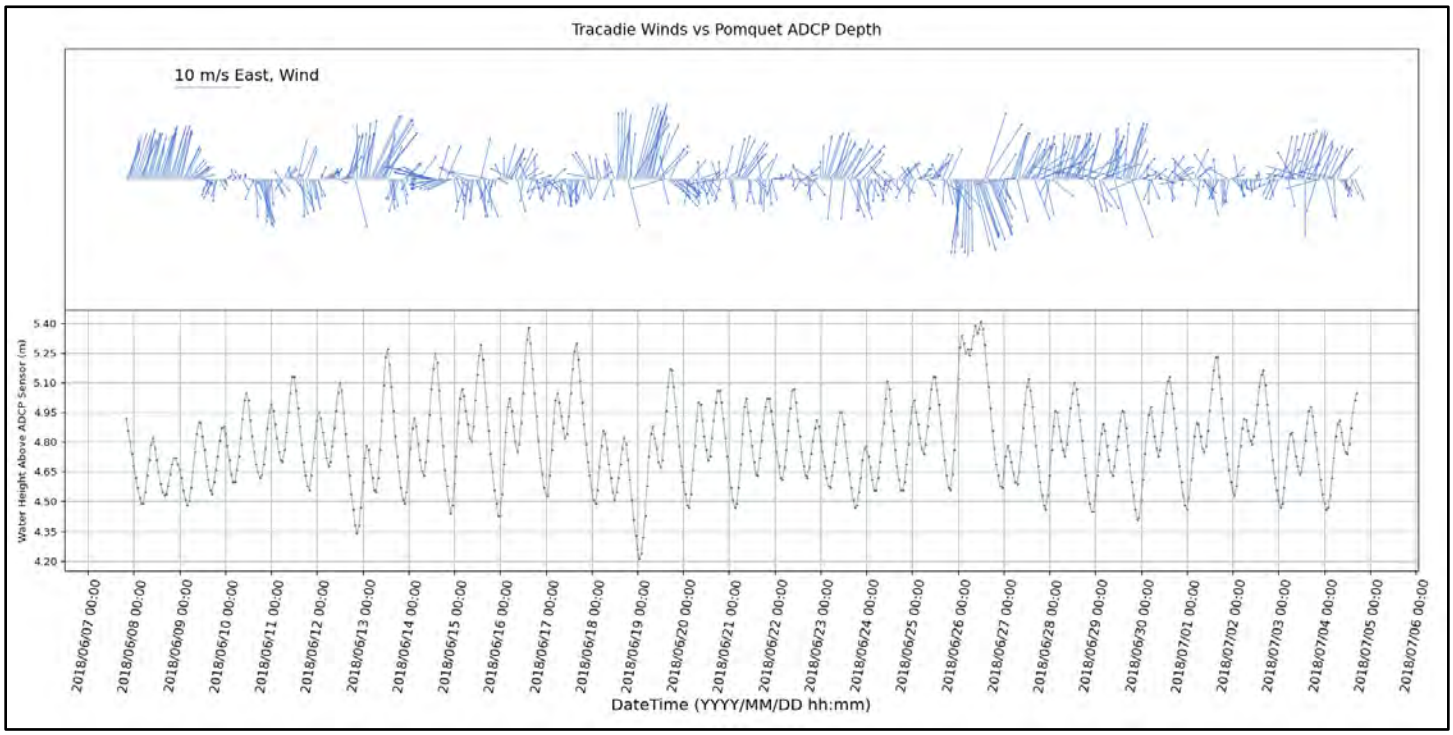

Figure 55: Wind from Tracadie weather station (top) and water height above the ADCP (bottom) for the June-July 2018.

3.7 Hydrodynamic Model Products

Several map products were derived from the results of the hydrodynamic modelling, including mean and maximum monthly currents, flushing time, significant wave height from the predominant wind based on data from Tracadie from 2003-2020, particle tracking for oyster spat, and the impact of a 1.5 m storm surge.

3.7.1 Mean and Maximum Currents

Mean and maximum monthly currents were extracted directly from the hydrodynamic model. A Txstat tool from Mike Zero toolbox was used to calculate the statistics on the converted unstructured mesh file. The continuous mean currents raster showed the actual values (Figure 56). The classification scheme chosen for the currents showed that the mean currents in most of the harbour, including the deep pools in Church Cove, were less than 0.1 m/s (Figure 57).

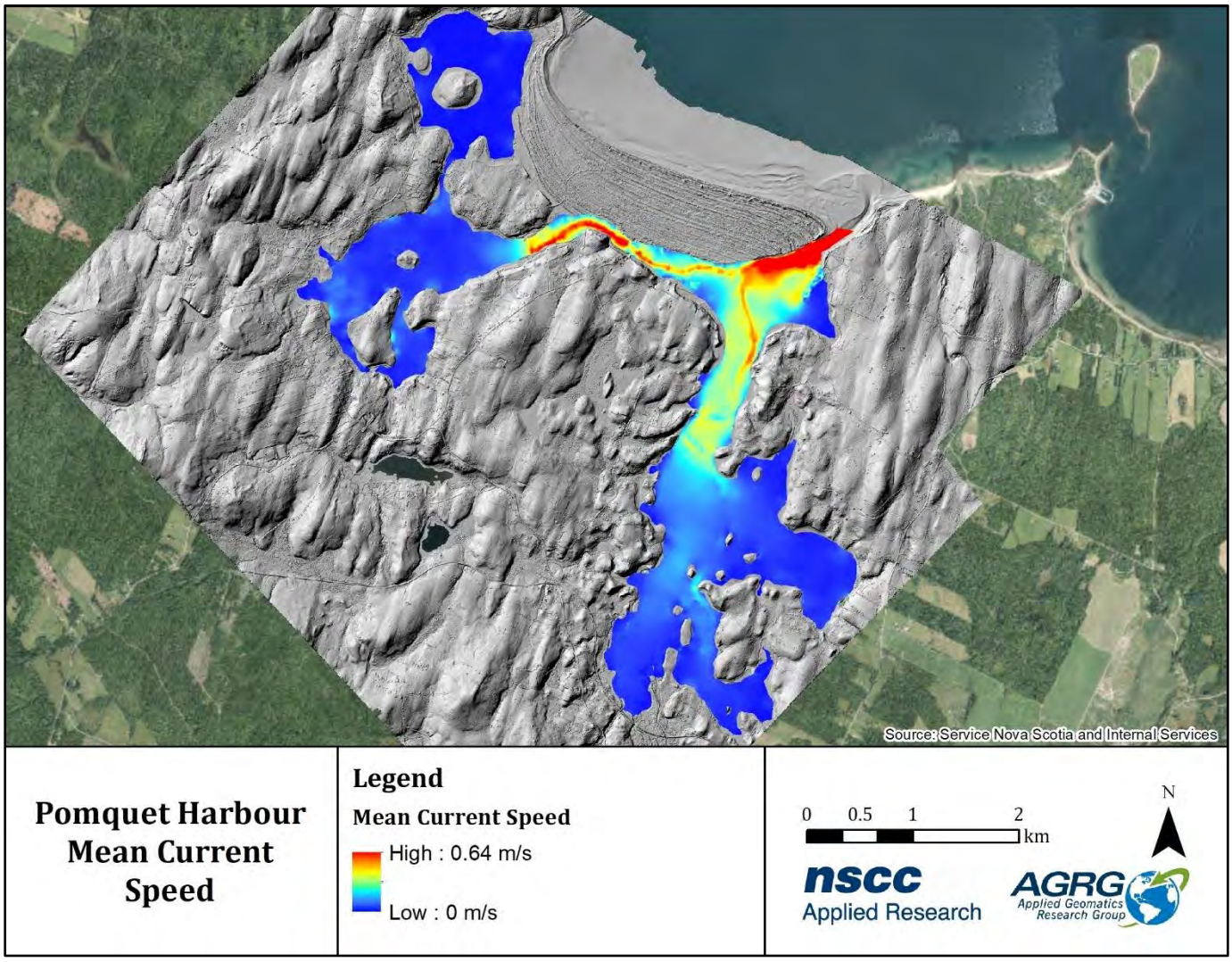

Figure 56: Mean of current magnitudes (m/s) during a 33-day simulation of the hydrodynamic model displayed as a continuous raster.

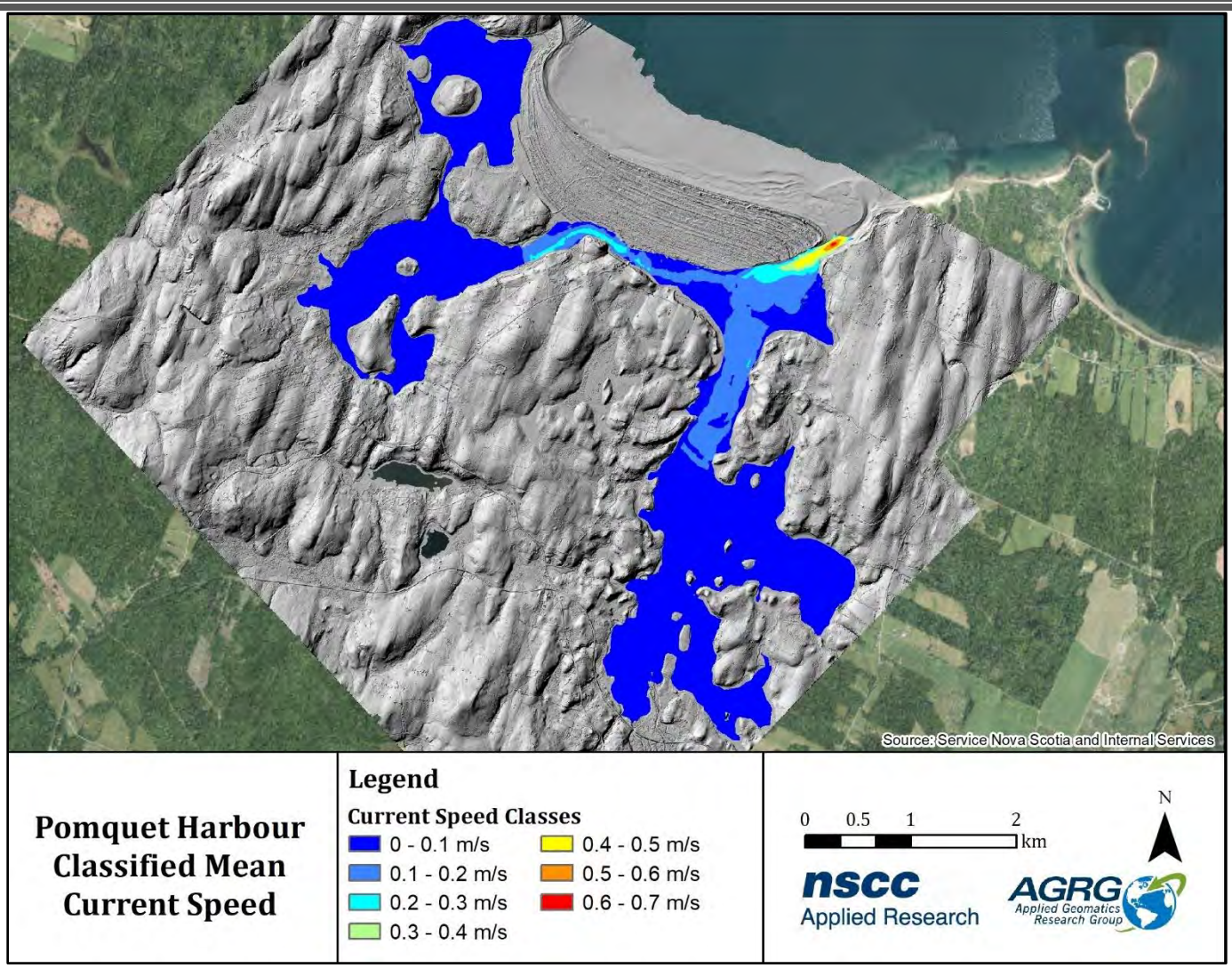

Figure 57: Mean of current magnitudes (m/s) during a 33-day simulation of the hydrodynamic model classified into seven speed categories.

The continuous maximum monthly current speed raster showed that near the mouth of the harbour, the speed was the fastest, with 1.27 m/s, and the current magnitudes varied in the channels coming to the east and west side of the bay (Figure 58). The monthly maximum current magnitudes were classified into thirteen categories (0.1 m/s increments) and show that the maximum currents were between 0 and 0.1 m/s in most of the harbour, faster in the channels (0.2 – 0.6 m/s) and were greater than 0.6 m/s at the mouth (Figure 59).

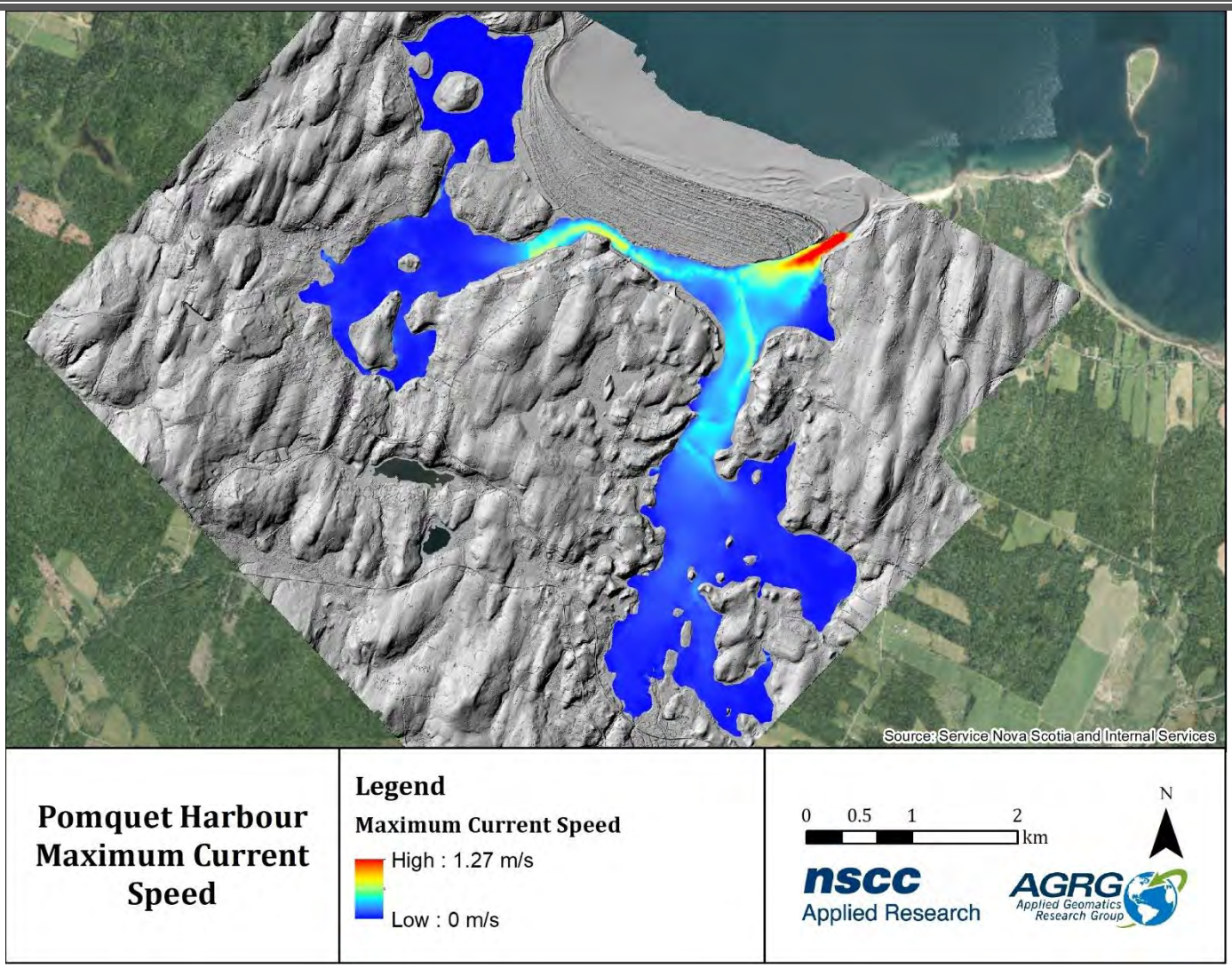

Figure 58: Maximum value of current magnitudes (m/s) during a 33-day simulation of the hydrodynamic model displayed as a continuous raster.

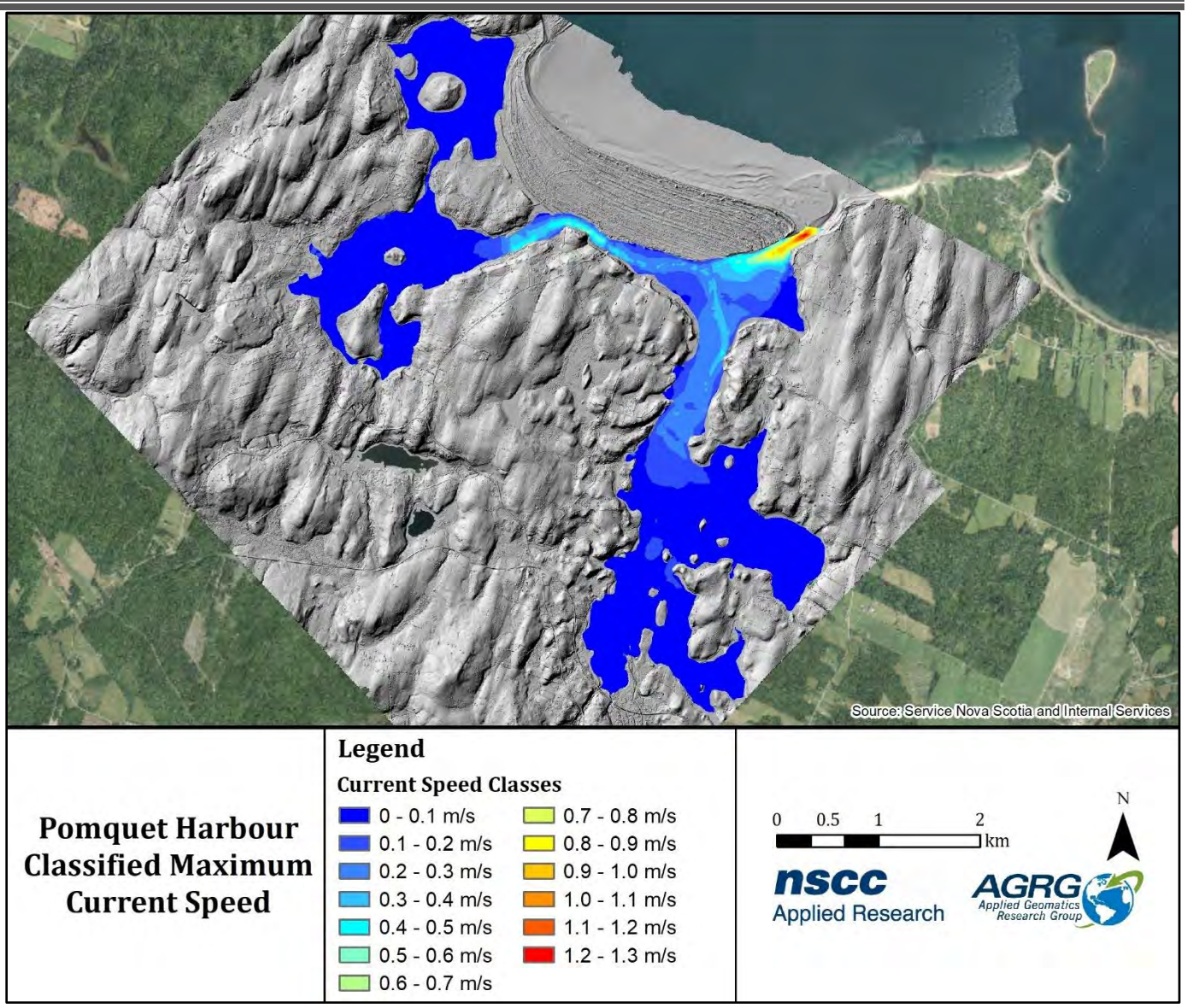

Figure 59: Maximum value of current magnitudes (m/s) during a 33-day simulation of the hydrodynamic model classified into thirteen speed categories.

3.7.2 Significant Wave Height (Hs)

Waves modelled using the Spectral Wave module showed that the Hs in the harbour was very minimal. The continuous raster showed that in most of the harbour Hs was less than 2 cm when strong south-southwest winds (200°) were applied (Figure 60). The classified raster showed that the harbour had low exposure to south winds which was likely due to the land mass surrounding it (Figure 61).

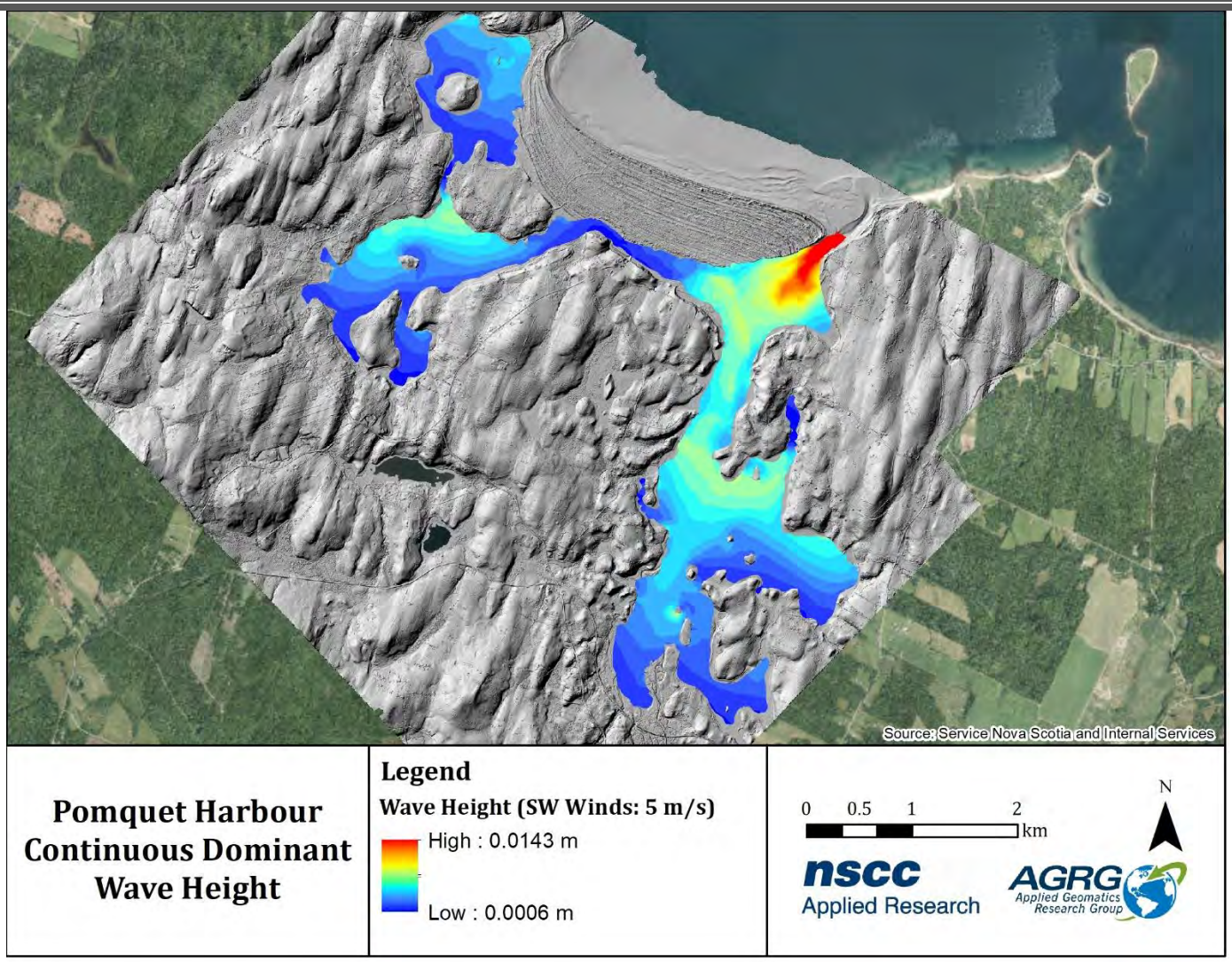

Figure 60: The continuous dominant wave height layer was generated by applying strong south-southwest winds to the model.

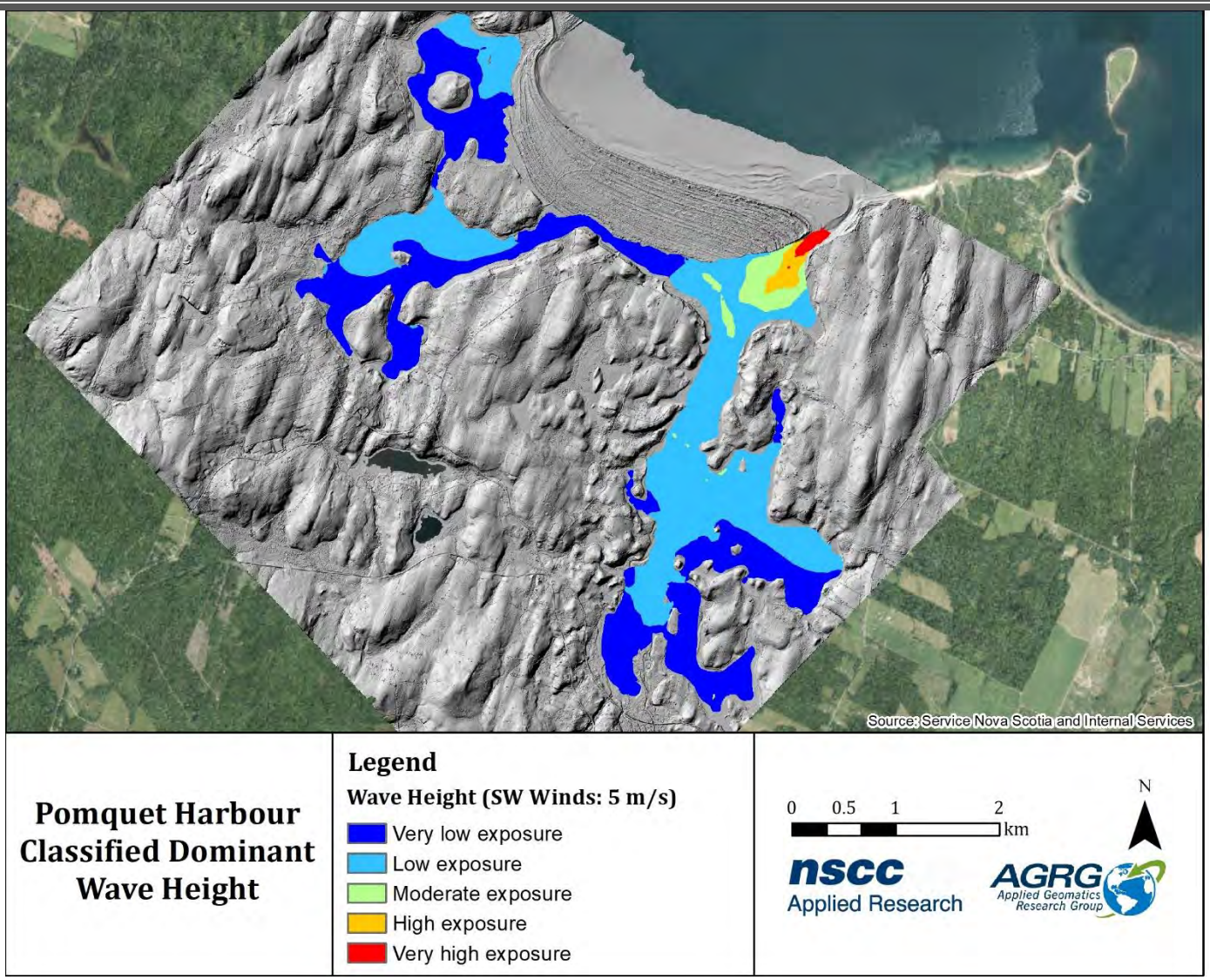

Figure 61: The classified dominant wave height layer was generated from modelled exposure to a south-southwest wind.

3.7.3 Flushing Rate

The minimum concentration left in the harbour after an initial concentration of one was added on the first day and then the transport model was run for 33 days indicated that the Church Cove area was flushed slowly compared to the rest of the harbour (Figure 62).

The flushing rate showed that the channels got flushed at a faster rate than at Church Cove and Monks Head. Fresh water into the bay also helped to flush the concentration (Figure 63). The classification of the flushing rate values represented five classes from very well flushed (0 - 20% concentration after one month), well flushed (20 - 40% concentration), 50% flushed (40 – 60% concentration), poorly flushed (60 – 80% concentration), and not flushed after one month (80 – 100% concentration) (Figure 63).

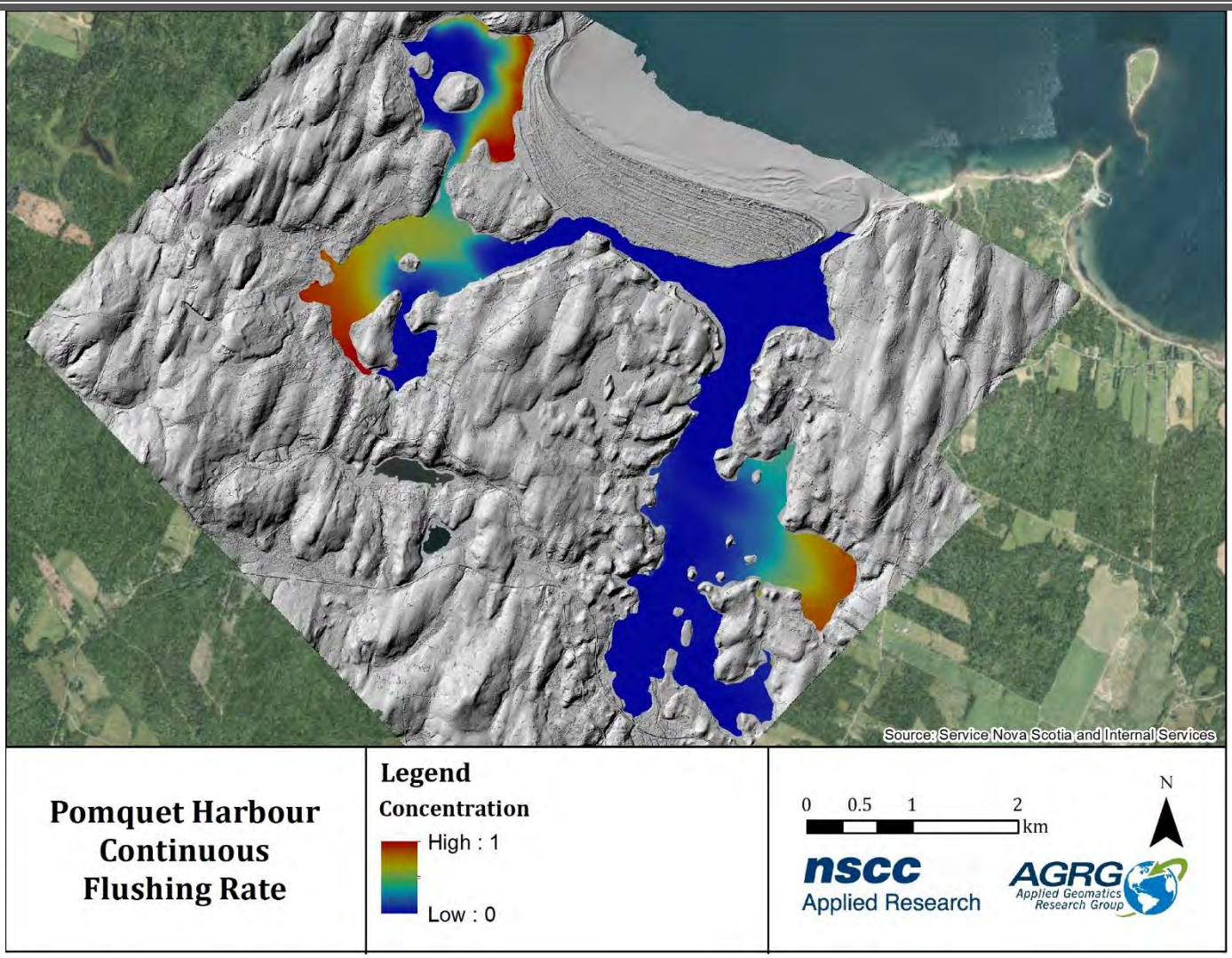

Figure 62: The continuous flush layer was generated from the minimum concentration left in the harbour after a 33-day simulation of the hydrodynamic model. The blue indicates faster flushing rates than the red areas.

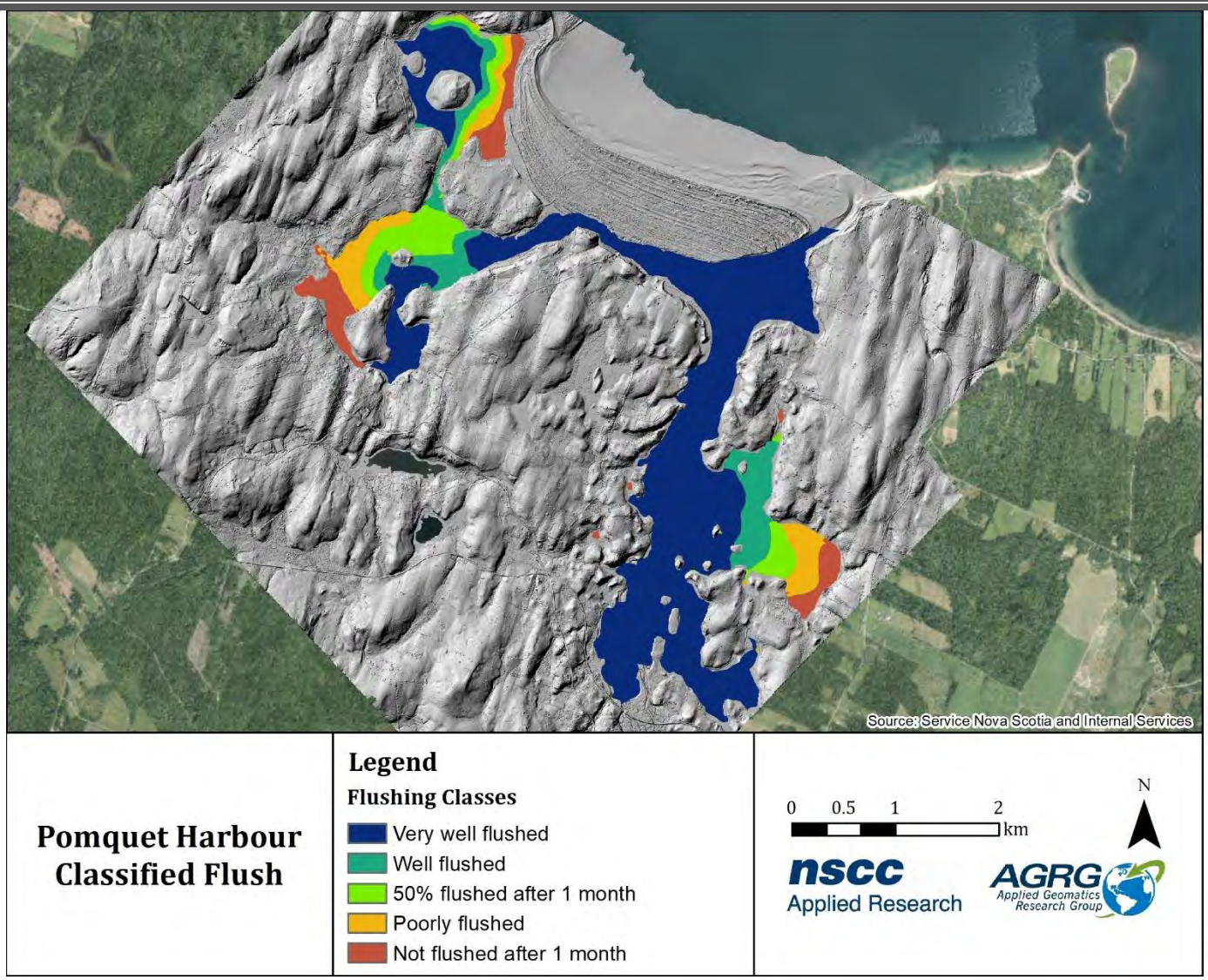

Figure 63: The minimum concentration left in the harbour after the hydrodynamic model simulation was classified into five flushing classes.

3.7.4 Storm Surge

The additional water levels of a 1.5 m storm surge were added to the tidal boundary condition of the hydrodynamic model that showed that the areas around the island and many parts in the harbour were potential zones for flooding (Figure 64). A water level with a high of 1.95 m could be observed in the harbour during a storm event.

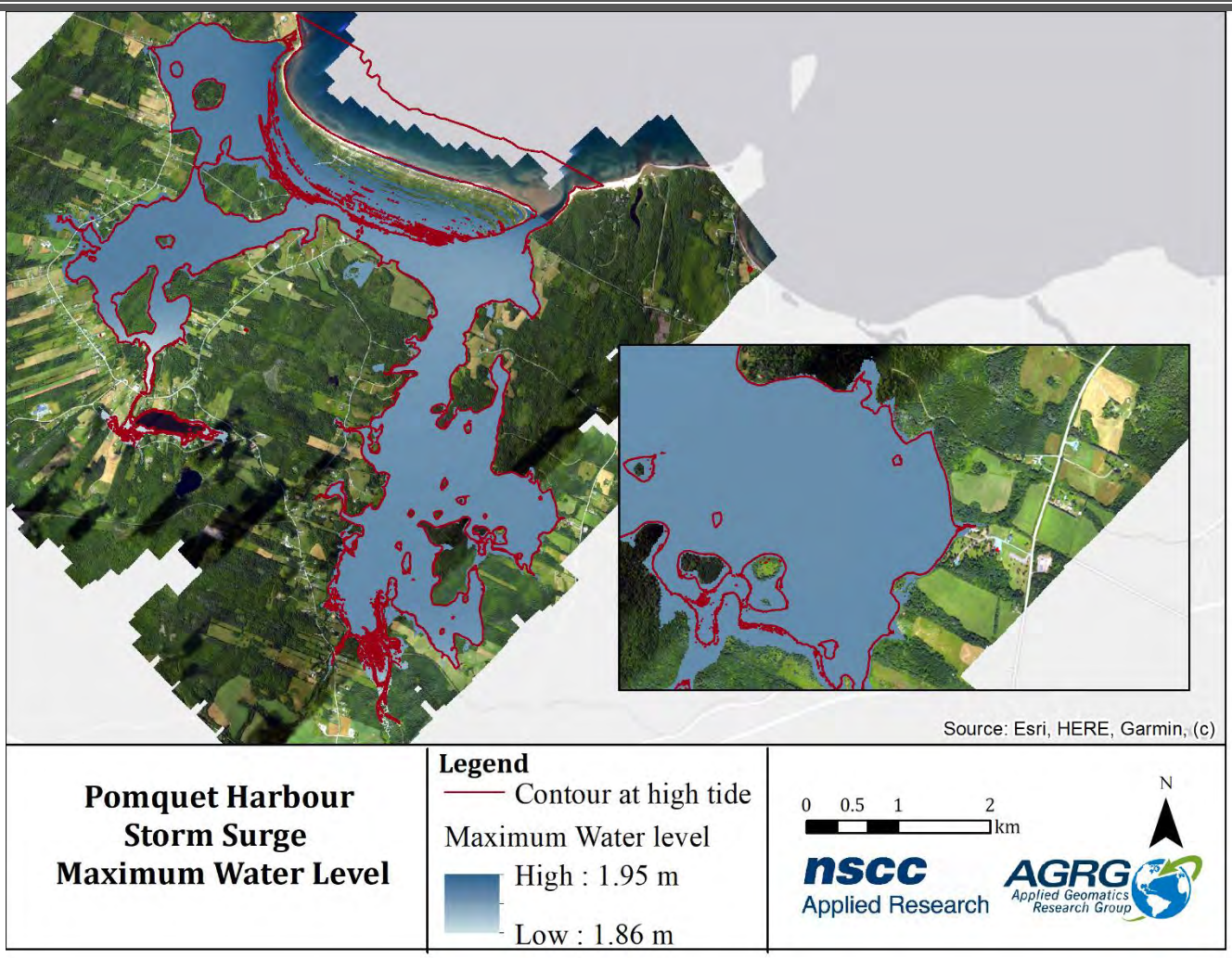

Figure 64: Maximum water level during storm surge, modelled in Mike 21 and a contour at high tide. Inset shows the water level in Church Cove.

Mean and maximum current speeds were slightly greater, especially near the mouth of the harbour, when compared to regular tides (Figure 65; Figure 66). Maximum current speed near the mouth on a storm surge, as modelled in Mike 21, showed a value of 1.78 m/s. It was also observed that the current speed in the channel to the Monks Head harbour was greater than usual.

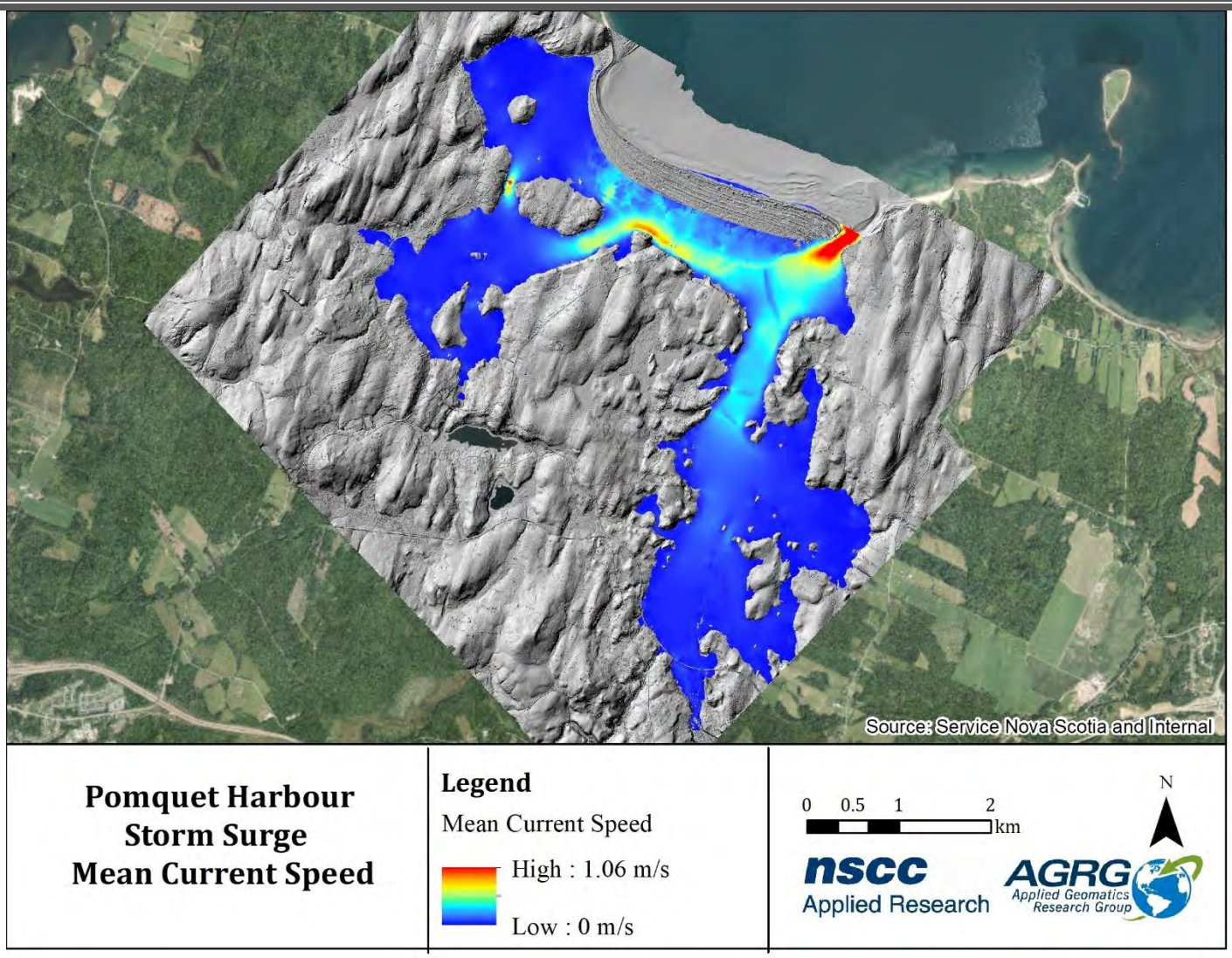

Figure 65: Mean Current magnitudes during a storm event modelled in Mike 21 Flex Mesh.

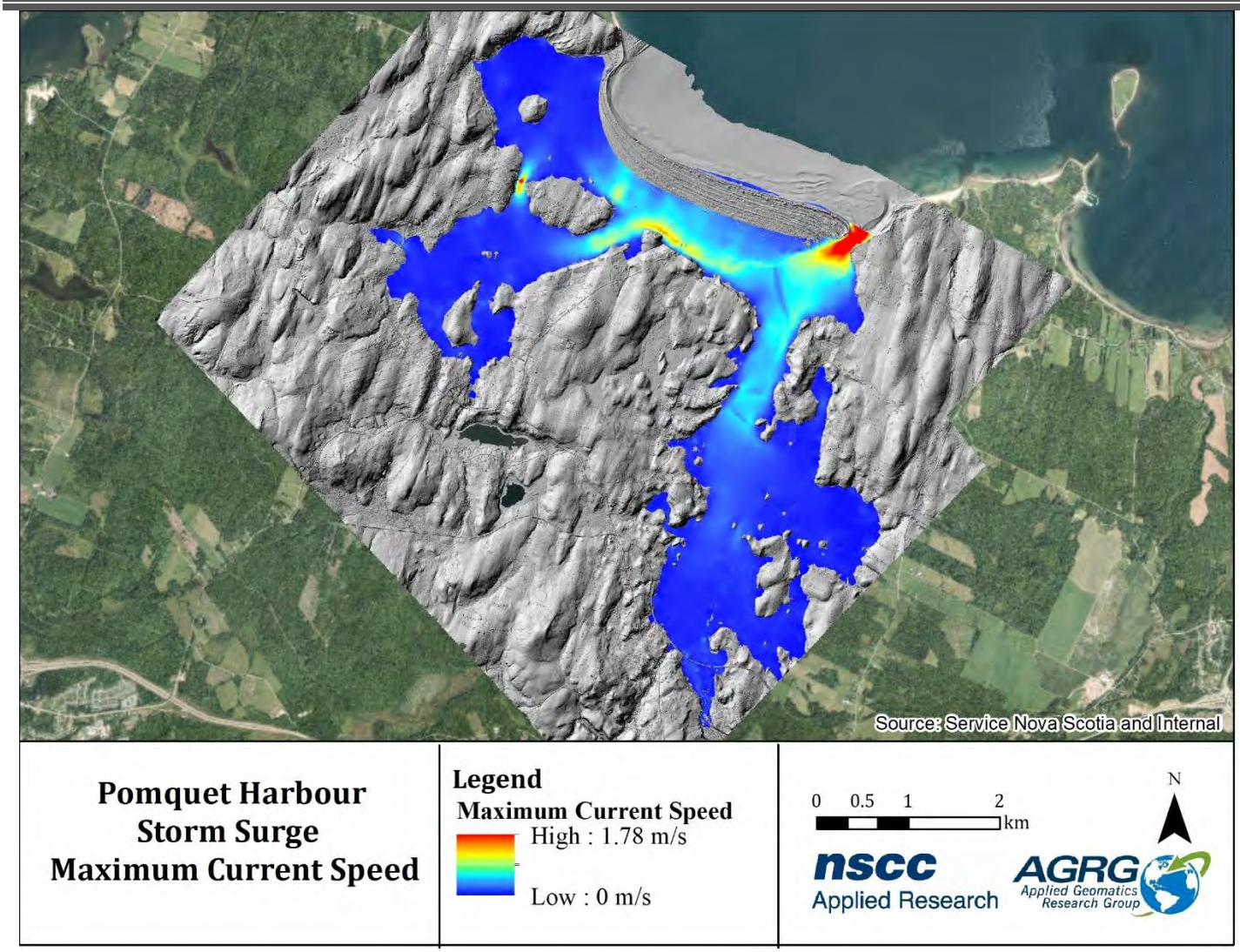

Figure 66: Maximum current magnitudes during a storm event modelled in Mike 21 Flex Mesh.

3.7.5 Particle Tracking

The validated hydrodynamic model was used to support a particle tracking simulation developed to model an oyster spat release event. Spat particles were dispersed by water movement generated in the HD model and natural horizontal dispersion (0.01 m^2/s). Initial release concentrations varied based on the release potentials of each of the identified natural oyster reef production areas (Figure 67).

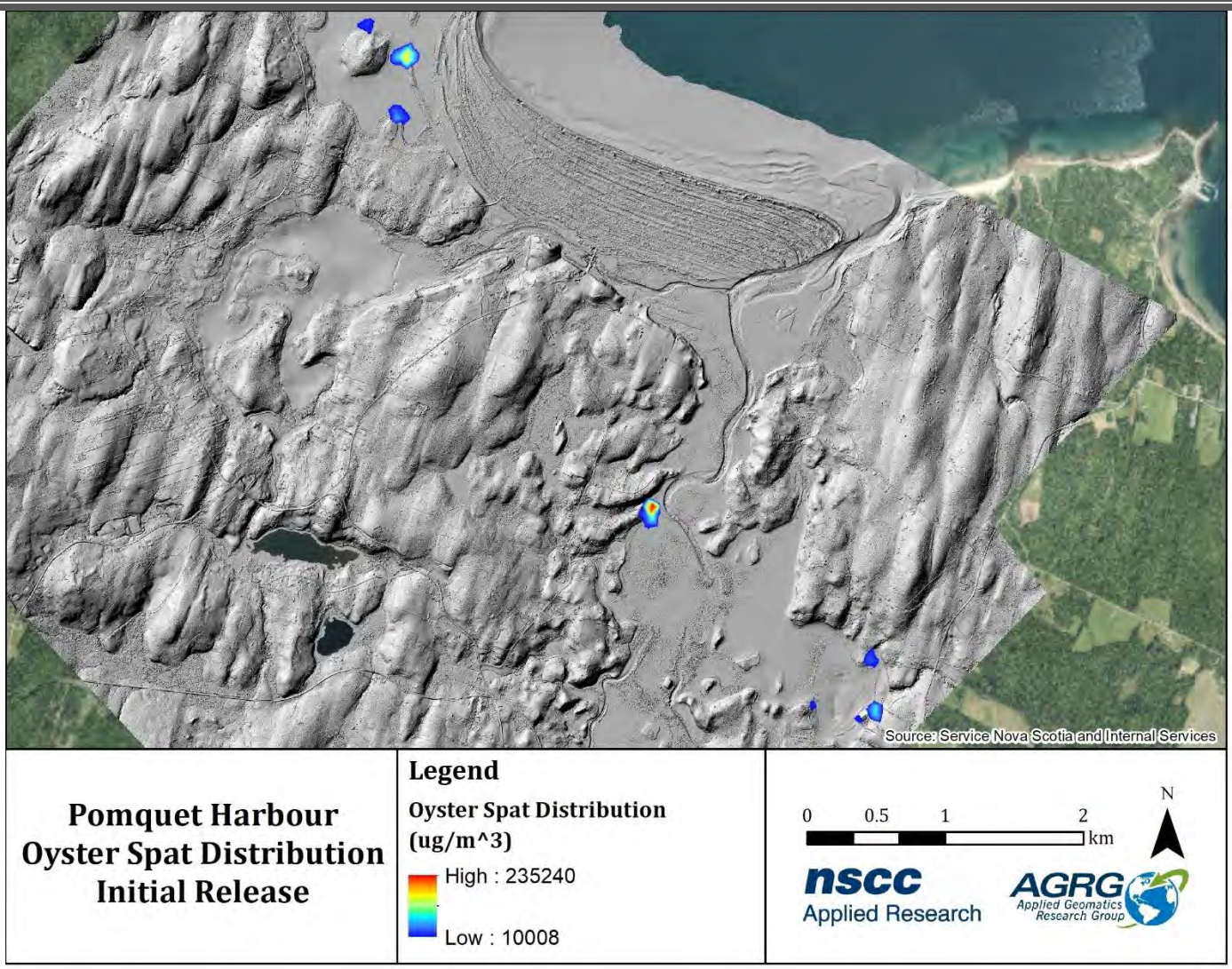

Figure 67: Simulated oyster spat concentrations during the initial model timesteps.

The fate of spat particles was heavily determined by the tidal action at the time of settling roughly two weeks after initial release. Since this variability could not be predicted, it was determined that spat distribution results should be generated for both an outgoing tide settling event and an incoming tide settling event. Particle tracking results were qualitatively assessed for each of the events and showed that outgoing tides presented a linear distribution of particles along the main channel with a significant concentration occurring along the western coast of the bay. High concentrations were also found to be present in the coastal areas around the eastern bay where natural spat producers were identified. Additionally, very high concentrations were modelled for the northwest bay where little to no tidal influence impacted the distribution of spat (Figure 68).

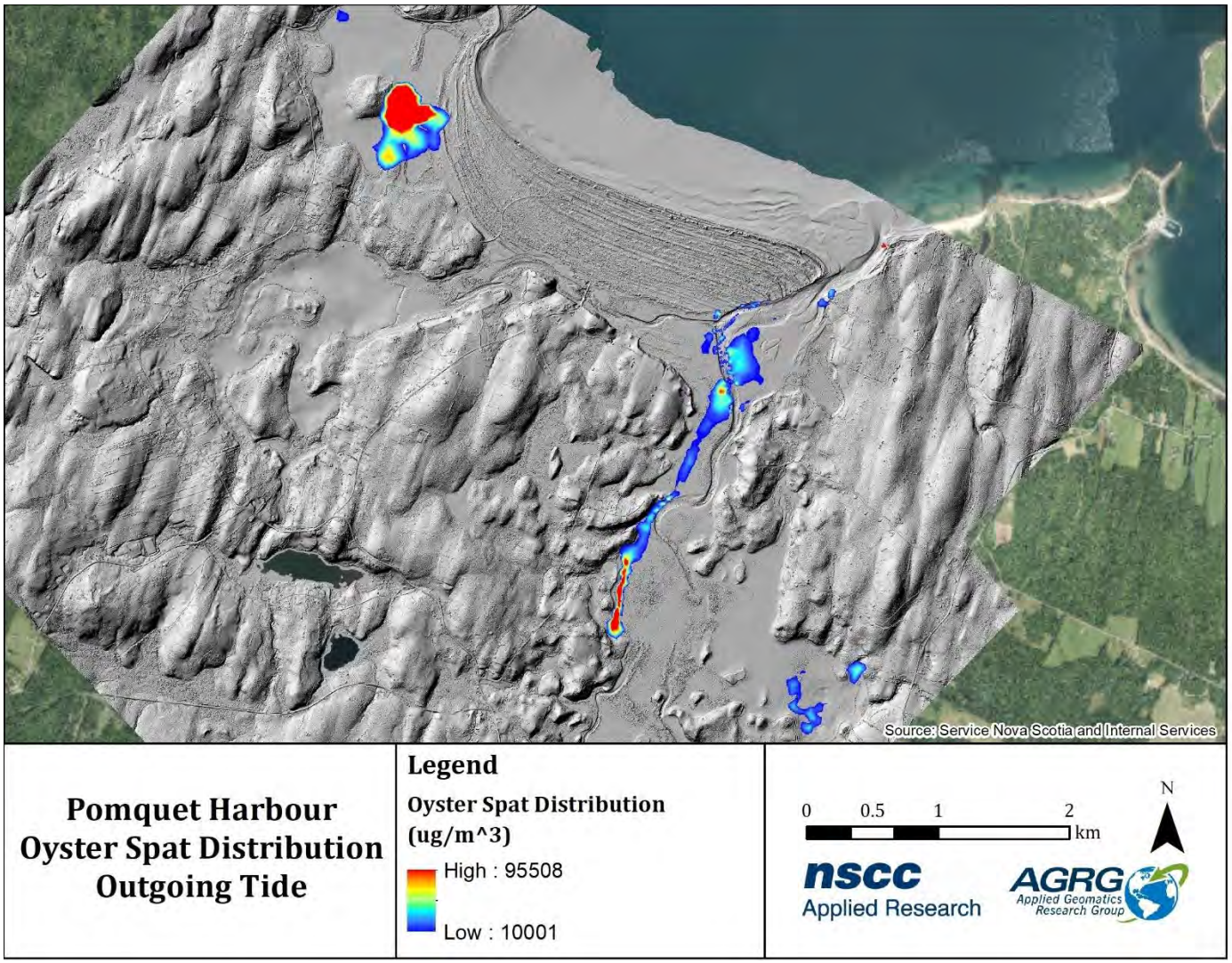

Figure 68: Modelled spat distribution during an outgoing tide scenario. Highest concentrations were observed in the northwestern bay which exhibited minimal tidal distribution.

The fate of particles was found to be much different if settling occurred on an incoming tide. More spreading was observed as water was pushed outward from the main channels resulting in the distribution of particles along the surrounding shallow-water areas. Three main areas were identified as having high concentrations of spat distribution on incoming tides, including the northwest isolated bay, the western shore south of a major contributing oyster reef, and the northern shore of the east bay where particles from several sources were concentrated on incoming tides (Figure 69).

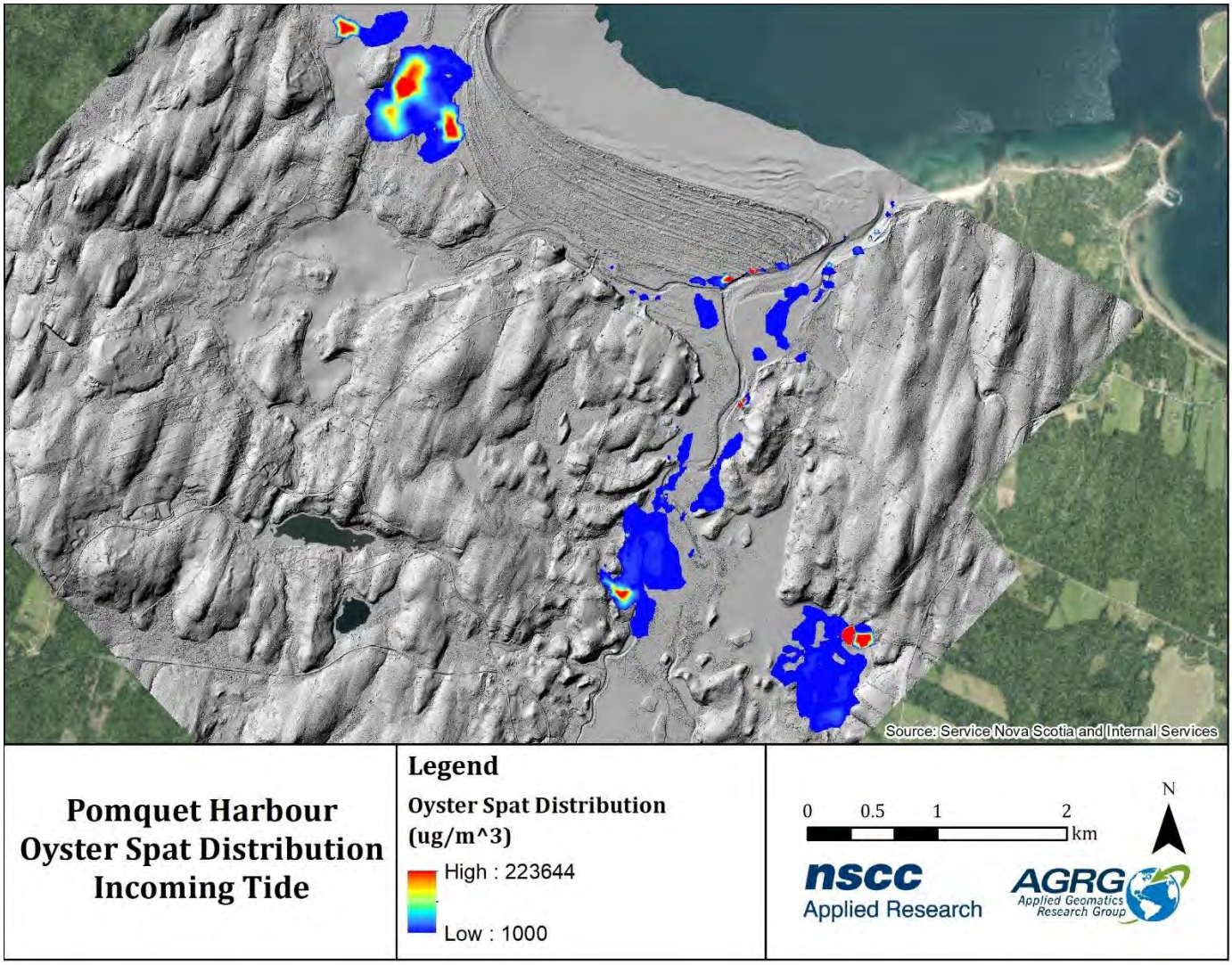

Figure 69: Modelled spat distribution during an incoming tide scenario. Highest concentrations were observed in the southeastern bay where onshore forcing concentrated particles on the north shore.

4 Validation

4.1 Lidar Validation

4.1.1 Topographic Validation

To validate topographic lidar returns on areas of hard and flat surfaces, ground elevations were obtained using a Real-Time Kinematic GPS with corrections transmitted via SmartNet network. The GPS unit was mounted on a vehicle and was driven around while collecting points every second. A total of 1,364 GPS points was collected along roads and bridges in the study site. 1,216 GPS points were within the tolerance of survey grade position precision. The elevation difference (Dz) was calculated by extracting the Z from the DEM at the points and subtracting them from the GPS elevations. A mean of 0.03 m with a standard deviation of ± 0.10 m showed that the topographic lidar points met the validation requirements within the specifications of the system (Figure 70).

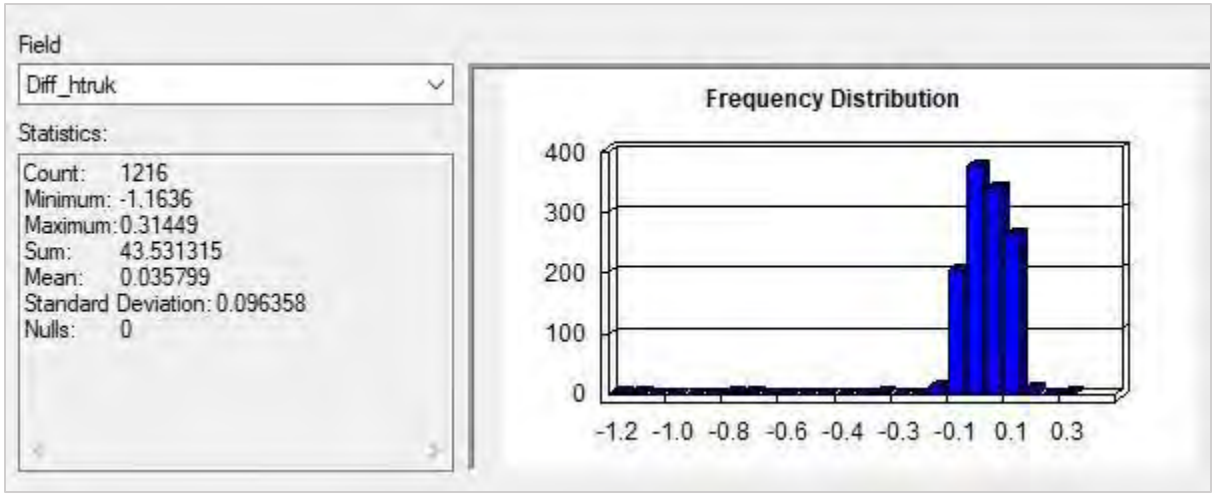

Figure 70: Validation statistics for topographic points.

4.1.2 Bathymetric Validation

For bathymetric lidar validation, several GPS points were collected at various locations in the harbour using a receiver with RTK corrections mounted on a painter's pole. A total of 11 points were collected. The elevation difference (Dz) was calculated by extracting the Z from the DEM at the points and subtracting these from the GPS elevations, which gave a mean of -0.04 m with a standard deviation of ± 0.19 m, as shown in the below figure (Figure 71).

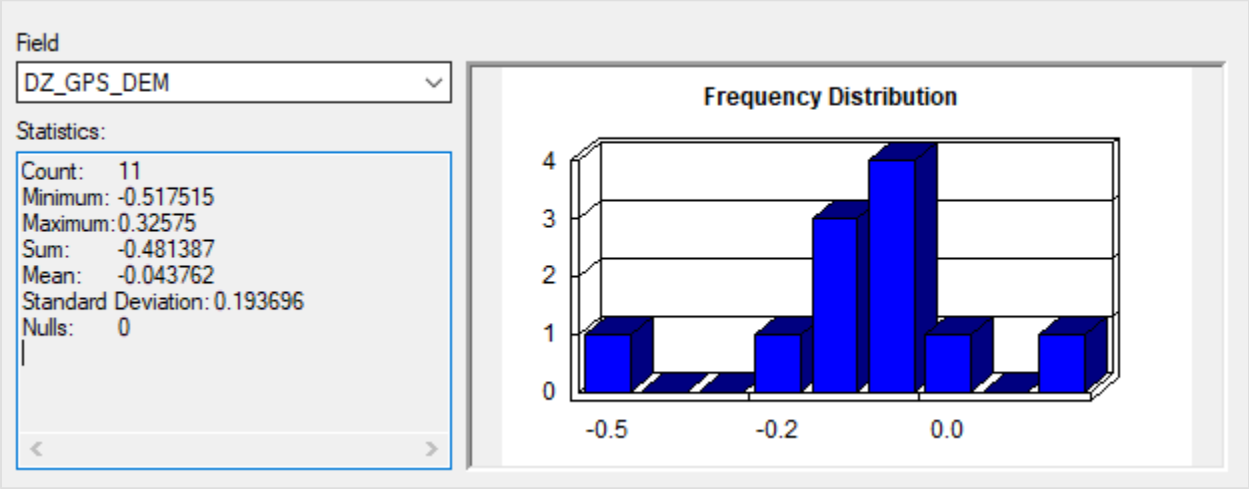

Figure 71: Validation statistics for bathymetric points.

There were certain areas where the lidar could not penetrate and hit the seabed due to the clarity of the water or depth, and other areas where the underwater vegetation was very thick which resulted in the higher standard deviation than on land. The GPS points where the lidar did hit the bottom showed that the bathymetric lidar points meet the validation requirements within the specifications of the system.

4.2 Hydrodynamic Model Validation

Simulated water levels and current characteristics were extracted from the hydrodynamic model at the point where the ADCP was deployed for the duration of the deployment. These data were compared against ADCP observations to validate the accuracy of the developed model. Simulated water levels matched ADCP observations for the majority of deployment period and were superior to standard predicted tidal elevations which severely over-predicted low tide values (Figure 72).

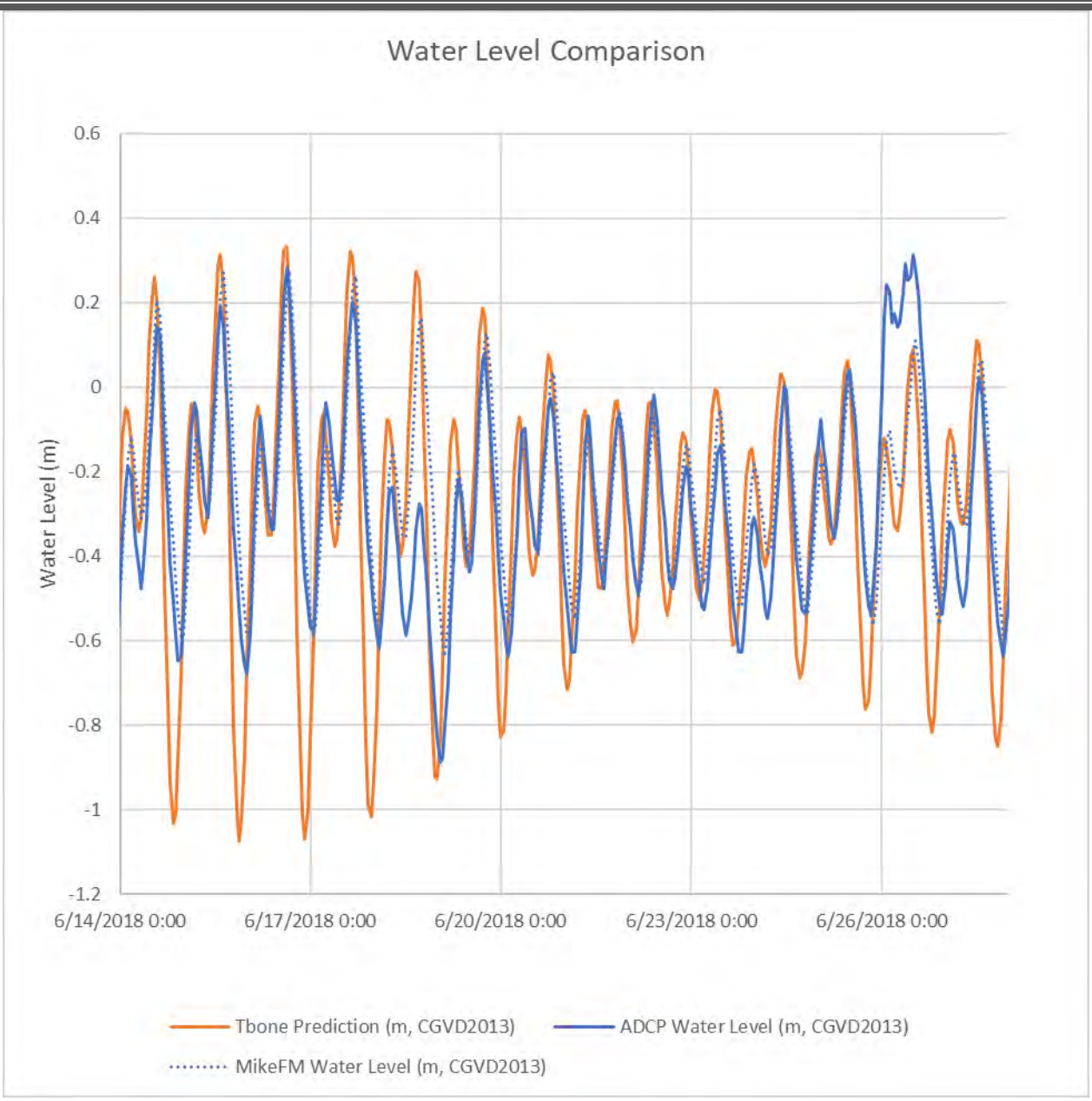

Figure 72: Simulated water levels from the Mike FM hydrodynamic model (blue dash) show good agreement with ADCP observations (blue line) over the validation period in contrast to tidal predictions (orange line).

Major deviations occurred on June 19th during a low-pressure system which occurred with strong offshore winds and similarly on June 26th during a high-pressure system which also occurred with strong onshore winds. The model was not able to force the volume of water necessary to allow the simulated events to match observed water levels during the anomalous events (Figure 73). Simulation results may be improved by extending the model boundary 5 to 10 km north to allow for additional fetch and transfer of water from the Northumberland Strait into the Pomquet system.

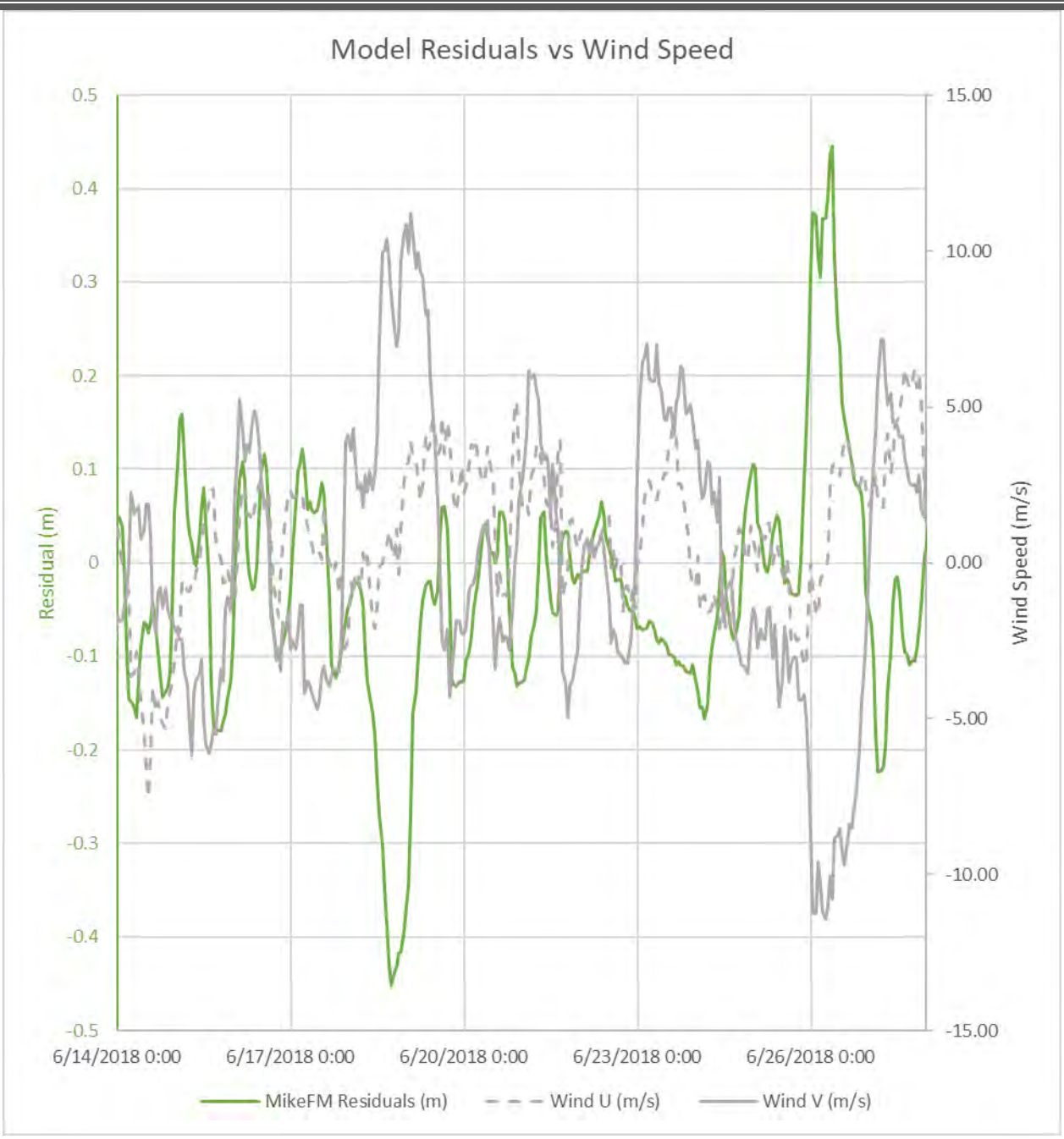

Figure 73: Residual water level (+ observation above simulation, - observation below simulation; green line) plotted against wind velocity components as Wind U (+ East, - West; grey dash) and Wind V (+ North, - South; grey line) showing inverse relation between residual water level and V component velocity.

Hydrodynamic model results demonstrated that simulated water levels matched ADCP observations. When comparing current magnitudes and directions it was found that simulated current magnitudes matched ADCP values in many cases, but simulated directions did not agree with ADCP observations in several cases (Figure 74).

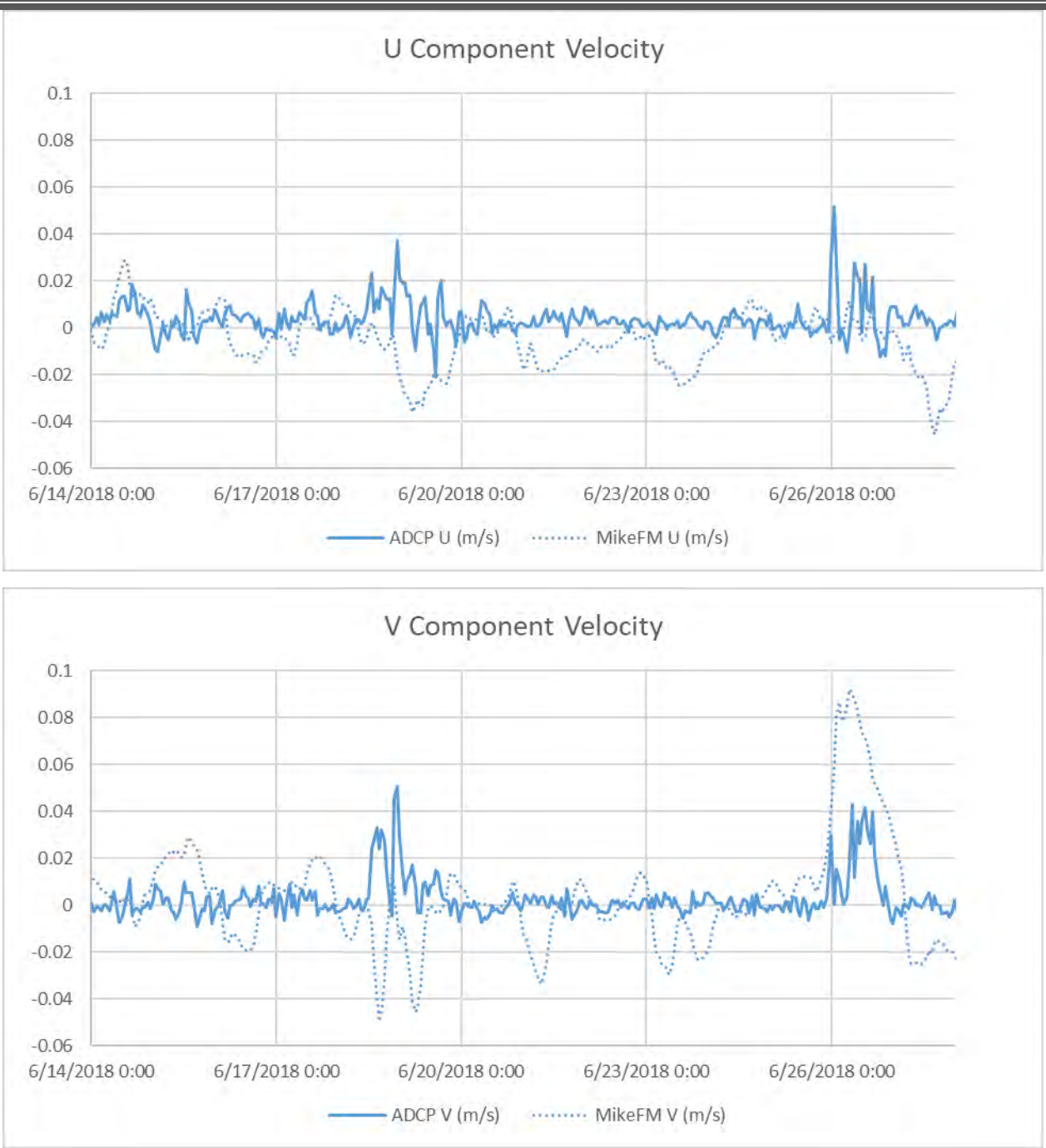

Figure 74: Simulated and observed current velocities presented as Velocity U (+ East, - West; top) and Velocity V (+ North, - South; bottom) showing a dominant V component in both the simulated and observed currents with a high degree of variation between the modelled and observed values.

This disagreement was most likely caused by the complex eddying pattern within the ADCP deployment area. Deviations between the true and modelled coastal morphology could have affected the simulated eddy locations which would result in erroneous current directions. The complexity of the modelled system is evident when comparing an incoming spring tide which produced northward currents over the ADCP and a neap tide which produced southeastward currents over the ADCP location (Figure 75).

Figure 75: Comparison of incoming spring and neap tidal currents which were found to produce complex and variable eddy patterns over the ADCP validation point (red).

While this result was not optimal, it is often the case that simulated current directions are not in good agreement with ADCP observations. The complexities of the true environment are often not perfectly reflected in the model parameters.

Additionally, current directions and magnitudes were calculated as depth averaged values in the hydrodynamic model which produced two-dimensional results that do not fully represent the layering of current velocities throughout the water column. For these reasons, model results were determined to be acceptable for the study area while accepting that directional errors existed within the complex bay areas. Hydrodynamic model simulations produced stable realistic current results throughout the study area (Figure 76).

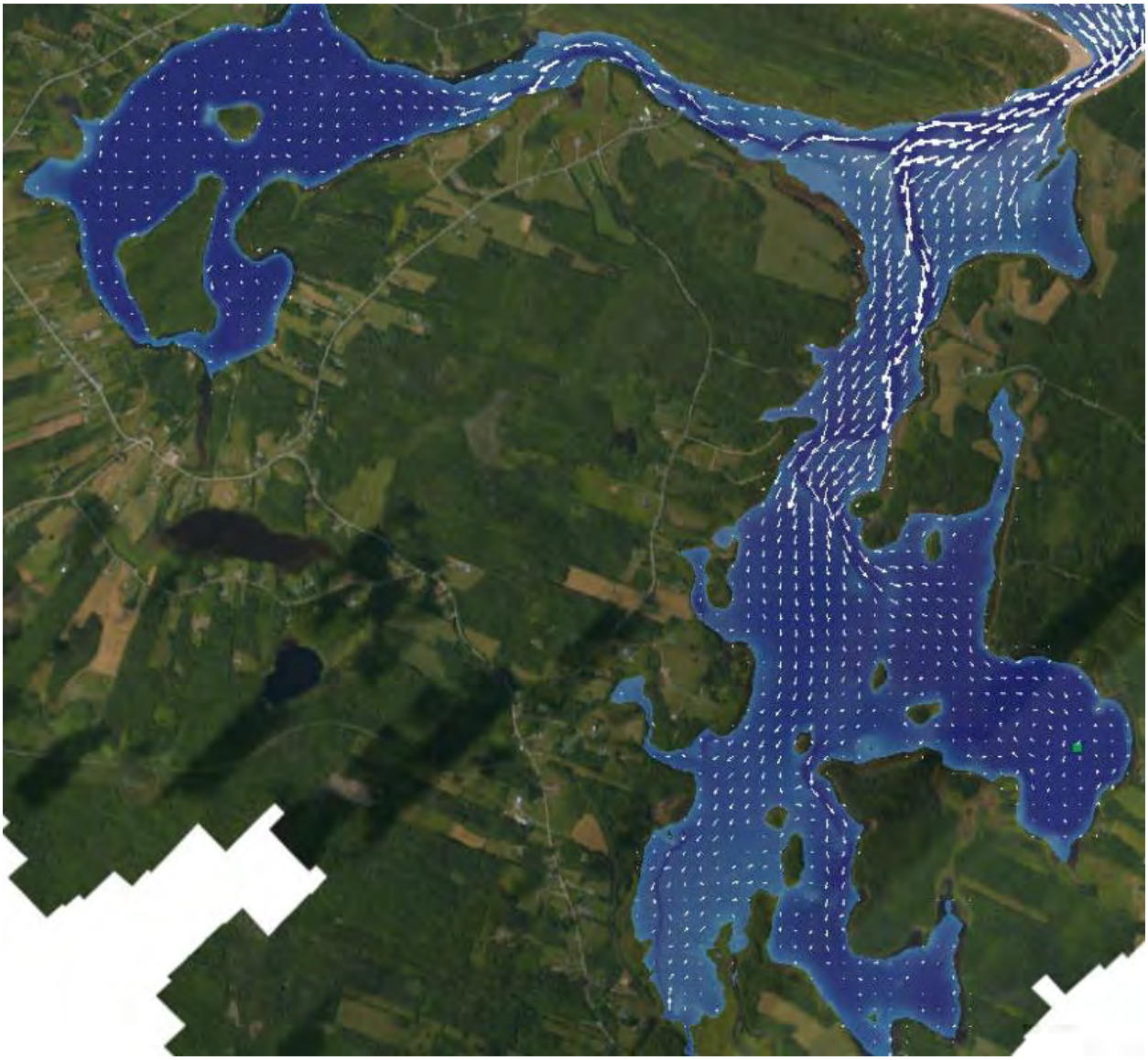

Figure 76: Simulated current magnitudes and directions modelled during the peak flow of an incoming tide.

5 Aquaculture Suitability Index

5.1 GIS Data Layers

Data layers generated for the Web Visualization Application and the Weighted Overlay tool were derived from a variety of sources. ArcMap Desktop version 10.8.3 was used to process and project the layers to Universal Transverse Mercator projection (UTM, Zone 20N), and reference them to the North American Datum: Canadian Spatial Reference System of 1983 (CSRS NAD83) and the Canadian Geodetic Vertical Datum of 2013 (CGVD2013). Table 6 shows each of the data layers and the source from which they were generated.

Data Source	Data Layer
DEM	Intertidal Zone
	Classified Ice Impact-free Depth Map
	Continuous Depth
	Classified Depth
	Depth Contours
	DEM Colour Shaded Relief
	DEM Hillshade
DSM	DSM Colour Shaded Relief
	DSM Hillshade
Lidar Intensity	Intensity Model
	Normalized Bathymetric Intensity Model
DEM + Lidar Intensity	DEM Colour Shaded Intensity Model
Orthophoto	RGB Orthophoto
	Near IR Orthophoto
DEM + Orthophoto	Classified Channel
	Classified Eelgrass Presence
Hydrodynamic Model	Continuous Mean Monthly Currents
	Classified Mean Monthly Currents
	Continuous Maximum Monthly Currents
	Classified Maximum Monthly Currents
	Continuous Dominant Wave Height
	Classified Dominant Wave Height
	Continuous Flushing Rate
	Classified Flushing Rate
	Oyster Spat Distribution: Initial Release
	Oyster Spat Distribution: Outgoing Tide
	Oyster Spat Distribution: Incoming Tide
DFO Traditional Ecological Knowledge (polygons)	Alewife
	American Eel
	American Smelt
	Atlantic Salmon
	Sea Trout
	American Oyster
	Blue Mussel
	Quahog
	Razor Clam
	Softshell Clam
DFO Traditional Ecological Knowledge (points)	Green Crab
Stuart Oyster Stock Survey (points)	Wild Oyster Locations
	Wild Oyster Spat Producers
	Number of Oysters Times Average Size
	Temperature
	Salinity
	Number of Oysters per Length (0 – 20 mm)
	Number of Oysters per Length (20 – 30 mm)
	Number of Oysters per Length (30 – 40 mm)
	Number of Oysters per Length (40 – 50 mm)
	Number of Oysters per Length (50 – 60 mm)
	Number of Oysters per Length (60 – 80 mm)
	Number of Oysters per Length (80 – 100 mm)
	Number of Oysters per Length (>100 mm)
Observed Data (points)	ADCP Deployment
NSFA (polygons)	Aquaculture Leases

Table 6: Data layers utilized by the Web Application and its components.

The index used to inform the aquaculture suitability map is described in the following section. For additional information on oyster site selection, the New Brunswick Department of Agriculture, Aquaculture and Fisheries provides a document that goes into detail about many of the main parameters (Doiron, 2008).

5.2 Weighted Overlay Suitability Model

Suitability modelling, also known as site selection or overlay analysis, involves the combination of spatial data from diverse sources which satisfy a set of criteria to produce an output map of potential (Bonham-Carter, 1994; AGRG, 2018). Suitability models identify the best location for specific phenomena; in this case, the most ideal locations for oyster aquaculture development in Pomquet Harbour. In raster overlay analysis, each cell or pixel of each input layer references the same geographic location, which makes combining characteristics of numerous layers into a single output map appropriate (ESRI, 2016a). Numeric values, or weights, are assigned to each characteristic or variable, allowing the user to mathematically combine the layers and assign a new value to each cell in the output layer.

The suitability model for this project was generated by using ArcMap's Weighted Suitability, which implements several of the steps for weighted suitability in one tool (ESRI, 2016b). Experts from DFO, NSFA, and CMAR were consulted for map weights and scores for this example. The process for this method begins with assigning each raster layer a weight in the suitability analysis (the sum of weights must add to 100%). For use in the Weighted Overlay tool, continuous rasters must first be grouped in to ranges and assigned a single value by using the Reclassify tool. The values in these rasters are then scored for the suitability analysis (1 to 9, with 9 being the most favorable). The next step in the process involves overlaying the rasters and using a layer weight to multiply each raster's suitability score. The total values are used to determine a suitability value which is written to new cells in an output layer. The resulting symbology of the suitability layer is reflective of the derived suitability values.

5.3 Suitability Model Parameter Weighting

A portion of the GIS layers described in the previous sections were selected to be used in the Weighted Suitability Model (Table 7; Figure 77). Each of the layers was assigned a weight (to add to 100%), and each of the classes was assigned a score (0-9). Classes that were assigned a score value of 0 were assigned a "Restricted" score in the Weighted Overlay tool, as the evaluation scale ranged from 1 - 9. The Restricted value assigns the minimum value of the evaluation scale set, minus 1, which equated to 0 in the output raster cells. The final Aquaculture Suitability Index was produced using the sum of the weighted layers and scored classes. This index indicates areas most and least suitable for oyster aquaculture development. Figure 78 shows the resulting Oyster Suspension Aquaculture Suitability map that was generated from the Weighted Overlay tool.

Layer	Layer Weight (%)	Class	Class Score (0-Not acceptable, 1-low 9-high)
Depth from low tide (m)	20	0 - 1	0
		1 – 2	2
		2 – 3	3
		3 - 4	7
		4 – 5	8
		5 – 6	9
		6 – 7	9
		7 – 8	9
		8 – 9	9
		9 – 10	9
Ice impact-free depth map	25	Ice Impact Zone	0
		Ice Free Zone 1 m	1
		Ice Free Zone 2 m	5
		Ice Free Zone 3 m	9
		Ice Free Zone 4 m	9
Eelgrass	20	Presence	1
		Absence	9
Average monthly current speed (m/s)	5	0 – 0.1	2
		0.1 – 0.2	8
		0.2 – 0.3	9
		0.3 – 0.4	9
		0.4 – 0.5	8
		0.5 – 0.6	7
		0.6 – 0.7	5
Flushing rate	10	Very well flushed	9
		Well flushed	7
		50% flushed after 1 month	5
		Poorly flushed	3
		Not flushed after 1 month	1
Dominant wave height (SW winds)	10	Very low exposure	9
		Low exposure	8
		Moderate exposure	7
		High exposure	4
		Very high exposure	2
Channel	10	Presence	1
		Absence	9

Table 7: Data layers used to inform the Aquaculture Suitability Map.

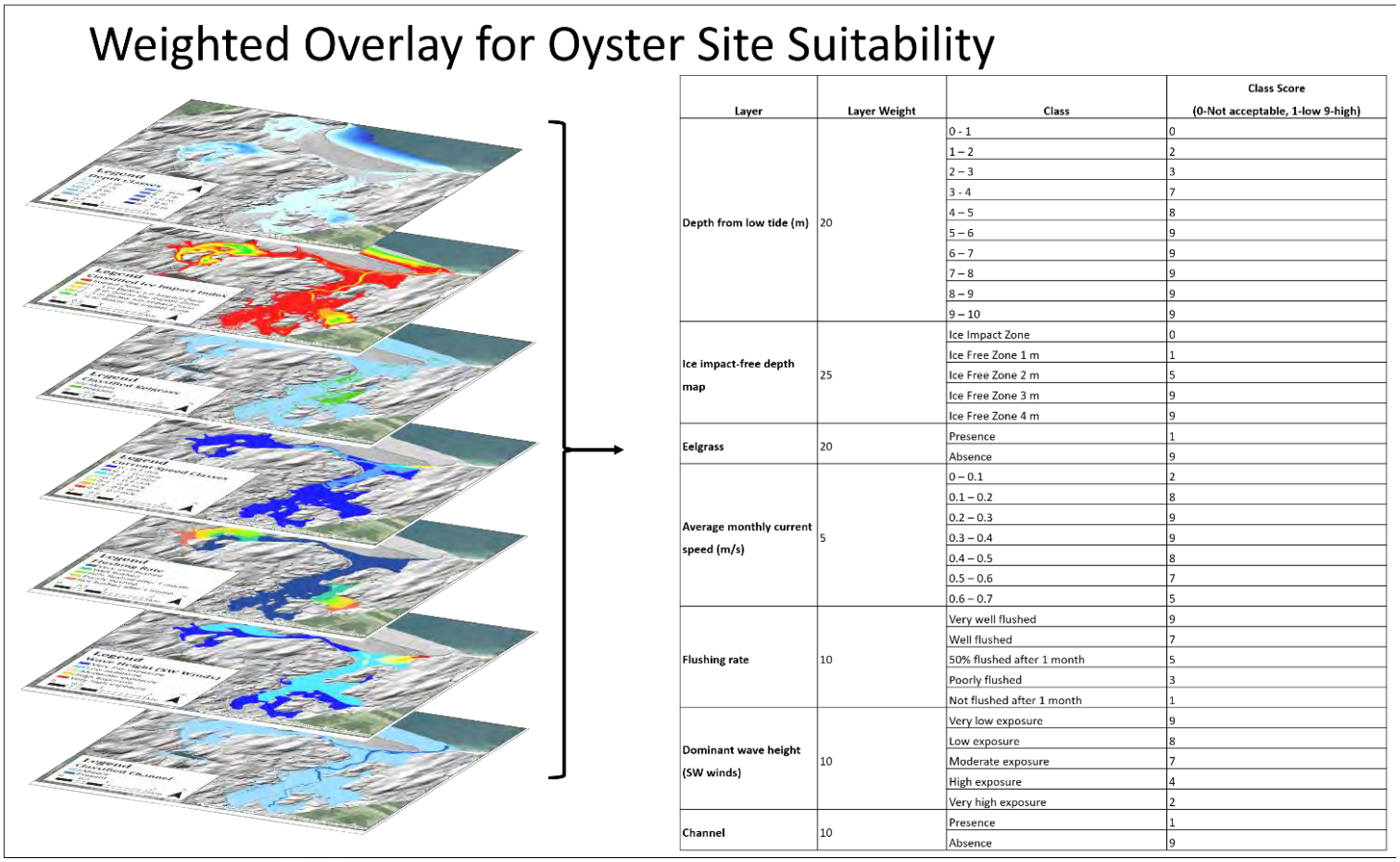

Layer	Layer Weight	Class	Class Score (0-Not acceptable, 1-low 9-high)
Depth from low tide (m)	20	0 - 1	0
		1 – 2	2
		2 – 3	3
		3 - 4	7
		4 – 5	8
		5 – 6	9
		6 – 7	9
		7 – 8	9
		8 – 9	9
		9 – 10	9
Ice impact-free depth map	25	Ice Impact Zone	0
		Ice Free Zone 1 m	1
		Ice Free Zone 2 m	5
		Ice Free Zone 3 m	9
		Ice Free Zone 4 m	9
Eelgrass	20	Presence	1
		Absence	9
Average monthly current speed (m/s)	5	0 – 0.1	2
		0.1 – 0.2	8
		0.2 – 0.3	9
		0.3 – 0.4	9
		0.4 – 0.5	8
		0.5 – 0.6	7
		0.6 – 0.7	5
Flushing rate	10	Very well flushed	9
		Well flushed	7
		50% flushed after 1 month	5
		Poorly flushed	3
		Not flushed after 1 month	1
Dominant wave height (SW winds)	10	Very low exposure	9
		Low exposure	8
		Moderate exposure	7
		High exposure	4
		Very high exposure	2
Channel	10	Presence	1
		Absence	9

Figure 77: The Pomquet Aquaculture Suitability Index includes seven classified raster layers: depth from low tide, ice impact-free depth, eelgrass presence, average monthly current speed, flushing rate, dominant wave height, and the channel location.

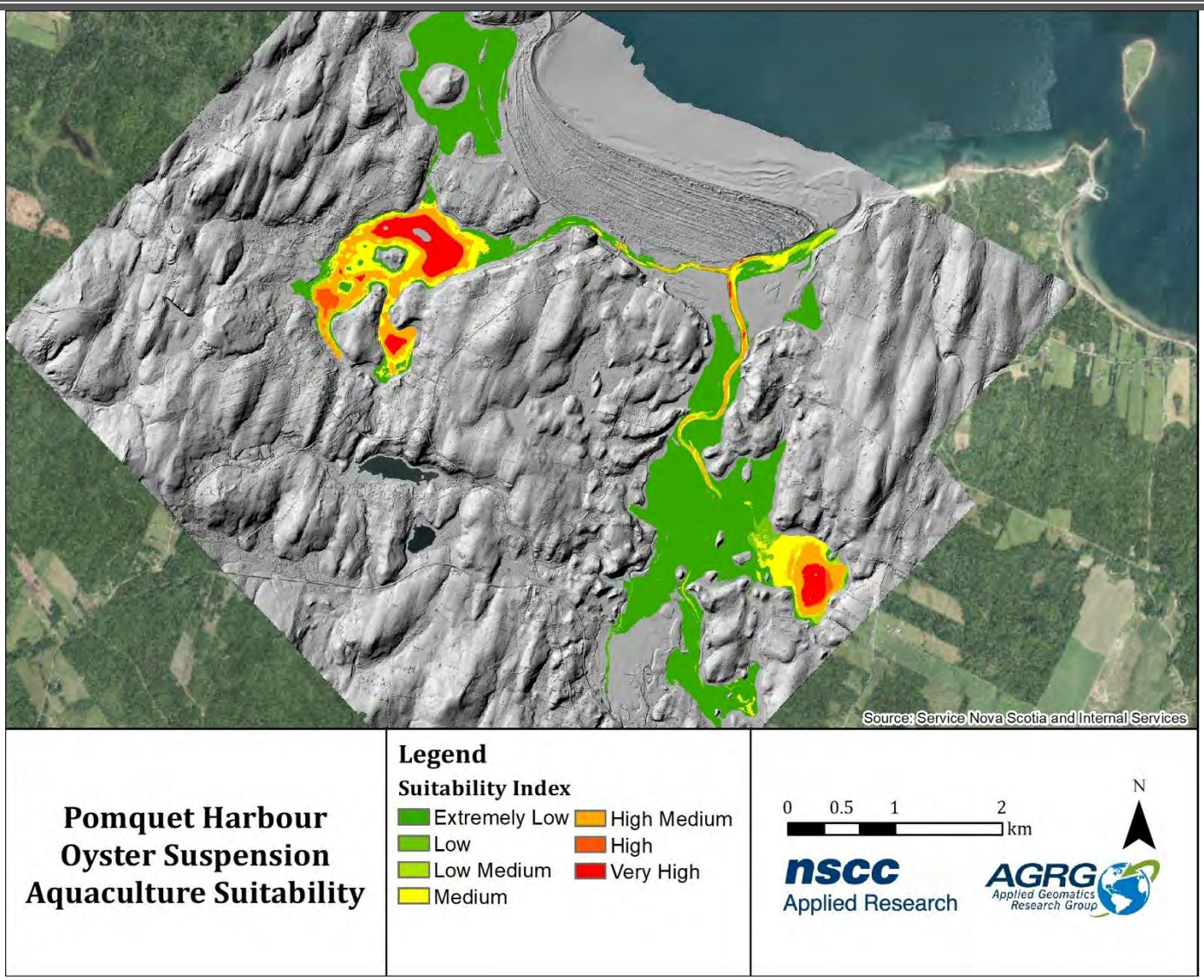

Figure 78: Pomquet Harbour Oyster Suspension Aquaculture Suitability map.

6 Web Visualization

Development and hosting of the web-based suitability modeller application required the following programs and tools:

- ArcGIS Pro 2.01 or newer
- ArcGIS Enterprise 10.5 or newer
- ArcGIS Image Server
- GeoPlanner for ArcGIS or Web AppBuilder
- Weighted Raster Overlay Service toolbox (https://github.com/Esri/weighted-raster-overlay-service-toolbox)

Suitability modeling input datasets that were originally presented in a vector format were converted to rasters with 1 metre cell sizes. The Weighted Raster Overlay Service toolbox contained tools for assembling the input raster datasets into a mosaic dataset and assigning the class ranges and default rankings to be used in the application. The mosaic dataset

was published to an ArcGIS Server. All input datasets and supplemental datasets, such as colour shaded relief models and orthophotos, were symbolized and published to the ArcGIS Server for visualization in the web application. Larger, high-resolution datasets were tiled prior to publishing to the ArcGIS Server for smoother delivery over the internet, while smaller datasets are tiled and served dynamically.

https://agrgims.cogs.nscc.ca/PomquetAFF/

The finalized web application displays the GIS data layers (hydrodynamic model output, lidar-derived layers, etc.) and the suitability maps for users to interact with. The application can be used to select from a list of layers, adjust their transparency, and overlay various datasets to examine overlapping areas and data trends (Figure 79). The user may also click on any vector layer to view a pop-up showing the attributes associated with that feature. For more detailed instructions on how to use the web application, see the *Pomquet AFF Aquaculture Suitability User Guide* in Appendix 3.

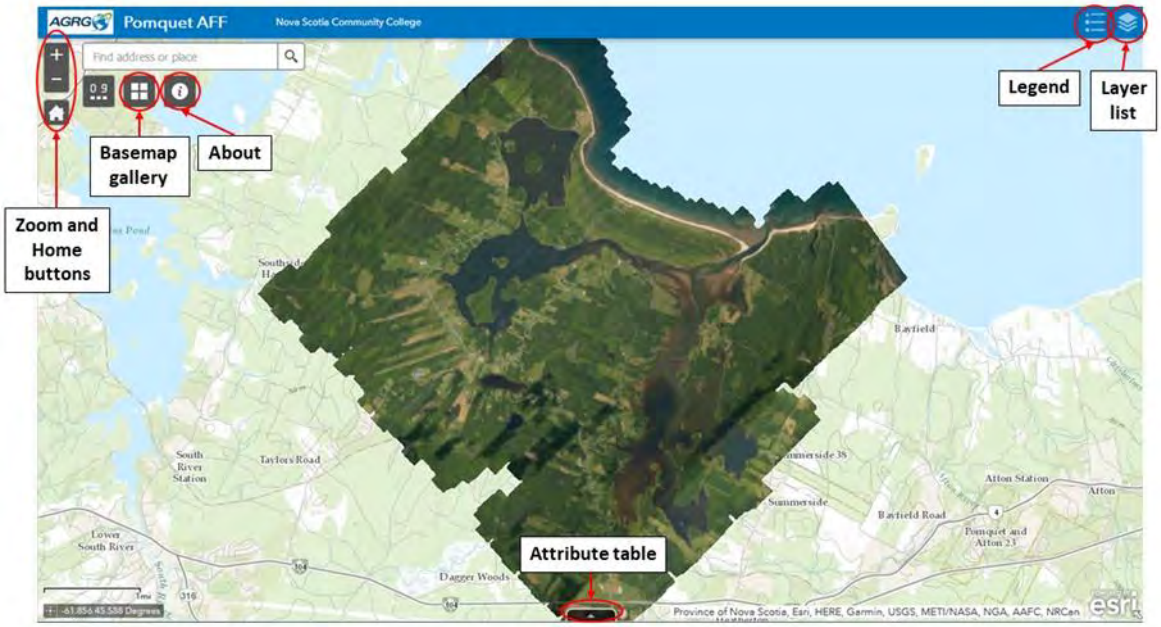

Figure 79: Pomquet AFF suitability web application, https://agrgims.cogs.nscc.ca/PomquetAFF/

6.1 Aquaculture Suitability Modeller

The weighted suitability tool is one of many widgets available within the ArcGIS Web AppBuilder environment. The widget allows the user to evaluate several factors at once by combining and weighting different raster layers (ESRI, 2020). For this project, the weighted suitability tool was configured to allow the user to generate a model of suitable oyster growing sites within Pomquet Harbour, similar to the model described in Section 5. The location of the tool is displayed in Figure 80.

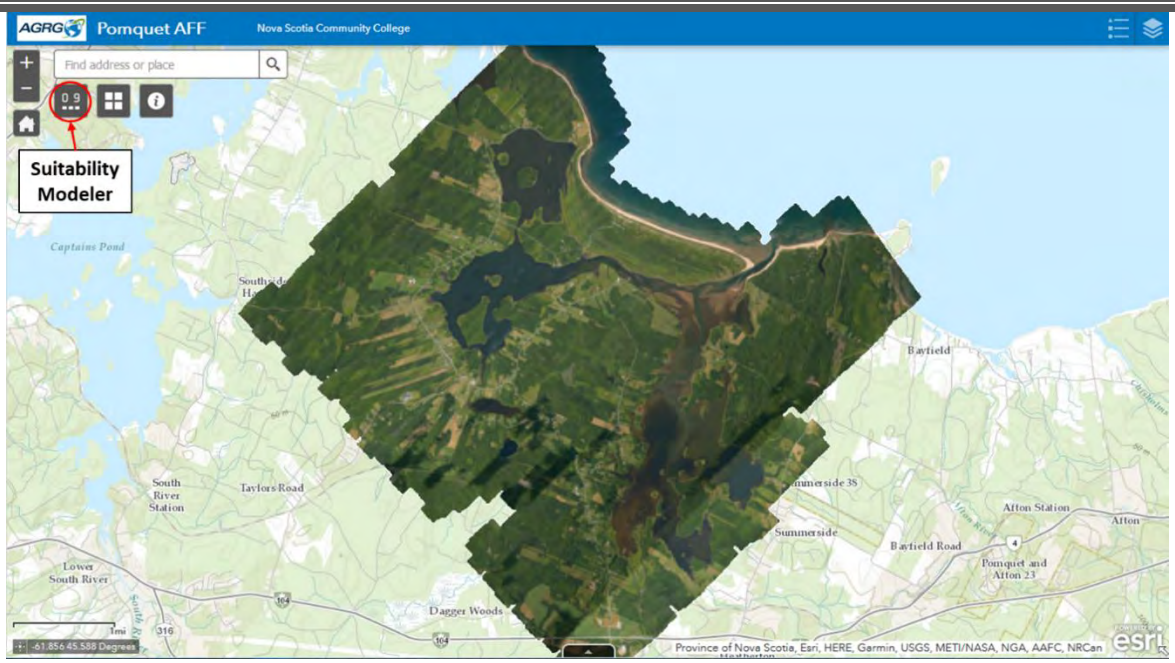

Figure 80: Location of suitability modeller tool on the Pomquet AFF web application.

To begin the analysis, the user should select their desired layers that will be incorporated into the model (Figure 81).

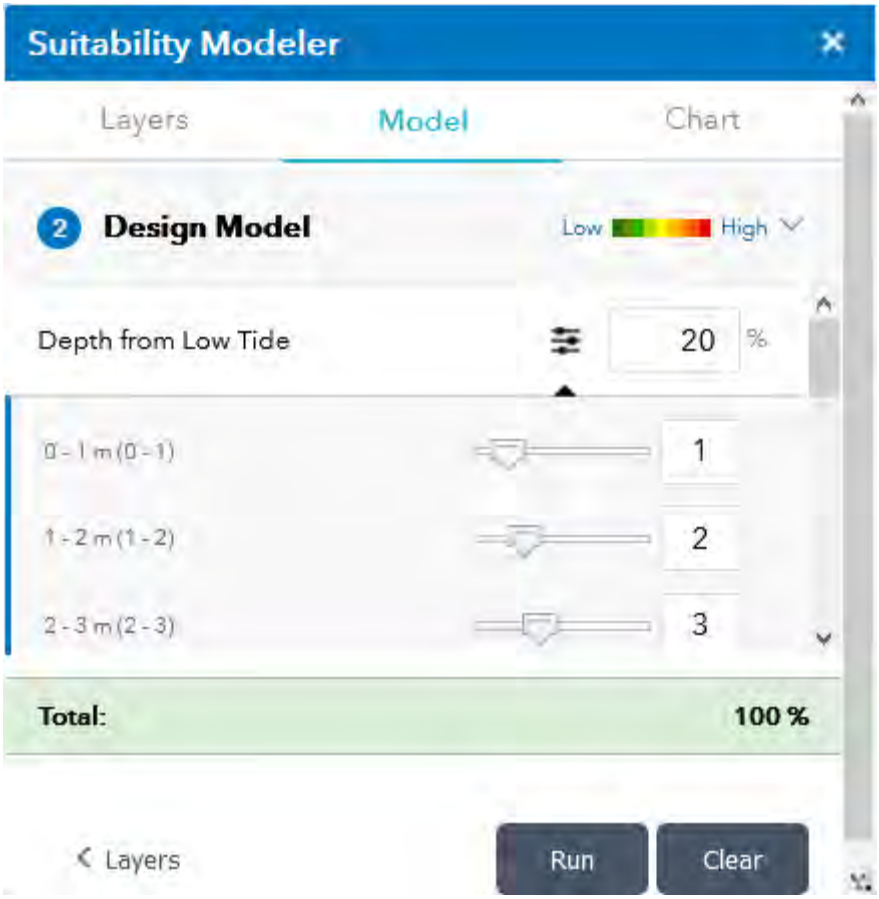

Figure 81: Partial list of layers available to conduct suitability analysis.

A percentage corresponding to each layer must be entered to assign it a relative importance in the analysis (Figure 82). The total percentage of these layers should equate to 100. Users can optionally expand each of the layers to adjust the class weights (0 – restricted, 1 being least suitable; 9 being most suitable). The class weights will decide how layer values are mapped to a suitability scale.

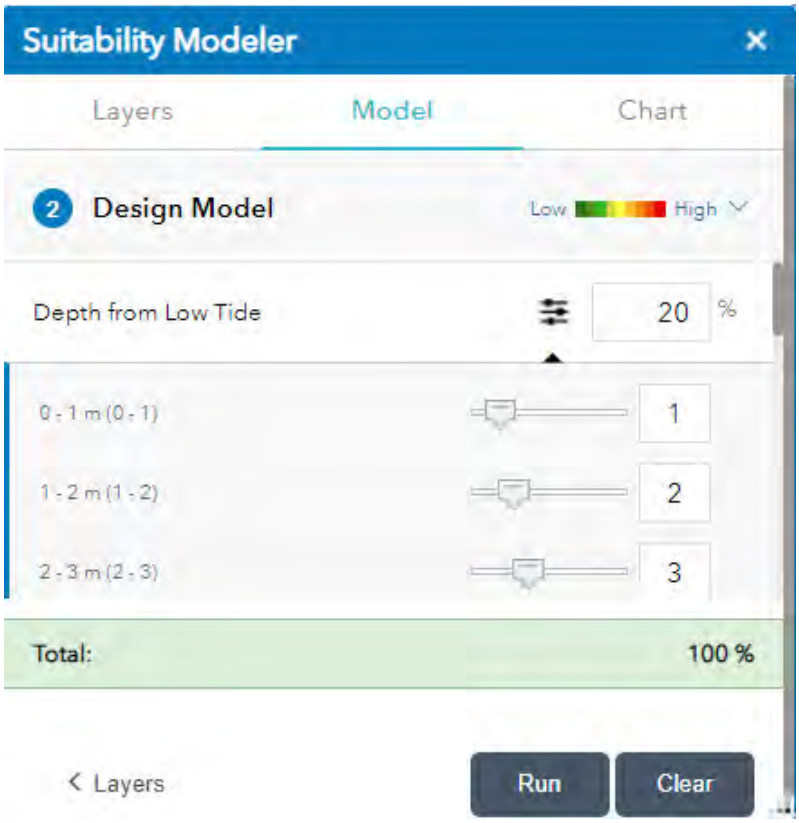

Figure 82: Relative importance assigned to each layer in the suitability analysis, as determined by the user.

When the user is satisfied with their suitability criteria, the analysis can be executed, and the resulting model will appear as an additional layer on the map and in the layer list as "rest- Pomquet_Suitability_1_Low_9_High" (Figure 84; Figure 84).

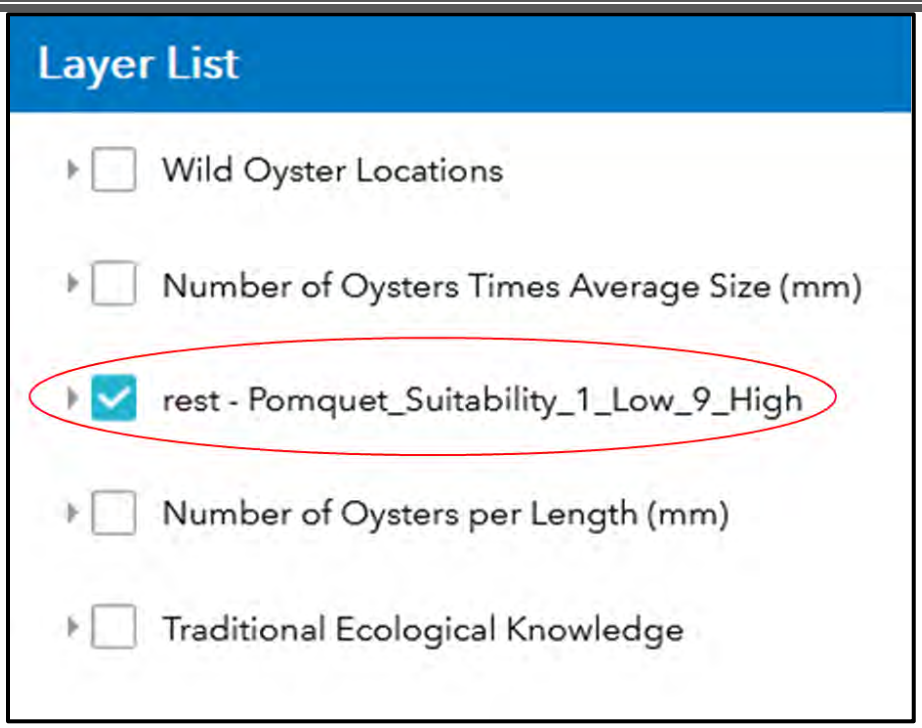

Figure 83: The suitability model will appear in the list of layers when the analysis is complete.

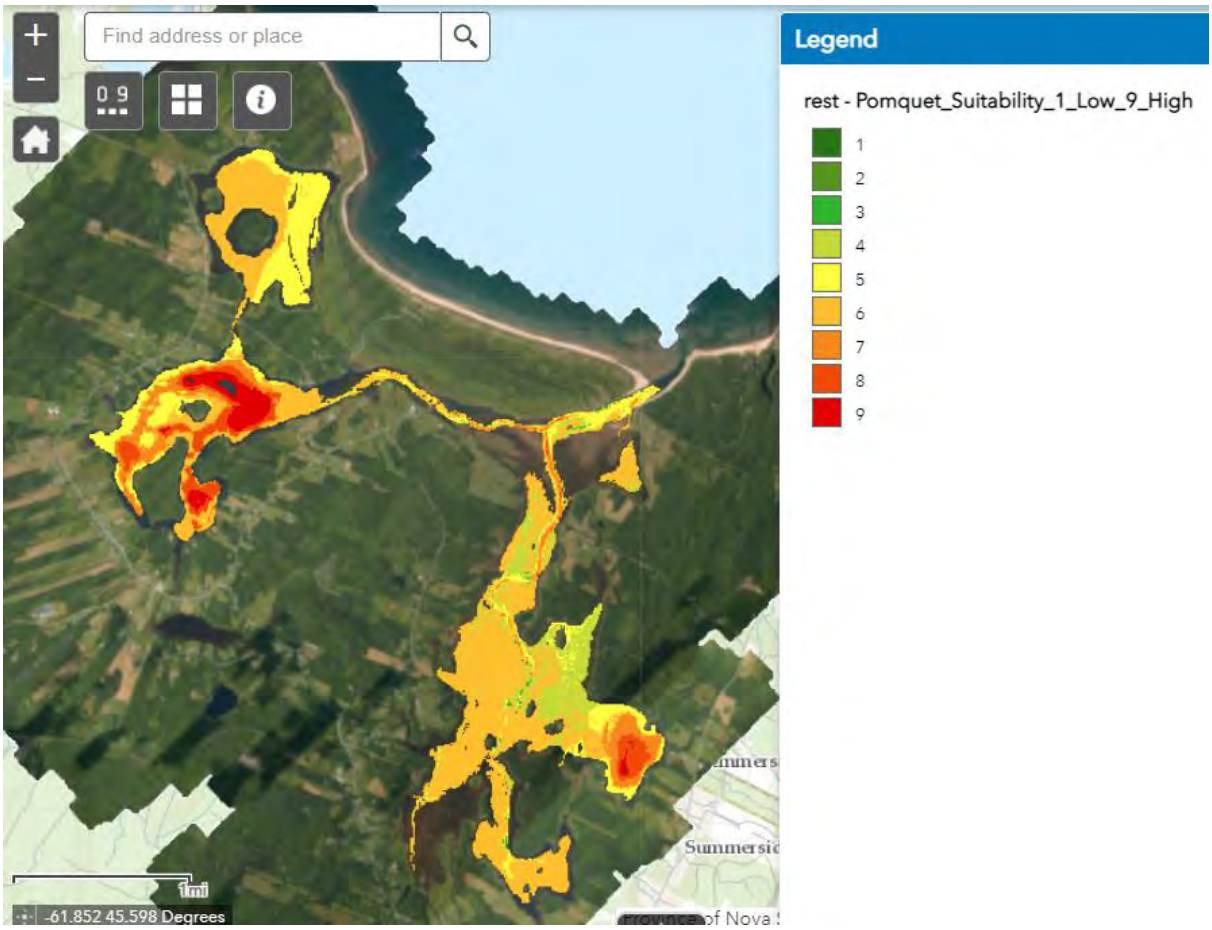

Figure 84: Output of suitability model. The visualization of the model will change as the user selects different layers and assigns different values of relative importance. Scores go from least suitable (1) to most suitable (9).

Once the suitability map is generated, the user can choose to design a chart of the model from one of the available features. The first feature allows the user to design a polygon by constructing vertices around their area of interest (Figure 85). The user can also choose to draw a freehand polygon around their desired selection or select a feature from a list of available layers.

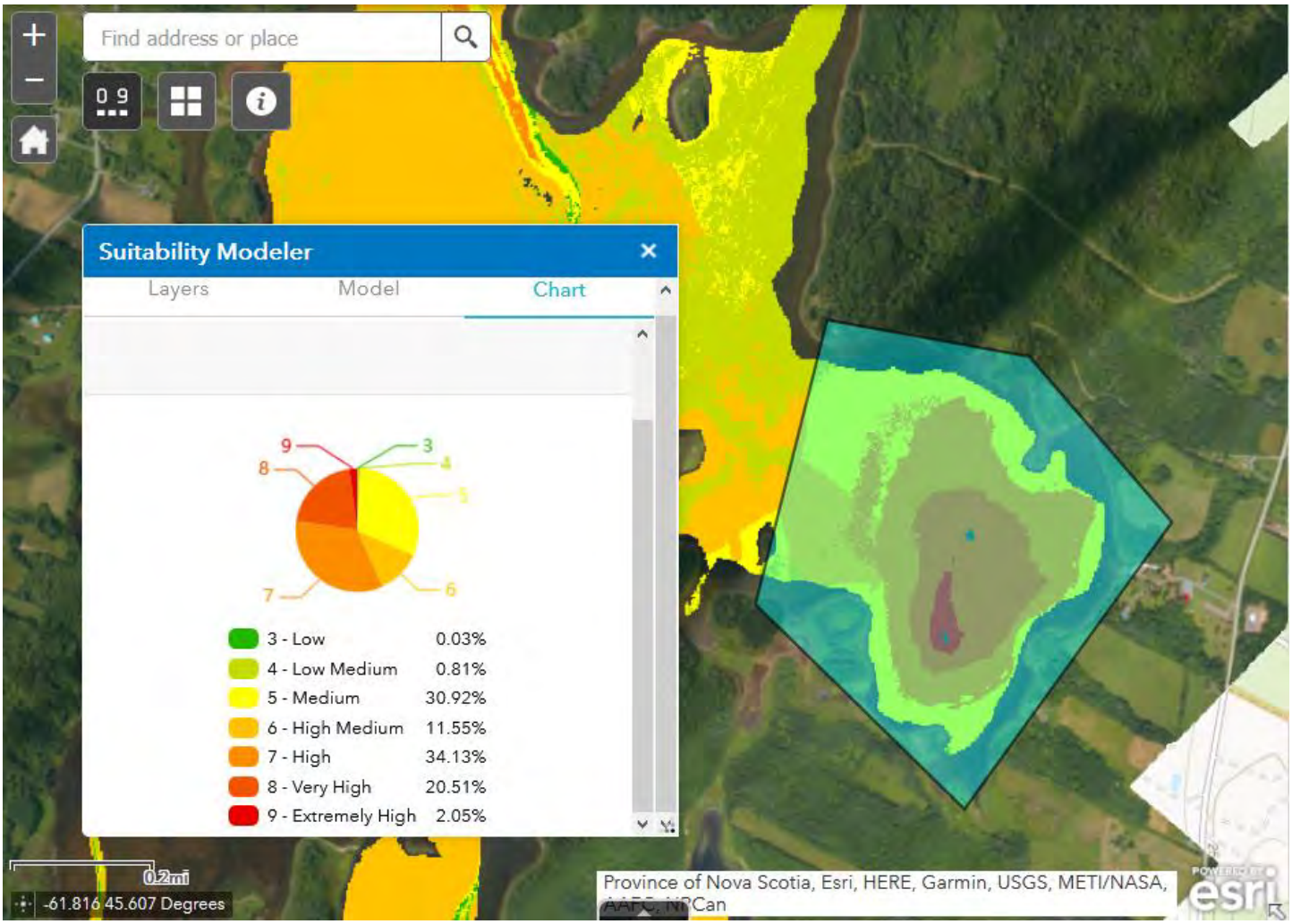

Figure 85: Chart of the suitability model generated by drawing a polygon around the area of interest.

7 Conclusion

This project has demonstrated the multiple uses of data derived from a single airborne topo-bathymetric lidar survey, supplemented by an ADCP deployed for one month, to support shellfish aquaculture site selection and possible spat collection areas. Several key data layers were derived from the lidar seamless land-sea elevation data including water depth, ice impact zone, intertidal area, the channel location and from the orthophotos the eelgrass presence map. The lidar elevations were supplemented with a multibeam survey conducted by AGRG and depth sounding from CHS charts where the lidar did not penetrate to the bottom because of water clarity limitations. The resultant DEM was used to construct a hydrodynamic (HD) model using the DHI Mike-21 suite of modelling tools. The model results were compared

and validated against the ADCP measurements. The water levels agreed quite well apart from some significant wind events. There was more variability between the current velocities modelled and those measured by the ADCP. This was interpreted to be a result of the complex movement of the water in Church Cove. The results of the HD model included the mean and maximum monthly current speeds, an estimate of flushing times and the significant wave height from the predominant wind. These additional layers were used as important site selection criteria. The results from the oyster stock survey conducted by Robin Stuart in Pomquet Harbour in 2014 were used to estimate spat release in the harbour which was represented as a series of particles that were then tracked using the HD model. Maps showing the distribution of the spat particles on an incoming and outgoing tide can be used to determine potential sites for spat collection. The ADCP data were analyzed with weather data, specifically wind, from the nearest Environment and Climate Change Canada weather station at Tracadie. It was observed that strong wind events influence both water level and current velocities but did not increase the wave height significantly for Church Cove. Animations were constructed to aid in visualizing the dynamic nature of the ADCP and HD model output. A suitability map was constructed in GIS for potential oyster growing sites. This used a weighted overlay technique where each map was assigned a weight and then each class within the map was assigned a score (1 low suitability, 9 high suitability). Advise was obtained by aquaculture experts from DFO, NSFA and CMAR to assign the weights and scores.

The various layers derived during this study as well as existing layers such as Traditional Ecological Knowledge and aquaculture leases were made available through a web mapping system. These layers can be toggled on and off and their transparency can be set so that multiple maps can be viewed at once. As well the attributes of any GIS layer are also available to query, for example the data collected by Stuart (2014) for the oyster stock survey are now available on-line and can be queried. The web-system also allows the user to construct their own site suitability map. This involves selection the layer for the overlay from those available in the list. The layers available on the website include both continuous data as well as classified data. A User Guide is available on the website accessed through the About icon ***i*** as well as a description of the project and funders. The classified data are recommended for use in this overlay system. Once the user selects the layers of interest, weights are assigned to each ensuring the sum of all the weights is equal to 100. Each map class is then scored from 0-unacceptable, flagged to be unacceptable regardless of how high the scores are for other map layers, to a range of scores between 1- low and 9 high. The weighted overlay is then executed, and a new suitability map is displayed on the web (rest – Pomquet_Suitability_1_Low_9_High). A chart can also be constructed showing the area of each suitability class. A polygon of interest can be digitized within the web mapping system over the suitability map to calculate a graph of the area for each class within the polygon.

Overall, this project has demonstrated the benefits of high-resolution coastal data for shellfish management and site selection. The ability to access these large data set through a web viewer allows easy access for multiple stakeholders. The ability to overlay maps to calculate possible suitable areas for siting farms was also built into the web-mapping system as part of the project making it easy for non-GIS experts. These results of this project could be expanded to other bays

within the Maritimes to improve our understanding of the coastal processes and assist in marine spatial planning and aquaculture site selection.

8 Acknowledgements

We would like to thank Paqtnkek Mi'kmaw Nation and the Atlantic Fisheries Fund - Fisheries and Oceans Canada - DFO-MPO and Nova Scotia Fisheries and Aquaculture for funding support. We would especially like to thank Sean Dzafovic and Thomas Allen of NSCC's AGRG for their assistance with data collection and processing. Thanks to staff from Airborne Hydrography and Leica Geosystems, and LEG staff for operations support and AGRG staff for administrative support. We are grateful for the eelgrass ground truthing information supplied by Dr. David Garbary and Sarah Silver Slayter of St. FX Biology Department. Support from the following individuals and organizations for the discussion of maps weights and class scores for the suitability overlay including Monique Niles – DFO Gulf Region, Matthew King – NSFA, Gregor Reid, Laila Nargis, and James Cunningham of CMAR-Perennia.

9 References

AGRG. (2018). Aquaculture Decision Support Tool Demonstration Project. Technical report, Applied Geomatics Research Group, NSCC Middleton, NS.

Bonham-Carter, G. F. (1994). Geographic Information Systems for Geoscientists Modelling with GIS. (G. F. Bonham-Carter, & D. F. Merriam, Eds.) New York: Elsevier.

Doiron, S. (2008). Reference Manual for Oyster Aquaculturists. New Brunswick Department of Agriculture, Aquaculture, and Fisheries.

Pentcheff, D. WWW Tide and Current Predictor. Tide/Current Predictor. http://tbone.biol.sc.edu/tide Website accessed Sept. 2020.

ESRI. (2016a). Overlay analysis – Help | ArcGIS for Desktop.

ESRI. (2016b). How Weighted Overlay works – Help | ArcGIS for Desktop.

ESRI. (2020). Suitability Modeler widget – ArcGIS Web AppBuilder.

Stuart, R. (2014). Proposal to determine the Best Location to Collect Wild Oyster Seed in Pomquet Harbour, N.S. Englishtown, NS. Report to Paqtnkek First Nation.

10 Appendix 1: Number of Oysters per Length

The following maps represent the count values of eight different oyster shell size classes observed in Pomquet Harbour during oyster stock surveys (Figure 86; Figure 87; Figure 88; Figure 89; Figure 90; Figure 91; Figure 92; Figure 93). These observations were made in areas identified as having a suitable oyster habitat. Station 21 reported the highest count of oysters in the shell size classes between 0 – 80 mm. Market size oysters, defined as having a shell length of greater than 76 mm, had the highest count at station 13 with 156 oysters.

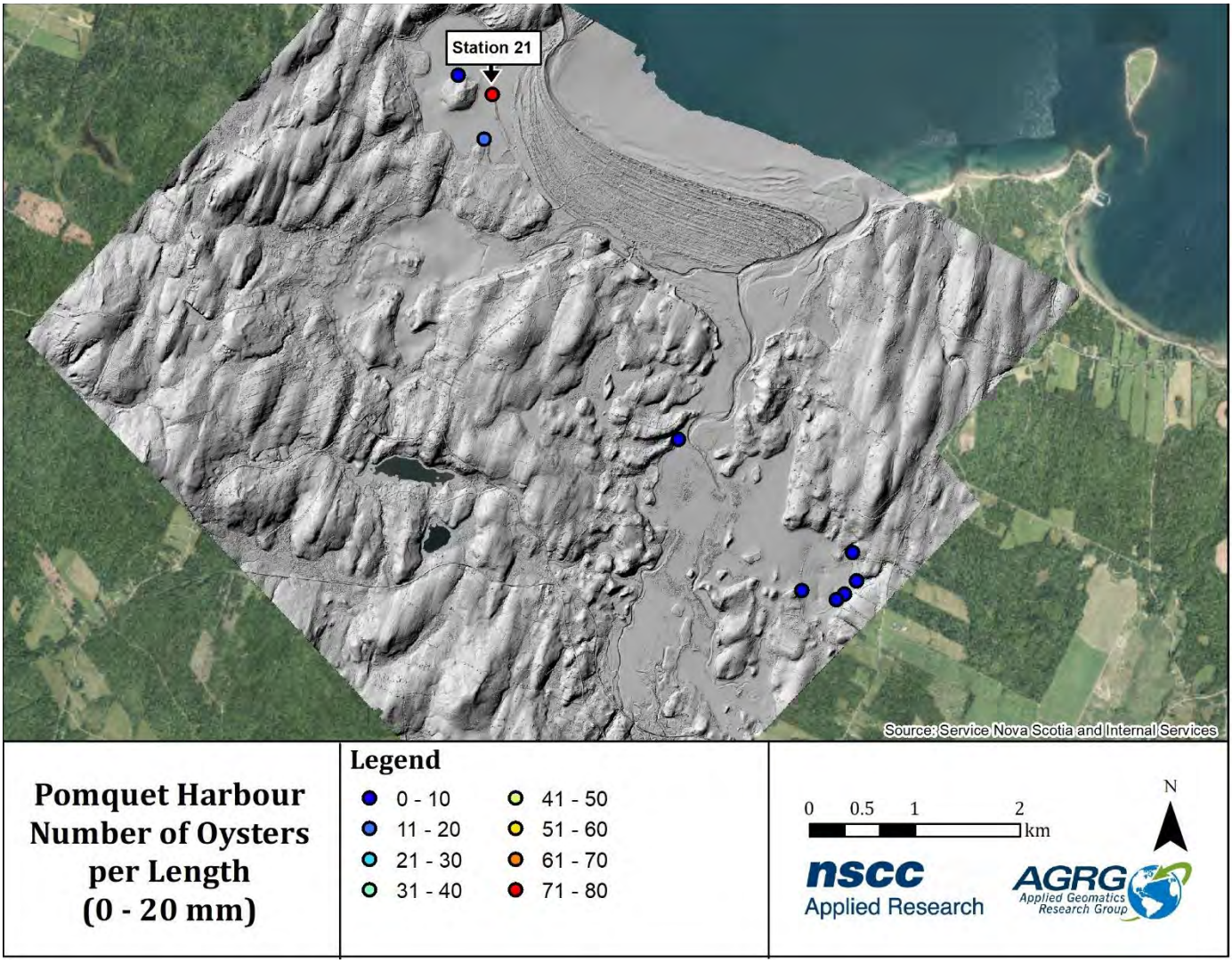

Figure 86: Count values of the 0 – 20 mm oyster shell size class collected at each station during oyster stock surveys conducted by Robin Stuart on Paqtnkek First Nation's behalf.

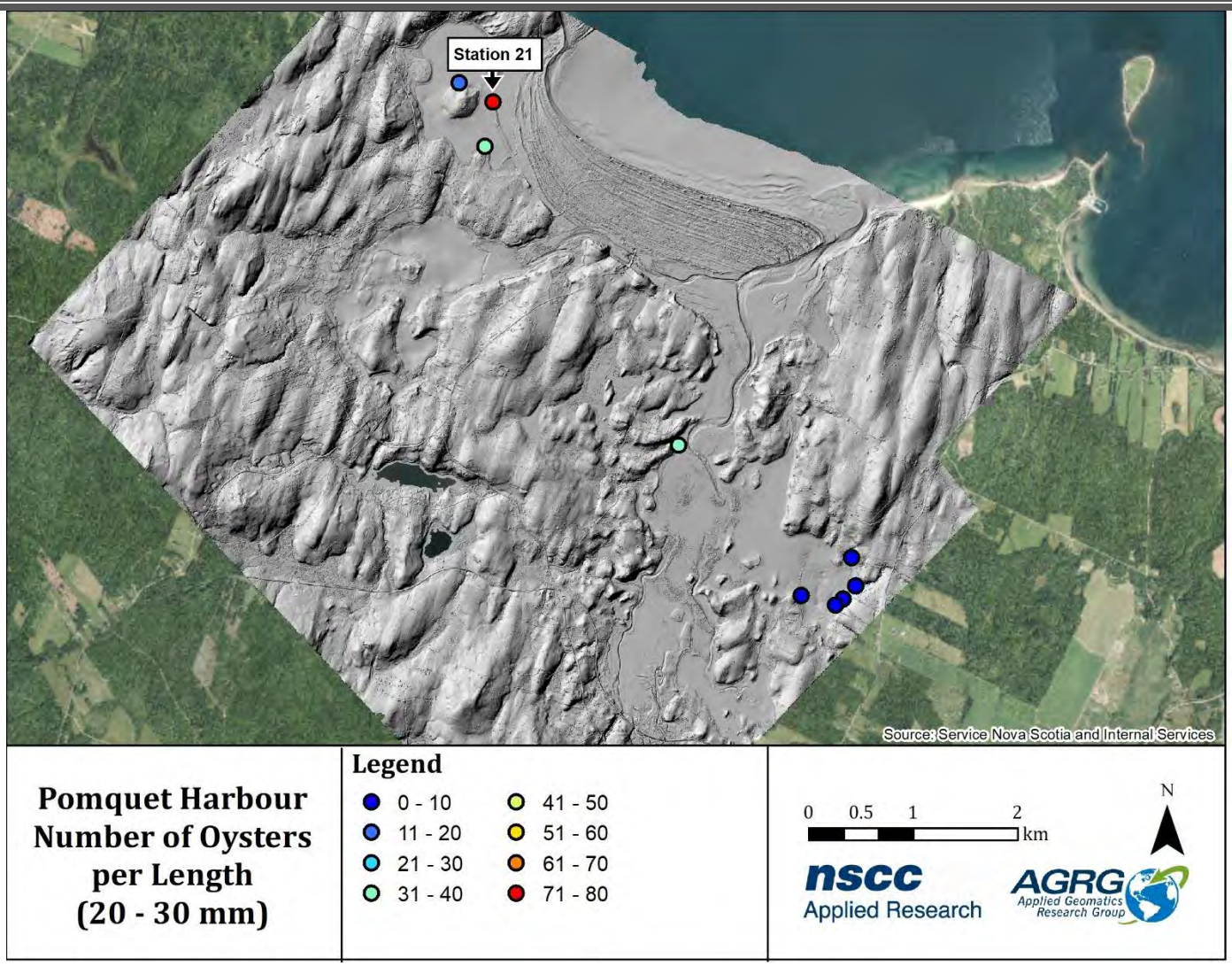

Figure 87: Count values of the 20 – 30 mm oyster shell size class collected at each station during oyster stock surveys conducted by Robin Stuart on Paqtnkek First Nation's behalf.

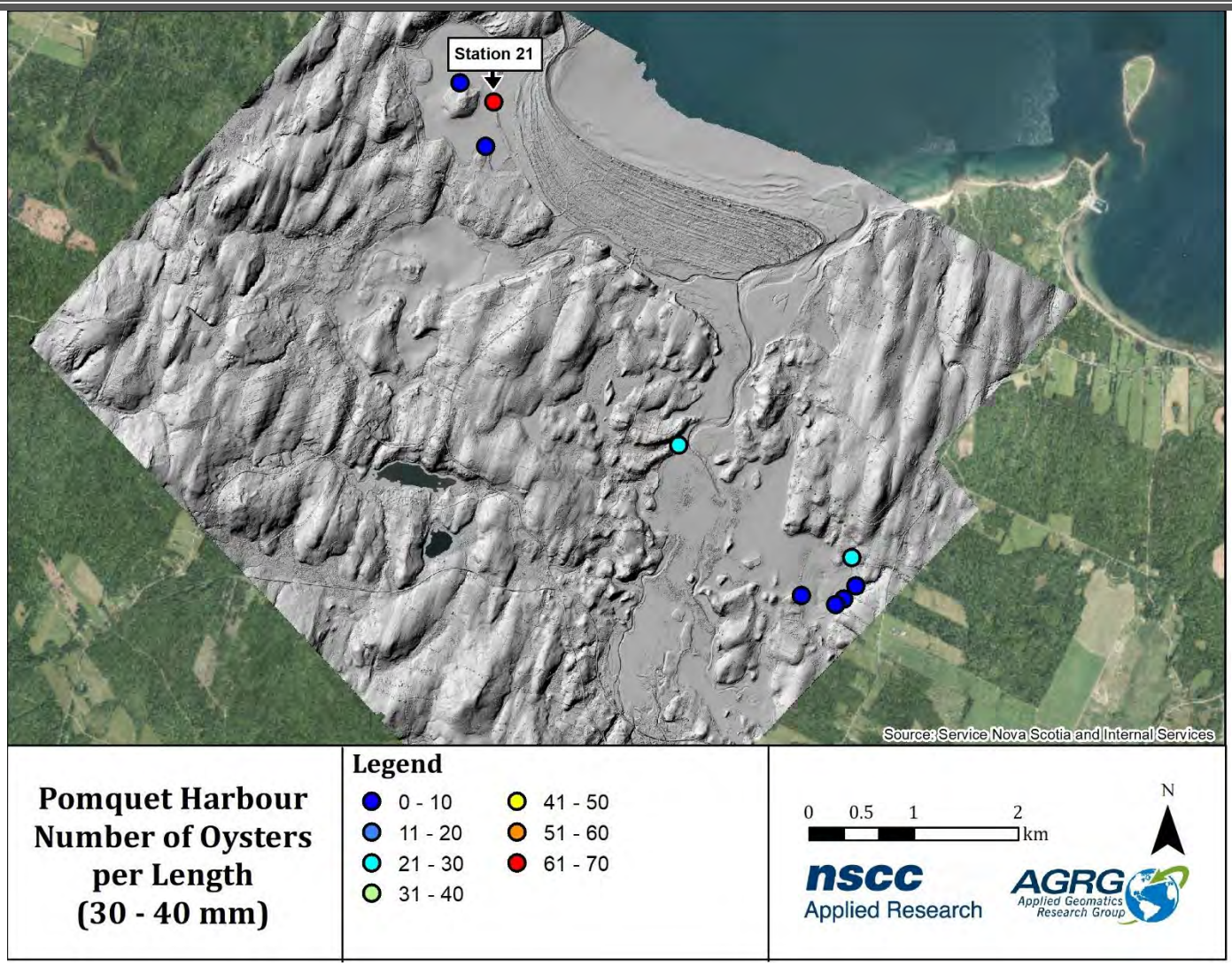

Figure 88: Count values of the 30 – 40 mm oyster shell size class collected at each station during oyster stock surveys conducted by Robin Stuart on Paqtnkek First Nation's behalf.

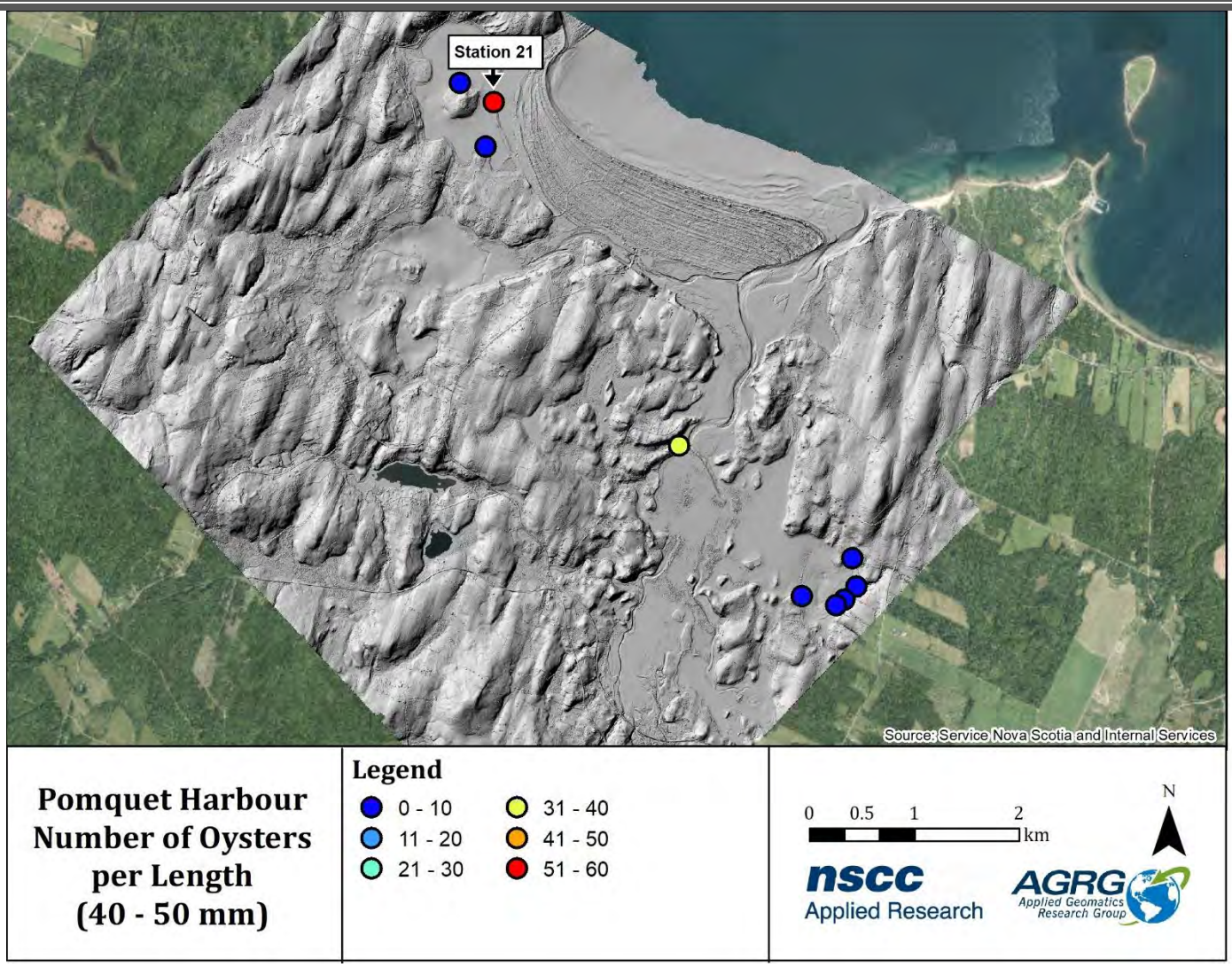

Figure 89: Count values of the 40 – 50 mm oyster shell size class collected at each station during oyster stock surveys conducted by Robin Stuart on Paqtnkek First Nation's behalf.

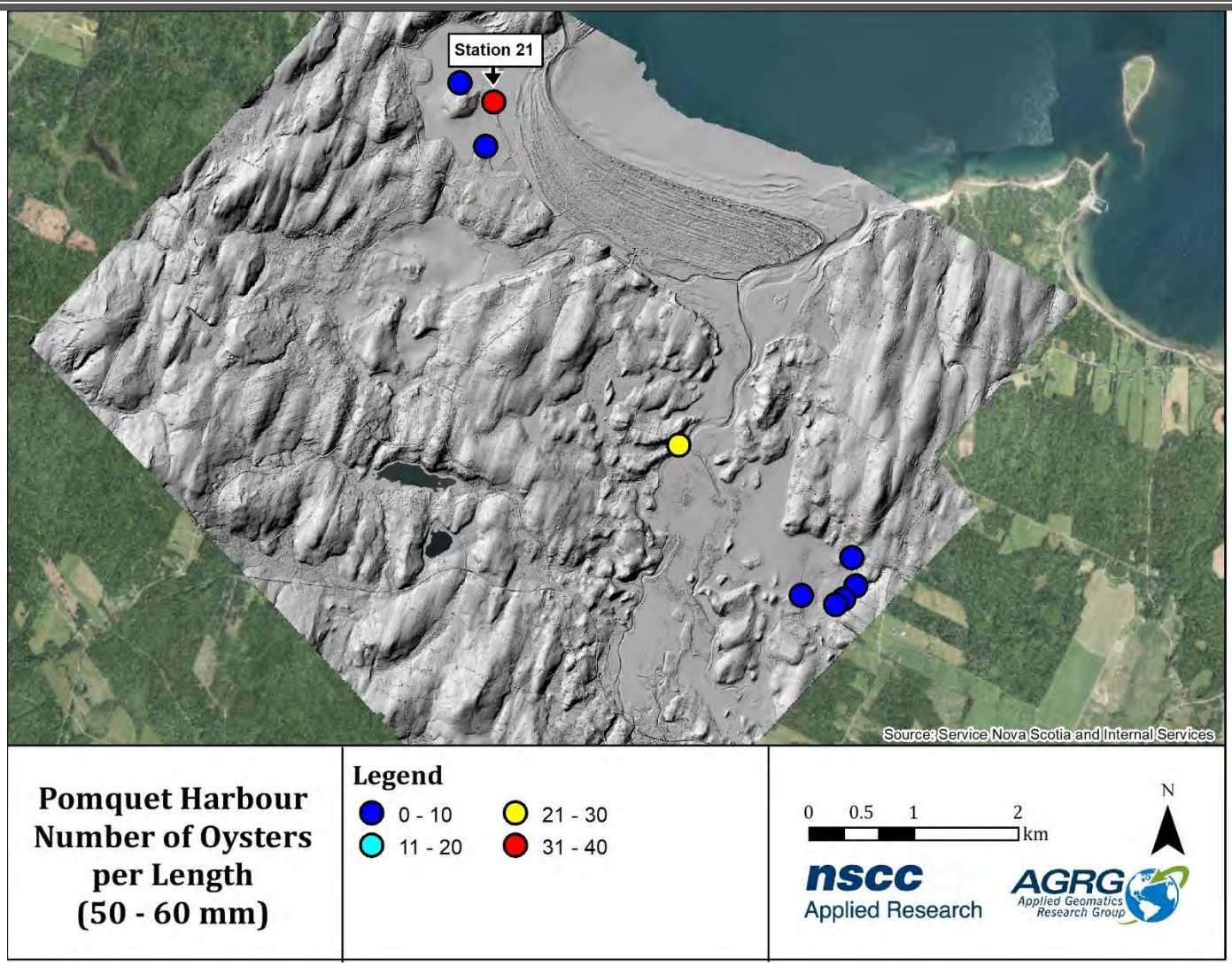

Figure 90: Count values of the 50 – 60 mm oyster shell size class collected at each station during oyster stock surveys conducted by Robin Stuart on Paqtnkek First Nation's behalf.

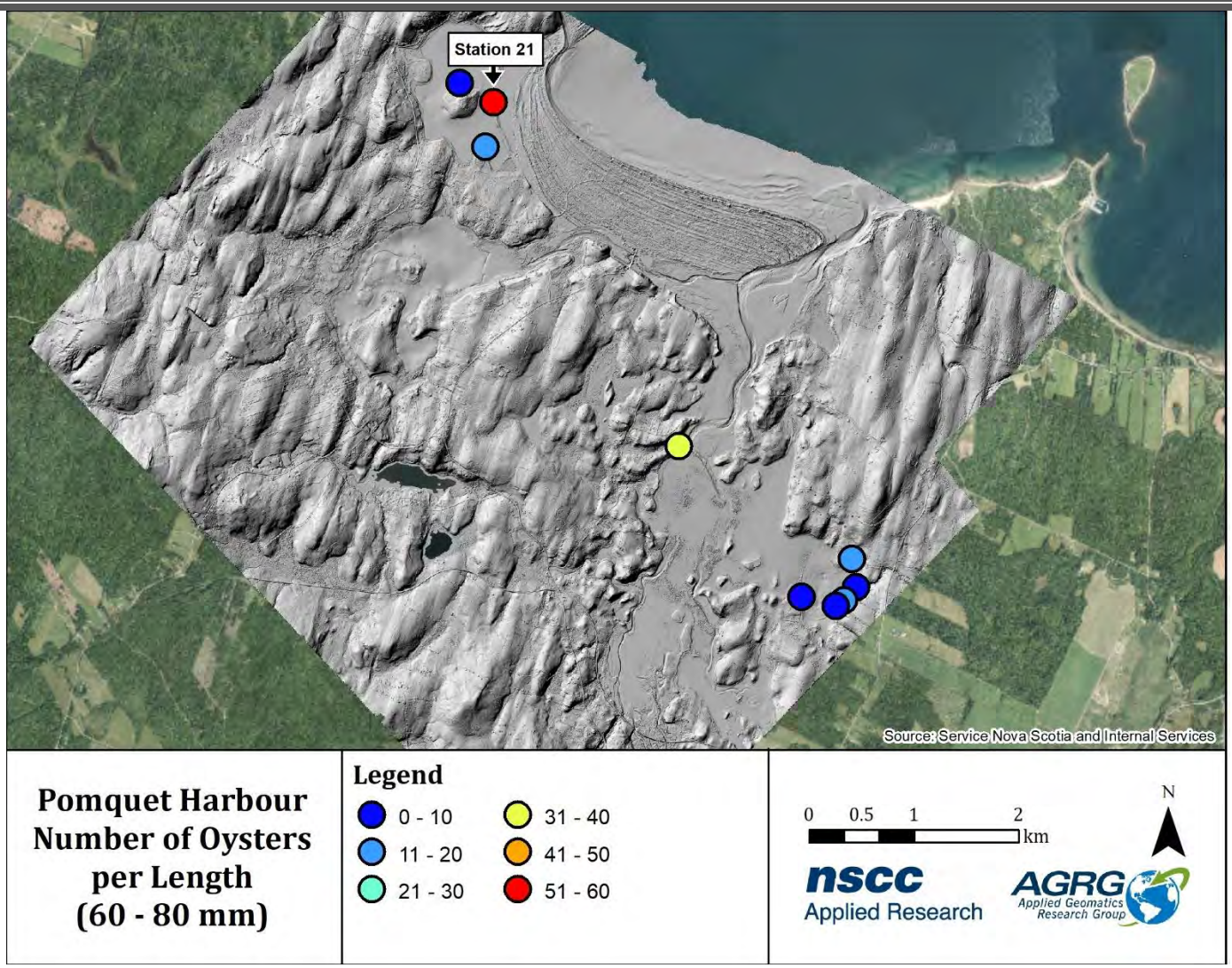

Figure 91: Count values of the 60 – 80 mm oyster shell size class collected at each station during oyster stock surveys conducted by Robin Stuart on Paqtnkek First Nation's behalf.

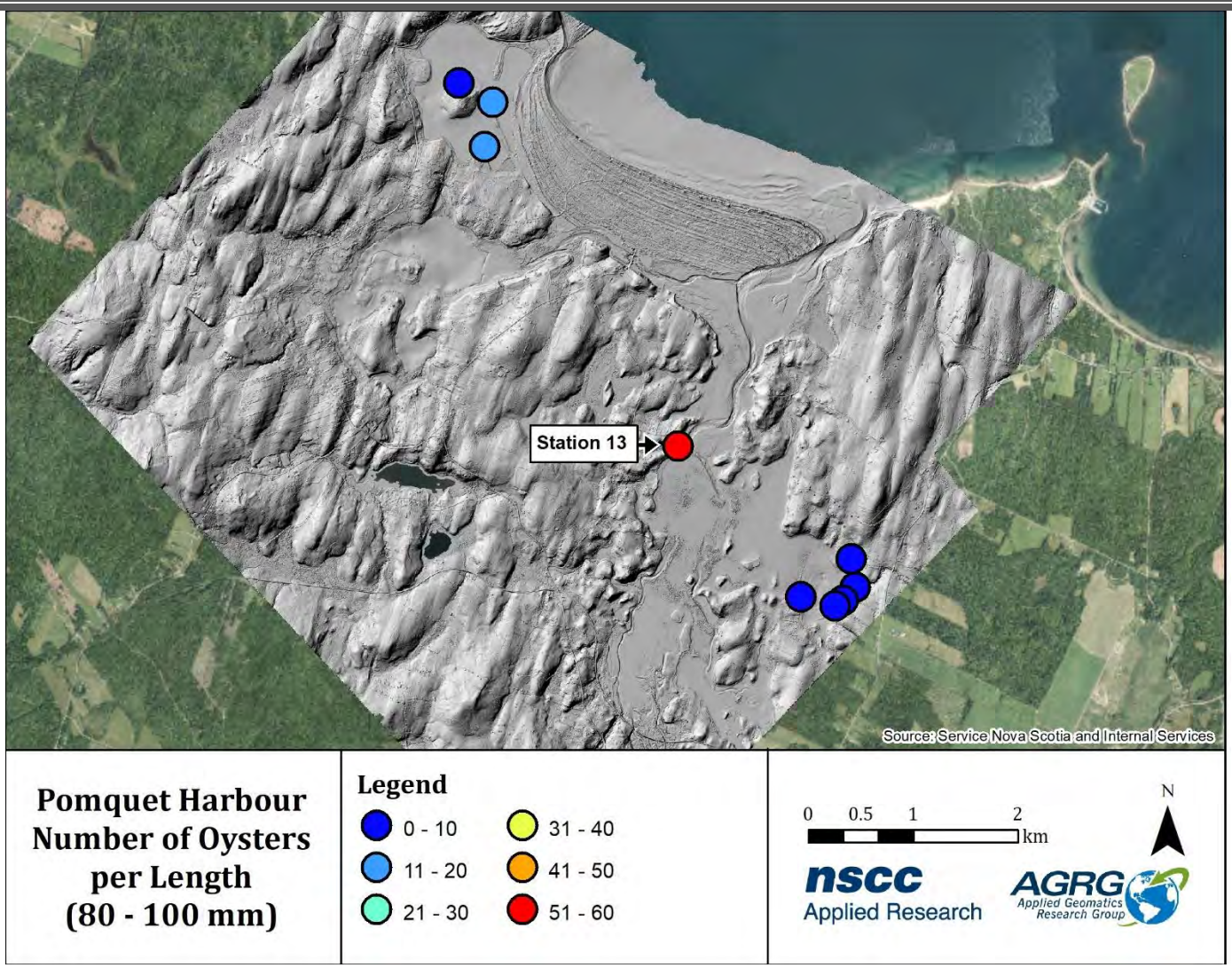

Figure 92: Count values of the 80 – 100 mm oyster shell size class collected at each station during oyster stock surveys conducted by Robin Stuart on Paqtnkek First Nation's behalf.

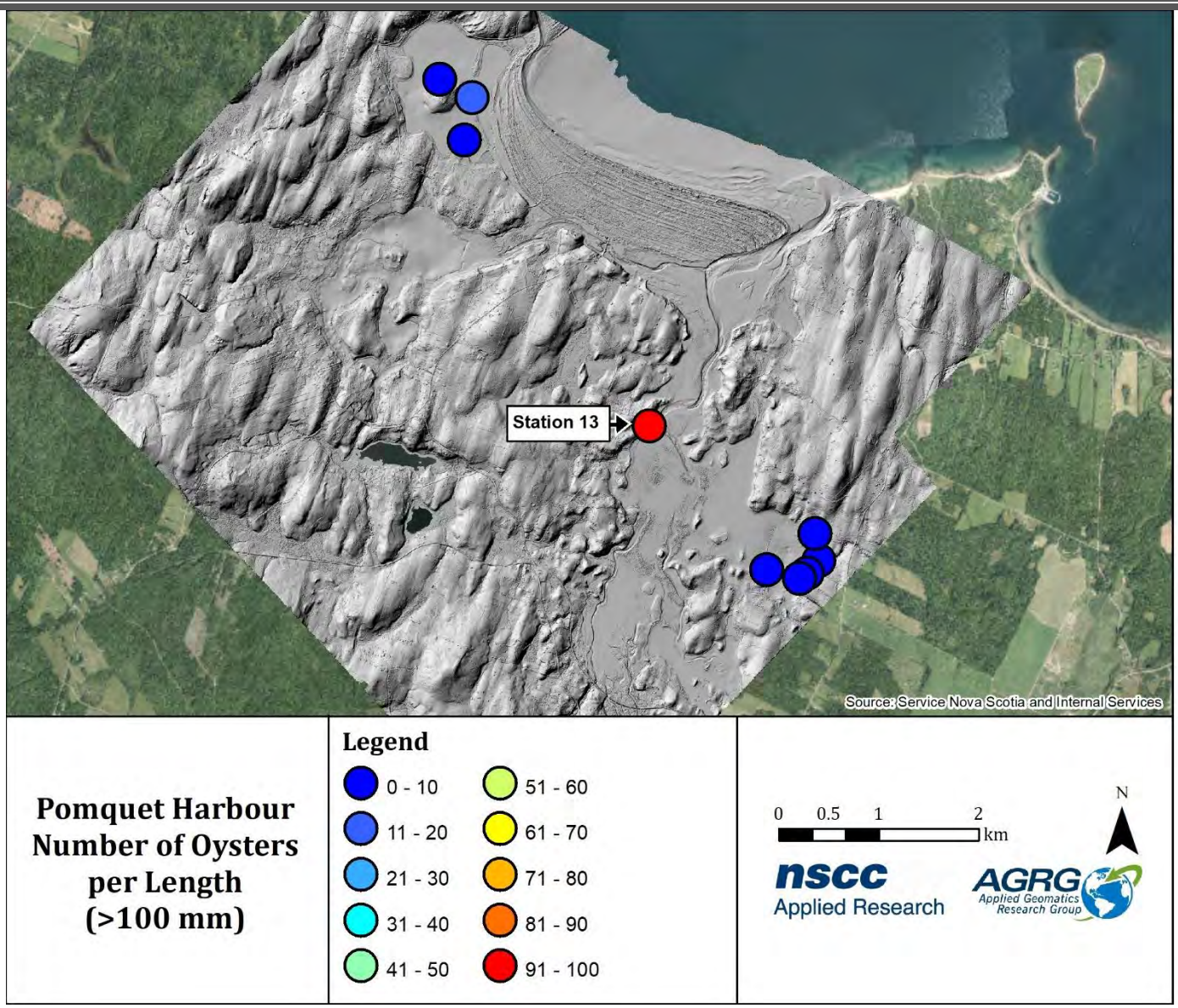

Figure 93: Count values of the >100 mm oyster shell size class collected at each station during oyster stock surveys conducted by Robin Stuart on Paqtnkek First Nation's behalf.

11 Appendix 2: Hillshade Models

The maps in this section show hillshade models of the DEM and the DSM (Figure 94; Figure 95).

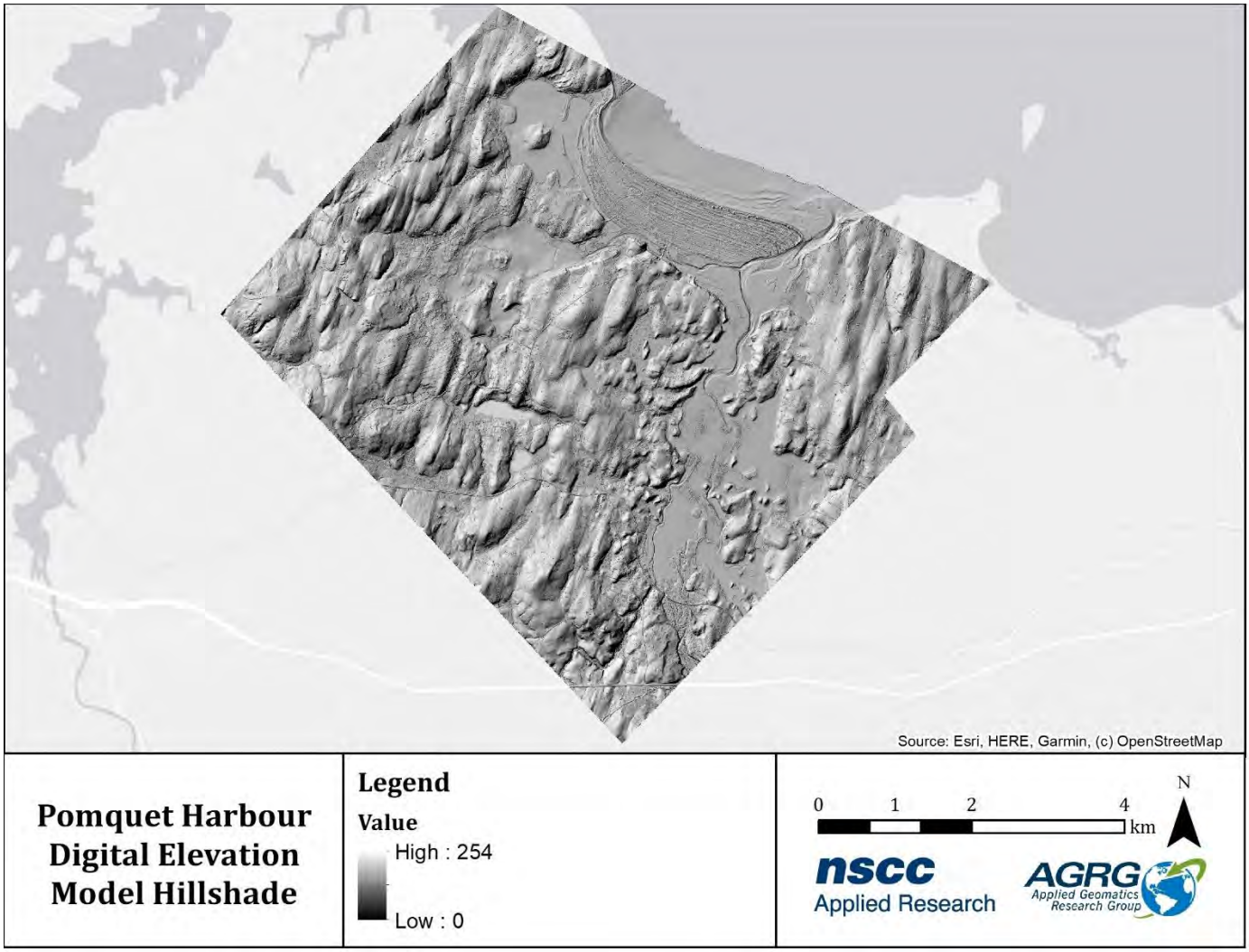

Figure 94: Hillshade generated from the digital elevation model.

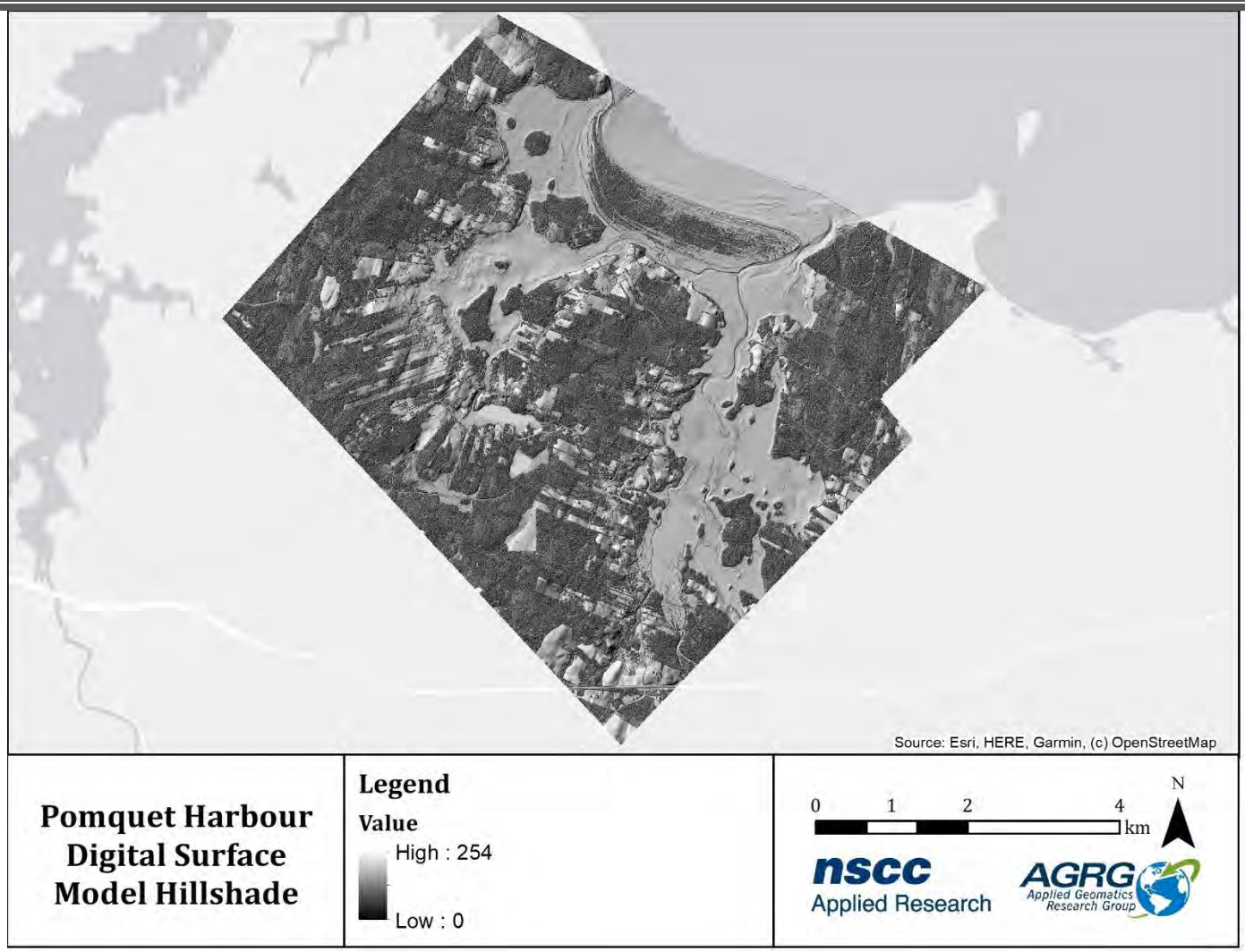

Figure 95: Hillshade generated from the digital surface model.

12 Appendix 3: Pomquet AFF Aquaculture Suitability Modeller User Guide

Pomquet AFF Aquaculture Suitability Web Map

User Documentation

Prepared by:

Applied Geomatics Research Group
NSCC, Middleton
Tel. 902 825 5475
email: tim.webster@nscc.ca

Getting Started

- When initially landing the Pomquet AFF Aquaculture Suitability Map's main page, the user will see a 5 cm resolution aerial image of the Pomquet Harbour study area.

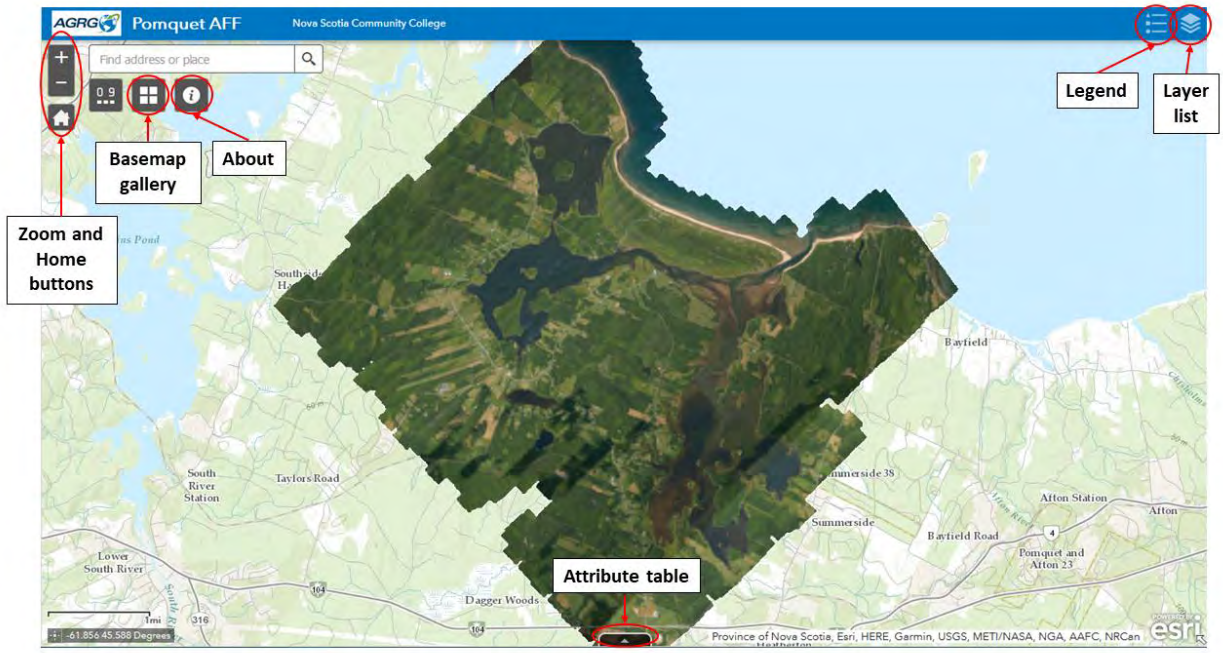

- To zoom in and out of the map, click the "+" and "-" buttons located in the web application's top left corner. To return to the default map extent, click the home button located below the zoom buttons.
- To find a specific address or place, type into the search bar located next to the zoom buttons.
- To change the default basemap, click the basemap gallery button positioned below the search bar. The user can select one of ten available Esri basemaps to change the display on the web application.
- The user can click on an activated vector layer to display a popup of the associated attributes.

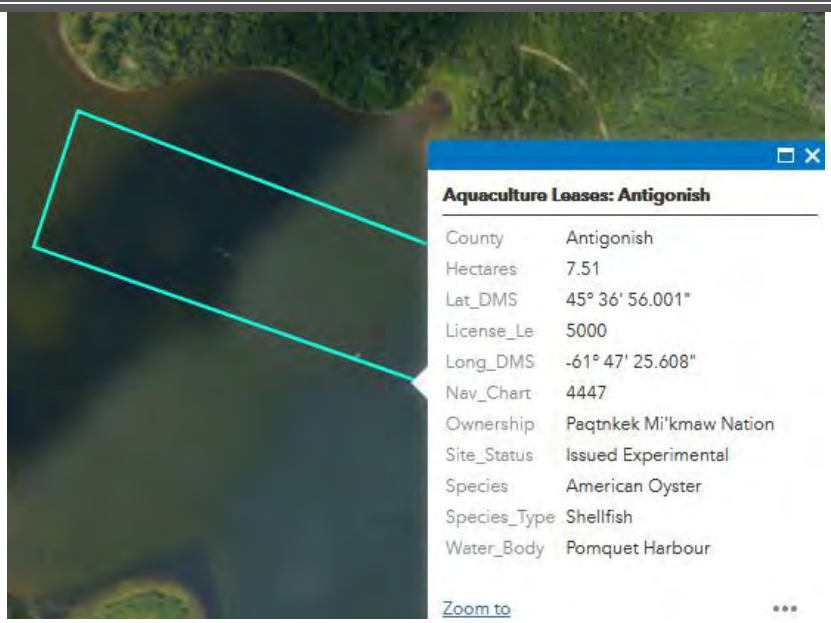

- The user can also view any vector layer's attribute table by clicking the arrow at the bottom of the map.

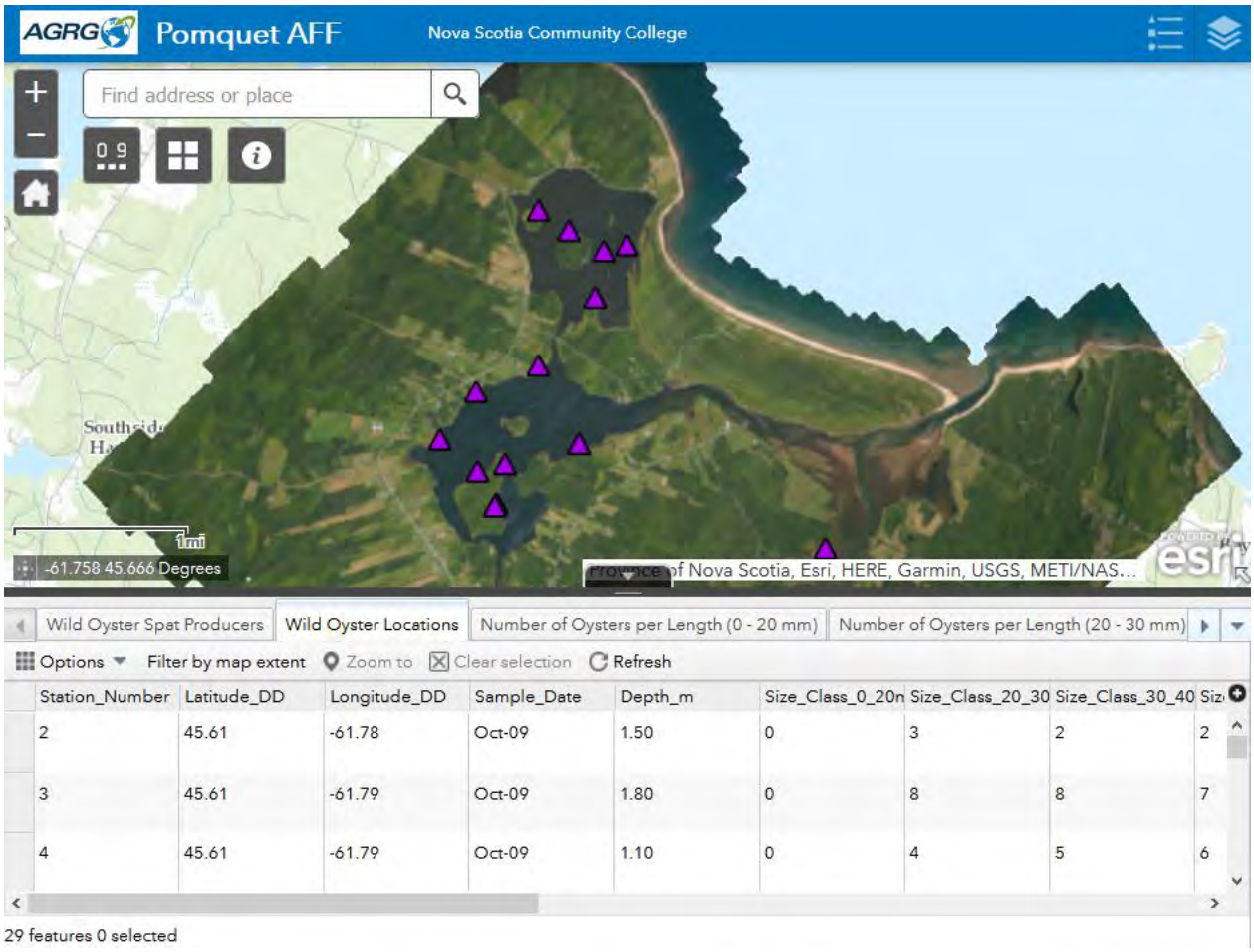

- A description of the key layers and the Suitability Modeller tool is outlined in the following section.

12.1 GIS Data Layers

- The user can activate any of the layers in the layer list by clicking the checkbox next to it.
- By clicking the three dots next to one of the layers, a list of options, such as adjusting the transparency or setting a visibility range, will appear.

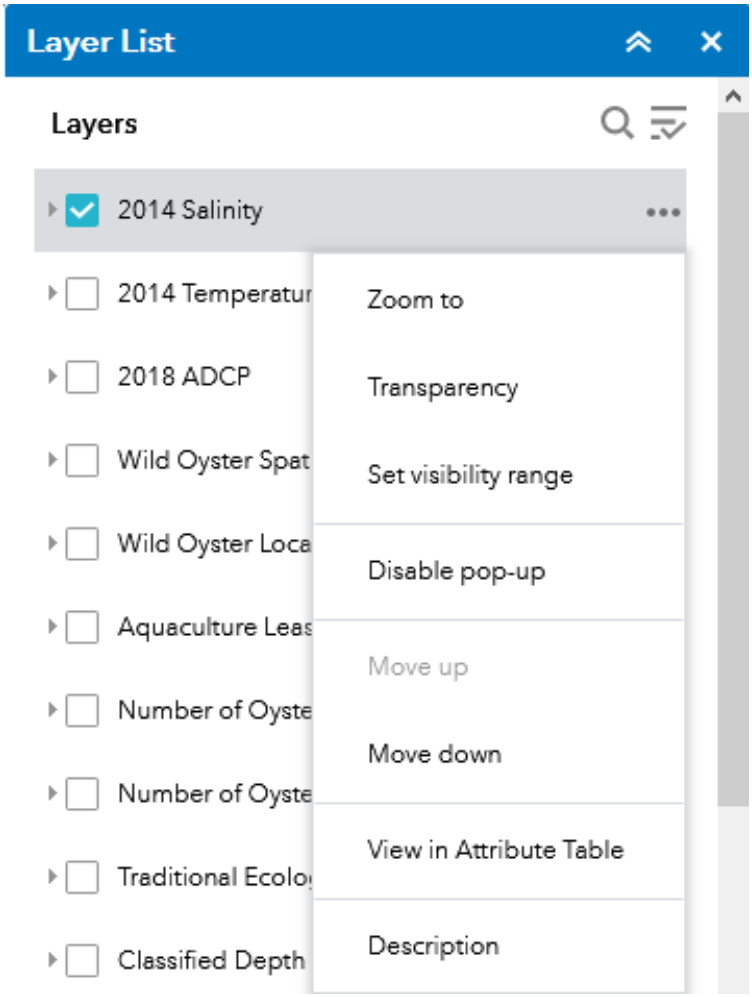

12.1.1 Traditional Ecological Knowledge (TEK): Molluscs

- Polygon locations representing the habitat of several mollusc species (American oyster, blue mussel, quahog, razor clam, softshell clam) are displayed on the map when activated by the user. These layers were provided by the Department of Fisheries and Oceans (DFO) and clipped to the study area.

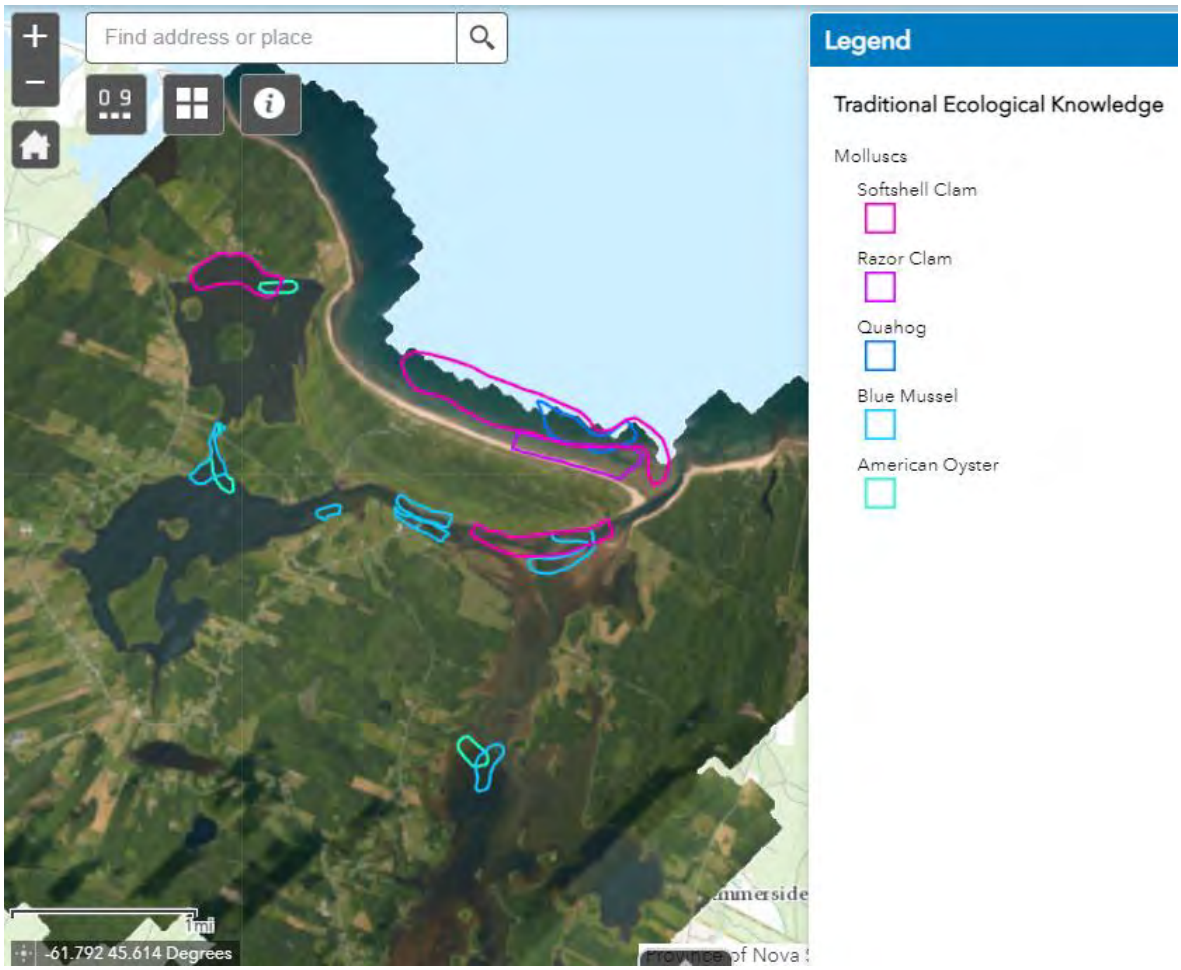

12.1.2 Channel Location

- The classified channel layer was derived from the continuous depth layer.

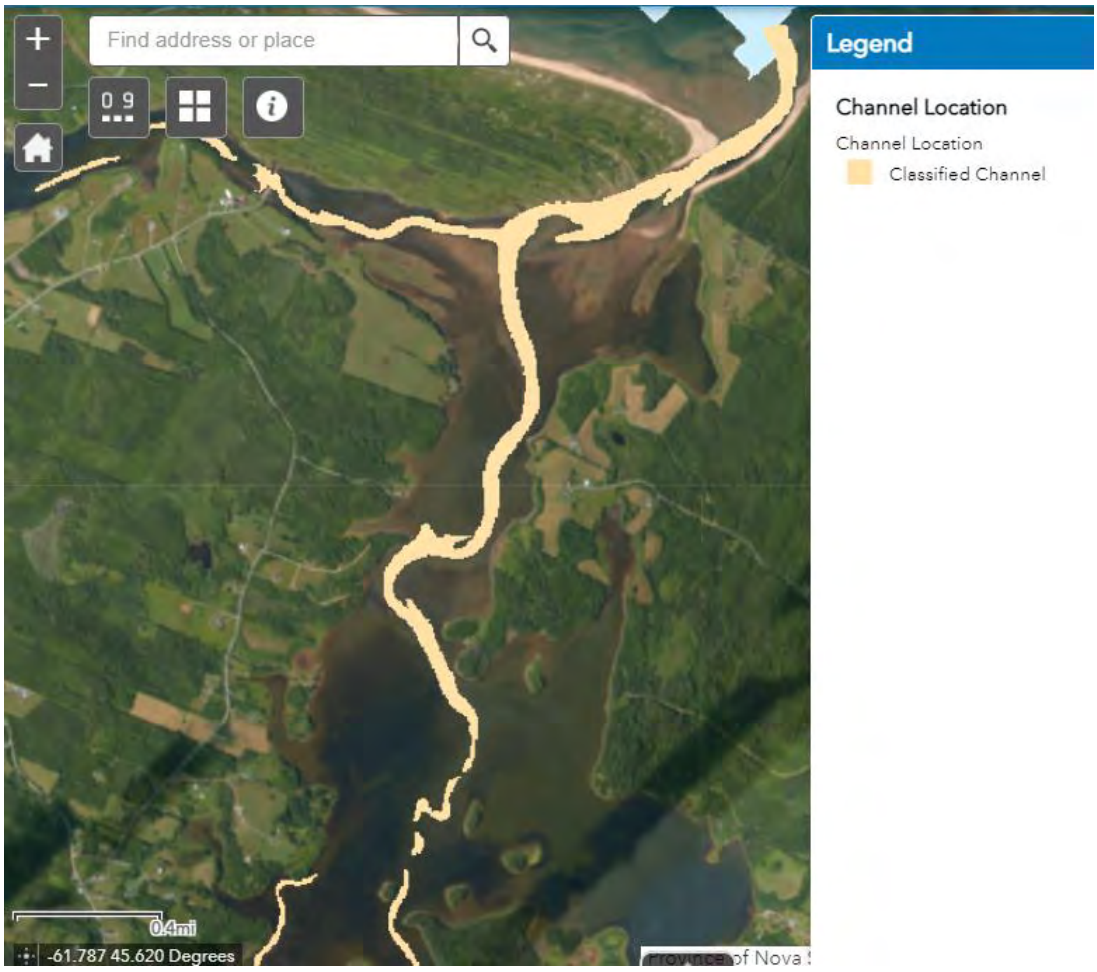

12.1.3 Classified Depth from Low Tide

- The classified depth layer relative to low tide layer was generated from the seamless Digital Elevation Model and is binned in 1 m increments.

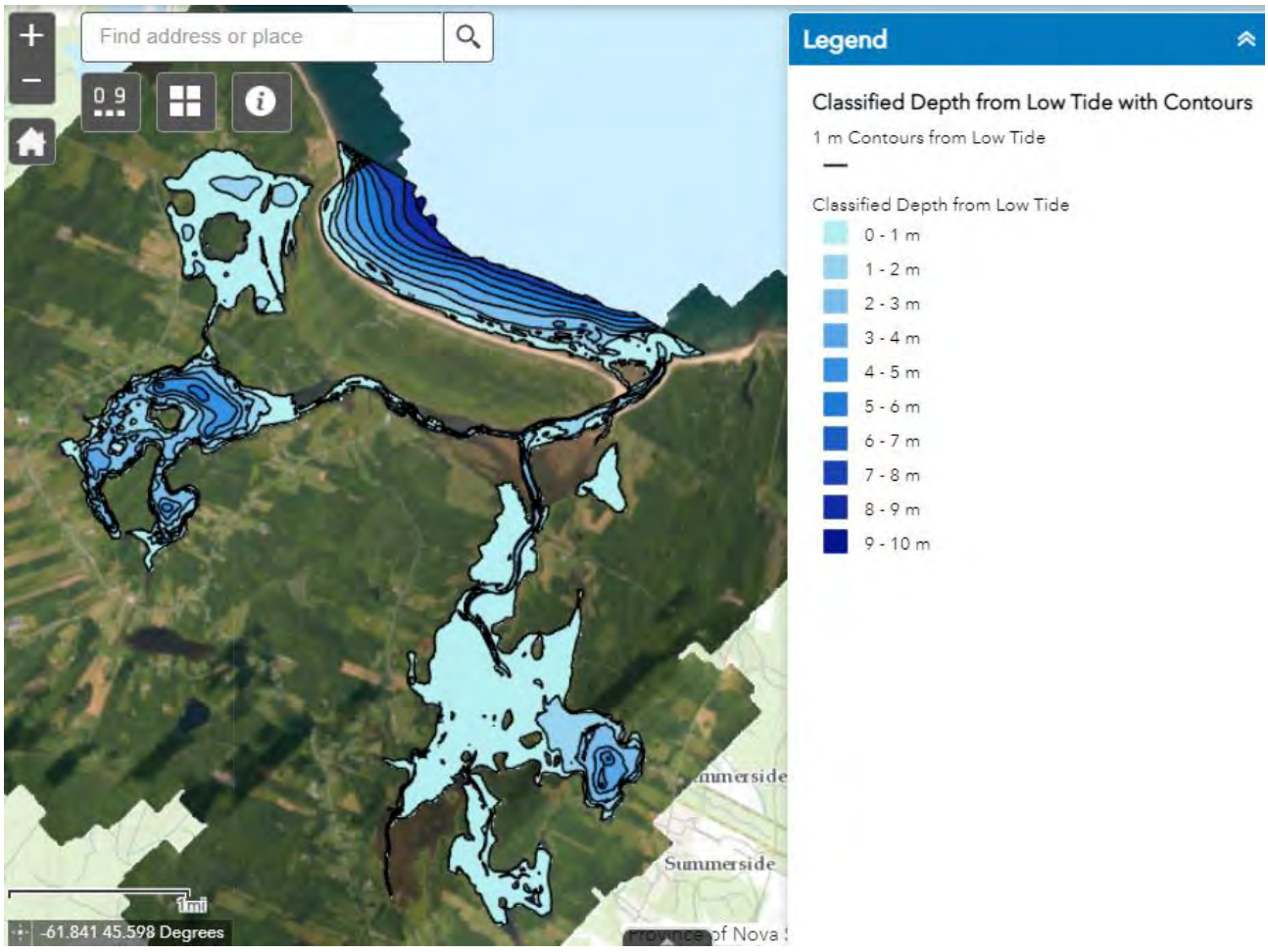

12.1.4 Classified Dominant Wave Height

- The classified dominant wave height layer was generated by using the hydrodynamic modelling software, Mike 21, to apply strong south winds to the Pomquet Harbour study area over two tidal cycles. Wave height was determined to be a suitable proxy for fetch.

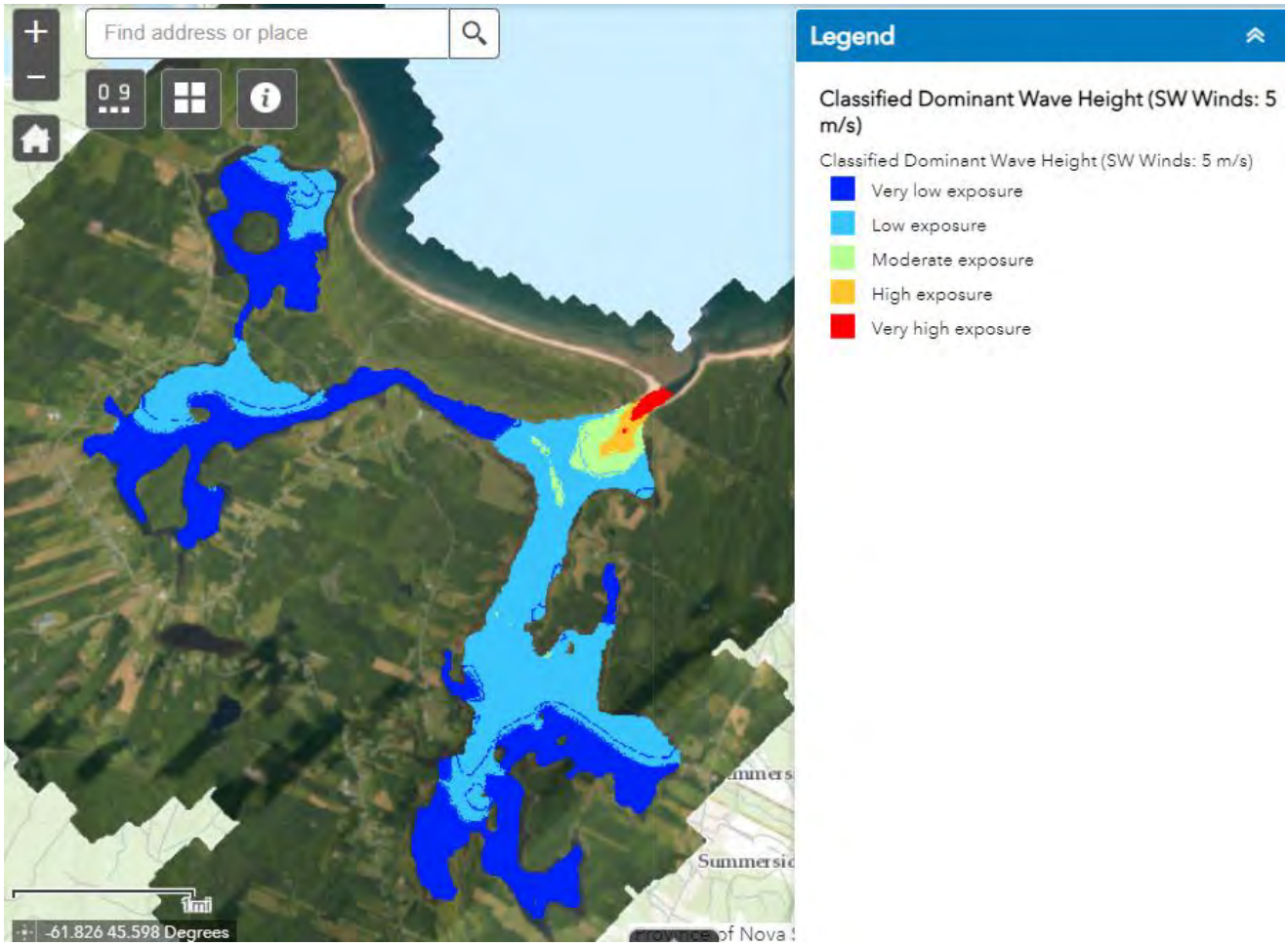

12.1.5 Classified Flushing Rate

- The classified flushing rate layer was generated by using an arbitrary concentration of 1 on the first day of a 30-day simulation in the Transport Model of Mike 21. The resulting raster represents the minimum concentration in Pomquet Harbour during this simulation.

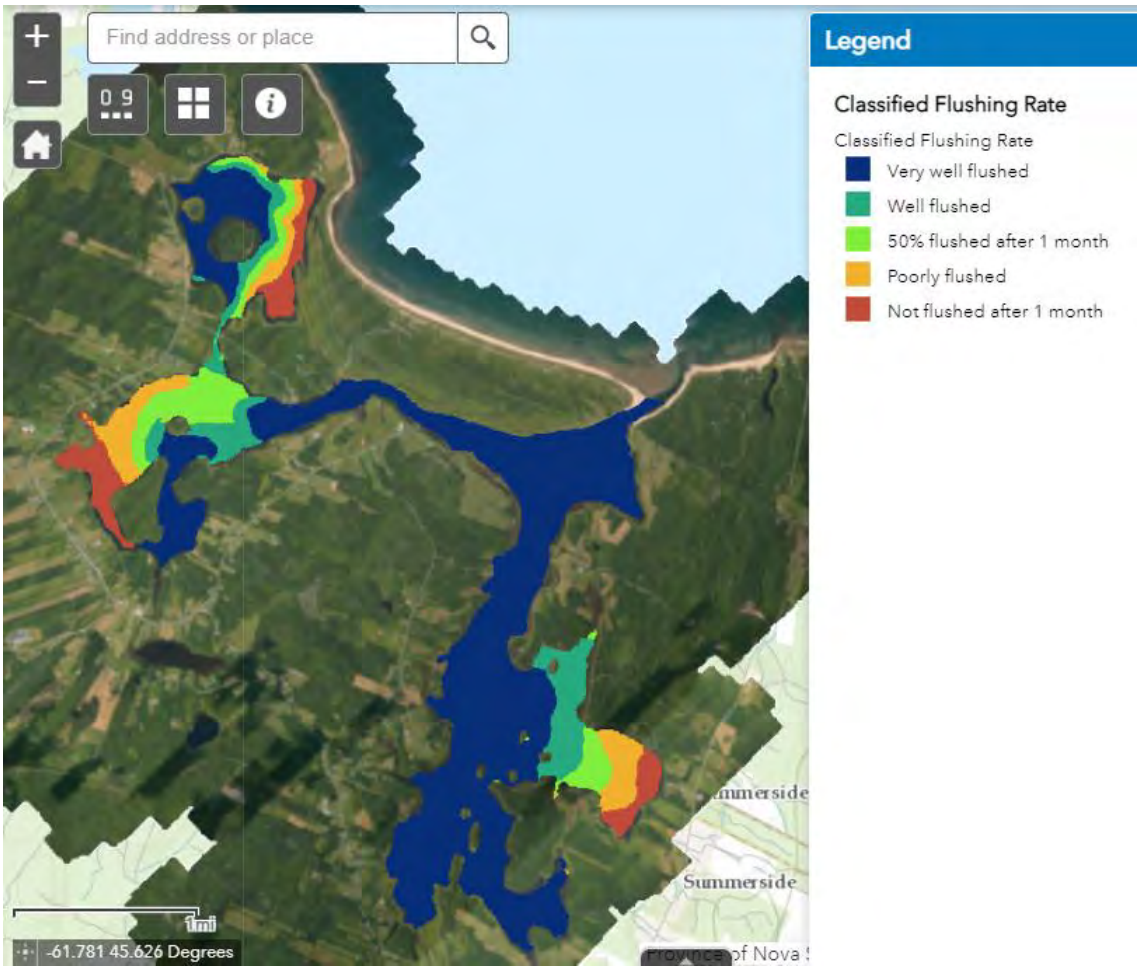

12.1.6 Classified Mean and Maximum Monthly Current Speed

- The classified mean and maximum current speed layers were derived directly from the hydrodynamic model simulation in Mike 21, which ran throughout the ADCP deployment.

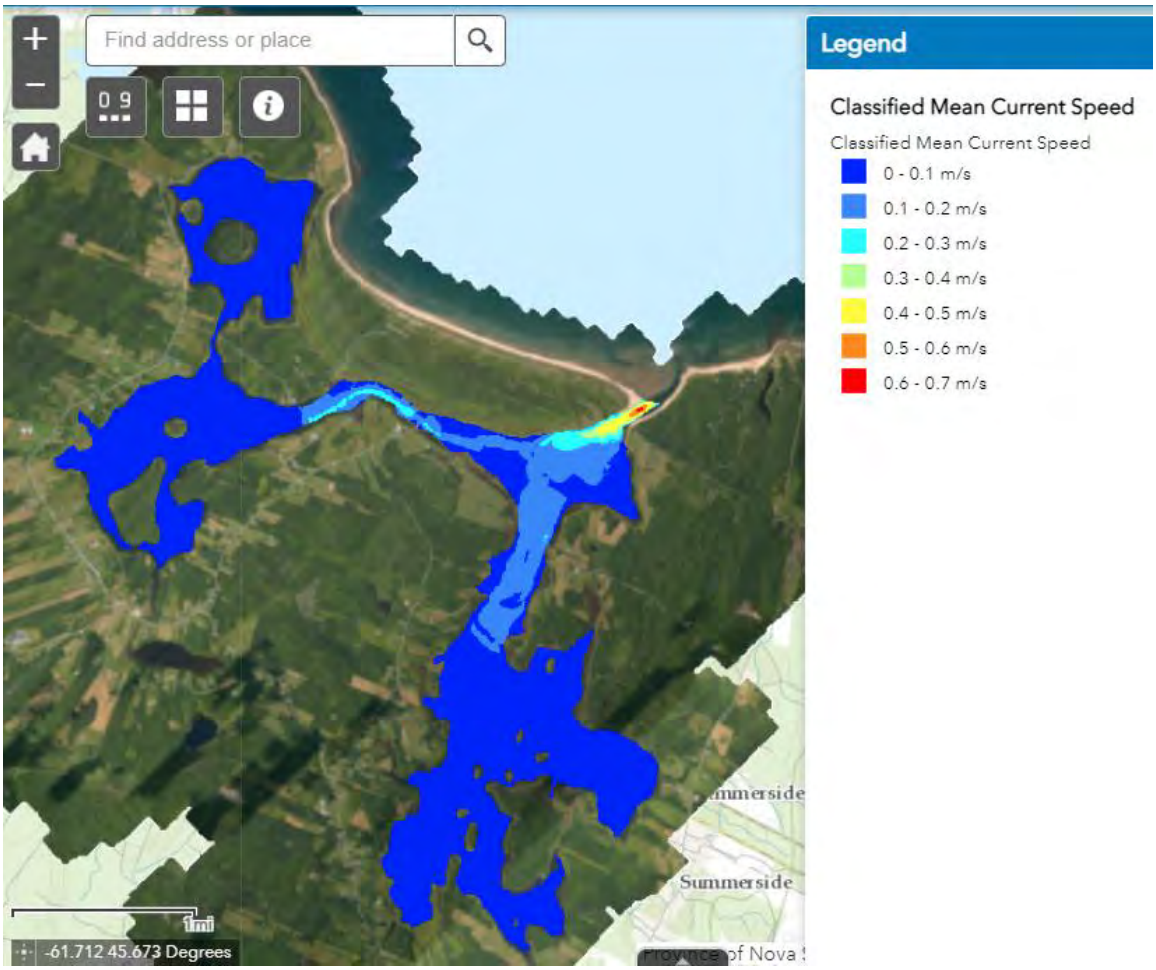

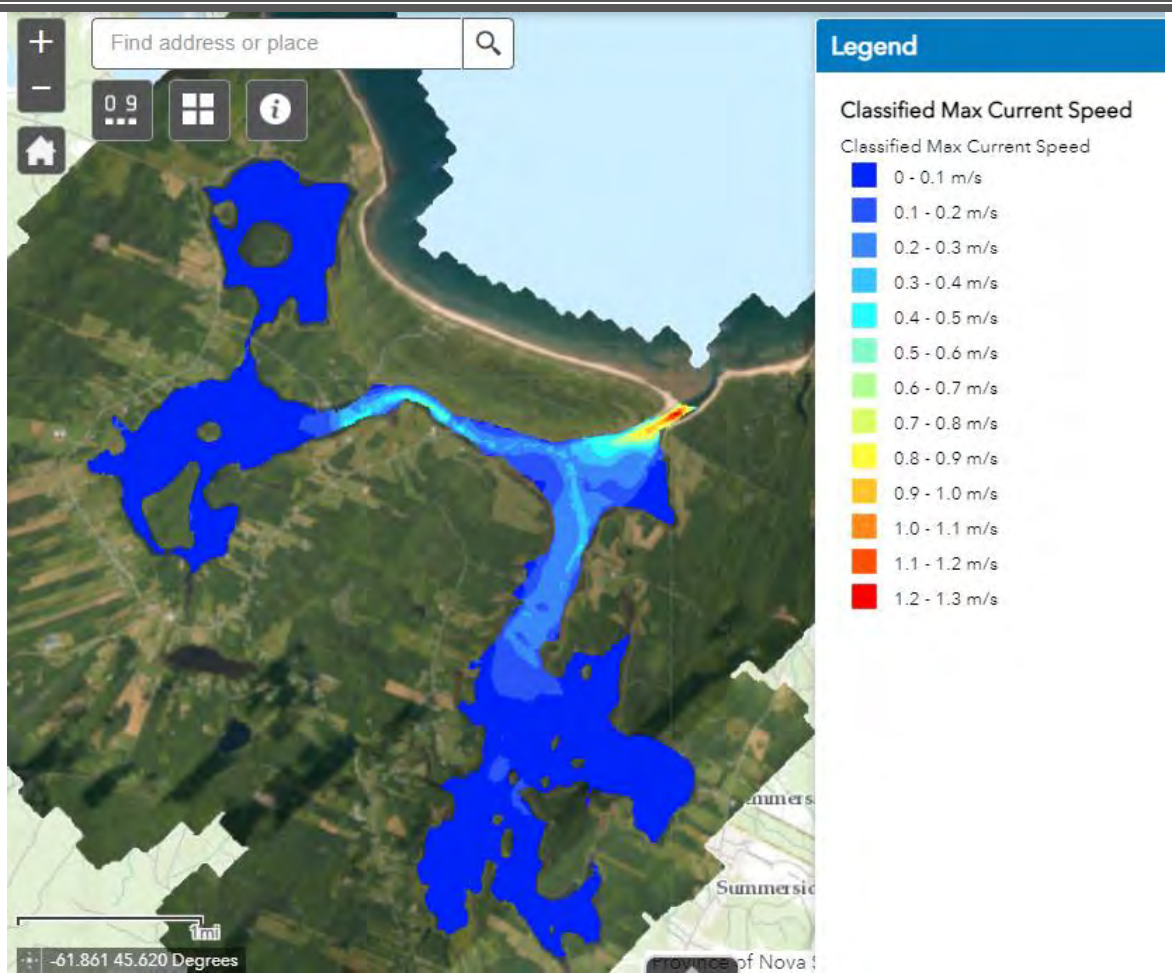
Find address or place
Legend
Classified Max Current Speed
Classified Max Current Speed
0 - 0.1 m/s
0.1 - 0.2 m/s
0.2 - 0.3 m/s
0.3 - 0.4 m/s
0.4 - 0.5 m/s
0.5 - 0.6 m/s
0.6 - 0.7 m/s
0.7 - 0.8 m/s
0.8 - 0.9 m/s
0.9 - 1.0 m/s
1.0 - 1.1 m/s
1.1 - 1.2 m/s
1.2 - 1.3 m/s
1mi
-61.861 45.620 Degrees

12.1.7 Classified Eelgrass

- The eelgrass layer was derived from a Fuzzy K-Means unsupervised classification of the benthic habitat in Pomquet Harbour.

12.1.8 Ice Impact-Free

- The Ice Impact Zone layer was generated from the seamless Digital Elevation Model (DEM). The ice impact zone was defined as the area between Higher High Water Large Tide (HHWLT) and 1 m below Lower Low Water Large Tide (LLWLT). Ice impact-free zones were defined as areas deeper than 1 m below LLWLT.

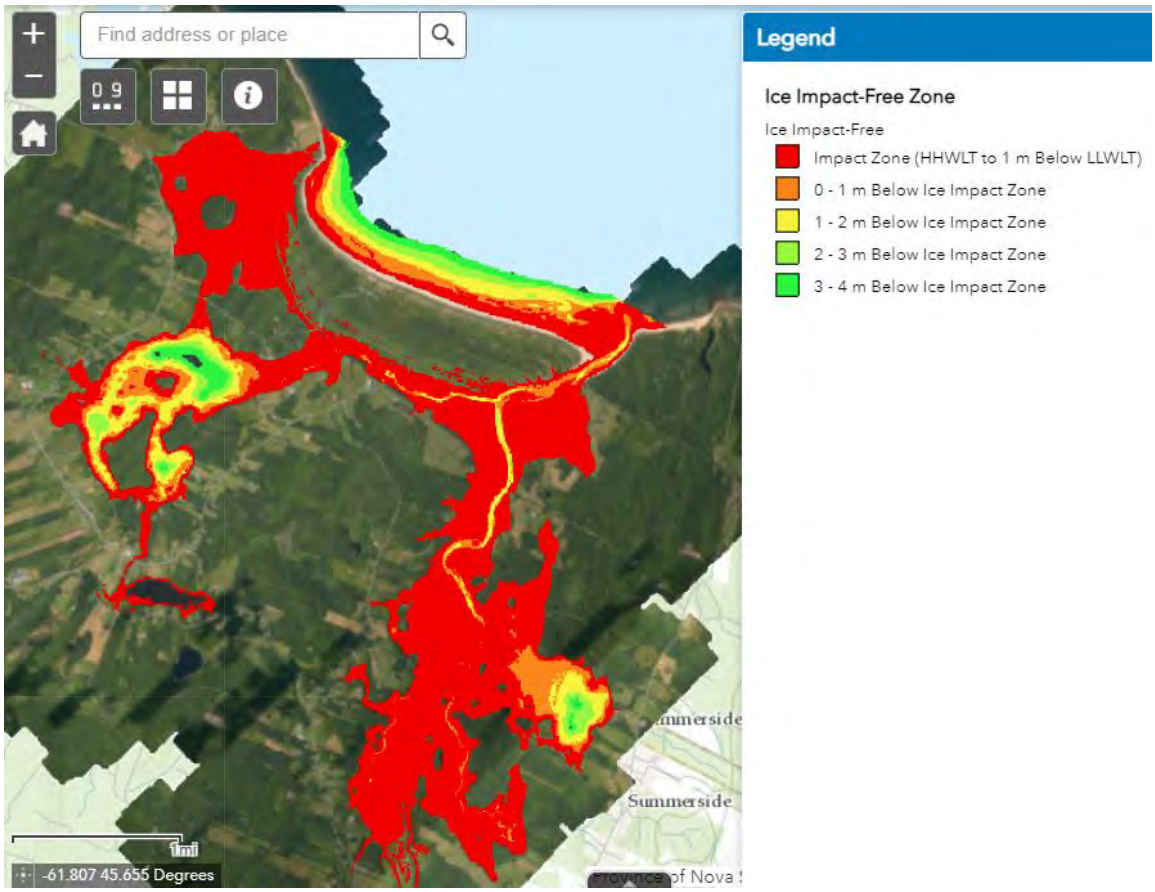

12.1.9 NS Marine Aquaculture Leases

- Polygon locations of issued aquaculture leases within Pomquet Harbour are displayed on the map when activated by the user. This layer was provided by Nova Scotia Fisheries and Aquaculture (NSFA) and clipped to the study area.

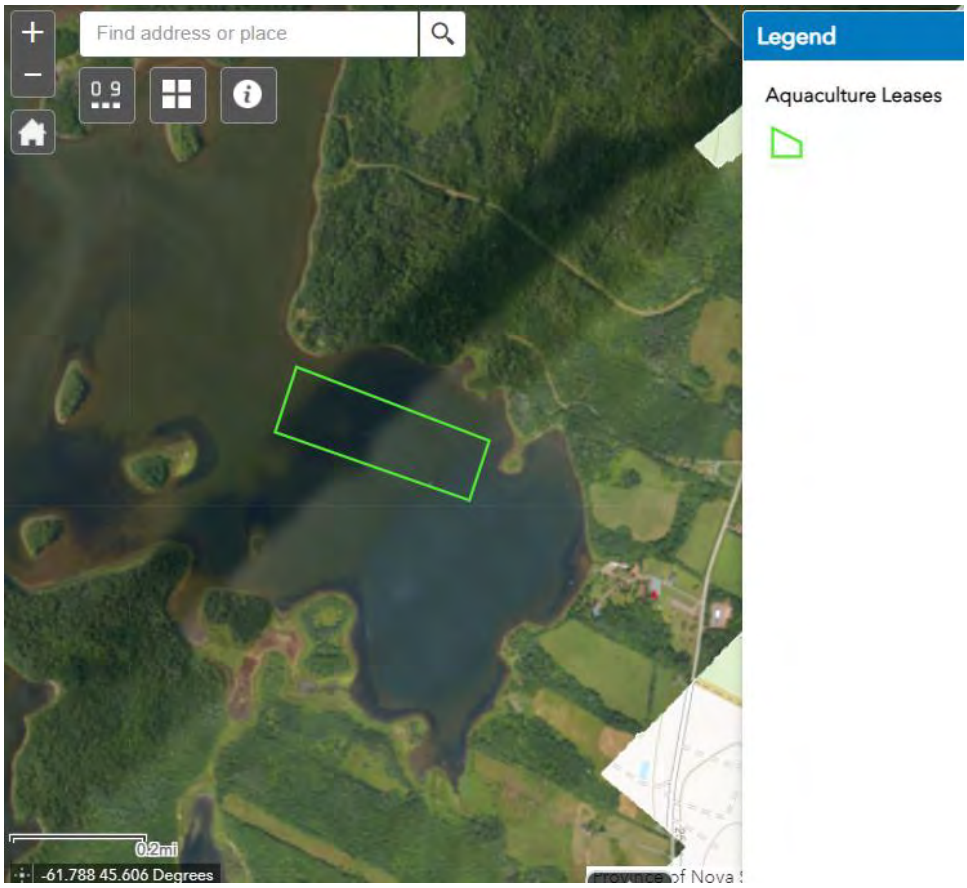

12.2 Suitability Modeller Tool

- The suitability modeller tool allows the user to generate a model of suitable oyster spat collection sites within Pomquet Harbour by conducting a weighted raster overlay analysis.

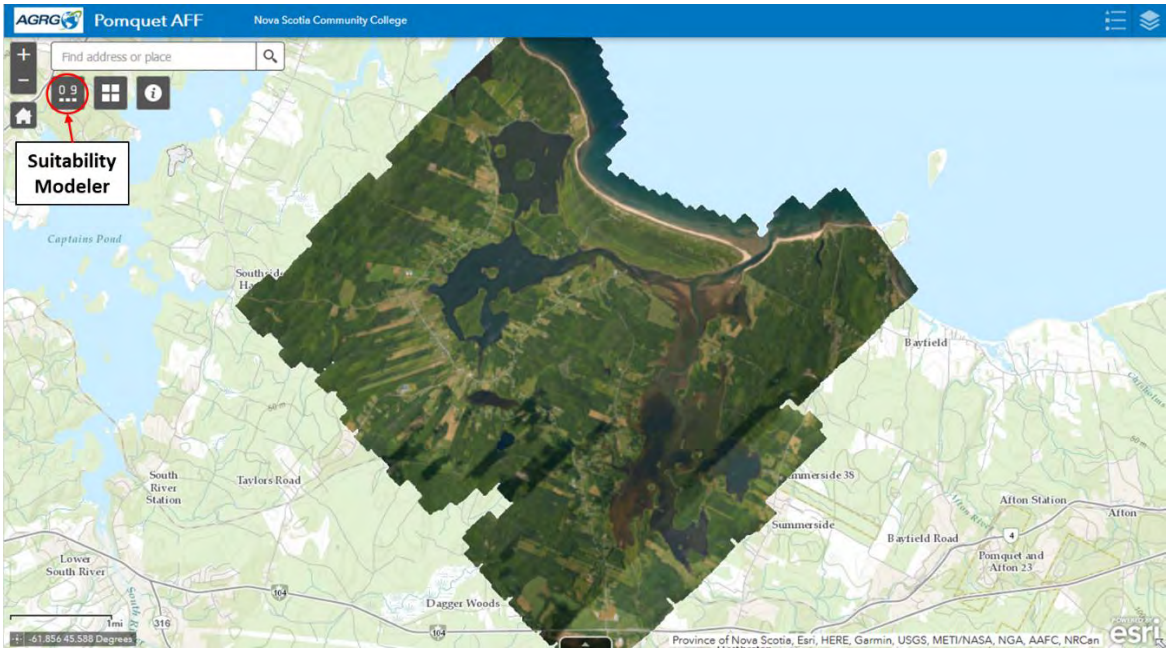

- To design the model, begin by selecting the layers you want to use in your analysis. Scroll down to see the full list of available layers.

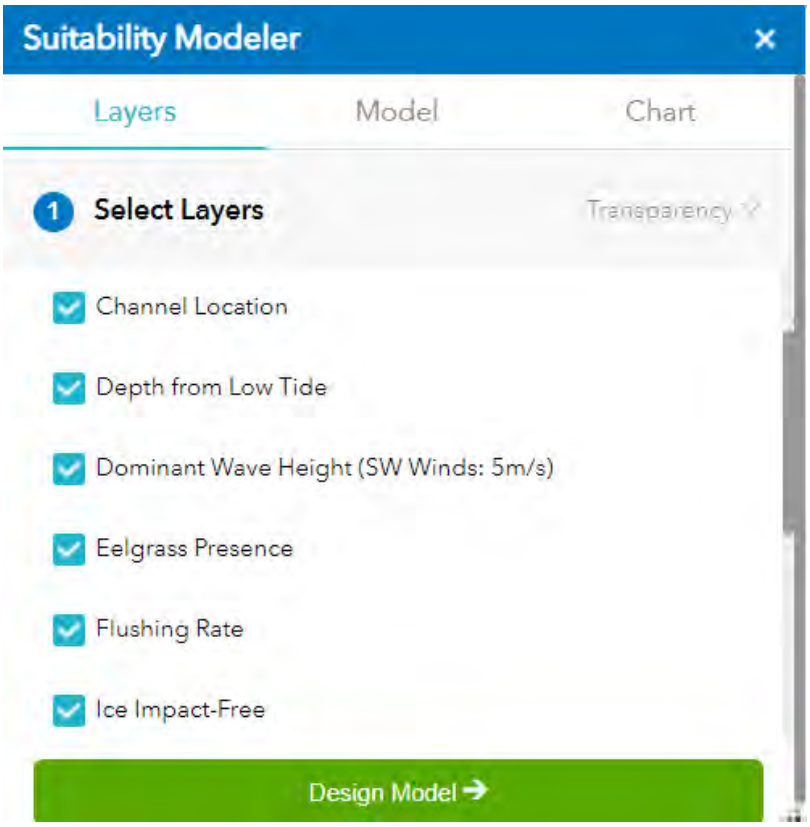

- Click "Design Model".
- Under the Model section, type a number into the percentage (%) text box to assign each layer a relative importance in the analysis. The total percentage must equate to 100 before the analysis can be run.

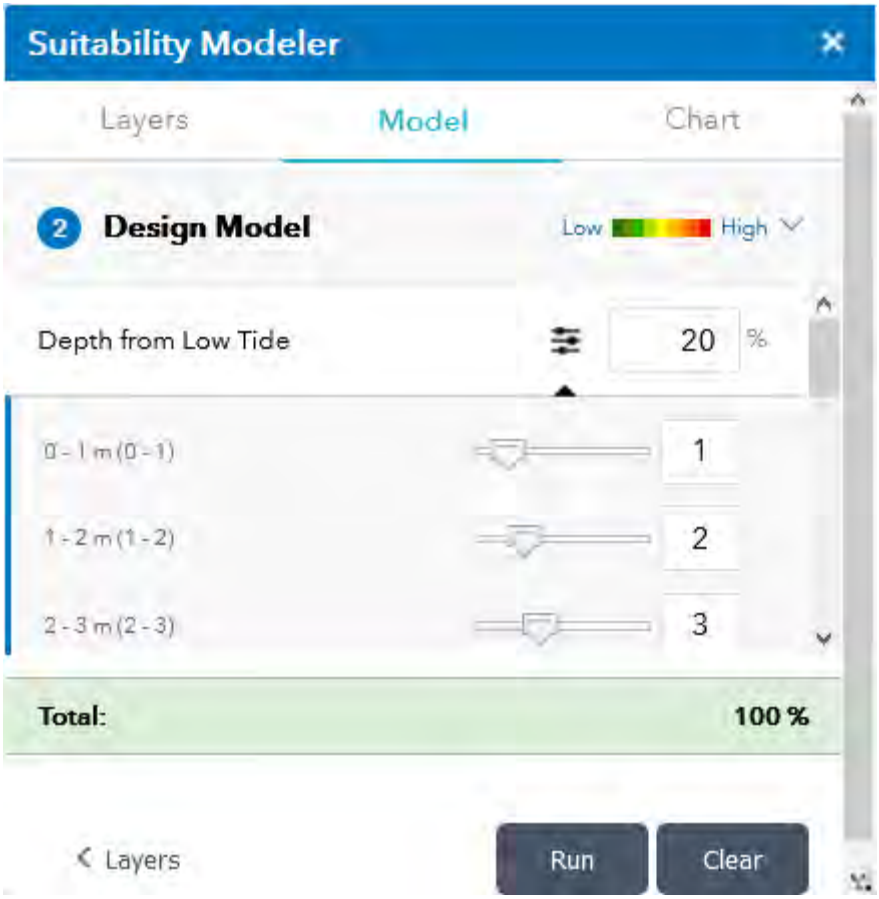

- Users can optionally expand each of the layers to adjust the class weights (1 being least suitable and 9 being most suitable). The class weights will decide how layer values are mapped to a suitability scale.
- To change your model's colour ramp, select the ramp labelled "Low" to "High" in the top right corner of the Suitability Modeller window.
- Click "Run" for a model to appear on the map as a layer.

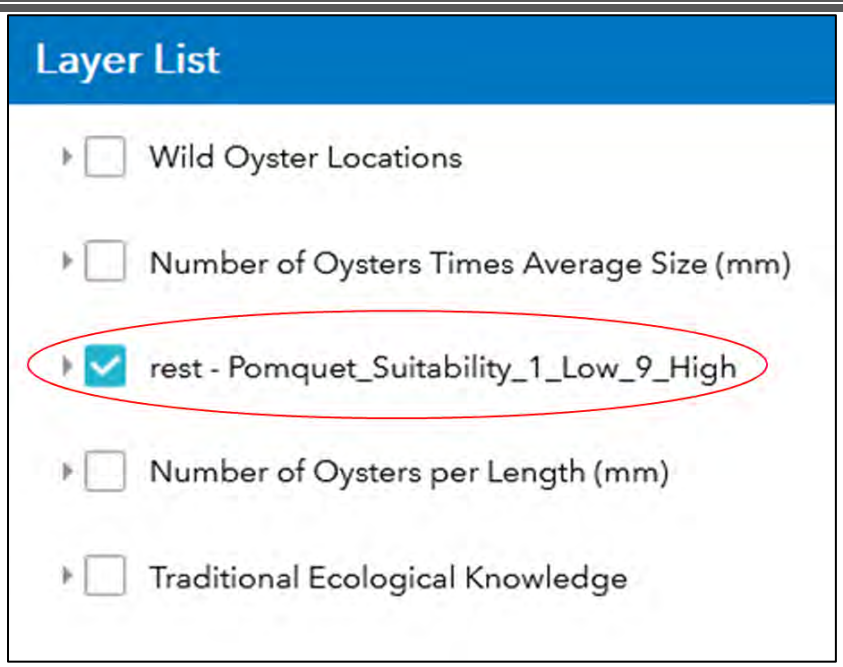

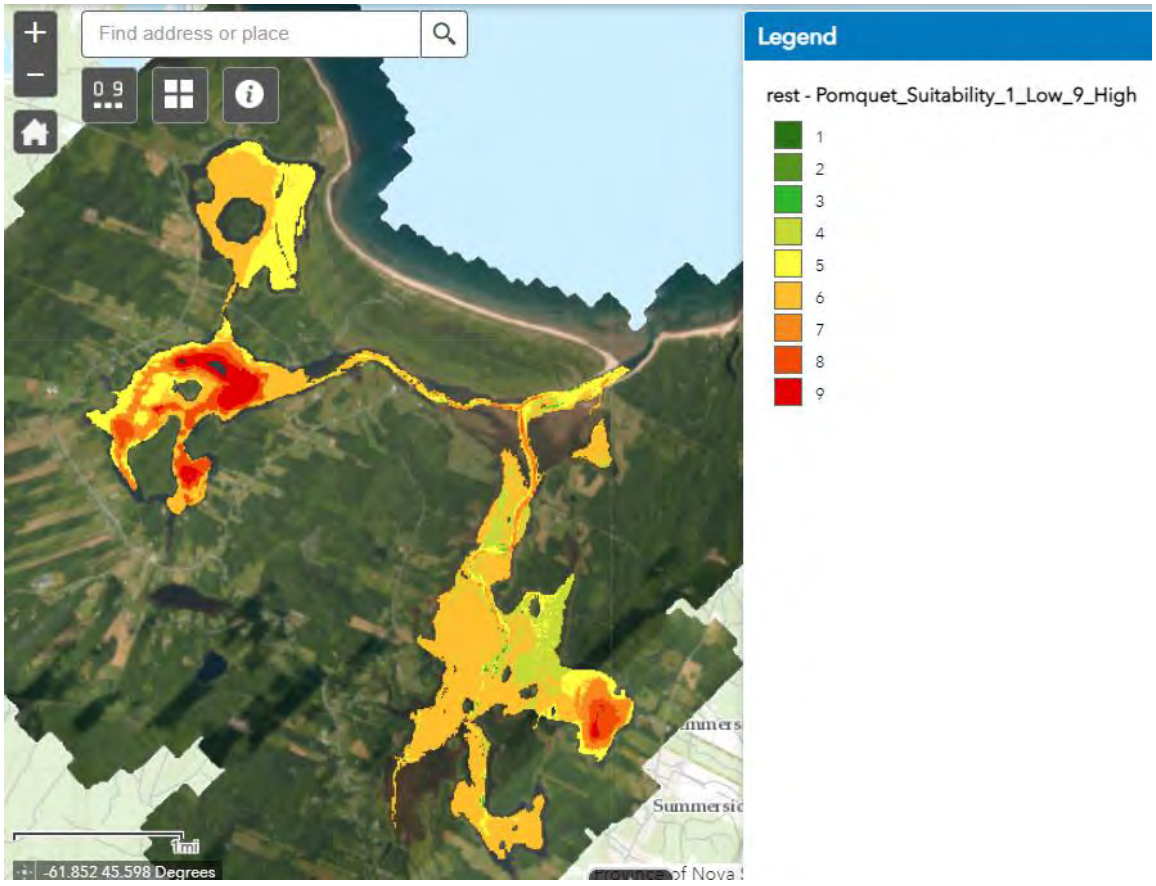

- Under the Chart section, choose between the features to design a chart of your model. The tools you can use are:
    - Draw a polygon.
        - Click the map to start drawing polygon vertices around your area of interest.

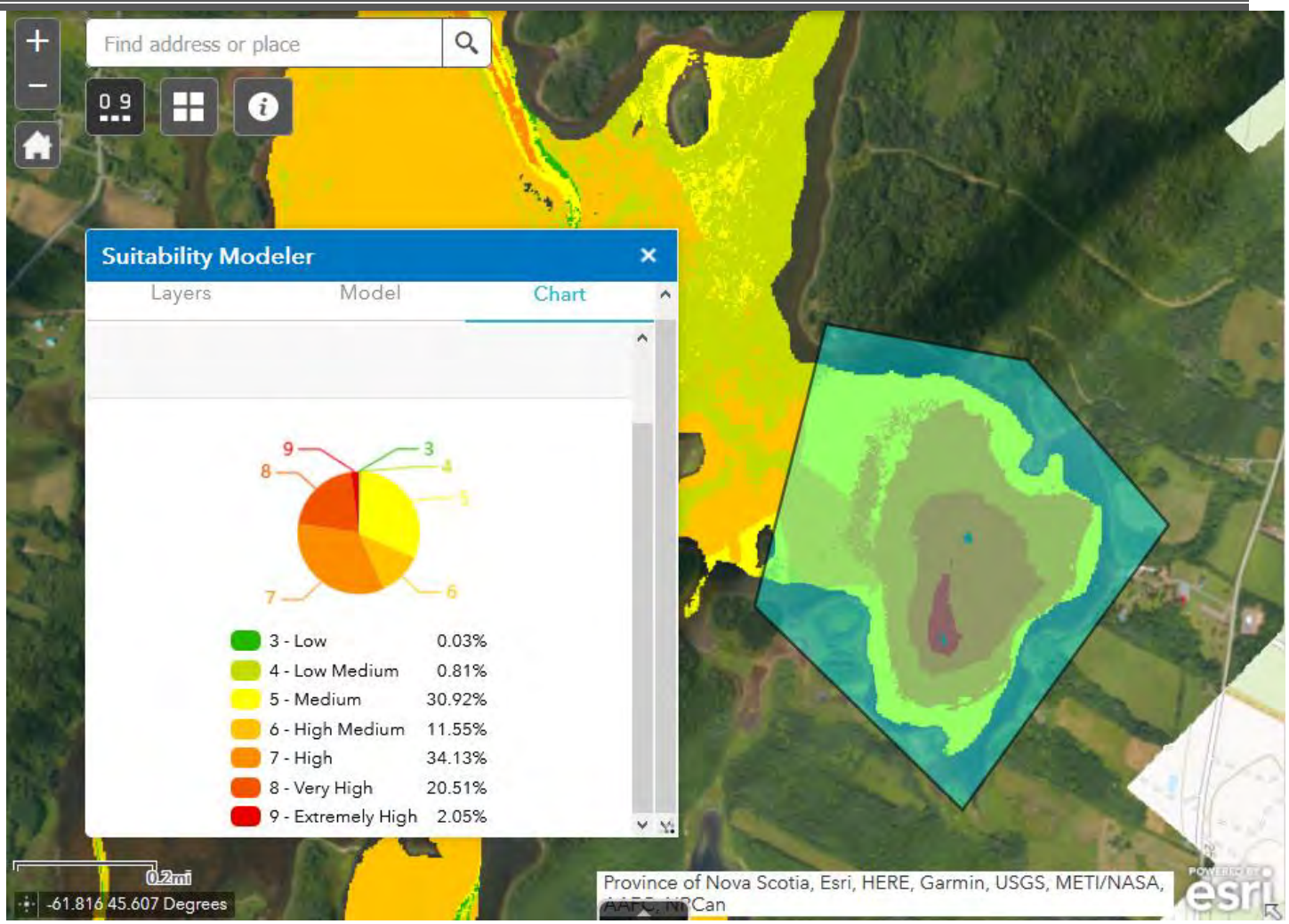

- Draw a freehand polygon.
  - Click and press down your mouse to draw a freehand polygon around your area of interest. Finish your polygon by letting go of the mouse.
- Select from a layer.
  - Begin by choosing one of the available layers from the drop-down list. Users can then click and press down their mouse to select the desired feature from a layer.
- Pan.
  - Click this tool to pan around the model.

- To design a new chart, the user must first select "clear".